NASA / CR—1998-206597

Energy Efficient Engine Low Pressure Subsystem Flow Analysis

Edward J. Hall, Sean R. Lynn, Nathan J. Heidegger, and Robert A. Delaney
Allison Engine Company, Indianapolis, Indiana

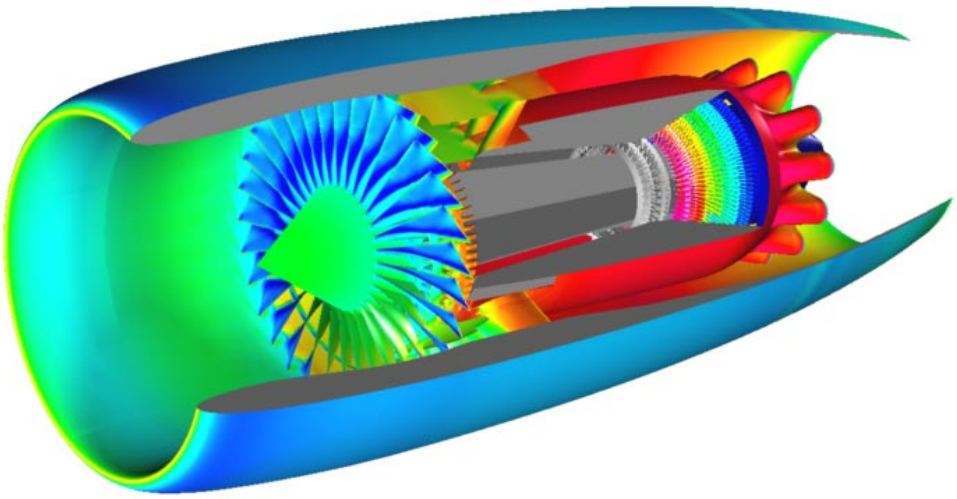

April 1998

The NASA STI Program Office . . . in Profile

Since its founding, NASA has been dedicated to the advancement of aeronautics and space science. The NASA Scientific and Technical Information (STI) Program Office plays a key part in helping NASA maintain this important role.

The NASA STI Program Office is operated by Langley Research Center, the Lead Center for NASA's scientific and technical information. The NASA STI Program Office provides access to the NASA STI Database, the largest collection of aeronautical and space science STI in the world. The Program Office is also NASA's institutional mechanism for disseminating the results of its research and development activities. These results are published by NASA in the NASA STI Report Series, which includes the following report types:

- TECHNICAL PUBLICATION. Reports of completed research or a major significant phase of research that present the results of NASA programs and include extensive data or theoretical analysis. Includes compilations of significant scientific and technical data and information deemed to be of continuing reference value. NASA's counterpart of peer-reviewed formal professional papers but has less stringent limitations on manuscript length and extent of graphic presentations.

- TECHNICAL MEMORANDUM. Scientific and technical findings that are preliminary or of specialized interest, e.g., quick release reports, working papers, and bibliographies that contain minimal annotation. Does not contain extensive analysis.

- CONTRACTOR REPORT. Scientific and technical findings by NASA-sponsored contractors and grantees.

- CONFERENCE PUBLICATION. Collected papers from scientific and technical conferences, symposia, seminars, or other meetings sponsored or cosponsored by NASA.

- SPECIAL PUBLICATION. Scientific, technical, or historical information from NASA programs, projects, and missions, often concerned with subjects having substantial public interest.

- TECHNICAL TRANSLATION. English-language translations of foreign scientific and technical material pertinent to NASA's mission.

Specialized services that complement the STI Program Office's diverse offerings include creating custom thesauri, building customized data bases, organizing and publishing research results . . . even providing videos.

For more information about the NASA STI Program Office, see the following:

- Access the NASA STI Program Home Page at ***http://www.sti.nasa.gov***

- E-mail your question via the Internet to help@sti.nasa.gov

- Fax your question to the NASA Access Help Desk at (301) 621-0134

- Telephone the NASA Access Help Desk at (301) 621-0390

- Write to:
  NASA Access Help Desk
  NASA Center for AeroSpace Information
  800 Elkridge Landing Road
  Linthicum Heights, MD 21090-2934

NASA / CR—1998-206597

Energy Efficient Engine Low Pressure Subsystem Flow Analysis

Edward J. Hall, Sean R. Lynn, Nathan J. Heidegger, and Robert A. Delaney
Allison Engine Company, Indianapolis, Indiana

Prepared under Contract NAS3–27394

National Aeronautics and
Space Administration

Lewis Research Center

April 1998

This report contains preliminary findings, subject to revision as analysis proceeds.

Available from

NASA Center for Aerospace Information
800 Elkridge Landing Road
Linthicum Heights, MD 21090-2934
Price Code: A08

National Technical Information Service
5287 Port Royal Road
Springfield, VA 22100
Price Code: A08

Preface

This report was prepared by Edward J. Hall, Sean R. Lynn, Nathan J. Heidegger, and Robert A. Delaney of the Allison Engine Company, Indianapolis, IN. The work was performed under Task 13 of NASA Contract NAS3-27394 from March, 1996 to September, 1997. The Principal Investigator for this program was Edward J. Hall. The Allison Program Manager for this contract was Robert A. Delaney. The NASA Project Manager was Joseph P. Veres.

Contents

1 SUMMARY **1**

2 INTRODUCTION **3**
2.1 Description of Engine Balance Design Problem 3
2.2 NASA Programs Addressing Advanced Engine Design 3
2.2.1 NASA High Performance Computing and Communications (HCCP) Program [1] 4
2.2.2 The Computational Aerosciences (CAS) Project [2] 4
2.2.3 The Numerical Propulsion System Simulator (NPSS) [3] . . . 5
2.3 Integration of NASA Program Objectives and the Engine Balance Design Problem 5
2.4 NPSS and the Energy Efficient Engine (EEE) 6
2.5 Objectives of the Present Study 7

3 DESCRIPTION OF THE ENERGY EFFICIENT ENGINE **9**

4 GEOMETRY MODELING **13**

5 COMPONENT MESH GENERATION **17**

6 *ADPAC* CODE DESCRIPTION **23**

7 PARALLEL COMPUTING **29**
7.1 *davinci* Workstation Cluster 29
7.2 *babbage* Workstation Cluster 30
7.3 *LACE* Workstation Cluster 31
7.4 Allison Silicon Graphics Power Challenge XL 32

8 *NEPP* CODE DESCRIPTION **35**

9 Component Performance Validation **37**
9.1 EEE Fan Section Analysis 37
9.1.1 Description of Design 37
9.1.2 Mesh System 38
9.1.3 Design Point Analysis 40
9.1.4 Off-Design Analysis 42

9.2 EEE Low Pressure (LP) Turbine Analysis 45
9.2.1 Description of Design 45
9.2.2 Mesh System 45
9.2.3 Design Point Analysis 47
9.2.4 Effect of Variations in First Vane Setting Angle 49
9.2.5 Effect of Variations in Inlet Profile 49
9.2.6 Effect of Variations in Endwall Geometry 49
9.2.7 Summary of Variations in Turbine Parameters on Design Point Performance 54
9.2.8 Off-Design Analysis 56
9.3 EEE Core Compressor Analysis 62
9.3.1 Description of the Design 62
9.3.2 Mesh System 62
9.3.3 Design Point Analysis 62
9.4 EEE HP Turbine Analysis 67
9.4.1 Description of the Design 67
9.4.2 Mesh System 67
9.4.3 Design Point Analysis 69
9.5 Lobed Exhaust Mixer Analysis 72
9.5.1 Description of the Design 72
9.5.2 Mesh System 72
9.5.3 Design Point Analysis 72

10 EEE/LP Subsystem Analysis **81**
10.1 LP Subsystem Mesh Construction 81
10.2 EEE LPS Processing Strategy 83
10.3 EEE LPS Design Point Simulation 86
10.4 EEE LPS Shaft Power Balance 86

11 *ADPAC/NEPP* Engine Analysis **91**
11.1 *ADPAC/NEPP* Coupling Procedure 91

12 CONCLUSIONS **95**
12.1 Geometry Manipulation 95
12.2 Mesh Generation 96
12.3 Solution Initialization 97
12.4 Application of Parallel Computing 97
12.5 Full-Scale Engine Simulation 97
12.6 Interpretation of Computational Results 98
12.7 Recommendations for Future Study 98

A *ADPAC07* Input Files for EEE/LP Simulation **113**

B *SEARCH* Program Source Code **139**

List of Figures

3.1 Energy Efficient Engine layout and design features. 10
3.2 Energy Efficient Engine component description and CFD mesh representation. 11

4.1 Energy Efficient Engine test rig hardware. 14
4.2 PATRAN representation of the Energy Efficient Engine Master Engine Geometry Database. 14

5.1 Component mesh generation procedure for EEE LPS analysis. 18
5.2 Illustration of the *GRIDGEN* user interface display for the meridional projection of the EEE fan section mesh system. 19
5.3 Axisymetric mesh projection for the EEE LP turbine. 20
5.4 Three-dimensional mesh projection for the EEE LP turbine. 21

6.1 Summary of variety of problems which can be analyzed using the *ADPAC* code. 24
6.2 Illustration of *ADPAC* mixing plane boundary formulation for steady prediction of multistage turbomachinery flows. 26
6.3 Illustration of mixing plane analysis (predicted Mach contours and mesh system) for a 3-1/2 stage compressor. 26

7.1 NASA Ames Research Center Silicon Graphics (*davinci*) workstation cluster schematic diagram (configuration circa 1995). 30
7.2 NASA Ames Research Center IBM RS-6000 (*babbage*) workstastion cluster schematic diagram (configuration circa 1995). 31
7.3 NASA Lewis Research Center IBM RS-6000 (*LACE*) workstastion cluster. 32
7.4 Allison Engine Company Silicon Graphics Power Challenge XL parallel computer. 33

8.1 Screen illustration of NEPP analysis with NPAS user interface. 36

9.1 Axisymmetric projection of EEE fan+1/4-height booster stage configuration ilustrating test data instrumentation plane locations. 38
9.2 Axisymmetric projection of EEE fan section multi-block H-type mesh system. 41

9.3 Predicted surface static pressure contours for EEE fan plus 1/4-height booster stage configuration. 41
9.4 Comparison of predicted and experimental spanwise total pressure distributions at bypass vane exit and 1/4-stage vane leading edge for EEE fan plus 1/4-height booster stage configuration. 42
9.5 Comparison of predicted and experimental total pressure ratio and adiabatic efficiency versus corrected flow rate for the core inlet of the EEE fan section. 43
9.6 Comparison of predicted and experimental total pressure ratio and adiabatic efficiency versus corrected flow rate for the bypass duct flow of the EEE fan section. 44
9.7 Axisymmetric projection of EEE LP turbine component validation mesh system. 46
9.8 Predicted surface static pressure contours for EEE LP turbine. 47
9.9 Comparison of predicted and experimental spanwise total pressure and total temperature distributions for fifth stage exit of the EEE LP turbine 2/3-scale test rig. 48
9.10 Comparison of predicted and experimental spanwise variation in fifth stage exit total temperature distributions for EEE LP turbine analyses with variations in first vane reset and endwall modeling. 50
9.11 Comparison of spanwise variation of inflow total pressure and total temperature ratio profiles for profiles for the EEE LP turbine analyses with variations in inlet profile. 51
9.12 Comparison of predicted and experimental spanwise variation in fifth stage exit total temperature distributions for EEE LP turbine analyses with variations in inlet profile. 52
9.13 Illustration of realistic LP turbine endwall irregularities and CFD modeling techniques for the EEE LP turbine component validation study. 53
9.14 Comparison of axisymmetric projection of mesh systems for the EEE LP turbine with smooth endwalls (upper) and with modeled shrouded rotor seal cavities (lower). 55
9.15 Illustration of predicted axisymmetric-averaged Mach number contours for the EEE LP turbine with shrouded rotor cavity endwall model. . 56
9.16 Comparison of predicted and experimental spanwise variation in fifth stage exit total temperature distributions for EEE LP turbine analyses with variations in inlet profile. 57
9.17 Comparison of predicted (ADPAC) and measured equivalent energy extraction for the Energy Efficient Engine (EEE) LP turbine. 58
9.18 Comparison of predicted (ADPAC) and measured inlet flow function for the Energy Efficient Engine (EEE) LP turbine. 59
9.19 Comparison of predicted (ADPAC) and measured total to total adiabatic efficiency for the Energy Efficient Engine (EEE) LP turbine. . . 60
9.20 Comparison of predicted (ADPAC) and measured total to static adiabatic efficiency for the Energy Efficient Engine (EEE) LP turbine. . . 61

9.21 Axisymmetric projection of EEE core compressor component validation mesh system. 63
9.22 Comparison of predicted and experimental spanwise total temperature distribution aft of the sixth stage rotor for the EEE HP compressor (design point operation). 65
9.23 Comparison of predicted and experimental spanwise total temperature distribution aft of the tenth stage stator for the EEE HP compressor (design point operation). 66
9.24 Axisymmetric projection of EEE HP turbine multi-block H-type mesh system. 69
9.25 Predicted surface static pressure contours for EEE HP turbine. 70
9.26 Comparison of predicted and experimental spanwise distributions of second stage exit total pressure and total temperature profiles for the EEE HP turbine. 71
9.27 Illustration of EEE lobed exhaust mixer geometric surfaces modeled during the component validation study. 73
9.28 Illustration of EEE lobed exhaust mixer symmetry plane mesh surfaces employed during the component validation study. 74
9.29 Illustration of EEE lobed exhaust mixer exit plane mesh system employed during the component validation study (analysis employs one lobe and assumes periodicity from lobe to lobe). 75
9.30 Predicted surface static pressure contours and axial plane total temperature contours (one diameter aft of nozzle exit) for the EEE lobed exhaust mixer. 77
9.31 Predicted iso-temperature surfaces for EEE lobed exhaust mixer simulation illustrate temperature distribution patterns due to mixing. . . 78
9.32 Comparison of predicted and experimental radial total temperature surveys for the EEE lobed exhaust mixer. 79

10.1 Axisymmetric projection of Energy Efficient Engine (EEE) Low Pressure (LP) Subsystem analysis component layout and mesh system. . . 82
10.2 Illustration of aerodynamic/mechanical balance required for single-spool and twin-spool gas turbine engines. 87
10.3 Illustration of *NEPP* solution along constant *operating lines* and *ADPAC* solution along constant *speed lines*. 89

11.1 Coupled ADPAC/NEPP analysis schematic data flow representation. 92
11.2 Illustration of coupled ADPAC/NEPP prediction for the EEE LP Subsystem (color contours indicate predicted static pressure ratio: red-10.0, blue-0.36, grey scale components are represented by the NEPP cycle analysis). 93

List of Tables

3.1 Energy Efficient Engine Flight Propulsion System cycle characteristics. 10

9.1 EEE fan section aerodynamic design parameters. 39
9.2 Tabulated mesh block sizes for EEE fan section component performance validation analysis. 40
9.3 EEE LP turbine aerodynamic design parameters. 45
9.4 Tabulated mesh block sizes for EEE LP turbine component performance validation analysis. 46
9.5 Comparison of predicted overall performance parameters due to variations in inlet profile, endwll model, and first vane reset for the EEE LP turbine 2/3 scale test rig. 54
9.6 EEE core compressor aerodynamic design parameters. 63
9.7 EEE HP turbine critical operating data. 67
9.8 EEE HP turbine stage aerodynamic parameters. 68
9.9 EEE HP turbine stage blade aerodynamic geometry. 68
9.10 Tabulation of EEE lobed exhaust mixer mesh block sizes and total number of computational cells employed during the component validation study. 73

10.1 Tabulation of parallel computing CPU time estimates for platforms employed for the EEE LP Subsystem analysis (all times given are wall clock time on non-dedicated systems with precautions taken to eliminate outside loading factors). 84
10.2 Tabulation of coarse mesh EEE LP Subsystem shaft power balance iterative results. 88

NOTATION

A list of the symbols used throughout this document and their definitions is provided below for convenience.

Roman Symbols

a . . . speed of sound
c_p . . . gas specific heat at constant pressure
c_v . . . gas specific heat at constant volume

e... total internal energy
i... first grid index of numerical solution
j... second grid index of numerical solution
k... third grid index of numerical solution or thermal conductivity
k... turbulent kinetic energy
l... Van Driest damping function or mixing length
n... rotational speed (revolutions per second) or time step level
p... pressure
r... radius or radial coordinate
t... time
v_x... velocity in the Cartesian coordinate system x direction
v_y... velocity in the Cartesian coordinate system y direction
v_z... velocity in the Cartesian coordinate system z direction
v_r... velocity in the cylindrical coordinate system radial direction
v_θ... velocity in the cylindrical coordinate system circumferential direction
w_{rel}... relative velocity in the circumferential direction $(= v_\theta - r\omega)$
x... Cartesian coordinate system coordinate
y... Cartesian coordinate system coordinate
z... Cartesian coordinate system coordinate
$ADPAC07$... Advanced Ducted Propfan Analysis Code Version 07
$ADSPIN$... ADPAC post processing program
$ASCII$... American Standard Code for Information Interchange
CFL... Courant-Freidrichs-Lewy number $(\Delta t/\Delta t_{max,stable})$
D... diameter
DOC... Direct Operating Costs
EEE... Energy Efficienct Engine
F... i coordinate direction flux vector
FPS... Flight Propulsion System
G... j coordinate direction flux vector
$GRIDGEN$... Multiple block general purpose mesh generation system
H... k coordinate direction flux vector
H_{total}... total enthalpy
HP... high pressure
$ICLS$... Integrated Core/Low Spool
ISA... Industry Standard Atmosphere
K... cylindrical coordinate system source vector
L... reference length
LP... low pressure
LPS... low pressure subsystem
M... Mach number
$MFLOP$... million floating point operations per second (CPU speed factor)
N... Number of blades
Q... vector of conserved variables
R... gas constant or residual or maximum radius
$\mathcal{R}$... turbulent Reynolds number

Re ... Reynolds Number
P ... turbulence kinetic energy production term
Pr ... gas Prandtl Number
S ... surface area normal vector
$SDBLIB$ ... Scientific DataBase Library (binary file I/O routines)
T ... Temperature
U ... Freestream velocity (units of length/time)
$\mathcal{V}$ ... volume

Greek Symbols

γ ... specific heat ratio
Δ ... calculation increment
ϵ ... turbulence dissipation parameter
∇ ... gradient vector operator
ω ... vorticity
ρ ... density
μ ... coefficient of viscosity
τ ... fictitous time or shear stress
$\mathbf{\Pi}_{i,j}$ ... fluid stress tensor

Subscripts

$[\,]_1$ ... inlet value
$[\,]_2$ ... exit value
$[\,]_{ax}$ ... pertaining to the axial (x) cylindrical coordinate
$[\,]_{coarse}$ ... coarse mesh value
$[\,]_{effective}$ ... effective value
$[\,]_{fine}$ ... fine mesh value
$[\,]_{freestream}$ ... freestream value
$[\,]_{i,j,k}$ ... grid point index of variable
$[\,]_{laminar}$ ... laminar flow value
$[\,]_{max}$ ... maximum value
$[\,]_{min}$ ... minimum value
$[\,]_{nearwall}$ ... near wall value
$[\,]_{non-dimensional}$ ... non-dimensional value
$[\,]_r$ ... pertaining to the radial (r) cylindrical coordinate
$[\,]_{ref}$ ... reference value
$[\,]_{stable}$ ... value implied by linear stability
$[\,]_t$ ... turbulent flow value
$[\,]_{total}$ ... total (stagnation) value
$[\,]_{turbulent}$ ... turbulent flow value
$[\,]_{wall}$ ... value at the wall

$[\,]_x \ldots$ pertaining to the x Cartesian coordinate
$[\,]_y \ldots$ pertaining to the y Cartesian coordinate
$[\,]_z \ldots$ pertaining to the z Cartesian coordinate
$[\,]_\theta \ldots$ pertaining to the circumferential (θ) cylindrical coordinate

Superscripts

$[\,]^+ \ldots$ Turbulent velocity profile coordinate
$[\,]^* \ldots$ Intermediate value
$[\,]^n \ldots$ Time step index
$[\,] \ldots$ (no overscore) nondimensional variable
$\hat{[\,]} \ldots$ Dimensional variable
$\overline{[\,]} \ldots$ Time-averaged variable
$\tilde{[\,]} \ldots$ Density-weighted time-averaged variable $\vec{[\,]} \ldots$ Vector variable
$\vec{\vec{[\,]}} \ldots$ Tensor variable

This Page Intentionally Left Blank

Chapter 1

SUMMARY

The objective of this project is to provide the capability to analyze the aerodynamic performance of the complete low pressure subsystem (LPS) of the Energy Efficient Engine (EEE). The analyses were performed using three-dimensional Navier-Stokes numerical models employing advanced clustered processor computing platforms. The analysis evaluates the impact of steady aerodynamic interaction effects between the components of the LPS at design and off-design operating conditions. Mechanical coupling is provided by adjusting the rotational speed of common shaft-mounted components until a power balance is achieved. The Navier-Stokes modeling of the complete low pressure subsystem provides critical knowledge of component aero/mechanical interactions that previously were unknown to the designer until after hardware testing.

(This page intentionally left blank)

Chapter 2

INTRODUCTION

2.1 Description of Engine Balance Design Problem

Competitive market conditions in the gas turbine industry have placed stringent demands on engine manufacturers to respond to customer requirements with efficient, cost effective products with significant reductions in development time. During the engine development period, component efficiencies often fall short of desired goals by significant margins. The engine cycle rebalance which results causes other components to operate at non-optimal (off-design) flow conditions, further reducing efficiency and complicating the identification of the original source of inefficiency. Expensive, multiple build rig testing, representing a major portion of the overall development cost, has, in the past, been required to balance component performance and optimize the engine system design.

2.2 NASA Programs Addressing Advanced Engine Design

Efforts to attack the problems associated with aircraft gas turbine engine development have been addressed through several NASA Programs. The Advanced Subsonic Technology (AST) program specifically supports technology development to improve the performance of subsonic aircraft, both in flight characteristics and propulsion. The High Performance Computing and Communication (HPCC) Program and more specifically, the Computational Aerosciences (CAS) Project are directed to accelerate the availability of high performance computing technology for use by the U.S. aerospace community. Finally, the Numerical Propulsion System Simulation (NPSS) project represents an interdisciplinary program to unite the various disciplines used in gas turbine engine design. A primary goal of the NPSS program is to numerically solve the entire flow through a realistic gas turbine engine using high fidelity computational tools. Additional details of these programs and their relation to the present work is given in the sections below.

2.2.1 NASA High Performance Computing and Communications (HCCP) Program [1]

NASA is a key participant in the Federal High Performance Computing and Communications (HPCC) Program. As a key participant of the Federal Program, the primary purpose of NASA's HPCC Program is to extend U.S. technological leadership in high-performance computing and communications for the benefit of NASA stakeholders: the U.S. aeronautics, earth and space sciences, and spaceborne research communities. As international competition intensifies and as scientists push back the frontiers of knowledge, leading-edge computational science is more important than ever.

The NASA Program is structured to contribute to broad Federal efforts while addressing agency-specific computational problems called Grand Challenges. NASA provides resources to develop tools to solve Grand Challenges in four HPCC project areas: Computational Aerosciences (CAS), Earth and Space Sciences, Remote Exploration and Experimentation, and Information Infrstructure Technology and Applications. The NASA Research and Education Network (NREN) also supports the four projects.

2.2.2 The Computational Aerosciences (CAS) Project [2]

CAS is a computer science-related program oriented around the needs of the aeroscience community. The CAS project [2] directly supports other NASA aeronautics programs and is driven by the needs of the aeronautics industry. The CAS goal is to:

"Accelerate development and availability of high-performance computing technology of use to the U.S. aerospace community, to facilitate adoption and use of this technology by the U.S. aerospace industry, and to hasten emergence of a viable commercial market for hardware and software vendors to exploit this lead."

The science and engineering requirements inherent in the NASA Grand Challenge applications like aeronautics require orders of magnitude improvement in high-performance computing and networking capabilities over the capabilities that existed at the beginning of the NASA HPCC Program in FY1992. Without an accelerated development program, this level of improvement may not be available for many years.

CAS has traditionally been oriented around the longer term thrust of the exploration of future high-end supercomputing for aerospace needs - extreme high-performance computing (TeraFLOPS). As a result of increased interactions with industry, CAS has added research efforts in a new direction - the use of networked workstations in the design environment. Networked workstations is a shorter term thrust oriented around the effective use of current generation computing hardware to reduce costs.

The goals of the Grand Challenges in Computational Aerosciences are to:

1 Provide focus for the entire HPCC Program by providing requirements for Testbeds and Networks and Systems Software

2 Assure relevance of HPCC Program to the U.S. aerospace community by providing base computational technology for multi-disciplinary analysis and design of aerospace vehicles and propulsion systems on HPCCP platforms, demonstrating superiority of HPCCP systems for solution of relevant aerospace problems, assisting U.S. aerospace industry in implementing HPCCP technologies within their organizations and realizing real improvement in their design cycle process and final products.

The goal of the Computing Testbeds of the CAS Project is to support the accelerated development of cost-effective, high performance computing machinery from domestic vendors in order to benefit the aerospace industry through the:

1. Creation of "beta-test" prototype computing facilities scalable to TeraFLOPS, and through the evaluation of the functionality and robustness of associated system software.
2. Creation of prototype networked workstation clusters, that are representative of existing clusters in aerospace companies, in order to provide the environment to develop and test the software necessary to make clusters an alternative to the traditional supercomputer.

The goal of CAS System Software research is to identify, define, and provide the critical software and tools not available from others sources that will enable the effective utilization of networked, heterogeneous, high performance scalable computing environments.

2.2.3 The Numerical Propulsion System Simulator (NPSS) [3]

The Numerical Propulsion System Simulator (NPSS) [3] is an interdisciplinary project to unite the various disciplines used in gas turbine engine design. The project is coordinated by NASA Lewis and is designed to bring together different groups and codes in order to create a system to engineer advanced jet engine designs. NPSS can be represented by three main concepts: "zooming," " coupling," and "integration." *Zooming* enables the simulation of complete engine systems at a level of analysis required by the physics. *Coupling* refers to the joining of the various disciplines in a single analysis. *Integration* refers to the integration of the various engine component simulations.

2.3 Integration of NASA Program Objectives and the Engine Balance Design Problem

A jet engine can be characterized by a number of different components working together very efficiently within a range of demanding operating conditions. Several of these engine components are sensitive to interactions with neighboring components. For example: the efficiency of the compressor is very sensitive to steady inlet and outlet conditions, outlet pressure fluctuations can unstart a supersonic inlet and expel the

shock, substantially increasing drag and reducing engine performance. Consequently, during the design process it is important to consider not only isolated components but the engine as a system of components which influence each other.

Historically, the design process has started with a study of the complete proposed engine using performance maps and one-dimensional analysis. Then individual engine components are simulated and designed in detail by component design teams. Some engine components are designed by the airframe manufacturer. These results improve the performance maps and one-dimensional analysis, which helps address component interactions. These components are experimentally tested in isolation, progressively integrated, and adjusted to finalize the engine design.

Component design teams depend on numerical analysis techniques to achieve the best performance. Streamline curvature methods continue to be extensively used to analyze multistage turbomachinery. More recently, the trend has been to apply advanced 2-D and 3-D numerical techniques [4] to engine components to understand the details of their operation in isolation. These applications range from quasi-three-dimensional blade calculations which predict the behavior of a transonic blade to multistage compressor calculations which simulate the behavior of transonic compressors to simulation of nacelles and combustor chemistry. Multistage analyses for turbomachinery are also becoming increasingly more valuable [5], [6].

These advanced component analysis techniques do not systematically account for inter-component interactions. Multistage analyses may someday provide adequate representation of interaction effects between blade rows in an axial compressor, for example, but do not presently provide information related to inter-component interactions (HP/LP turbine systems, e.g.).

One goal of NPSS is to create a system which will allow these individual component codes to be coupled to create a full engine simulation system. This system will allow analysis at different levels of accuracy by coupling codes of all levels from 1-D models to full 3-D computational fluid dynamics codes. This system would then allow the design engineer to "zoom" between levels of detail, while still providing some indication of the overall system interaction effects.

2.4 NPSS and the Energy Efficient Engine (EEE)

Several examples of multistage turbomachinery aerodynamic performance prediction techniques [7], [5], [6] exist which demonstrate the viability of large scale simulation in the gas turbine engine design environment. Unfortunately, many of these models have only explored aerodynamic interaction effects for a specific subcomponent of an engine (HP compressor, or fan section in isolation, e.g.). Improvements in the power and availability of high speed processors, and a streamlining of the problems associated with large scale simulation data management has afforded the opportunity to perform large scale simulations of coupled subsystem components, and perhaps even an entire engine.

In 1976 NASA initiated the Aircraft Energy Efficiency (ACEE) Program to assist in the development of technology for more fuel-efficient aircraft for commercial airline

use. The Energy Efficient Engine (EEE) Project of the ACEE program was intended to lay the advanced technology foundation for a new generation of turbofan engines. This project, planned as a seven-year cooperative government-industry effort, was aimed at developing and demonstrating advanced component and systems technologies for engines that could be introduced into airline service by the late 1980's or early 1990's. In addition to fuel savings, these new engines offered the potential for being economically attractive to the airline users and environmentally acceptable.

The goals of the EEE program were:

- 12% reduction in installed specific fuel consumption compared to a CF6-50C at maximum cruise thrust, M=0.8 at 35,000 ft ISA
- Comply with FAR 36 (1978) with provisions for growth
- Comply with EPA Proposed (1981) Standards for new engines
- 50% reduction in the rate of performance deterioration in-service as compared to the CF6-50C

The EEE Program consisted of four major technical tasks structured as follows:

1 Propulsion System Analysis, Design, and Integration (Establish the component design and performance requirements for future tasks).
2 Component Analysis, Design, and Integration (Design, fabrication, test, and post-test analysis of the components and supporting technologies).
3 Core Test (Design, fabrication, test, and post-test analysis of the core test vehicle (HP compressor, combustor, and HP turbine).
4 Integrated Core/Low Spool (ICLS) Test (Design, fabrication, test, and post-test analysis of the ICLS turbofan ground test vehicle).

The data obtained during these tasks yielded insight into the evaluation of core components operating in isolation and in the engine environment, and also permitted accurate measurements of important internal conditions which would be impractical in a complete turbofan engine.

The EEE provides a natural vehicle for the type of large scale simulation planned for this study due to the availability of both subcomponent test rig data, as well as fully coupled, assembled engine test data.

2.5 Objectives of the Present Study

This project represents a consolidation of industry goals, NASA vision, and the growing maturity of computational tools for predicting gas turbine engine flow physics. The overall objective of this project is to provide the capability to analyze the aerodynamics in the complete low pressure subsystem (LPS) of the Energy Efficient Engine (EEE) using three-dimensional Navier-Stokes numerical models. The analysis evaluates the impact of steady aerodynamic interaction effects between the components of the LPS at the design and at off-design operating conditions. The LPS modeling

capability will be integrated into the NPSS and be available as an option to the designer. The long range goal of the LPS modeling project, and NPSS, is to provide a tool that can significantly reduce the design, development, and certification time of gas turbine engines.

The approach for creating the LPS model is to select a validated Navier-Stokes (N-S) analysis code for accuracy and to minimize turnaround time. The EEE LPS model was developed from the geometric components in the LPS including: external flow, nacelle, inlet, fan blades, bifurcated bypass and core inlet, bypass vanes, core inlet guide vanes, quarter height booster stage, low pressure turbine blades, mixer, and exhaust nozzle. Initially, the engine core components were modeled using appropriate boundary conditions. At a later stage in the program, an engine cycle performance deck was used to set the core operating conditions for the analysis. The complete LPS analysis was constructed following a verification of the performance of the individual subcomponents in the LPS. The N-S analysis of the fully coupled LPS enabled a torque balance on the low pressure spool at quasi-steady state operating conditions.

This study was divided into five major milestone areas:

1 **Geometry Definition:** Detailed geometry definitions of the components of the Energy Efficient Engine primary gas flowpaths were assembled.
2 **Mesh Generation:** Geometry definitions described above were employed to develop discrete mesh systems suitable for CFD analysis.
3 **Component validation study:** Block components of the LP and HP subsystems were analyzed using CFD tools to verify the accuracy of the geometry definitions, and to validate the CFD analysis with available rig test data.
4 **LP Subsystem Analysis:** Various components were assembled to form the discrete representation of the LP Subsystem, and a quasi-steady CFD analysis was applied to predict both the aerodynamic and mechanical coupling of the LP Subsystem.
5 **Core Cycle Specification:** An engine cycle performance model was coupled with the 3-D CFD analysis to represent the operating parameters for the engine core in the LP Subsystem Analysis.

Each of the five milestone topics are described in more detail in the chapters which follow. The ultimate objective of this study was to develop a simulation capability for the LP Subsystem of modern high bypass ratio turbofan engines which would address the goals of the NASA NPSS program.

Chapter 3

DESCRIPTION OF THE ENERGY EFFICIENT ENGINE

The Energy Efficient Engine (EEE) program [8]-[103] was developed to create fuel saving technologies for transport aircraft engines which would be introduced into service in the late 1980's and 1990's. The EEE development cycle included candidate engines from two manufacturers: Pratt & Whitney and General Electric. Both manufacturers designed and tested various components as part of the technology demonstrations necessary to validate the final engine designs. The General Electric design was selected for engine testing, and included separate tests of the core [92] and integrated core/low spool (ICLS) [99] configurations. In the course of this discussion, reference will also be made to the *flight propulsion system* (FPS), which is essentially the integrated core/low spool with a flight-ready nacelle and inlet, rather than the bellmouth arrangement used in the static propulsion tests.

An illustration of the General Electric EEE flight propulsion system layout and some of the design features is given in Figure 3.1. A table of cycle characteristics for the EEE FPS are given in Table 3.1. Based on corrections to test data, the flight propulsion system was projected to have a thrust specific fuel consumption of 0.551 lbm/hr/lbf at the maximum cruise design point (35,000 ft. ISA). The ICLS achieved a static corrected take-off thrust of 37,415 lbf.

An illustration of the major subcomponent arrangement for the EEE Low Pressure spool is given in Figure 3.2. The elimination of the high pressure spool from the proposed analysis is illustrated in the sample numerical mesh system depicted in this figure. The analysis of the LP spool entails considerable detail in managing both aerodynamic and mechanical performance of the fan section, LP turbine, exhaust mixer, and inlet/nozzle/external flowfields. Detailed presentations of design expectation, test measurement, and CFD prediction of the individual component performance data are presented in the following chapters. Coupled analysis of the HP/LP spool systems are presented in the final chapters dealing with the LP subsystem analysis. Numerous sources of information related to the EEE program are provided in the reference section of this report.

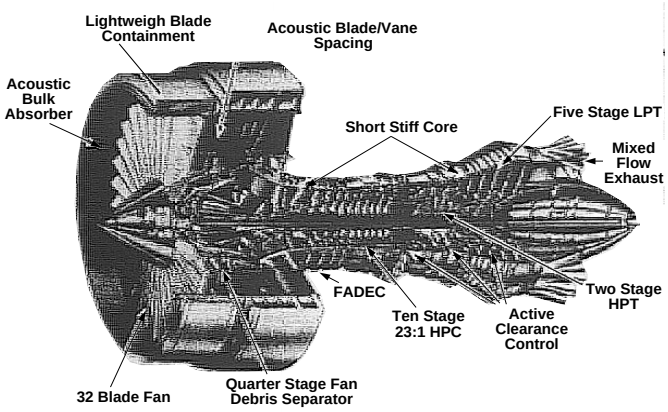

Figure 3.1: Energy Efficient Engine layout and design features.

Cycle Pressure Ratio at Max Climb[1]	**38**
Bypass Ratio at Max Climb[1]	**6.8**
Fan Pressure Ratio at Max Climb[1]	**1.65**
Turbine Rotor Inlet Temperature at Static Warm Day[2] Take−off Power	**2450 F**
Specific Fuel Consumption at Max Cruise[3], Bare Engine	**0.542 lbm/(lbf−hr)**
Specific Fuel Consumption at Max Cruise[3], Installed Engine	**0.564 lbm/(lbf−hr)**

1 Max Climb is the aerodynamic design point, M=0.8, 35,000 ft., standard day +18 F.

2 Sea level static warm day refers to a standard 59 F.

3 Max cruise is the performance evaluation design point, M=0.8, 35,000 ft., standard day.

Table 3.1: Energy Efficient Engine Flight Propulsion System cycle characteristics.

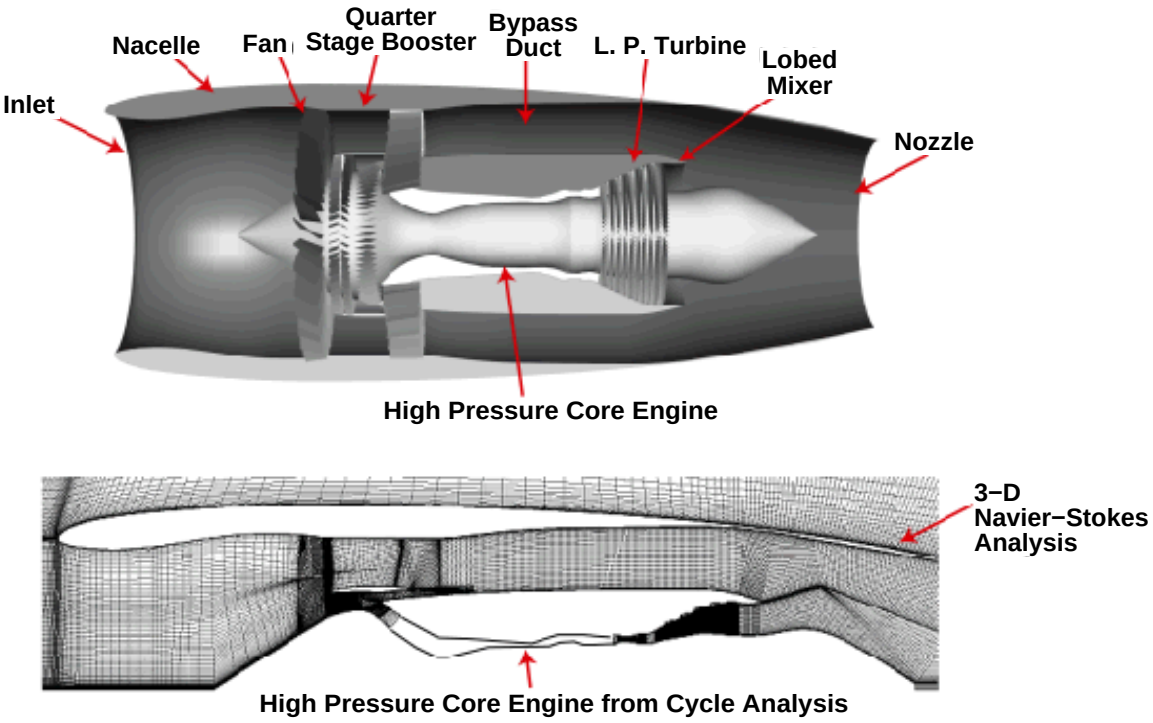

Figure 3.2: Energy Efficient Engine component description and CFD mesh representation.

(This page intentionally left blank)

Chapter 4

GEOMETRY MODELING

Detailed geometry for the EEE model was extracted from the NASA Energy Efficient Engine Master Geometry Database. This database was developed specifically for NPSS-related applications which employ the EEE design for demonstration. The database consists of NASA IGES curve-based and surface-based entities describing the major components of the engine core and bypass gas flowpaths. Exact geometric definitions of the EEE LPS are employed, with the exception of the outer nacelle and inlet, which have been designed consistent with the Energy Efficient Engine design philosophy in order to take the place of the test rig bellmouth. A picture of the Energy Efficient Engine test rig hardware is given in Figure 4.1.

The geometry database consists of individual elements (separate blade rows, for example) as well as "assembled" systems, which consist of more complete coupled collections of components. Familiarization with the geometry database package was facilitated by using the PATRAN [104] geometry modeling software package. A PATRAN representation of the EEE hardware geometry is given in Figure 4.2.

Certain enhancements to the database will almost certainly be required for this type of geometry definition to be useful during the engine design process. The ability to reset blade stagger angle, for example, is a common operation in gas turbine engine design and test, but is still an overly complex operation with the current database. The EEE HP compressor employs variable geometry on several stators, for example, and rig test results were obtained with various stator settings which are difficult to reproduce in the current database arrangement. The blade restagger capability will require definition of the rotation axis in the database, and specific built-in stator reset schedules could be imported as "off-design" geometry definitions.

The current database does not contain any indication of rotor tip clearances, and this was essentially approximated from experience during most of the course of this study. The database should include at least a reasonable approximation of rotor tip clearances (and other important clearance dimensions as additional geometry components are incorporated into the database).

The flow in the primary gas flowpath of a modern turbine engines is complicated by the various networks of secondary flow systems for cooling, bleed, etc. Compressor flowpaths are affected by leakage flows through inner-banded stator seals, while turbine flows are complicated by the stepped, overlapped hub flowpath and inner

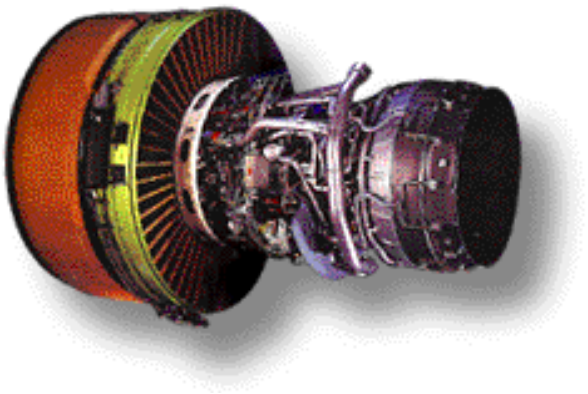

Figure 4.1: Energy Efficient Engine test rig hardware.

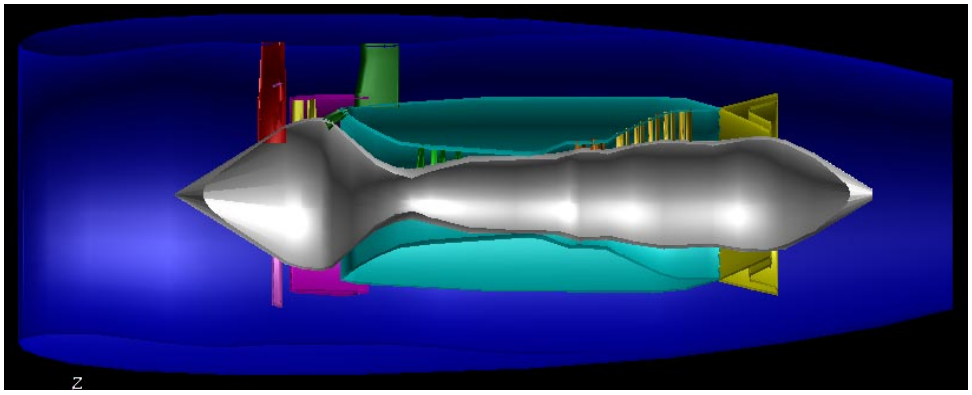

Figure 4.2: PATRAN representation of the Energy Efficient Engine Master Engine Geometry Database.

wheel purge flow. The contributions of these secondary flows in the engine play an important role in determining the overall performance of the machine. During the course of this study, the database flowpath representations were smooth walls with no representations of secondary system leakage flows. As experience is gained with large scale system aerodynamic analyses, and the analyses become more sophisticated, the influences of these systems must be included to accurately model the overall engine flow performance.

Finally, consideration must be given to the overall operational life of the engine and the potential for performance degradation through component erosion and wear. Over time, clearances become larger, blade leading edges can become warped due to foreign object damage, and erosion, in general, alters the blade surface quality and even the blade profile. If the database is to be useful for the overall engine life performance analysis, then these effects must necessarily be incorporated in some manner.

A UNIX *tar* archive listing of the geometric components included in the Master Engine Geometry Database for this study is included below for reference:

```
Engine Assembly Components:

rwxr-xr-x 2788/100  May 22 08:05 1996 assembly/
rw-r--r-- 2788/100  May 10 13:30 1996 assembly/eee_eng_3d_symall.nigs
rw-r--r-- 2788/100  May 10 13:24 1996 assembly/eee_eng_3d_symflow.nigs
rw-r--r-- 2788/100  May 10 13:40 1996 assembly/eee_eng_3d_unsymall.nigs
rw-r--r-- 2788/100  May 10 13:26 1996 assembly/eee_eng_3d_unsymflow.nigs

HP Compressor Components:

rwxr-xr-x 2788/100  May 22 08:06 1996 comp_schmidt/
rw-r--r-- 2788/100  May 20 13:04 1996 comp_schmidt/cmpr_igv_srf.nigs
rw-r--r-- 2788/100  May 20 13:04 1996 comp_schmidt/cmpr_rotor10_srf.nigs
rw-r--r-- 2788/100  May 20 13:04 1996 comp_schmidt/cmpr_rotor1_srf.nigs
rw-r--r-- 2788/100  May 20 13:04 1996 comp_schmidt/cmpr_rotor2_srf.nigs
rw-r--r-- 2788/100  May 20 13:04 1996 comp_schmidt/cmpr_rotor3_srf.nigs
rw-r--r-- 2788/100  May 20 13:04 1996 comp_schmidt/cmpr_rotor4_srf.nigs
rw-r--r-- 2788/100  May 20 13:04 1996 comp_schmidt/cmpr_rotor5_srf.nigs
rw-r--r-- 2788/100  May 20 13:04 1996 comp_schmidt/cmpr_rotor6_srf.nigs
rw-r--r-- 2788/100  May 20 13:05 1996 comp_schmidt/cmpr_rotor7_srf.nigs
rw-r--r-- 2788/100  May 20 13:05 1996 comp_schmidt/cmpr_rotor8_srf.nigs
rw-r--r-- 2788/100  May 20 13:05 1996 comp_schmidt/cmpr_rotor9_srf.nigs
rw-r--r-- 2788/100  May 20 13:05 1996 comp_schmidt/cmpr_stator10_srf.nigs
rw-r--r-- 2788/100  May 20 13:05 1996 comp_schmidt/cmpr_stator1_srf.nigs
rw-r--r-- 2788/100  May 20 13:05 1996 comp_schmidt/cmpr_stator2_srf.nigs
rw-r--r-- 2788/100  May 20 13:05 1996 comp_schmidt/cmpr_stator3_srf.nigs
```

```
rw-r--r-- 2788/100  May 20 13:05 1996 comp_schmidt/cmpr_stator4_srf.nigs
rw-r--r-- 2788/100  May 20 13:05 1996 comp_schmidt/cmpr_stator5_srf.nigs
rw-r--r-- 2788/100  May 20 13:05 1996 comp_schmidt/cmpr_stator6_srf.nigs
rw-r--r-- 2788/100  May 20 13:05 1996 comp_schmidt/cmpr_stator7_srf.nigs
rw-r--r-- 2788/100  May 20 13:05 1996 comp_schmidt/cmpr_stator8_srf.nigs
rw-r--r-- 2788/100  May 20 13:05 1996 comp_schmidt/cmpr_stator9_srf.nigs

HP Turbine Components:

rwxr-xr-x 2788/100  May 22 08:06 1996 hpt/
rw-r--r-- 2788/100  May 10 08:48 1996 hpt/hpt_rotor1_srf.nigs
rw-r--r-- 2788/100  May 10 08:50 1996 hpt/hpt_rotor2_srf.nigs
rw-r--r-- 2788/100  May 10 08:50 1996 hpt/hpt_stator1_srf.nigs
rw-r--r-- 2788/100  May 10 08:51 1996 hpt/hpt_stator2_srf.nigs

LP Turbine Components:

rwxr-xr-x 2788/100  May 22 08:06 1996 lpt/
rw-r--r-- 2788/100  May 10 09:04 1996 lpt/lpt_rotor1_srf.nigs
rw-r--r-- 2788/100  May 10 09:04 1996 lpt/lpt_rotor2_srf.nigs
rw-r--r-- 2788/100  May 10 09:04 1996 lpt/lpt_rotor3_srf.nigs
rw-r--r-- 2788/100  May 10 09:04 1996 lpt/lpt_rotor4_srf.nigs
rw-r--r-- 2788/100  May 10 09:04 1996 lpt/lpt_rotor5_srf.nigs
rw-r--r-- 2788/100  May 10 09:04 1996 lpt/lpt_stator1_srf.nigs
rw-r--r-- 2788/100  May 10 09:05 1996 lpt/lpt_stator2_srf.nigs
rw-r--r-- 2788/100  May 10 09:05 1996 lpt/lpt_stator3_srf.nigs
rw-r--r-- 2788/100  May 10 09:05 1996 lpt/lpt_stator4_srf.nigs
rw-r--r-- 2788/100  May 10 09:05 1996 lpt/lpt_stator5_srf.nigs

Fan + Quarter Height Booster Components:

rwxr-xr-x 2788/100  May 22 08:07 1996 qtr_stage/
rw-r--r-- 2788/100  May 14 10:01 1996 qtr_stage/booster_rotor_srf.nigs
rw-r--r-- 2788/100  May 14 10:01 1996 qtr_stage/booster_stator_srf.nigs
rw-r--r-- 2788/100  May 14 10:02 1996 qtr_stage/bypass_stator_srf.nigs
rw-r--r-- 2788/100  May 14 10:02 1996 qtr_stage/core_guide_vane_srf.nigs
rw-r--r-- 2788/100  May 14 10:02 1996 qtr_stage/fan_srf.nigs

Lobed Exhaust Mixer Components:

mixernew.igs
```

Chapter 5

COMPONENT MESH GENERATION

The development of the EEE/LPS CFD analysis requires numerical discretization of the Master Engine Geometry Database geometry definitions described in the previous chapter. The nature of this discretization is defined by the requirements of the *ADPAC* CFD flow solver, which is described in more detail in the following chapter. Numerous meshing strategies are possible with the *ADPAC* code, the simplest of which is simply to use a single sheared H-type mesh for each blade row (see e.g. [5]). This meshing strategy also has the direct benefit that the resulting mesh could also be used for other NPSS-related multistage turbomachinery flow analyses such as *APNASA*.

A key element of the meshing strategy in this project was to employ the Master Engine Geometry Database IGES entities directly in the grid generation process. Many mesh generation codes require discretized point data as input to define the geometry of interest. This discretized definition, and the subsequent interpolations which occur during the mesh generation process can lead to errors in the coordinates of the final mesh. One focus of the NPSS geometry definition has been to employ analytical definitions of geometric components in the form of IGES or NURBS-based entities. These analytical definitions would then form a consistent geometric database for all applications (aerodynamic, stress, heat transfer, etc.) and significantly reduce errors due to interpolations and interpretations of discrete point data. In order to address the mesh objectives described above, a procedure to generate meshes for the EEE LPS analysis directly from the NASA Energy Efficient Engine Master Engine Geometry Database was developed and is described in the paragraphs below.

Detailed geometry for the EEE engine was extracted from the NASA Energy Efficient Engine Master Geometry Database. This database was developed specifically for NPSS-related applications which employ the EEE design for demonstration. The database consists of NASA IGES curve-based and surface-based entities describing the major components of the primary gas flowpath. Exact geometric definitions of the EEE LPS are employed, with the exception of the outer nacelle and inlet, which have been designed with the Energy Efficient Engine design philosophy in order to take the place of the test rig bellmouth.

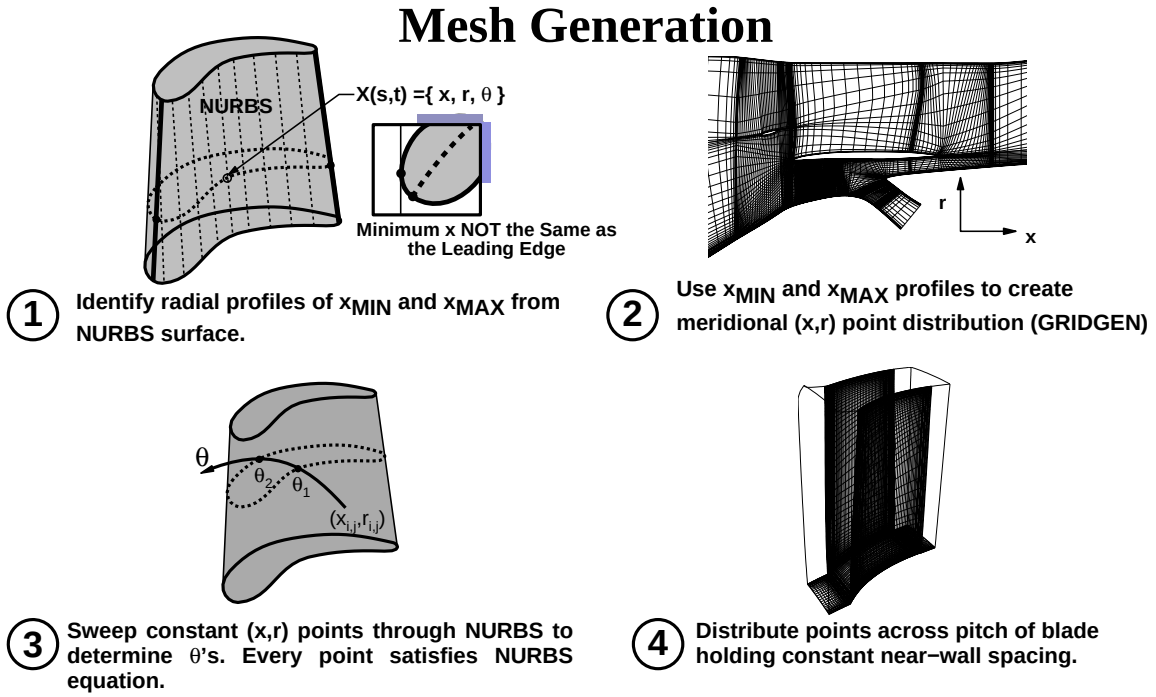

Figure 5.1: Component mesh generation procedure for EEE LPS analysis.

The construction of the numerical mesh system for each individual component is performed in a manner which permits a simple coupling of the component meshes for the complete LPS analysis. H-type computational meshes are employed for this purpose, although the analysis need not be limited in this fashion. A primary focus of the NPSS research is to employ a consistent geometry definition during all phases of the engine analysis. As such, a mesh generation strategy was developed whose only direct geometric input is the NASA-IGES based geometry of the Master Engine Geometry Database. A graphical illustration of the mechanics of the mesh generation procedure is given in Figure 5.1.

The procedure is initiated by defining the exact geometric axial extents of the blade elements in the axisymmetric projection of the flowpath. This procedure was accomplished by interrogating the geometric elements for each individual blade row, and extracting the geometric leading and trailing edge outlines (in this sense, the geometric leading and trailing edges are represented by the minimum and maximum axial coordinate locations, respectively). In essence, the radial profiles of the blade minimum and maximum axial coordinates were extracted from the blade IGES surface definition. These new entities are themselves represented in *GRIDGEN* database segment format and are added to the geometry database. The *SEARCH* program was developed for this purpose. Source code for the *SEARCH* program is listed in

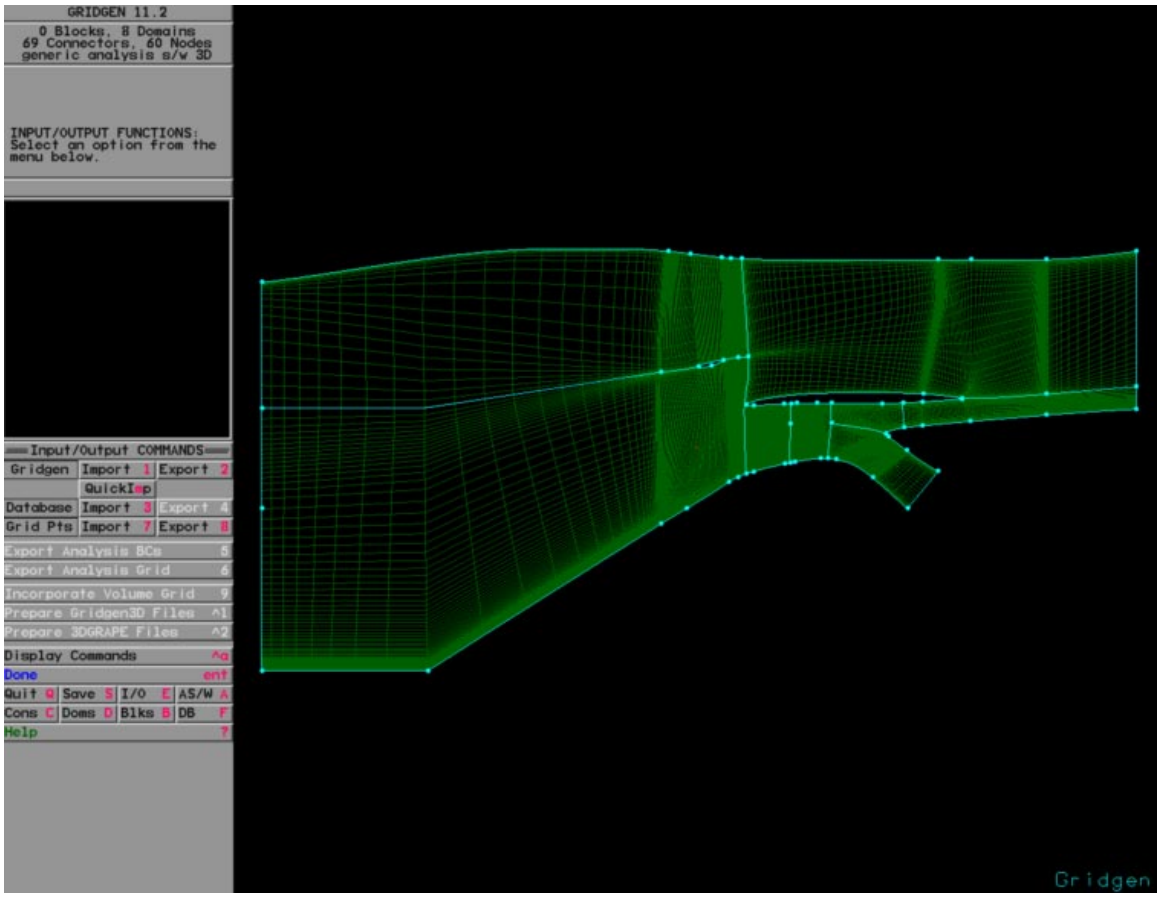

Figure 5.2: Illustration of the *GRIDGEN* user interface display for the meridional projection of the EEE fan section mesh system.

the Appendix for this report.

Once the blade row extents are defined, standard NASA-IGES capable mesh generation schemes (GRIDGEN [1] was used for this exercise) can be employed to define the meridional projection of the H-type meshes. A snapshot of the gridgen user interface screen for the EEE fan section is illustrated in Figure 5.2. The blade leading and trailing edge elements define the positions of the blade rows in the axisymmetric projection, while the Master Engine Geometry Database flowpath definitions define the endwalls. The *GRIDGEN* program (which can read in the IGES entities as a geometry database) is then used to define the axial (x) and radial (r) point distributions in the meridional projection. Typical mesh dimensions for the axisymmetric components of the meshes employed 49 points radially along the blade span, and 65 points axially along the chord of the blade.

Next, the (x, r) coordinate pairs from the meridional mesh projection are swept through the airfoil IGES surface definition to determine the blade surface circumferential (θ) point distributions. The remaining points in the circumferential direc-

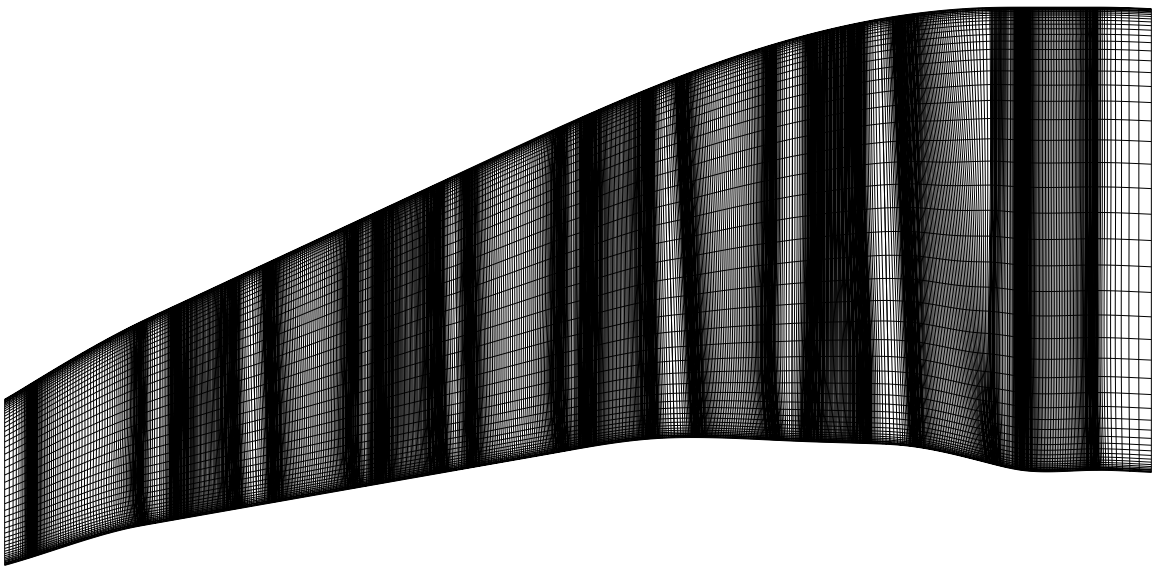

Figure 5.3: Axisymetric mesh projection for the EEE LP turbine.

tion (between airfoils) are defined using a simple hyperbolic distribution routine (see e.g. [105]). The circumferential distributions were constructed to maintain a fixed, specified near wall spacing in the circumferential direction (see Appendix for coding details).

A sample meridional mesh projection for the EEE LP turbine is given in Figure 5.3. The blade outlines are visible due to the mesh cluster near the leading and trailing edges. An illustration of the 3-D mesh system for the same turbine is given in Figure 5.4.

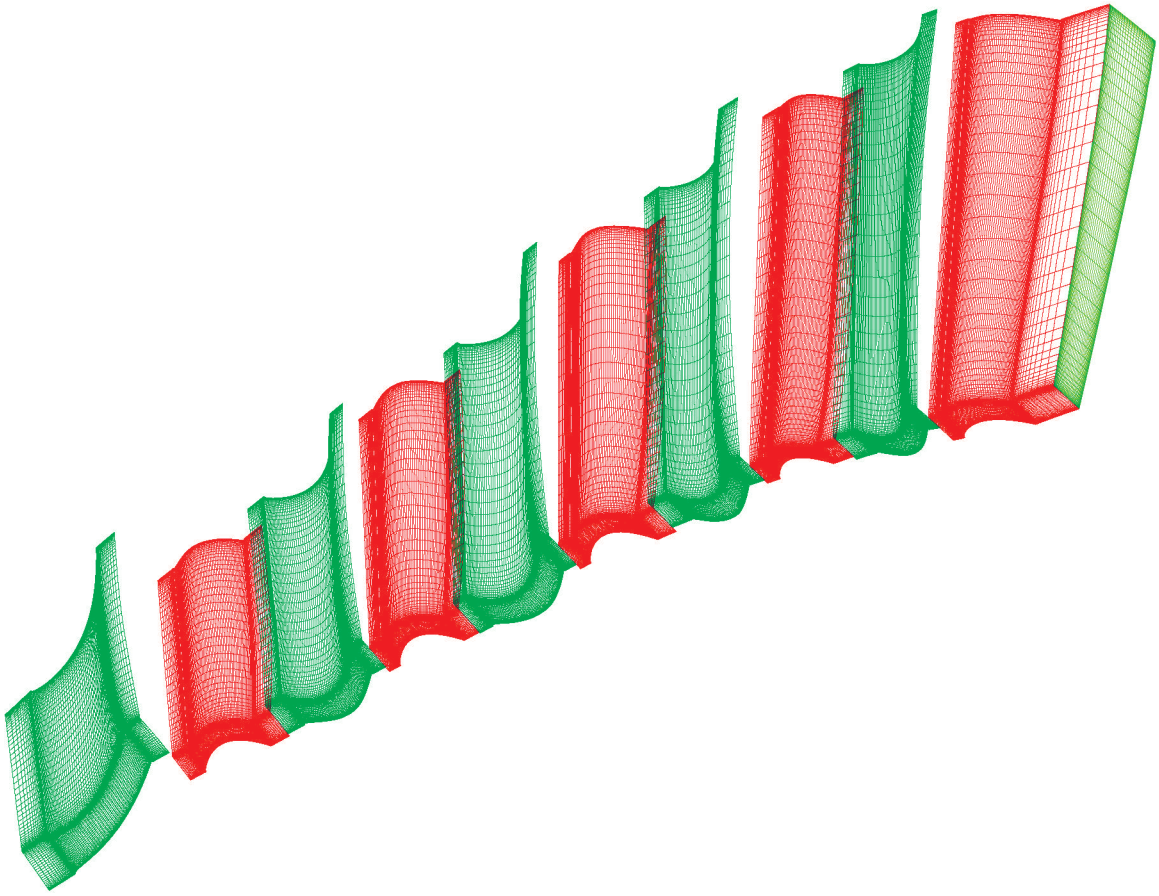

(This page intentionally left blank)

Chapter 6

ADPAC CODE DESCRIPTION

The aerodynamic predictions for the cases described in this study were obtained using the *ADPAC* analysis code. The *ADPAC* code is a general purpose aerospace propulsion aerodynamic analysis tool which has undergone extensive development, testing, and verification [106]. Detailed code documentation is also available for the *ADPAC* program [107].
The *ADPAC* analysis solves a time-dependent form of the three-dimensional Reynolds-averaged Navier-Stokes equations using a proven time-marching numerical formulation. The numerical algorithm employs robust numerics based on a finite-volume, explicit Runge-Kutta time-marching solution algorithm derived from the developmental efforts of Jameson et al. [108], Adamczyk et al. [7], and Arnone et al. [109]. Steady-state flows are obtained as the time-independent limit of the time-marching procedure. Several steady-state convergence acceleration techniques (local time stepping, implicit residual smoothing, and multigrid) are available to improve the overall computational efficiency of the analysis. A pseudo-time iterative implicit algorithm is available to permit large time steps for time-accurate flow predictions (see e.g. Melson et al., [110]). A relatively standard implementation of the Baldwin and Lomax [111] turbulence model with wall functions was employed to compute the turbulent shear stresses and turbulent heat flux.

An attractive feature of the *ADPAC* code is the versatility and generality of mesh systems upon which the analysis may be performed. The *ADPAC* code permits the use of a multiple-blocked mesh discretization which provides extreme flexibility for analyzing complex geometries. The block gridding technique enables the coupling of complex, multiple-region domains with common (non-overlapping) grid interface boundaries through specialized user-specified boundary condition procedures. An illustration of the wide variety of problems which have been analyzed using the *ADPAC* code is given on Figure 6.1.

ADPAC supports coarse-grained computational parallelism via block boundary-specified message passing. Interprocessor communication is controlled by the Application Portable Parallel Library (APPL) [112] with optional programming layers using the Parallel Virtual Machine (PVM) [113] and Message Passing Interface (MPI) [114] communication protocols. Both serial and parallel computations were employed during this study utilizing a wide range of high speed processors, workstation clusters,

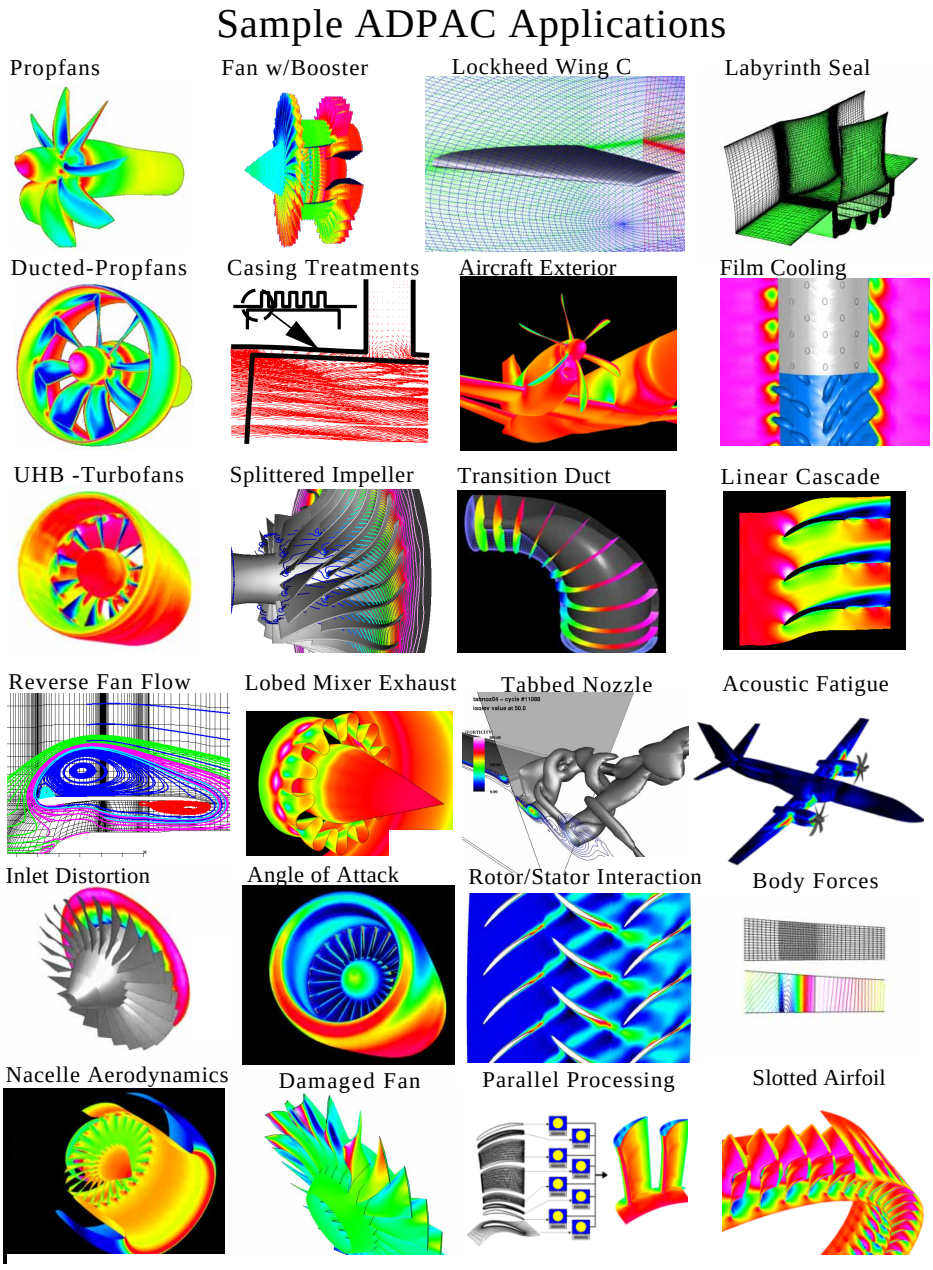

Figure 6.1: Summary of variety of problems which can be analyzed using the *ADPAC* code.

and massively parallel computing platforms, depending on availability.

Steady-state aerodynamic predictions for multistage turbomachinery are performed using a specialized boundary procedure known as a "mixing plane". The mixing plane strategy was developed to permit numerical simulations based on only a single blade passage representation for each blade row, regardless of the differences in circumferential spacing for each blade row. This simplification is afforded by circumferentially averaging data on either side of the interface between blade rows (the mixing plane), and then passing that information as a boundary condition to the neighboring blade row. This strategy is illustrated in Figure 6.2.

Several formulations for the mixing plane have been tested in the development of the *ADPAC* code, including varying the choice of variables to integrate and the use of "non-reflecting" boundary procedures (see e.g. Saxer [115]). A robust scheme results by simply averaging the conserved variables from the numerical scheme (ρ, ρu, ρv, ρw, and ρe) where ρ is density, u, v, w are the axial, radial, and circumferential velocity components, and e is the total internal energy. This scheme has the advantage of being numerically robust, conserves mass and momentum, and tends to preserve velocity triangle information across the interface plane more accurately than other approaches. A disadvantage of this scheme is that neither total pressure or total temperature are numerically conserved across the mixing surface. In practice, it was found that these conservation errors were detectable, but very small, and this scheme was therefore employed for the present set of calculations.

A graphic illustration of a mixing plane analysis for a multistage compressor is shown in Figure 6.3. The mixing planes are represented by the circumferential lines approximately midway between blade rows.

The solution procedure for the *ADPAC* analysis requires the definition of the numerical mesh, boundary conditions, and solution control input files. The meshing strategy for the EEE/LPS analysis was described in the previous chapter. The *ADPAC* boundary data file were created through a combination of hand construction, and data provide by the *PATCHFINDER ADPAC* tool program. The *PATCHFINDER* program interrogates the mesh system, and through a rigorous coordinate search routine determines where neighboring mesh blocks share coordinates and outputs the specific *ADPAC* boundary specifications to couple the neighboring block aerodynamic solutions. The *ADPAC* input file is essentially constructed by hand, and determines solution specific parameters such as reference pressure and temperature, number of iterations, etc.

The numerical solution proceeds with an initial flow specification from which the solution is advanced forward in time until the desired convergence criteria has been reached. The initial data is normally specified as a uniform flow, or may be read in as a "restart" of a previous existing solution. During the EEE/LPS simulations, the solution initialization procedure was complicated by the large range of pressures and temperatures encountered when doing large scale simulations of gas turbine engines. To ease the numerical problems with these wide variations in flow properties, the solution was initially started with very low pressure and temperature specifications in the boundary conditions, and was then iteratively restarted with subsequently larger values until the desired final conditions were achieved. The "full" multigrid

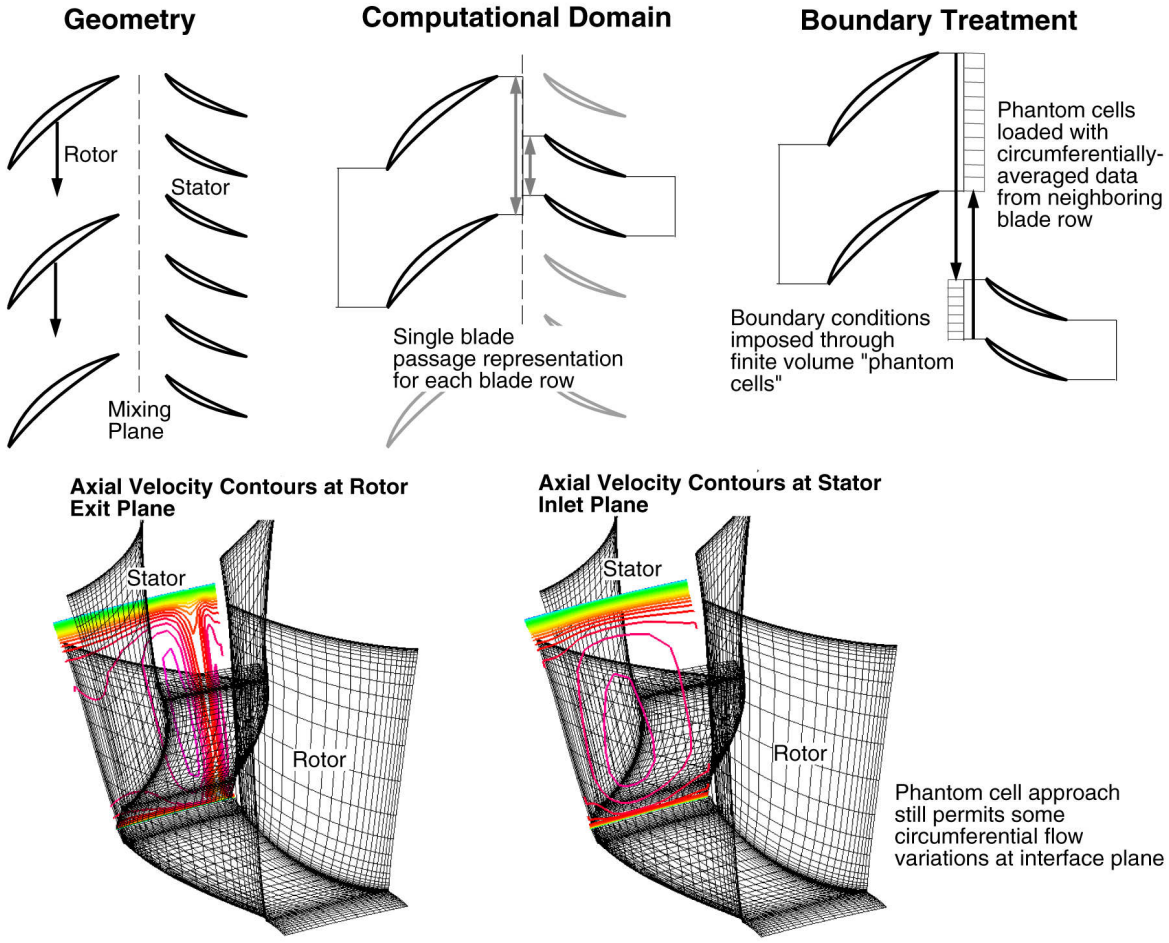

Figure 6.2: Illustration of *ADPAC* mixing plane boundary formulation for steady prediction of multistage turbomachinery flows.

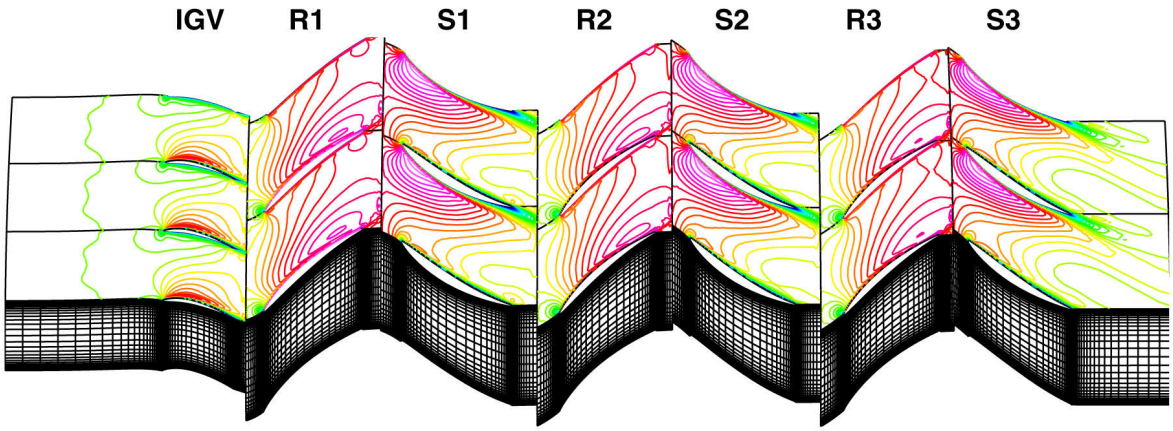

Figure 6.3: Illustration of mixing plane analysis (predicted Mach contours and mesh system) for a 3-1/2 stage compressor.

startup procedure was employed during this process such that this iterative startup procedure employs only the coarsest mesh system available.

Steady-state solutions were normally deemed converged when the average residual R was reduced by a factor of 10^{-3}, or when the residual has ceased to be reduced. Experience has shown that pressure-driven flow quantities generally converge first (e.g. mass flow, lift, etc.) while viscous driven flow quantities (loss) converge after a larger number of iterations. It is also therefiore necessary to monitor integrated performance parameters such as efficiency to determine when the solution is truly converged.

(This page intentionally left blank)

Chapter 7

PARALLEL COMPUTING

In order to address the goals of the HPCCP program described earlier, the EEE/LPS simulations were developed with the application of advanced parallel processing techniques as the computational foundation. Parallel processing computations using the ADPAC code are performed via a coarse-grained domain decomposition, and interprocessor message passing via either the Application Portable Parallel Processing (APPL) [112], Parallel Virtual Machine (PVM) [113], or Message Passing Interface (MPI) [114] message passing libraries. The LPS analysis was optimized for and performed on workstation cluster computing platforms using these parallel processing techniques. The NASA Ames Research Center *davinci* and *babbage* workstation clusters, and the NASA Lewis Research Center *LACE* workstation cluster were utilized for the analysis. The Allison Engine Company Silicon Graphics 16-processor Power Challenge XL server was also employed during this program. Details of each of these computing platforms are given in the sections which follow.

7.1 *davinci* Workstation Cluster

The *davinci* cluster consists of one front-end system and eight compute nodes. The front-end system (named *davinci*) is the host that users log into. The front-end is a Silicon Graphics Power Challenge L with four 75 MHZ R8000 CPUs and 384 MB memory, and serves as the system console, compile server, file server, user home server, PBS server, etc. There are eight compute nodes (four two-cpu nodes, and four eight-cpu shared-memory nodes) with the following configuration:

Machine	Cpu	Memory	Swap	/tmp	Use
davinci	4	384MB	1.2GB	1.2 GB	user home, fileserver
davinci-01	2	128MB	1.2GB	0.9 GB	compute node, console
davinci-02	2	128MB	1.2GB	0.9 GB	compute node
davinci-03	2	128MB	1.2GB	0.9 GB	compute node
davinci-04	2	128MB	1.2GB	0.9 GB	compute node
davinci-05	8	2GB	6GB	4 GB	compute node

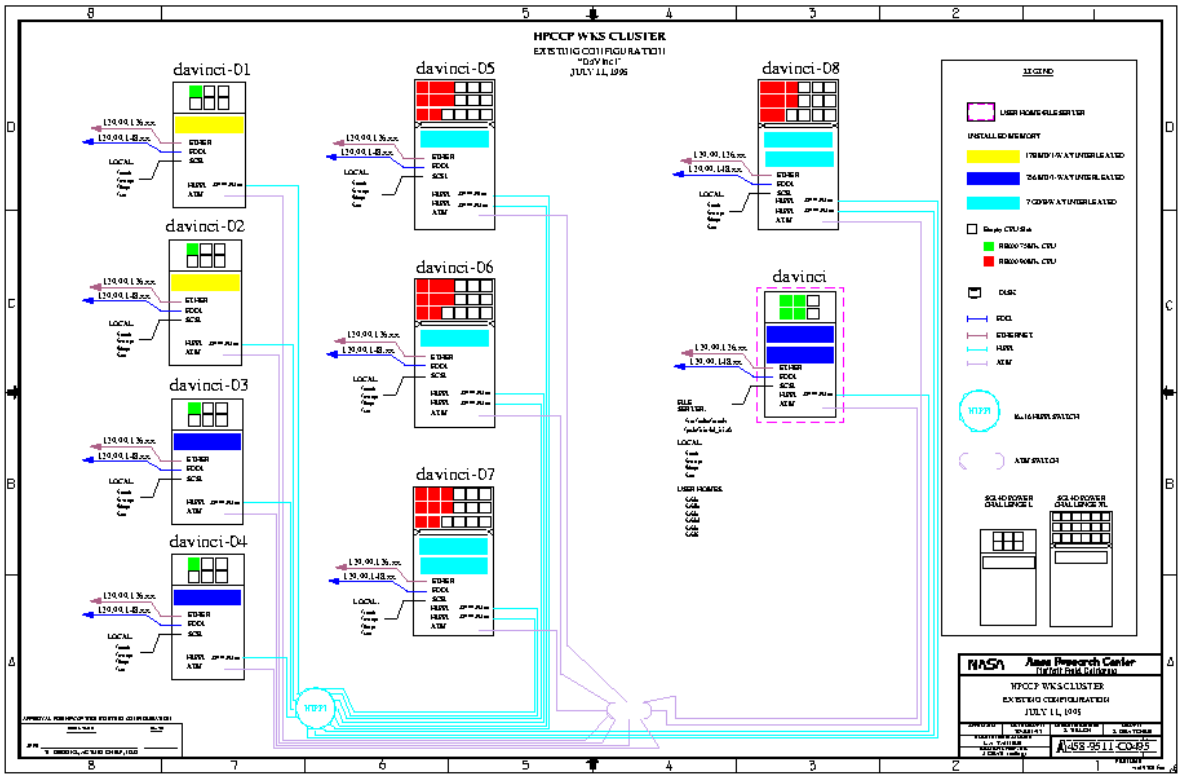

Figure 7.1: NASA Ames Research Center Silicon Graphics (*davinci*) workstation cluster schematic diagram (configuration circa 1995).

```
davinci-06    8    2GB     6GB    4 GB   compute node
davinci-07    8    4GB     6GB    4 GB   compute node
davinci-08    8    4GB     6GB    4 GB   compute node, console
```

All the machines were connected via Ethernet, FDDI, and HiPPI. ATM network adapters from both SGI and Fore Technology were also tested on this cluster. The eight compute nodes and the front-end were running the IRIX 6.2 operating system. PBS 1.1.8 was the job queuing system, and MPI 2.0 from SGI was the primary interprocessor communication library. A schematic illustration of the NASA-Ames Silicon Graphics (*davinci*) workstation cluster is given in Figure 7.1.

7.2 *babbage* Workstation Cluster

The NAS SP2 *babbage* workstation cluster is a 160-node MIMD parallel computer composed of IBM RS6000/590 workstations. On paper (and according to some benchmarks), the SP2 is capable of outperforming a 16-processor Cray C90. The NAS SP2 resulted from the HPCCPT-1 Cooperative Research Agreement (CRA) between NASA and a consortium led by IBM.

Each node has at least 128 Mbytes of main memory and 2 Gbytes of disk space.

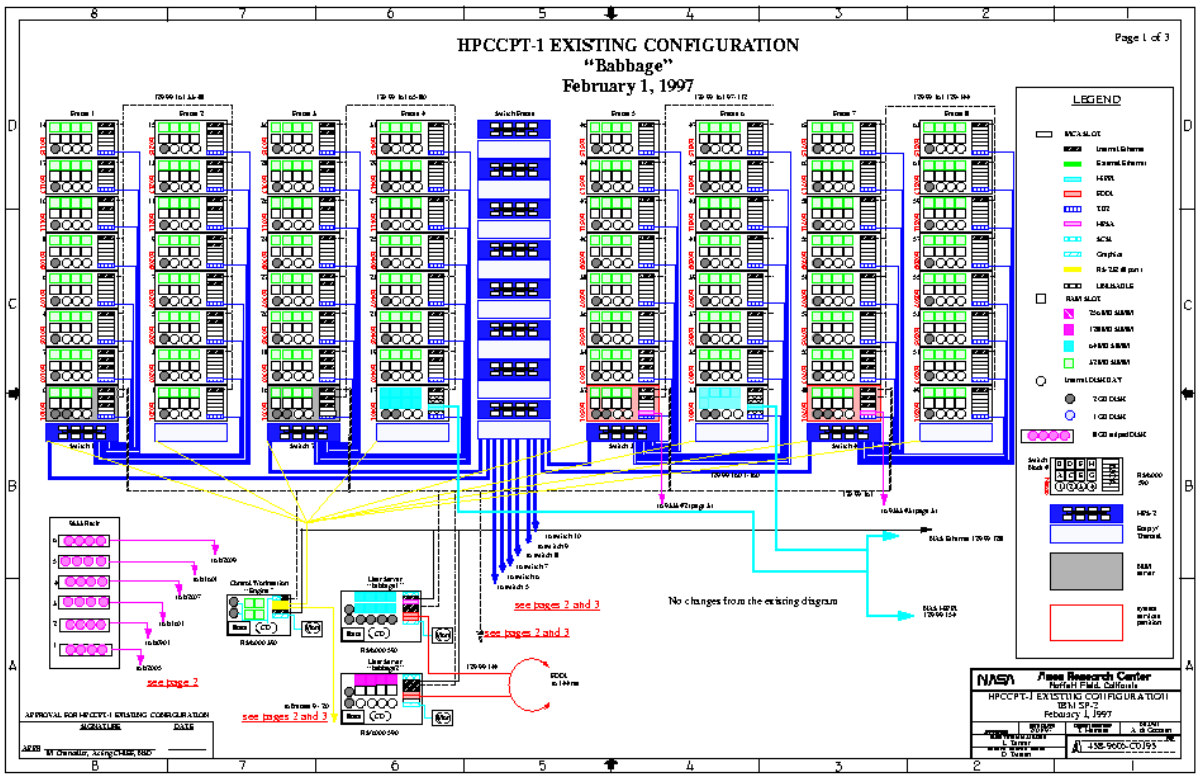

Figure 7.2: NASA Ames Research Center IBM RS-6000 (*babbage*) workstastion cluster schematic diagram (configuration circa 1995).

Some nodes have additional memory and disk space, as well as HiPPI or FDDI. The SP2 also has an external filesystem accessible by all nodes. The full 160-node SP2 has:

```
23.9 Gbytes of main memory
485 Gbytes of disk space
342 Gbytes/second main memory bandwidth
42.8 Gflops peak performance
```

An illustration of the NASA-Ames IBM SP2 (*babbage*) workstation cluster is given in Figure 7.2.

7.3 *LACE* Workstation Cluster

The NASA Lewis Research Center *LACE* cluster is a group of thirty-two networked IBM RS/6000 machines (*lace01-lace32*) plus one "control" node called *lace*. Job submission and queuing was moderated by the LSF (Load Sharing Facility) software.

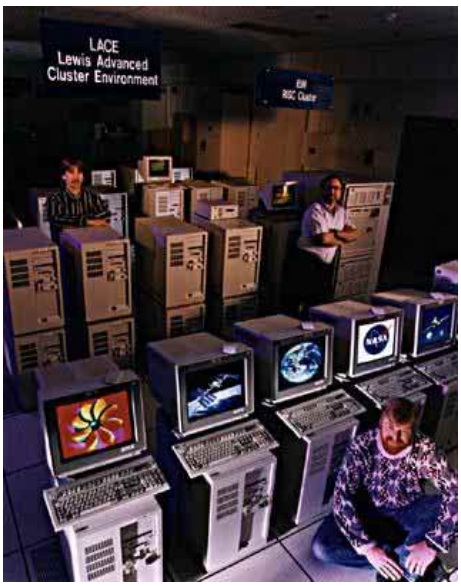

Figure 7.3: NASA Lewis Research Center IBM RS-6000 (*LACE*) workstastion cluster.

An image of the NASA-Lewis Research Center *LACE* IBM RS-6000 workstation cluster is given in Figure 7.3.

7.4 Allison Silicon Graphics Power Challenge XL

The Allison Engine Company Power Challenge XL workstation consists of a 16-processor shared-memory parallel computing platform. The machine consists of 16 R10000 CPU's with 2 gigabytes of main memory completely shared across all processors. The operating system during this study was IRIX 6.2, with job submission managed by the PBS software package Version 1.1.9b. A typical machine of this type is illustrated in Figure 7.4.

Figure 7.4: Allison Engine Company Silicon Graphics Power Challenge XL parallel computer.

(This page intentionally left blank)

Chapter 8

NEPP CODE DESCRIPTION

One facet of the analyses performed during this study was the desire to investigate aspects of the "zooming" feature of the planned NPSS engine performance analysis architecture. In this regard, the intention was to numerically couple detailed CFD simulations of the EEE LP spool with an engine cycle analysis of the EEE HP core. This coupled simulation, would, in fact, be a complete simulation of the two-spool EEE engine with varying levels of fidelity for the LP and HP subsystems. The *ADPAC* analysis described in the previous chapters was directed at the 3-D CFD portion of this simulation strategy, while the *NEPP* 1-D cycle analysis was directed at the HP spool simulation strategy. A brief description of the *NEPP* analysis code is given below.

The *NEPP* computer program [116]-[141] performs one-dimensional, steady-state thermodynamic performance analysis of aircraft gas turbine or jet engine configurations. Data inputs specify a standard set of components and their interconnections, allowing simulation of virtually any engine configuration. As many as six modes of engine operation may be configured to analyze multimode or variable cycle engines whose flowpaths and operating components vary over portions of the aircraft flight regimes. Physical components which may be used include propellers, inlets, ducts, combustors, fans, compressors, turbines, shafts, heat exchangers, flow splitters, subsonic mixers and/or supersonic ejectors, nozzles and water injectors or gas generators. Two options are available for gas thermodynamic properties. The default option uses built-in curve fits for mixtures of air and JP4, the standard hydrocarbon jet fuel. Alternatively, the Chemical Equilibrium Compositions (CEC) auxiliary program can model nearly any propellant combination or evaluate the effects of chemical dissociation of gases. The CEC option also permits simulation of rocket components and fuels in an engine configuration.

Although NEPP was originally intended to perform only thermodynamic analysis, additional capabilities have been implemented. Simplified aircraft installation effects give preliminary estimates of inlet and nozzle drag forces. A turbine cooling algorithm estimates the gas bleed flow required for high temperature engine operation. An approximation algorithm computes emissions of nitrogen oxides. Engine operation line data is accumulated for subsequent plotting on compressor and turbine performance maps (this feature presently requires software for plotting which varies

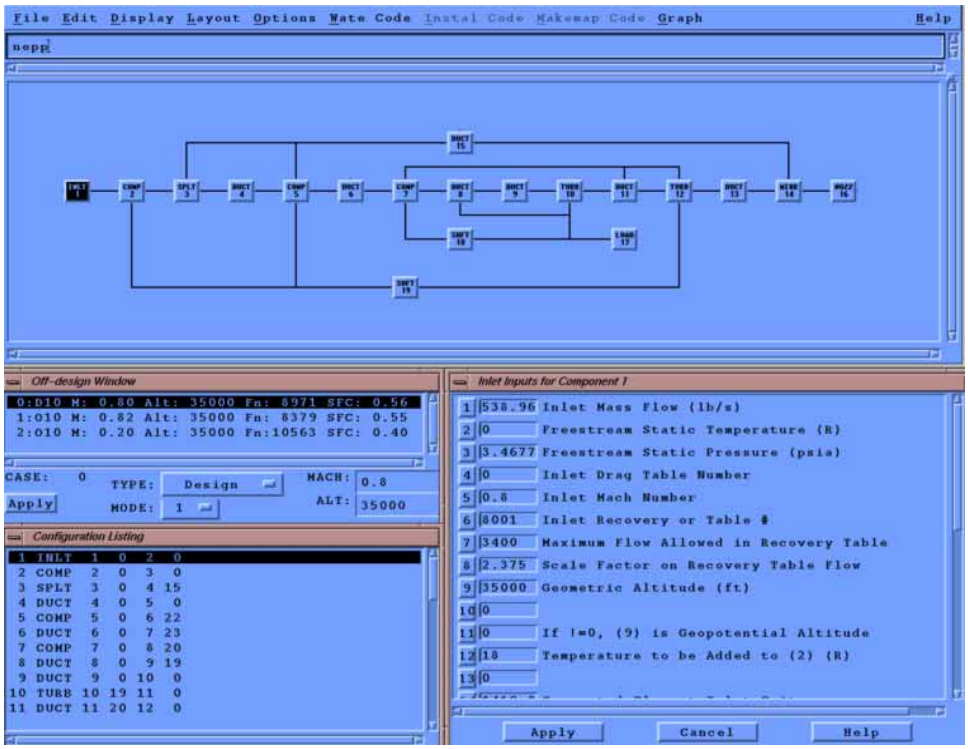

Figure 8.1: Screen illustration of NEPP analysis with NPAS user interface.

from installation to installation).

Two additional auxiliary programs further extend the capabilities of the NEPP system. WATE estimates engine component weights. INSTAL gives more accurate estimates of inlet and nozzle drag forces and inlet weights, provided design details are available.

There are several steps for putting together a NEPP input file to analyze an engine system.

- Select the engine cycle.
- Convert the cycle into a block diagram for NEPP.
- Define the compressor and turbine performance maps. Exact maps for the application are not required, the program can scale maps as required.

There exists a graphical user interface front-end for the *NEPP* code referred to as *NPAS* which simplifies the use of the code. An illustration of the *NPAS* user interface scheme for the analysis of the complete EEE engine is given on Figure 8.1. This complete engine model formed the basis for the reduced models described later in this report.

Chapter 9

Component Performance Validation

Component performance validation was considered a necessary milestone both in validating the accuracy of the analysis as well as verifying the accuracy of the geometry specifications in the EEE Master Engine Geometry Database. During this phase of the program, specific subcomponent geometries were selected and analyzed in isolation from the other major subcomponents of the overall EEE LPS analysis. The engine subcomponents analyzed during the component performance validation phase of the program were the fan/bypass/booster compressor, the LP turbine, and the lobed exhaust mixer. Design point validations were also performed for the core compressor and the HP turbine for completeness.

The component validation phase also served two additional purposes: the resulting simulations could be used as the initial conditions for the coupled EEE LPS analysis, and the results could also be used to evaluate, at least to some extent, the steady aerodynamic interaction effects resulting from subcomponent coupling in the EEE LPS analysis. Results from the component validation studies are summarized in the following sections.

9.1 EEE Fan Section Analysis

9.1.1 Description of Design

The EEE fan section design is based on a unique split flow configuration selected to minimize mission fuel burn and direct operating cost. An illustration of the EEE fan section flowpath and blade arrangement is given in Figure 9.1. The EEE fan section design employs a full span fan rotor with a design corrected tip speed of 1350 ft/s. and an inlet radius ratio of 0.342. The fan employs a part span shroud to improve structural rigidity. The fan rotor exit flow is split radially by an island splitter. The inner annulus of this island splitter is designed to capture 22% of the fan flow and employs a 1/4-height booster stage. The 1/4-height booster stage further supercharges the flow entering the core and enhances core protection from foreign

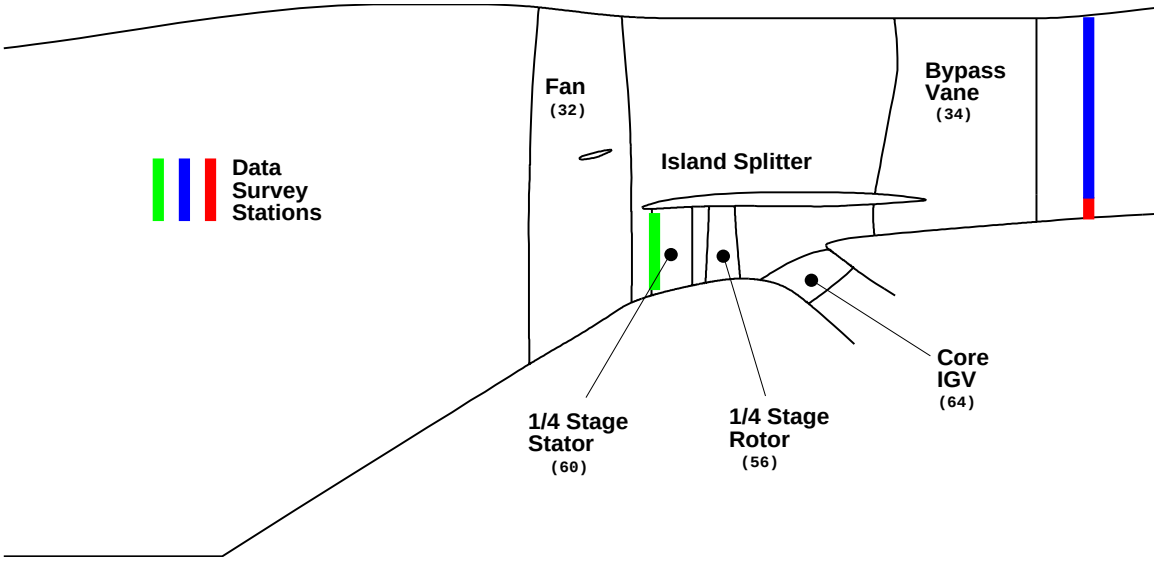

Figure 9.1: Axisymmetric projection of EEE fan+1/4-height booster stage configuration ilustrating test data instrumentation plane locations.

object damage. The use of the booster stage also permits a lower fan rotational speed, increased fan efficiency, lower fan hub aerodynamic loading, and provides for an easier engine growth path. The flow through the booster stage is subsequently split by the core inlet, with 68% of the booster flow entering the core and the remaining 42% of the booster flow reentering the bypass flowpath through the bypass vane. The outer annulus flow carries the remaining 78% of the fan rotor flow through the bypass vanes. A detailed listing of the EEE fan section design parameters is given in Table 9.1.

9.1.2 Mesh System

Three-dimensional Navier-Stokes computations were performed for the EEE fan section configuration using the *ADPAC* analysis code. The mesh generation procedure described in Chapter 4 was employed for this task. The analysis included the full height fan with part span shroud, 1/4-height booster stage, core inlet guide vane, and bypass vane as shown in Figure 9.1.

The mesh generation procedure previously described was employed to define a 1,605,000 cell mesh distributed among 8 mesh blocks. The mesh system for the fan section is somewhat more complicated than the other subcomponents (such as the LP turbine, for example) in that the mesh block structure is not a simple end-to-end stack of blade rows. The various radial divisions of the flow (by the part span shroud, island splitter and core splitter) all require block modeling, and must still be compatible with the mixing plane formulation and the H-type mesh structure developed for the individual blade rows. This complex mesh block structure is all

EEE Fan Section Aerodynamic Design Parameters
Engine Design Point: Max Climb (M=0.8, 35,000 ft ISA)

Inlet Radius Ratio	0.342
Fan Specific Flow	42.8 lbm/ft**2/s
Corrected Tip Speed	1350 ft./s.
Bypass Pressure Ratio	1.65
Core Pressure Ratio	1.67
Booster Mass Flow/ Fan Mass Flow	0.22
Core Mass Flow/ Booster Mass Flow	0.58
Bypass Ratio	6.8

Table 9.1: EEE fan section aerodynamic design parameters.

EEE Fan Section Component Performance Validation Mesh Block Size Tabulation

Block	I Index	J Index	K Index	# Pts
1	113	81	49	448497
2	113	21	49	116277
3	97	65	33	208065
4	97	65	33	208065
5	105	33	33	114345
6	29	33	33	31581
7	89	33	49	143913
8	137	37	49	248381

Table 9.2: Tabulated mesh block sizes for EEE fan section component performance validation analysis.

rather easily managed by the *GRIDGEN* mesh generation program, but does require some additional thought and planning by the user. The resulting mesh block sizes and general relationship to the fan section components is given in Table 9.2. An illustration of the axisymmetric projection of the mesh system is given in Figure 9.2.

9.1.3 Design Point Analysis

A design point analysis was performed for the EEE fan section using the mesh system described in the previous subsection. The EEE fan section design bypass ratio is 6.8, and the fan design point represents the engine maximum climb operating point. The analysis was performed on a 4-processor Silicon Graphics Power Challenge L multi-processor computer with 1 GB of main memory. A converged solution was obtained in a total of 6 hours (wall clock time) using all four processors. Figure 9.3 illustrates the predicted fan surface static pressure contours from the analysis. Numerical predictions for the EEE fan section were compared with experimental data derived from full scale rig tests of the fan section [74]. Figure 9.4 illustrates a comparison of predicted and experimental bypass vane exit and 1/4-stage vane leading edge spanwise total pressure distributions. The total pressure distributions are plotted and correlated with the colors of the data survey stations indicated on Figure 9.1. The character of the spanwise pressure distribution was very accurately captured, and was well within the range of test data.

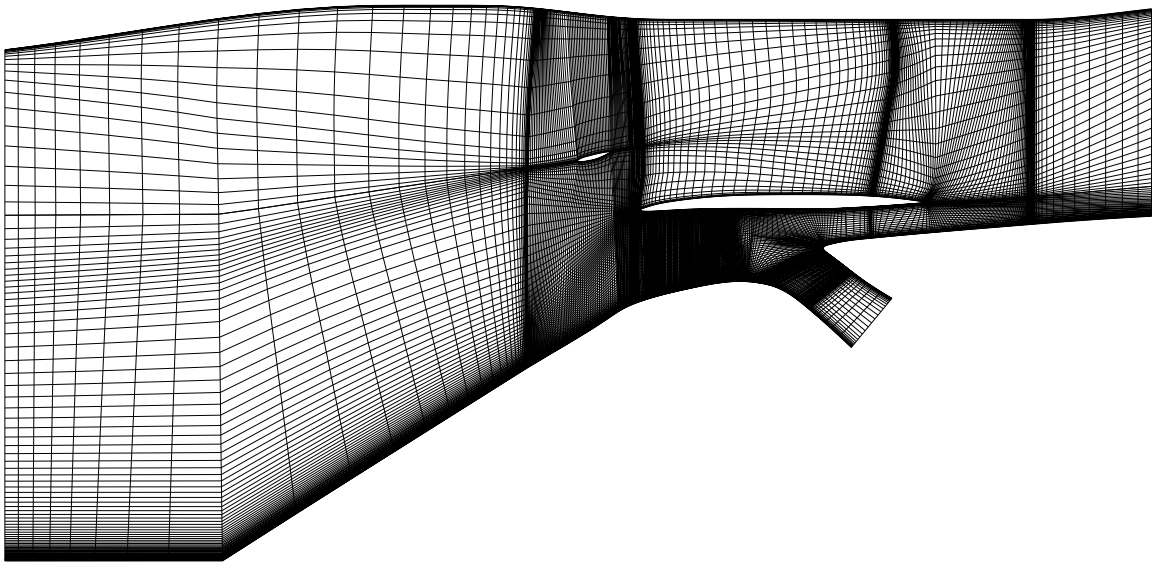

Figure 9.2: Axisymmetric projection of EEE fan section multi-block H-type mesh system.

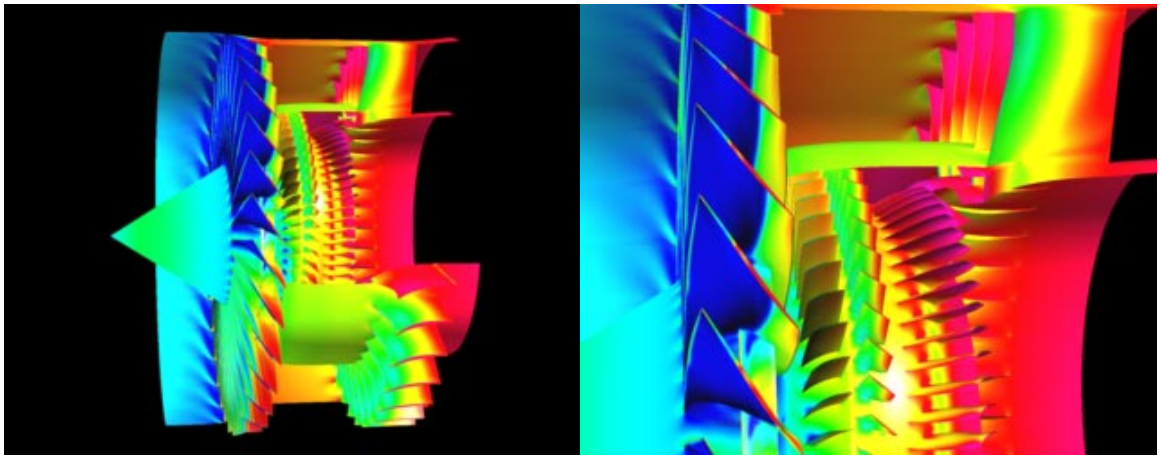

Figure 9.3: Predicted surface static pressure contours for EEE fan plus 1/4-height booster stage configuration.

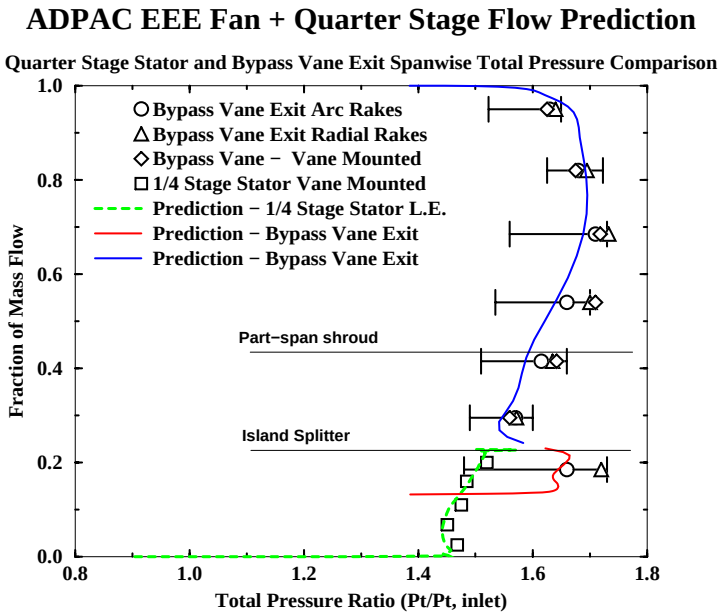

Figure 9.4: Comparison of predicted and experimental spanwise total pressure distributions at bypass vane exit and 1/4-stage vane leading edge for EEE fan plus 1/4-height booster stage configuration.

9.1.4 Off-Design Analysis

In order to investigate the off-design analysis capabilities of the EEE fan section model, a number of predictions were performed at 100% corrected speed with variations in both fan exit static pressure and fan section bypass ratio. These off-design results were obtained by prescribing the flow entering the core, and adjusting the bypass exit static pressure until the desired fan inlet flow was achieved. Excursions in predicted bypass ratio ranged from 6.0 to 10.8.

Predictions of overall performance were compared with measured data derived from full-scale rig tests of the fan section [74]. A comparison of predicted and experimental overall pressure ratio and adiabatic efficiency versus corrected mass flow rate for the core stream flow (downstream of the core inlet guide vane) of the EEE fan section is given in Figure 9.5. The corresponding maps for the fan bypass stream flow (downstream of the fan bypass vane) is given in Figure 9.6. The data on these figures illustrates the overall capabilities of the EEE fan design. Bold symbols on each figure illustrate the test performance at extreme high and low values of bypass ratio. It is interesting to note that in both the test and the prediction, bypass ratio did not significantly alter the characteristics of the bypass stream, but does have a significant effect on the core stream flow. The overall character of the off-design performance predictions displayed good agreement with the test data.

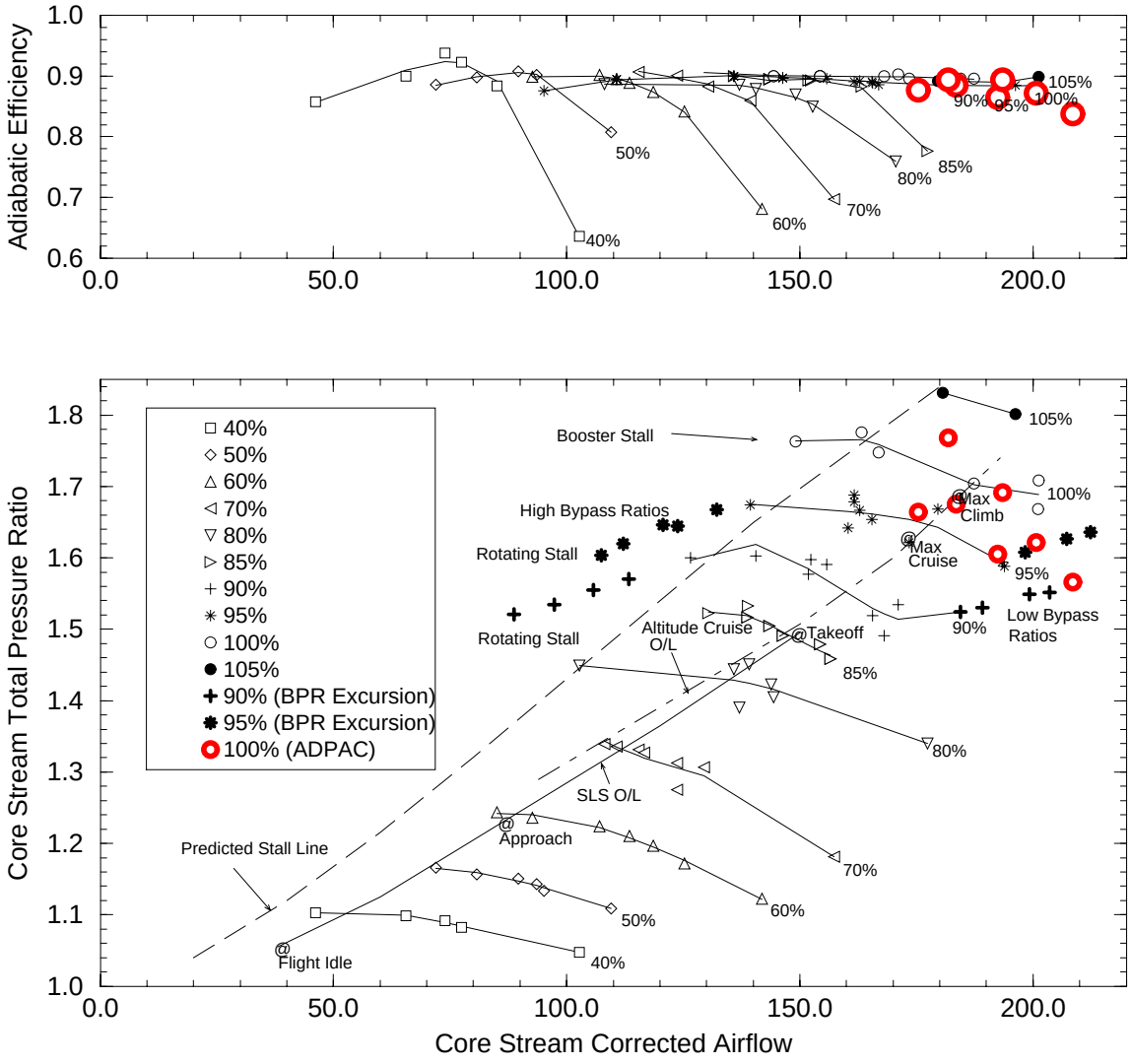

Figure 9.5: Comparison of predicted and experimental total pressure ratio and adiabatic efficiency versus corrected flow rate for the core inlet of the EEE fan section.

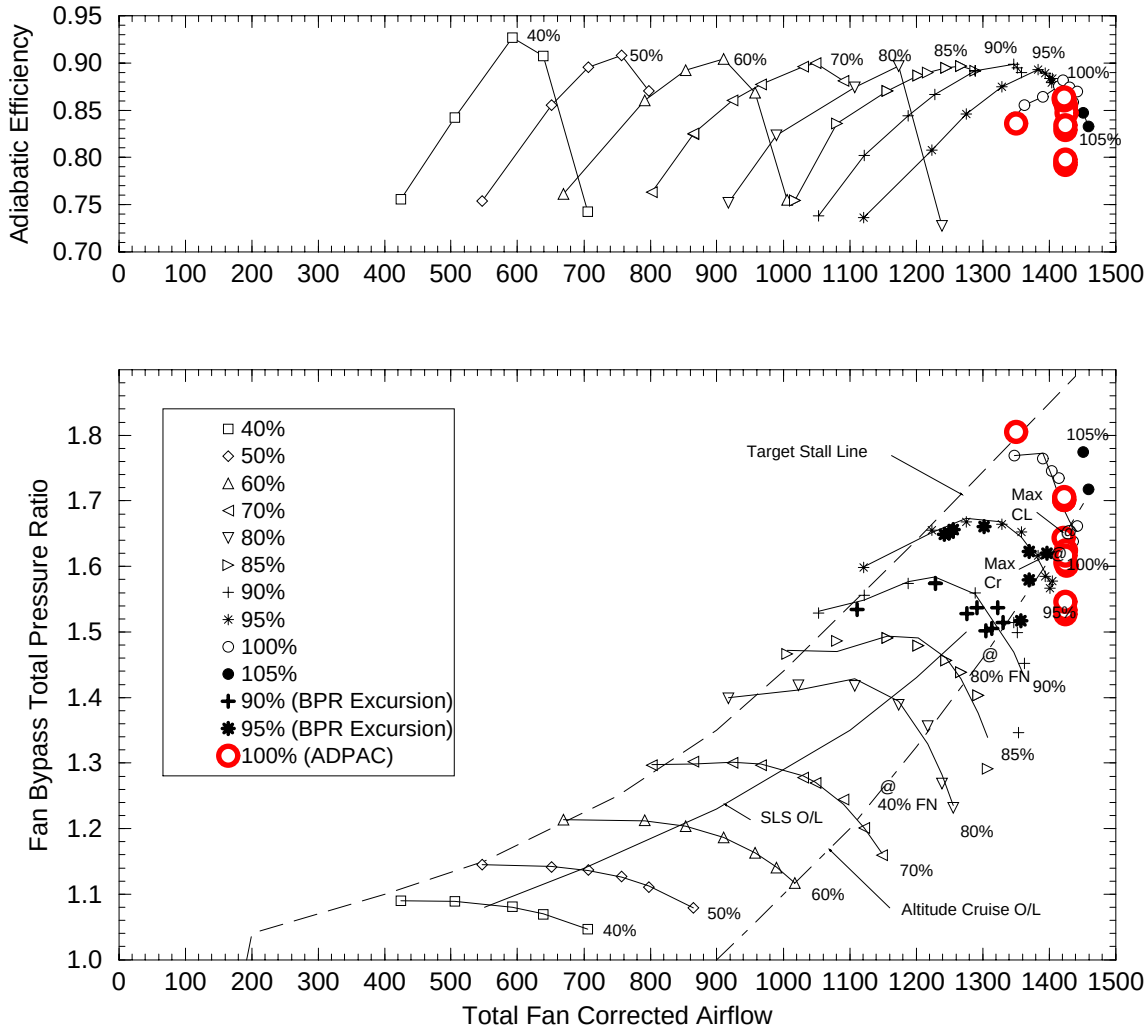

Figure 9.6: Comparison of predicted and experimental total pressure ratio and adiabatic efficiency versus corrected flow rate for the bypass duct flow of the EEE fan section.

9.2 EEE Low Pressure (LP) Turbine Analysis

9.2.1 Description of Design

The EEE LP turbine consists of a 5-stage design employing moderately loaded airfoils and a rather high (25 degrees) endwall slope. The 5-stage design was based in part on results obtained from studies of highly loaded fan turbine technology development at General Electric, and from system studies aimed at minimizing direct operating cost (DOC). The EEE engine LP turbine design is coupled to the HP turbine via a short (3 in.) transition duct. The relatively high bypass ratio (6.8) of the EEE fan section, and subsequent reduced core flow requires high specific energy from the fan-drive (LP) turbine. The design efficiency goals for the LP turbine were 91.1% for the integrated core/low spool (ICLS) test and 91.7% for the flight propulsion system (FPS) at the engine design point (M=0.8, 35,000 ft. altitude ISA). The LPT maximum tip diameter was set by mechanical and configuration control requirements at 46.5 in. The outer wall slope was also limited to 25 degrees (established as a maximum to maintain good aerodynamic performance) through stage 3, transitioning to a cylindrical outer wall at the stage 5 exit. A table of pertinent LP turbine design and operating parameters is given in Table 9.3.

9.2.2 Mesh System

Mesh generation was based on the 4-step procedure described in Chapter 5. A mesh system consisting of 10 mesh blocks (1 per blade row for 5 stages) containing 1,660,000 computational cells was assembled. A table of the mesh block sizes for the blade passage meshes is given in Table 9.4. An illustration of the axisymmetric projection of the LP turbine mesh system is given in Figure 9.7.

EEE LP Turbine Aerodynamic Design Parameters
Engine Design Point: Max Climb (M=0.8, 35,000 ft ISA)

	Stage 1	Stage 2	Stage 3	Stage 4	Stage 5
Energy Extraction Δh J/g (BTU/lbm)	73.04 (31.4)	79.09 (34.0)	82.11 (35.3)	70.25 (30.2)	49.31 (21.2)
Pressure Ratio (Pt/Pt)	1.30	1.35	1.40	1.36	1.26
Aero Loading $\Delta h/2u^2$	1.71	1.58	1.43	1.13	0.80
Flow Coefficiect Vz/u	1.25	1.08	1.04	0.98	1.07

Table 9.3: EEE LP turbine aerodynamic design parameters.

EEE LP Turbine Component Performance Validation Mesh Block Size Tabulation

Block	I Index	J Index	K Index	# Pts
1	97	49	33	156849
2	97	49	33	156849
3	97	49	33	156849
4	97	49	33	156849
5	97	49	33	156849
6	97	49	33	156849
7	97	49	33	156849
8	97	49	33	156849
9	97	49	33	156849
10	97	49	33	156849

Table 9.4: Tabulated mesh block sizes for EEE LP turbine component performance validation analysis.

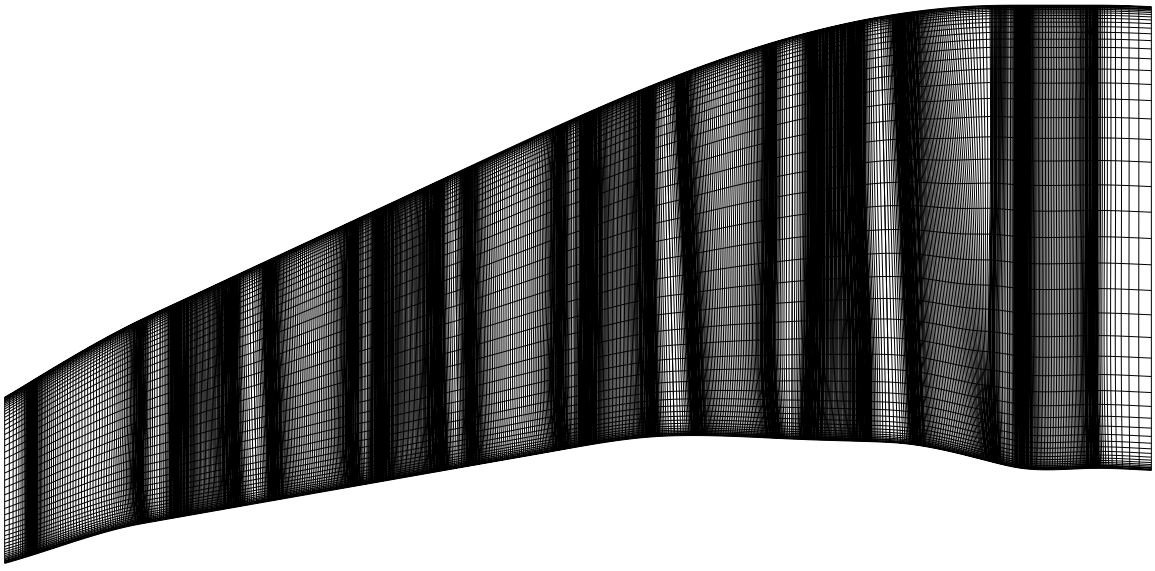

Figure 9.7: Axisymmetric projection of EEE LP turbine component validation mesh system.

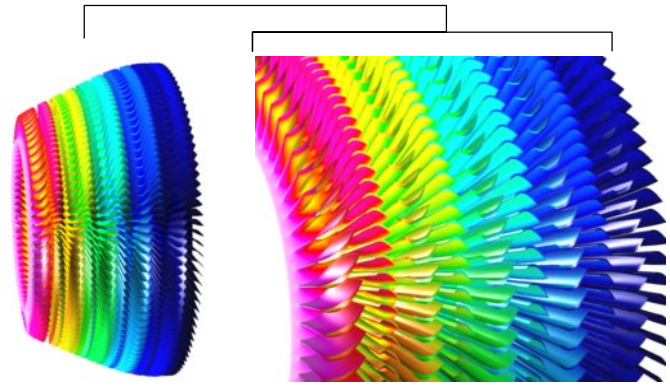

Figure 9.8: Predicted surface static pressure contours for EEE LP turbine.

9.2.3 Design Point Analysis

Design point numerical simulations of the EEE Low Pressure (LP) turbine were performed to permit comparison with 2/3 scale rig test data [101]. The analysis was performed on a Silicon Graphics Power Challenge L multiprocessor computer with 1 GB of main memory. Converged solutions were obtained in a total of 3 hours (wall clock time) using four processors. Note that the turbine simulation was nearly twice as fast as the fan section simulation in spite of the fact that approximately 20% more mesh points were involved. This feature results from the generally favorable pressure gradients involved in the turbine flow, leading to a rapid definition of the boundary layer flow. Conversely, the fan section flow involves predominantly adverse pressure gradients requiring significantly more computation time to resolve. The rapid computation time for the turbine clearly indicates the suitability of the analysis for design cycle studies. In fact, more time was involved in generating suitable meshes than was involved in the aerodynamic analysis itself. Predicted turbine surface static pressure contours are illustrated in Figure 9.8. This figure illustrates the three-dimensional nature of the blading and the general arrangement of the LP turbine.

A comparison of predicted and experimental spanwise variation of fifth stage exit total pressure and total temperature profiles is given in Figure 9.9. This preliminary analysis was based on a simple flat inlet profile of total pressure and total temperature and employed the exact blade and endwall definitions provided in the original Master Engine Geometry Database. The correlation between rig test and calculation is excellent in the 20%-80% radial span region. Noticeable discrepancies exist in the near endwall regions. These discrepancies were assumed to be due to the fact that no clearance flows, turbine hub overlap geometry, or shrouded rotor cavity geometries were modeled in this initial prediction.

In order to resolve differences between prediction and experiment near the endwalls, several additional calculations were performed to assess the effects of variations in geometry, flow parameters, etc. The variations tested included modifications to the first stage vane setting angle, modifications to the inlet flow profile, and the addition

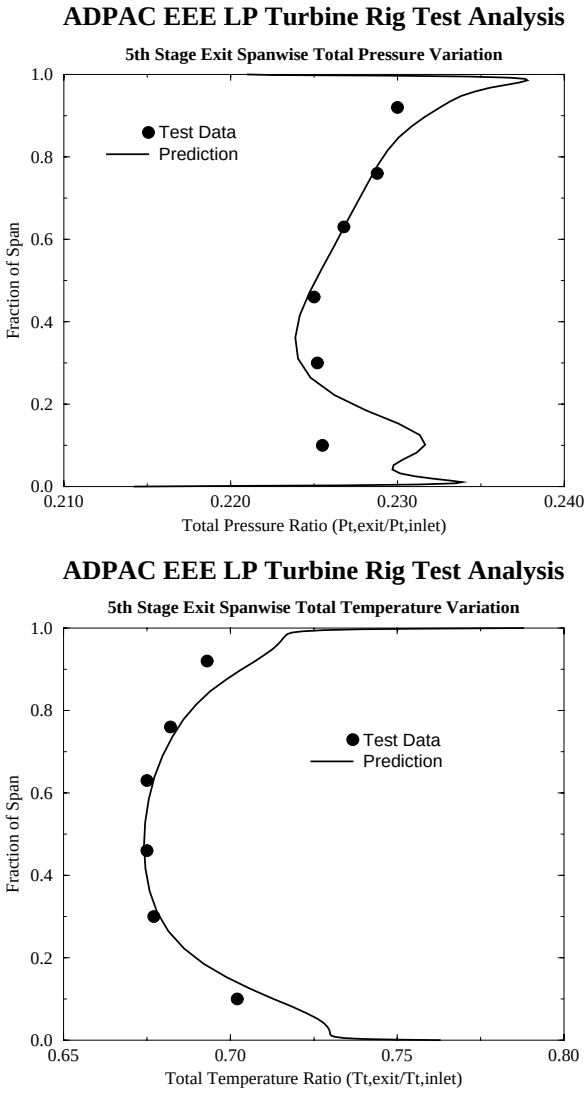

Figure 9.9: Comparison of predicted and experimental spanwise total pressure and total temperature distributions for fifth stage exit of the EEE LP turbine 2/3-scale test rig.

of a shrouded rotor endwall cavity model. Each of these variations are described in detail in the sections below. For each case, the effects are compared based on the predictions from the original, smooth endwall, flat inlet profile, unmodified LP turbine geometry as it existed in the EEE Master Engine Geometry Database at the beginning of this study. Each calculation was performed using a common static pressure ratio specification at the turbine exit hub surface.

9.2.4 Effect of Variations in First Vane Setting Angle

GE engineers familiar with the actual test rig and EEE engine geometry recommended a 1 degree (open) reset of the LP turbine first stage vane. The effect of the reset on the LP turbine exit spanwise flow profiles is illustrated on Figure 9.10. A distinct improvement in the predicted total temperature distribution was observed at the turbine exit, particularly near the tip, for the calculation involving the modified geometry. Given this observation, all further calculations were based on the modified first stage vane orientation.

9.2.5 Effect of Variations in Inlet Profile

Several multistage calculations were performed with variations in the first vane input spanwise total pressure, total temperature, and flow angle profile distributions. The profiles are categorized as flat (baseline, essentially no variation across the span except at the tip), boundary layer (BL - 10% thick total pressure deficit at the endwalls), and engine (derived from a simulation of the HP turbine exit flow). An illustration of the spanwise variation of inflow total pressure and total temperature from the three profiles is given in Figure 9.11.

Figure 9.12 illustrates the comparison of predicted and experimental LP turbine exit spanwise total pressure and total temperature profiles for each of the inlet profile variations described above. Note that there is not a significant change in the exit profile total pressure characteristics with variations in inlet profile specification. This is partially due to the fact that each calculation is run to the same exit static pressure ratio. There is some variation in the exit total temperature distributions, although this behavior essentially correlates with the inlet total temperature profile characteristics.

9.2.6 Effect of Variations in Endwall Geometry

The final comparison of results involved discrete modeling of the turbine shrouded rotor seal cavities. The calculations described above were all performed using a geometry model based on a smooth, continuous endwall definition. In reality, the endwalls are quite discontinuous and irregular due to the use of shrouded rotors and overlapping geometry, (see e.g. Figure 9.13) and these irregularities can have a significant impact on the primary gas path flow. Previous experience in predicting flows through compressor seal cavities suggests that the seal cavities themselves can often be modeled using two-dimensional techniques, and then subsequently coupled

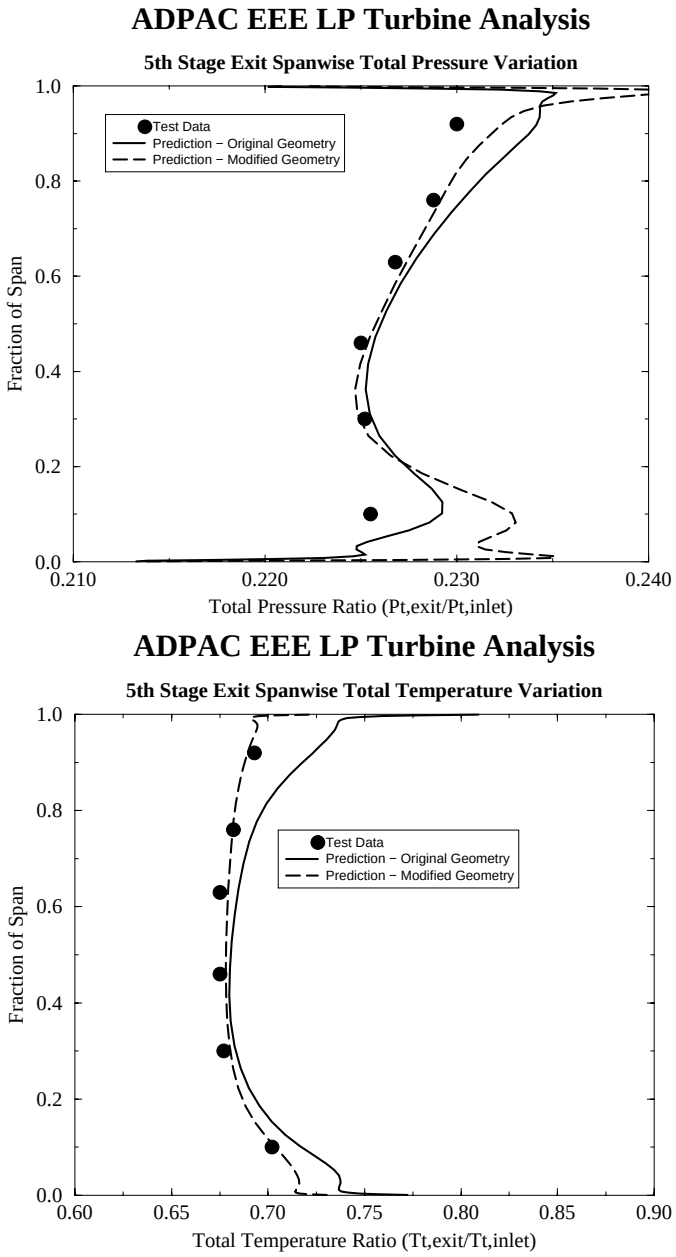

Figure 9.10: Comparison of predicted and experimental spanwise variation in fifth stage exit total temperature distributions for EEE LP turbine analyses with variations in first vane reset and endwall modeling.

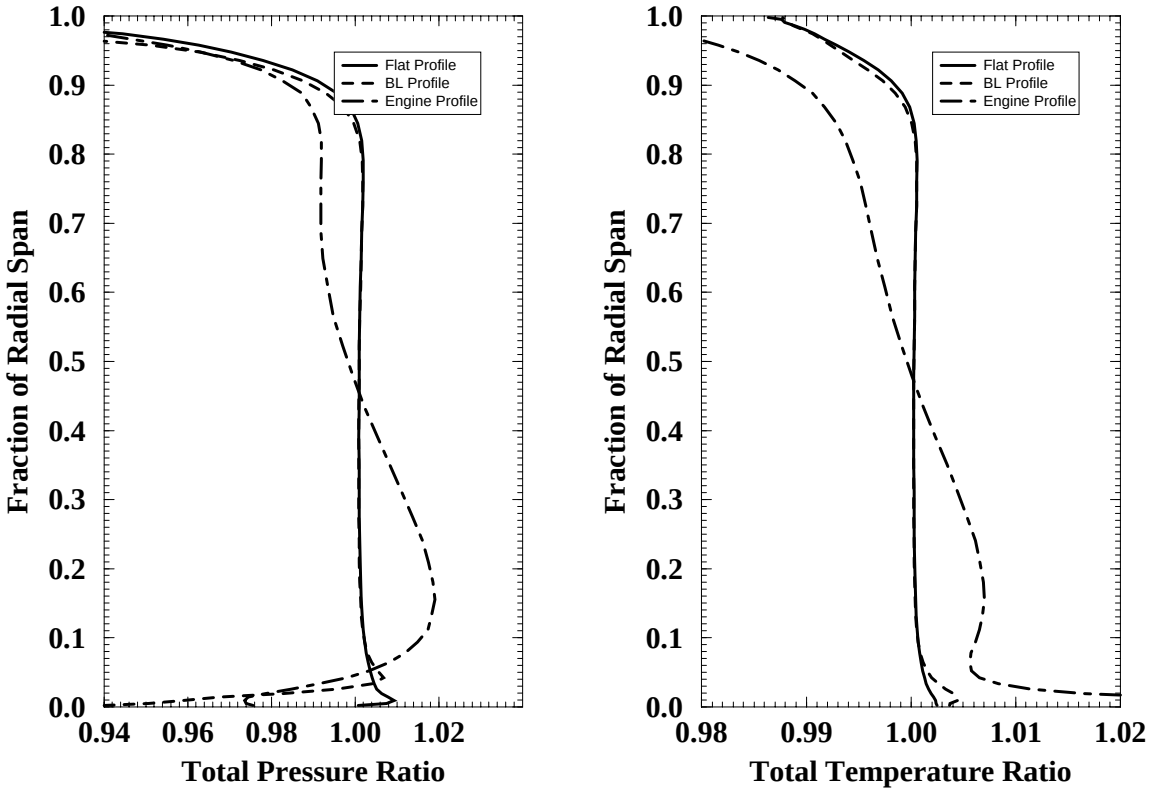

Figure 9.11: Comparison of spanwise variation of inflow total pressure and total temperature ratio profiles for profiles for the EEE LP turbine analyses with variations in inlet profile.

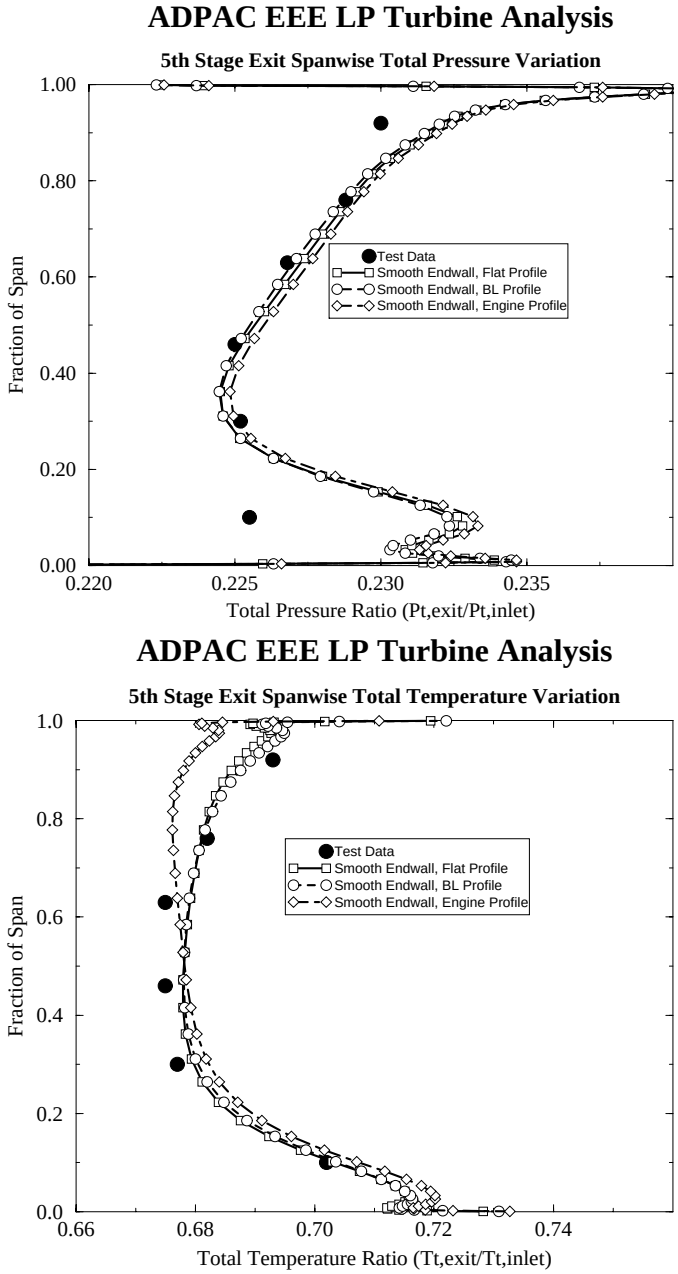

Figure 9.12: Comparison of predicted and experimental spanwise variation in fifth stage exit total temperature distributions for EEE LP turbine analyses with variations in inlet profile.

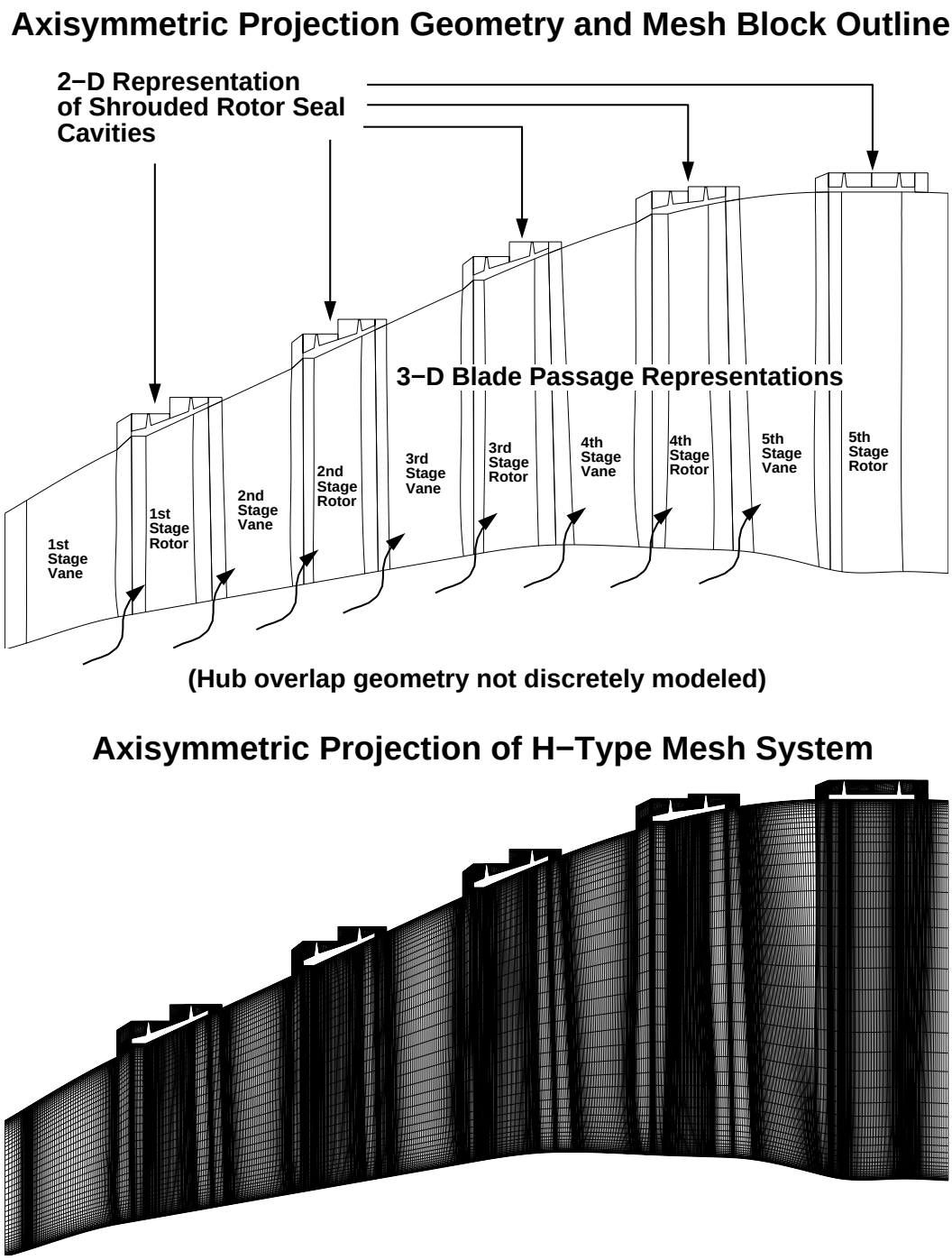

Figure 9.13: Illustration of realistic LP turbine endwall irregularities and CFD modeling techniques for the EEE LP turbine component validation study.

Inlet Profile Type	First Vane Reset	Endwall Type	Mass Flow (lb/s)	Pt, Exit (psia)	Tt,, Exit (deg. R)	Adiabatic Efficiency (Mass−Averaged)
Flat	0	Smooth	67.652	10.299	514.01	91.72%
BL	0	Smooth	67.366	10.292	514.49	91.60%
Engine	0	Smooth	68.228	10.314	512.70	91.99%
BL	1 open	Smooth	67.896	10.308	514.57	91.64%
Flat	0	Cavity	67.146	10.304	526.86	86.74%
BL	0	Cavity	66.705	10.284	522.92	88.27%
BL	1 open	Cavity	67.784	10.316	522.60	88.53%

Notes:
1. Nominal inlet total pressure = 45.0 psia
2. Nominal inlet total temperature = 750 deg. R
3. Approximate variation in computed mass flow from blade row to blade row:
   Smooth Endwall: 0.3%
   Cavity Endwall: 2.0%

Table 9.5: Comparison of predicted overall performance parameters due to variations in inlet profile, endwll model, and first vane reset for the EEE LP turbine 2/3 scale test rig.

with the 3-D blade passage flow through averaging techniques similar to a mixing plane. This was the approach adopted in this study to minimize the computational effort involved with modeling this more complicated flow case.

Figure 9.14 illustrates a meridional projection of the LP turbine mesh employing smooth endwalls (upper plot) and the same configuration where the shrouded rotor seal cavities are discretely modeled (lower plot). An illustration of the predicted axisymmetric-averaged Mach number contours for the EEE LP turbine with shrouded rotor cavity model is presented in Figure 9.15. The influence of the cavities would appear to be limited to local regions along the case near the inflow/outflow openings of the cavity. The resulting effect on the predicted spanwise profiles at the exit of the turbine are also illustrated on the plots on Figure 9.16. The characteristics of the spanwise profiles were not significantly altered due to the addition of the shrouded rotor cavity model; however, significant changes in the overall turbine performance parameters were detected. These changes are discussed in more detail in the following separate subsections.

9.2.7 Summary of Variations in Turbine Parameters on Design Point Performance

A summary of the overall performance characteristics due to the variations described above is given in Table 9.5. In terms of overall performance, variations in inlet profile did not appear to have a significant effect on the predicted mass flow rate, exit total pressure, total temperature, or efficiency for the smooth endwall model. In the cavity endwall model calculations, the differences due to inlet profile were more pronounced. Variations in first vane reset primarily affected the predicted mass flow rate. The 1 degree (open) reset of the first stage vane resulted in an increase in flow of 0.78% for the smooth endwall test case, and an increase of 1.59% for the cavity endwall model test case. Finally, in terms of the effects of variations in

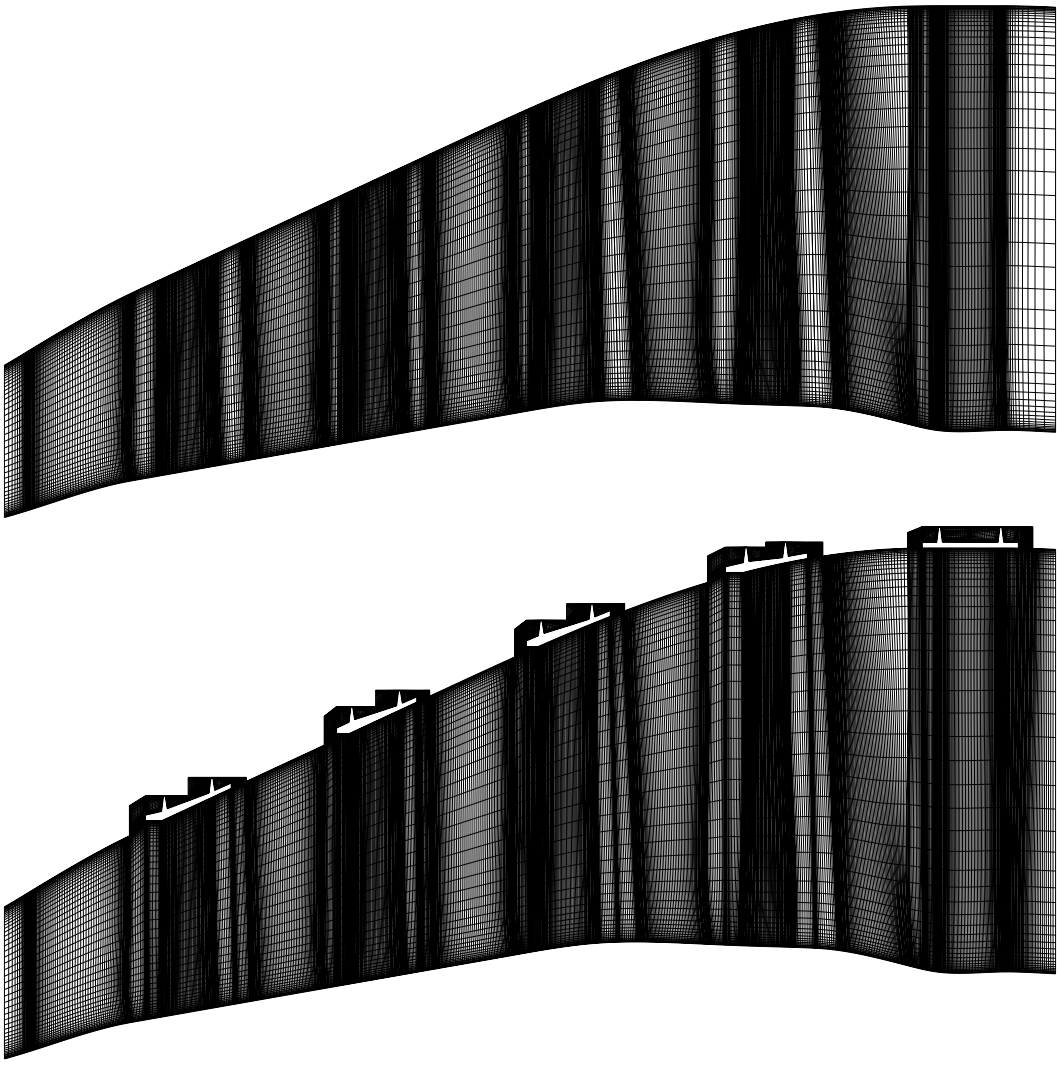

Figure 9.14: Comparison of axisymmetric projection of mesh systems for the EEE LP turbine with smooth endwalls (upper) and with modeled shrouded rotor seal cavities (lower).

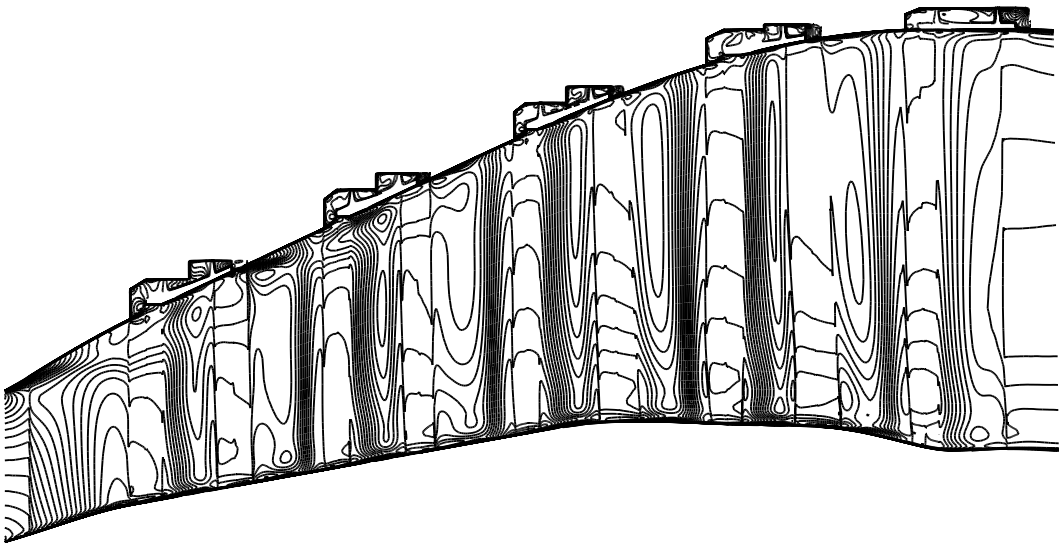

Figure 9.15: Illustration of predicted axisymmetric-averaged Mach number contours for the EEE LP turbine with shrouded rotor cavity endwall model.

the endwall model, the most prominent characteristics were reductions in predicted mass flow rate and adiabatic efficiency due to the cavity endwall flow model. The reduction in efficiency was quite dramatic - on the order of 3%-5% depending on the test case. One problem encountered during this evaluation was an inability to consistently maintain a constant mass flow from blade row to blade row in the cavity endwall solutions. Typical variations in mass flow from blade row to blade row in the multistage simulations using the smooth endwall model was 0.3%, while the cavity endwall model resulted in blade row to blade row variations as high as 2.0%. The large variation in the cavity flow model was a result of the complicated mixing-plane arrangement employed to numerically couple the 2-D cavity passage openings with both the upstream and downstream neighboring blade row 3-D mesh systems. Given this large level of mass flow variation, the large predicted efficiency reduction due to the addition of the shrouded rotor cavities should be interpreted qualitatively, not necessarily quantitatively.

9.2.8 Off-Design Analysis

A summary of the off-design component performance validation efforts for the EEE LP turbine are presented in this section. *ADPAC* solutions for the LP turbine were compared with GE scaled test rig Block II, Configuration 5 experimental data [101]. *ADPAC* was employed to generate several operating point solutions near the design blade-jet speed ratio ($u/C_o = 0.412$ where u is the turbine inlet mean axial velocity and C_o is the turbine tip speed) for the 2.4 million point LP mesh. The mesh included 2-D shrouded rotor seal geometries. A constant blade-jet speed ratio was set by fixing the inlet-to-exit pressure ratio and solving for the necessary shaft rotational speed. Pressure ratios of 2.0, 3.0 and 4.76 were used for computations and ADPAC data was

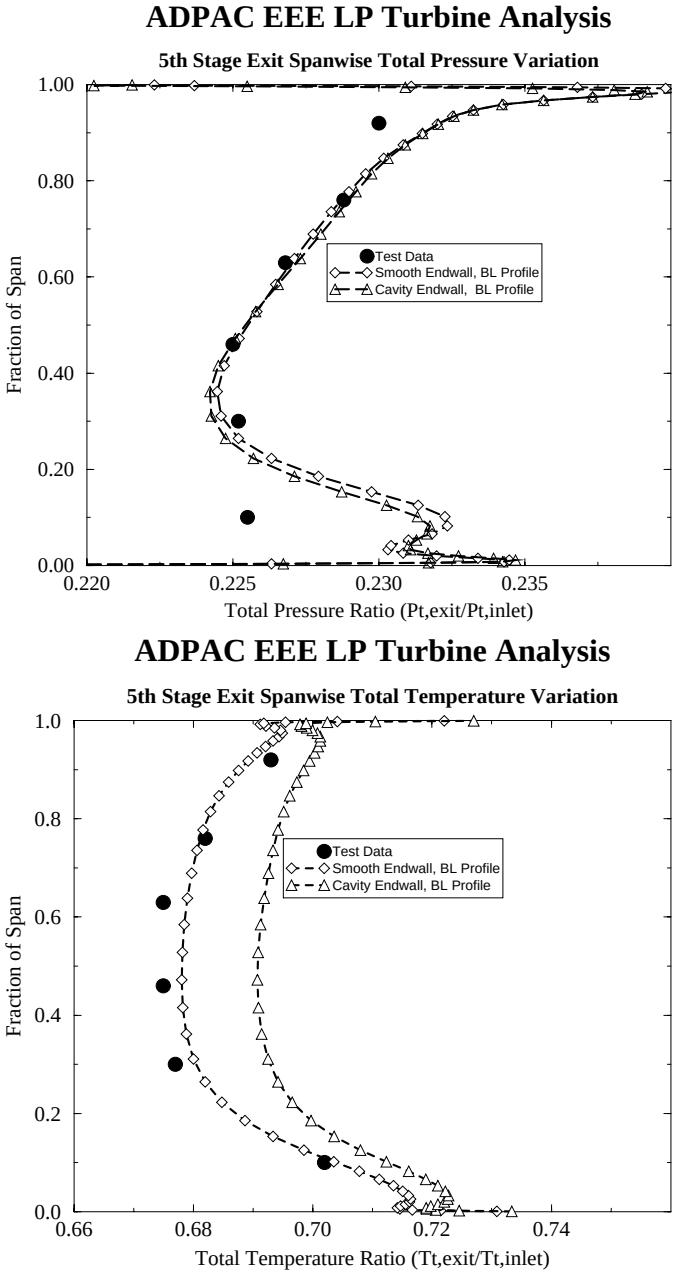

Figure 9.16: Comparison of predicted and experimental spanwise variation in fifth stage exit total temperature distributions for EEE LP turbine analyses with variations in inlet profile.

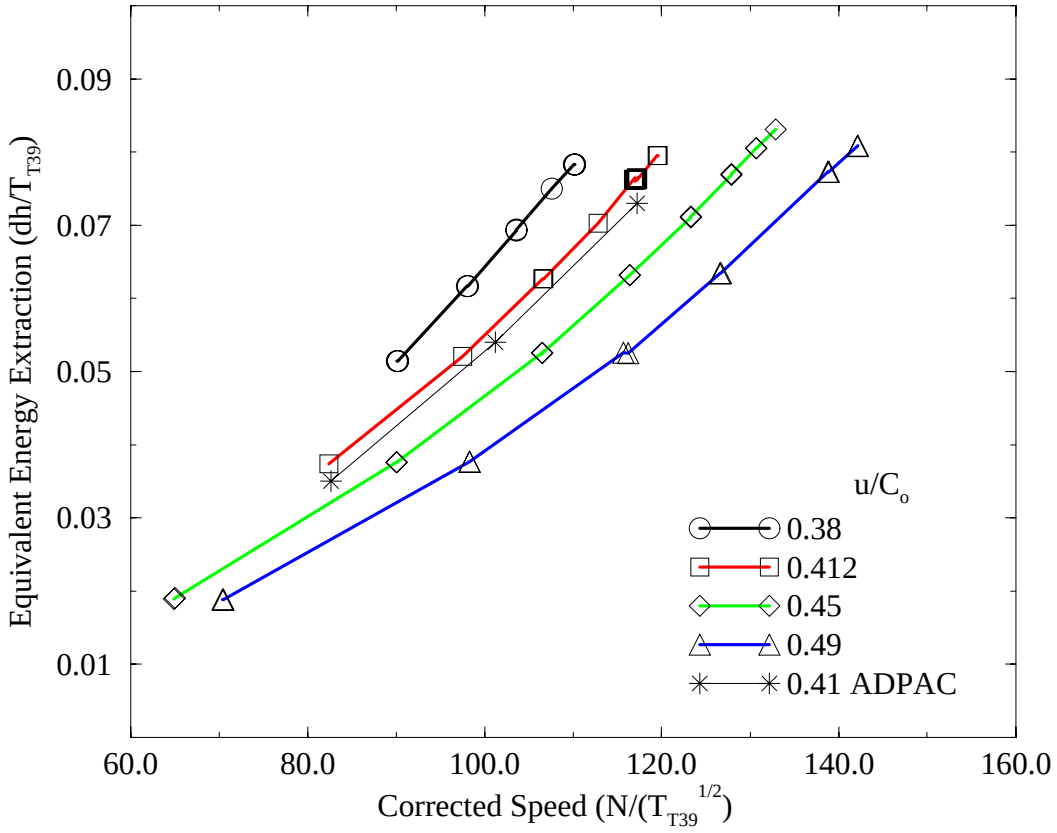

Figure 9.17: Comparison of predicted (ADPAC) and measured equivalent energy extraction for the Energy Efficient Engine (EEE) LP turbine.

reduced to enable comparison of equivalent energy extraction, inlet flow function, total-to-total efficiency and total-to-static efficiency. The comparisons are displayed in Figures 9.17-9.20.

The predicted trends for equivalent energy extraction and inlet flow function compare well with the scaled rig test data. The absolute levels of these performance parameters is also predicted reasonably well, in spite of the numerous uncertainties concerning the test vehicle and the data reduction procedures. The predicted trends in efficiency were also captured reasonably well; however, the predicted efficiencies are consistently 2%-4% low. This difference was due, in part, to the modeling of shrouded rotor seal flow, which caused a 3%-5% drop in adiabatic efficiency when compared to the smooth endwall prediction. The discrepancy in efficiency varied considerably based on the numerical method used to compute the efficiency (total temperature, angular momentum change, mass averaging versus area averaging, etc.). The large number of unpublished features of the test rig operation, and the uncertainties associated with the numerical cavity model prohibited timely investigation of this discrepency.

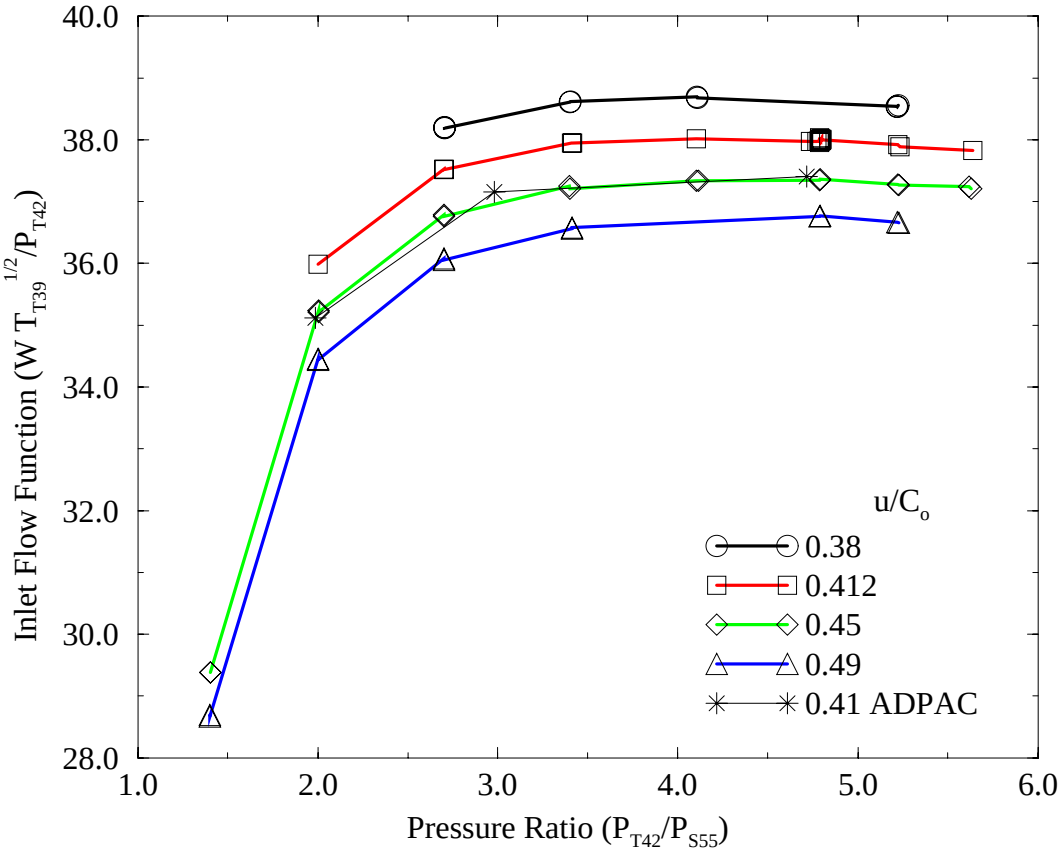

Figure 9.18: Comparison of predicted (ADPAC) and measured inlet flow function for the Energy Efficient Engine (EEE) LP turbine.

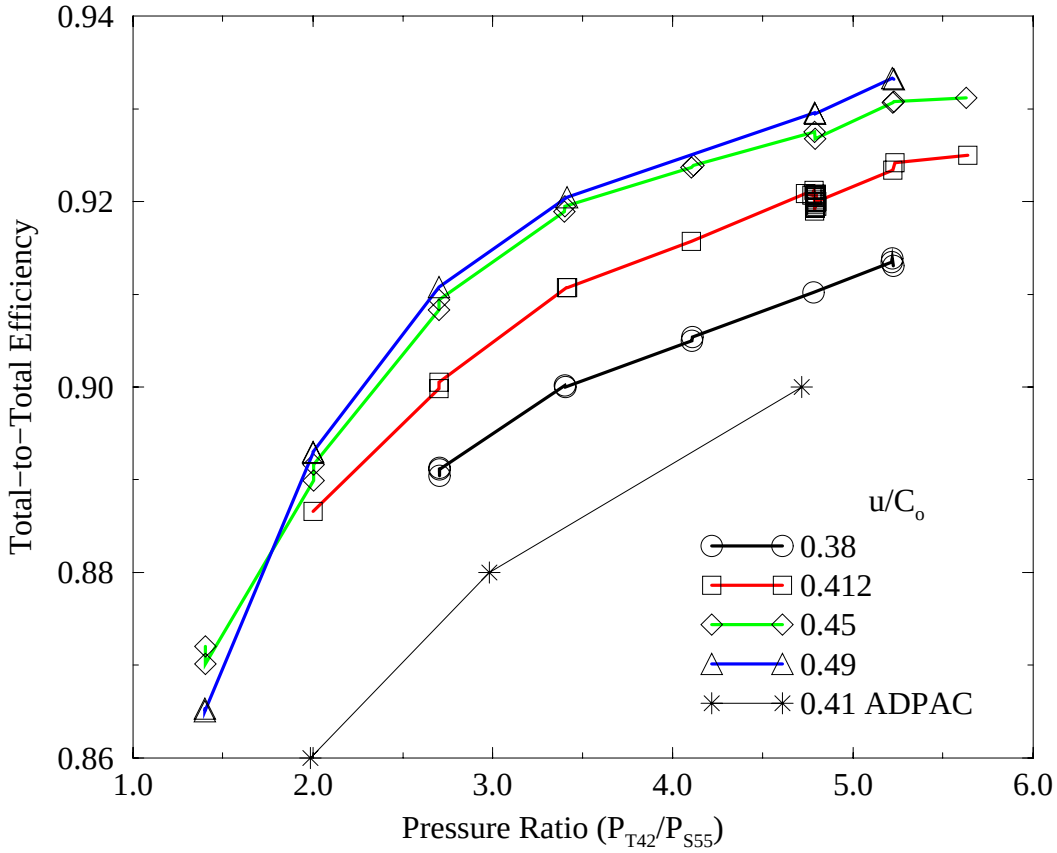

Figure 9.19: Comparison of predicted (ADPAC) and measured total to total adiabatic efficiency for the Energy Efficient Engine (EEE) LP turbine.

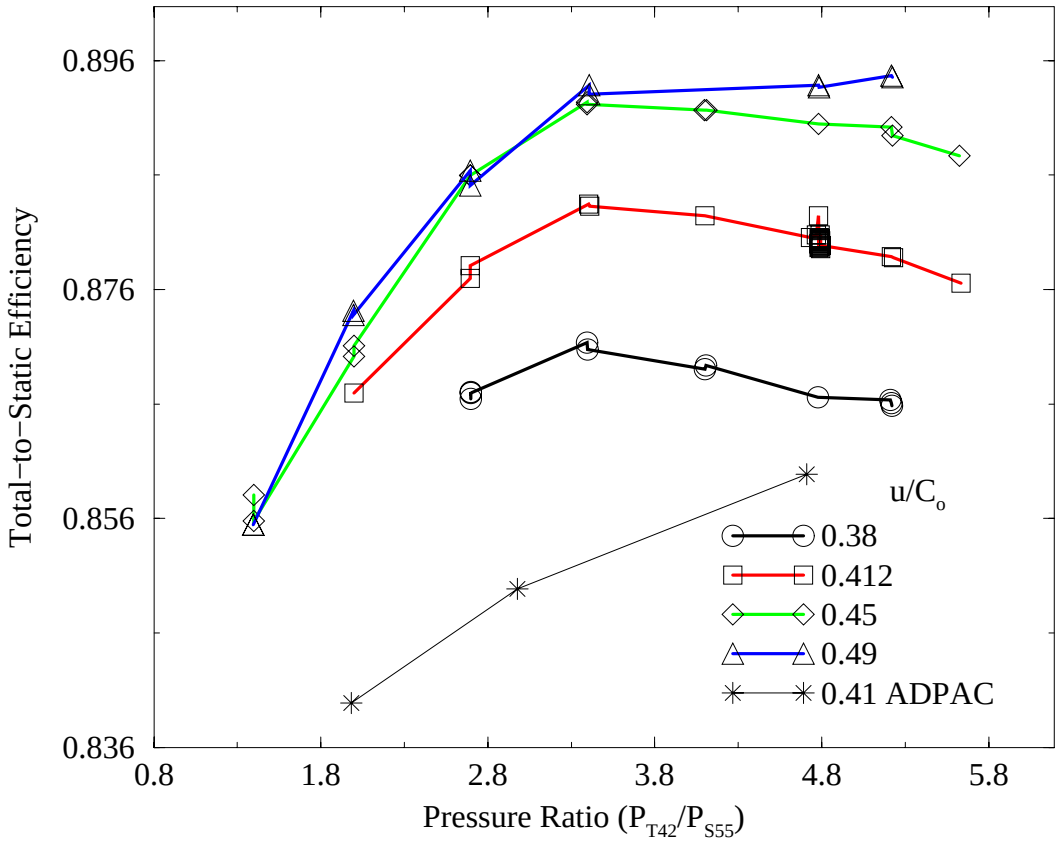

Figure 9.20: Comparison of predicted (ADPAC) and measured total to static adiabatic efficiency for the Energy Efficient Engine (EEE) LP turbine.

9.3 EEE Core Compressor Analysis

9.3.1 Description of the Design

The core (HP) compressor system for the EEE is a 10-stage axial flow compressor with a design pressure ratio of 22.6:1 [83]. The design corrected tip speed is 456 m/s (1495 ft/s), resulting in a corrected airflow of 53.5 kg/s (118 lb/s). The goal adiabatic and polytropic efficiencies for the EEE core compressor were 86.1% and 90.6%, respectively. The design was the result of an extensive compressor optimization study to identify desirable compressor design features for a subsonic transport engine. This optimization included analyses of the effects of aspect ratio, solidity, inlet specific flow, exit Mach number, reaction ratio, inlet radius ratio, exit radius ratio, and number of stages. The effects of each parameter were examined based on efficiency, weight, cost, aircraft direct operating cost (DOC) and fuel consumption. Two engine configurations were considered during this early study: an engine having a core compressor total pressure ratio of 14 with booster stages on the LP spool, and an unboosted core compressor with a total pressure ratio of 23. It was determined that best compressor performance was achieved using medium values of aspect ratio, solidity, and reaction ratio, and low values of inlet radius ratio, inlet specific flow, and exit Mach number. The 10-stage configuration offered the best overall combination of desirable features: compactness, low cost, high efficiency, low DOC and low fuel usage. Design parameters for the EEE core compressor are tabulated in Table 9.6.

9.3.2 Mesh System

Simulation of the core compressor was intended primarily as a check on the mesh generation system developed for the EEE IGES component definitions, and the fidelity of the EEE core compressor geometry database. As such, only a design point simulation was performed on the baseline core compressor geometry (variable stator schedules in their "design" setting). The resulting mesh system was composed of 21 mesh blocks (1 per blade row for IGV and 10 stages) and is illustrated in an axisymmetric projection in Figure 9.21. The total number of computational cells in this mesh is 3,553,000. A typical block size is 97x33x49 (axial, radial, tangential). This mesh density is typical of design analysis calculations.

9.3.3 Design Point Analysis

A design point analysis was performed for the EEE core compressor. The simulation was performed primarily as a check of the geometry database and the mesh generation and solution procedures. The solution was performed on a Silicon Graphics Power Challenge XL computer, employing 12 of the 16 available processors. This resulted in no more than two blade rows per processor. Subsequent calculations employed 21 processors with one blade passage per blade row. The resulting decrease in CPU time was nearly linear with the number of processors.

EEE Core Compressor Aerodynamic Design Parameters
Engine Design Point: Max Climb (M=0.8, 35,000 ft ISA)

Corrected Tip Speed	(m/s) (ft/s)	456 1495
Inlet Radius Ratio		0.503
Flow/Annulus Area	($kg/s/m^2$) ($lbm/s/ft^2$)	185.5 38.0
Rotor 10 Exit Hub Speed	(m/s) (ft/s)	352.7 1157
Rotor 10 Exit Radius Ratio		0.93
Outlet Guide Vane Exit Mach Number		0.30
Number of Rotors and Stators		1672
Average Aspect Ratio		1.48
Average Pitch Solidity		1.36
Adiabatic Efficiency		85.7%
Stall Margin Potential		25%

Table 9.6: EEE core compressor aerodynamic design parameters.

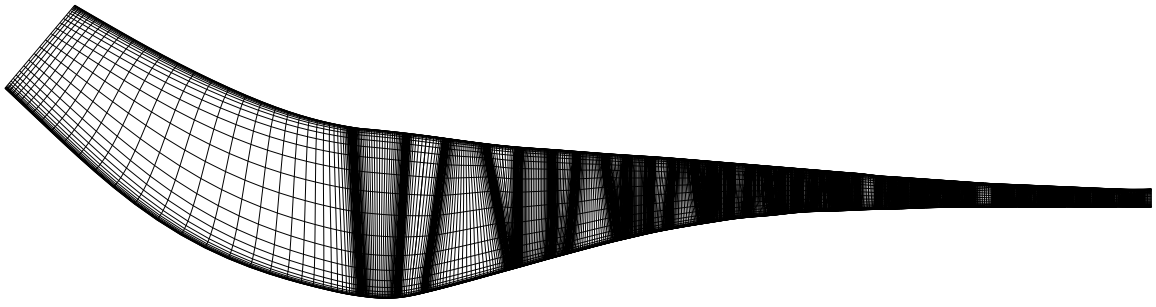

Figure 9.21: Axisymmetric projection of EEE core compressor component validation mesh system.

Including solution initialization, which was performed on coarser meshes using the ADPAC full multigrid initialization routine (essentially a combined grid sequencing/multigrid solution strategy), the complete design point simulation using the 12-processor configuration was obtained in 15 hours. This clearly indicates that a complete operating map could be derived in essentially one day given enough available processors. For example, using two 21-processor machines of current computing power, a single constant speed operating line (6 different pressure ratios at a constant speed) could be evaluated for this compressor in about 14 hours using the *ADPAC* solution strategy. This estimate includes the reduction in total solution time afforded by the ability to restart from previous solutions.

Mass-averaged estimates of performance from the HP compressor design point simulation were used to predict a mass flow rate, total pressure ratio, and adiabatic efficiency of 120.8 lbm/s, 22.37, and 86.6%, respectively. These estimates compare very well with the corresponding design values listed above. The prediction also demonstrated good agreement based on the measured data [83] for this compressor, although there were obvious potential sources of error such as bleed flows, clearance changes, etc.

A comparison of predicted and experimental spanwise total pressure distributions aft of the sixth stage rotor and aft of the tenth stage stator are presented on Figures 9.22 and 9.23, respectively. Test data from both the compressor rig test and the engine core test are included on both figures. Since the prediction and experiment represent operation at slightly different total pressure ratios, the absolute levels of total pressure are slightly mismatched, but it is clear from Figure 9.22 that the spanwise character of the flow is very accurately predicted. There is a large difference between the rig and core engine test data for the tenth stage stator exit data plotted on Figure 9.23. This large difference was attributed to a rather large difference in rotor tip clearance which degraded the performance of the outer endwall flow for the compressor rig test.

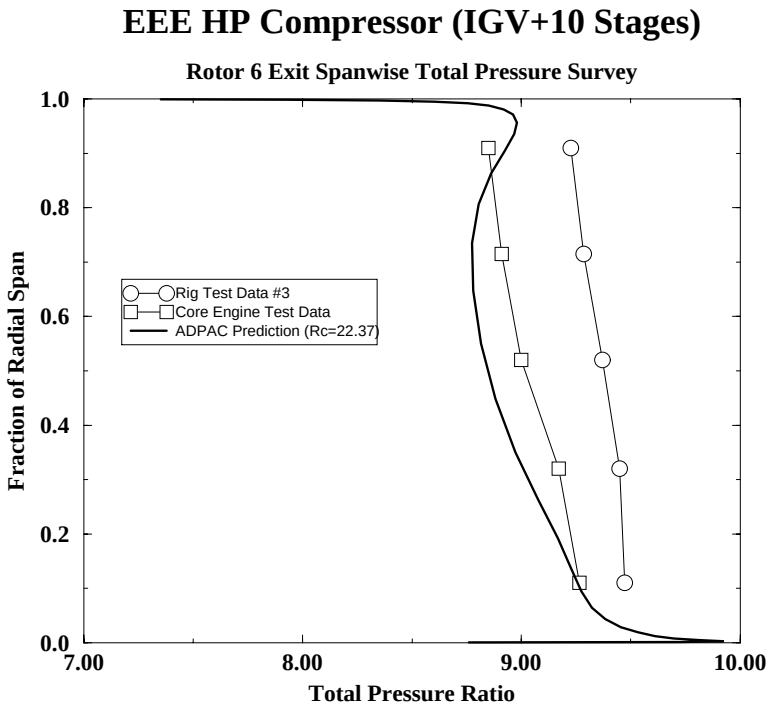

Figure 9.22: Comparison of predicted and experimental spanwise total pressure ratio distribution aft of the sixth stage rotor for the EEE HP compressor (design point operation).

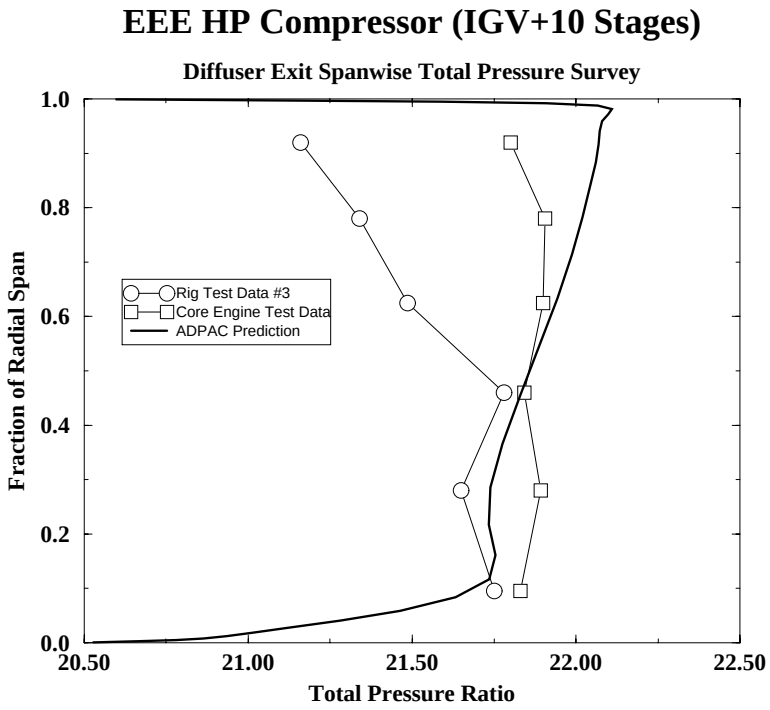

Figure 9.23: Comparison of predicted and experimental spanwise total pressure ratio distribution aft of the tenth stage stator for the EEE HP compressor (design point operation).

Parameter	(Units)	Max Climb	Max Climb+4%	Max Climb	Max Cruise	Sea Level Takeoff+27 F
Inlet Temperature	(deg. K)	1588	1591	1557	1515	1618
	(deg. R)	2858	2863	2802	2728	2913
Energy	(J/kg/de. K)	353.4	353.4	355.5	353.4	354.6
$\Delta h/T$	(But/lbm/deg. R)	0.0844	0.0844	0.0849	0.0844	0.0847
Speed	(rad/sec/$\sqrt{\text{deg. K}}$)	33.19	33.78	33.56	33.68	34.22
$N/\sqrt{T}$	(rpm/$\sqrt{\text{deg. R}}$)	236.2	240.4	238.9	239.7	243.6
Corrected Flow	(g$\sqrt{\text{deg. K}}$/sec/Pa)	0.8648	0.8913	0.8643	0.8638	0.8628
$W/\sqrt{T}/P$	(lbm$\sqrt{\text{deg. R}}$/sec/psi)	17.65	18.19	17.64	17.63	17.61
Loading $\Delta h/2U^2$		0.635	0.625	0.624	0.616	0.599
Efficiency (η, %)		91.9	91.9	92.4	92.4	92.1

Table 9.7: EEE HP turbine critical operating data.

9.4 EEE HP Turbine Analysis

9.4.1 Description of the Design

The EEE HP turbine design [84] evolved from overall engine integration and system studies performed at General Electric Corporation during the development of the EEE engine test vehicles. The design point for the HP turbine was operation at a Mach number of 0.8, at 35,000 ft. ISA. The efficiency goal was 92.4%. A summary of the EEE HP turbine critical operating data is given in Table 9.7.

The final HP turbine configuration was the result of detailed studies aimed at assessing the potential benefits of geometric alterations about a baseline design which resulted from the early cycle studies. The alterations considered were:

- number of stages
- outer diamater
- annulus height
- stage work distribution

The EEE HP turbine consists of a 2-stage design with moderately loaded airfoils. A summary of stage aerodynamic parameters for the EEE HP turbine is given in Table 9.8. The individual airfoil blade aerodynamic geometry parameters are listed in Table 9.9.

9.4.2 Mesh System

The mesh system for the EEE HP turbine consisted of 4 mesh blocks with a total of 627,396 points. A typical mesh block size for each blade row was 97x33x49 (axial, radial, tangential). An axisymmetric projection of the EEE HP turbine component validation mesh system is given in Figure 9.24.

Parameter		Stage	
		1	2
Pressure Ratio		2.18	2.18
$Dh/2U^2$		0.69	0.56
Tip Speed (Take−off)	(m/s)	513.9	535.2
	(ft/s)	1686.0	1756
Cooling and Leakage (%)		<−−−−−−−− 18.2 −−−−−−−−−−−−>	
Exit Mach Number		0.34	0.43
Reaction		0.38	0.35
Swirl, degrees		15	1
Number of Vanes		46	48
Number of Blades		76	70
Radius Ratio		0.88	0.82
%Tip Clearance		1.0	0.6

Table 9.8: EEE HP turbine stage aerodynamic parameters.

Parameter	Stage 1 Vanes	Stage 1 Vanes	Stage 2 Blades	Stage 2 Blades
Number	46	48	76	70
Solidity AW/t	0.71	1.07	0.96	1.06
Zweifel Number	0.67	0.79	1.08	1.03
% Trailing Edge Blockage	7.2	6.6	8.1	7.4
Aspect Ratio $AR=h/d_0$	3.3	4.4	3.8	4.6
Unguided Turn DB_S	8.4	11.0	13.0	15.5

Table 9.9: EEE HP turbine stage blade aerodynamic geometry.

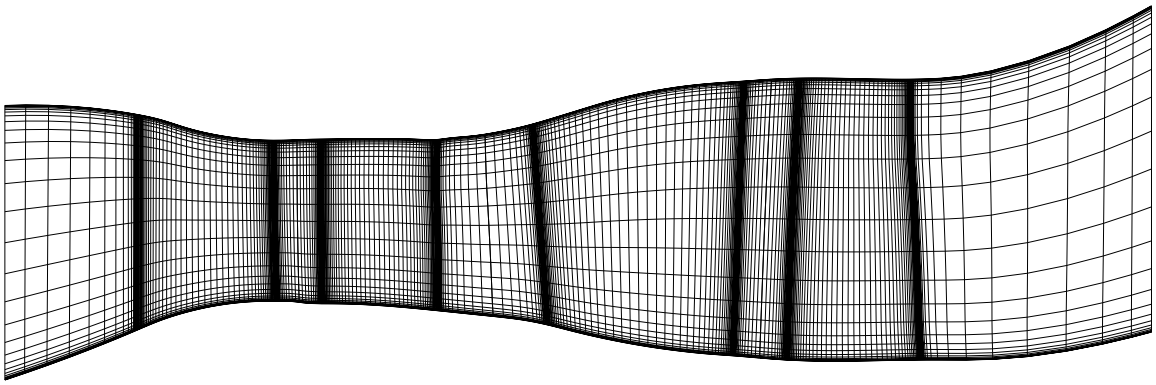

Figure 9.24: Axisymmetric projection of EEE HP turbine multi-block H-type mesh system.

9.4.3 Design Point Analysis

A design point numerical simulation of the EEE High Pressure (HP) turbine was performed to permit comparison with test data from the full scale warm air rig test performed during the EEE engine development cycle [100]. Although the warm air test rig included cooling flow, no attempt was made in the present numerical analysis to account for the effects (both aerodynamic and thermal) of the cooling flow system. The results must therefore be interpreted with this limitation in mind. The analysis was performed on a Silicon Graphics Power Challenge XL multiprocessor computer with 2 GB of main memory. Converged solutions were obtained in a total of 3 hours (wall clock time) using four processors.

Predicted turbine surface static pressure contours are illustrated in Figure 9.25. The orientation of the stages and nature of the blading is evident in this picture.

A comparison of predicted and experimental spanwise variation of second stage exit total pressure and total temperature profiles is given in Figure 9.26. The correlation between rig test and calculation displays a consistent deviation in both temperature and pressure across the entire span. This deviation (albeit small) is believed to be due to the fact that cooling air injection present in the warm air turbine rig test was not modeled in the numerical simulation. Since the only purpose of this simulation was to validate the geometry and solution procedure, the original solution was deemed sufficient for this purpose, and no further effort to identify this discrepency was attempted.

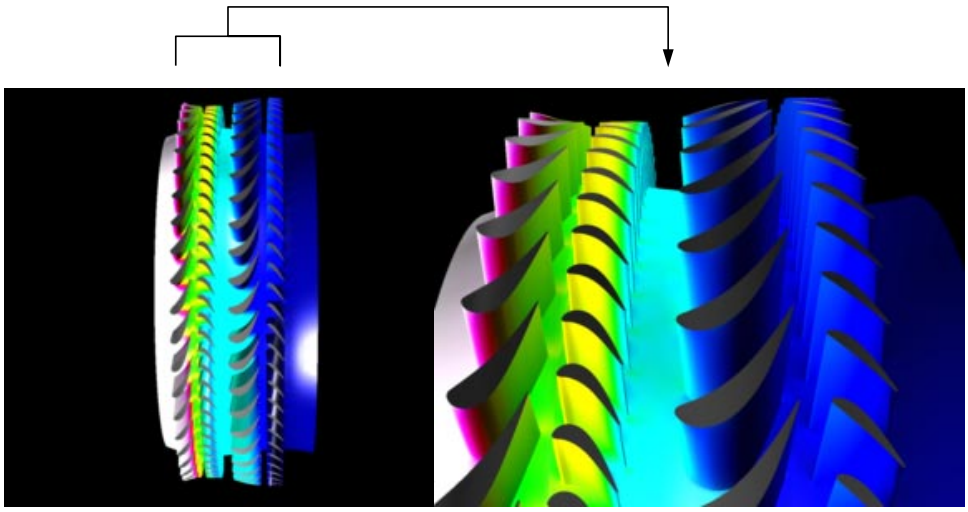

Figure 9.25: Predicted surface static pressure contours for EEE HP turbine.

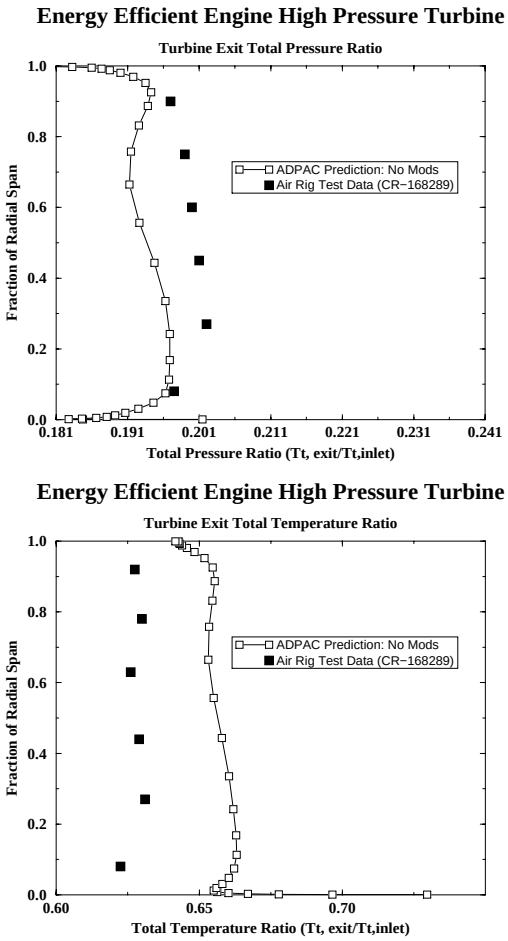

Figure 9.26: Comparison of predicted and experimental spanwise distributions of second stage exit total pressure and total temperature profiles for the EEE HP turbine.

9.5 Lobed Exhaust Mixer Analysis

9.5.1 Description of the Design

Static scale model tests were conducted to evaluate exhaust system mixers for a high bypass ratio engine as part of the NASA sponsored Energy Efficient Engine program [36]. Gross thrust coefficients were measured for a series of mixer configurations which included variations in the number of mixer lobes, tailpipe length, mixer penetration, and length. All of these parameters have a significant impact on exhaust system performance. In addition, flow visualization pictures and pressure/temperature traverses were obtained for selected configurations. Parametric performance trends were defined based on these results. Mixer configuration variables included lobe number, penetration and perimeter, as well as several cutback mixer geometries. Mixing effectiveness and mixer pressure loss were determined using measured thrust and nozzle exit total pressure and temperature surveys. These scaled results provided a data base to aid the analysis and design/development of the EEE mixed-flow exhaust system. The final EEE Flight Propulsion System (FPS) lobed exhaust mixer employed a scalloped, 12-lobe design based on the results of the extensive rig testing.

9.5.2 Mesh System

The mesh system for the EEE lobed exhaust mixer represented one of the more challenging aspects of this project. Since this geometry is dissimilar to the bladed flowpath geometries of the fan, compressor and turbine sections, mesh generation was performed essentially by hand using the *GRIDGEN* mesh generation program. A partial geometry database was constructed by NASA during this study and was employed for the EEE LPS simulations described in this section and the following chapter. The geometry is at least representative of the final design, but there remains some uncertainty as to the complete accuracy of the lobed surfaces. In addition, the actual test article employed scallops on the lobes to enhance mixing. Since no detailed information on scallop configuration was available, the cut-outs were not modeled in this study. An illustration of the modeled surfaces of the EEE lobed exhaust mixer is given in Figure 9.27. The EEE lobed exhaust mixer mesh system along the lobe plane of symmetry is given in Figure 9.28. A total of 9 mesh blocks were employed to define the coannular engine flow streams and the external flow stream. An illustration of the mesh system at the mixer plane is given in Figure 9.29.

The final mesh block sizes and total number of computational cells for the lobed exhaust mixer component validation study are tabulated in Table 9.10.

9.5.3 Design Point Analysis

A design flow analysis was performed for the EEE lobed exhaust mixer using the *ADPAC* code. Results from the analysis were integrated and qualitatively compared to the test data from the rig test study [36]. Only a qualitative comparison was

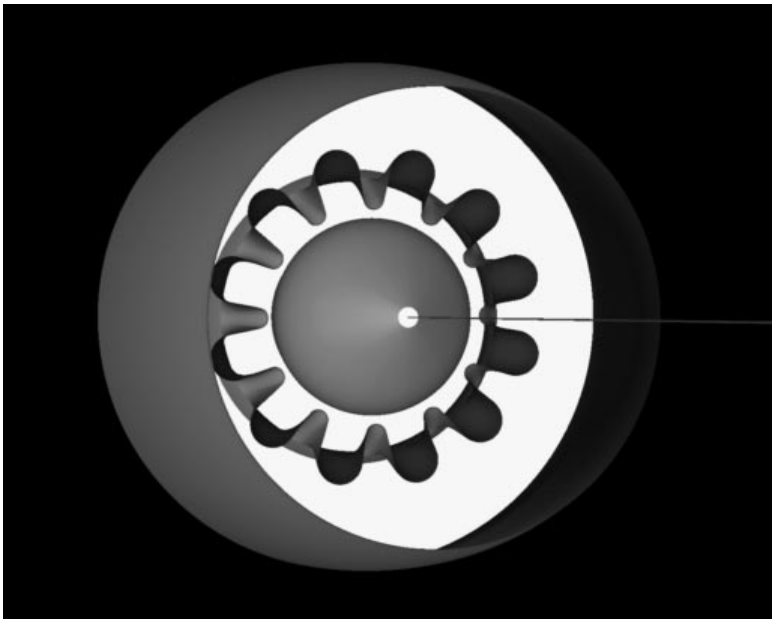

Figure 9.27: Illustration of EEE lobed exhaust mixer geometric surfaces modeled during the component validation study.

Number of blocks: 9

Block	I Size	J Size	K Size
1	65	45	81
2	81	9	81
3	81	49	81
4	81	49	81
5	73	49	81
6	73	49	81
7	49	49	81
8	65	49	81
9	49	49	81

Total Number of Computational Cells: 2,275,992

Table 9.10: Tabulation of EEE lobed exhaust mixer mesh block sizes and total number of computational cells employed during the component validation study.

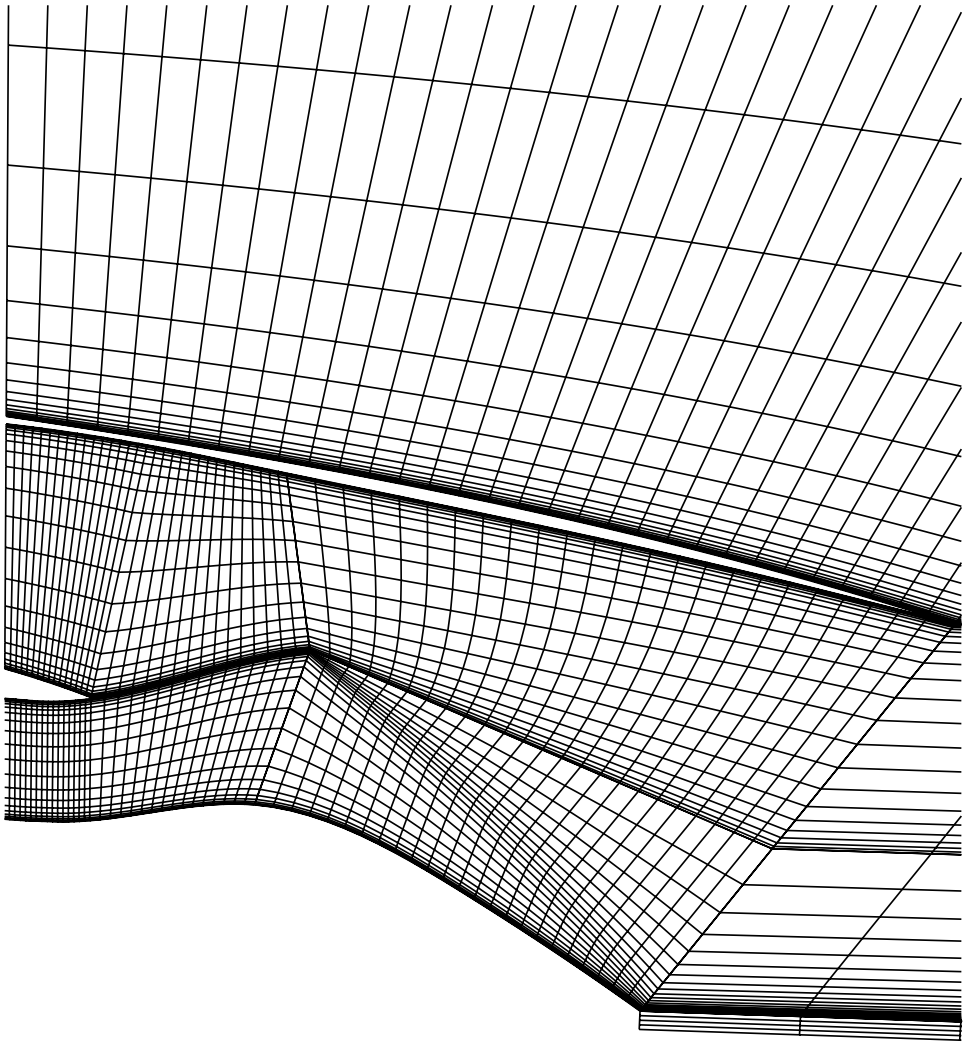

Figure 9.28: Illustration of EEE lobed exhaust mixer symmetry plane mesh surfaces employed during the component validation study.

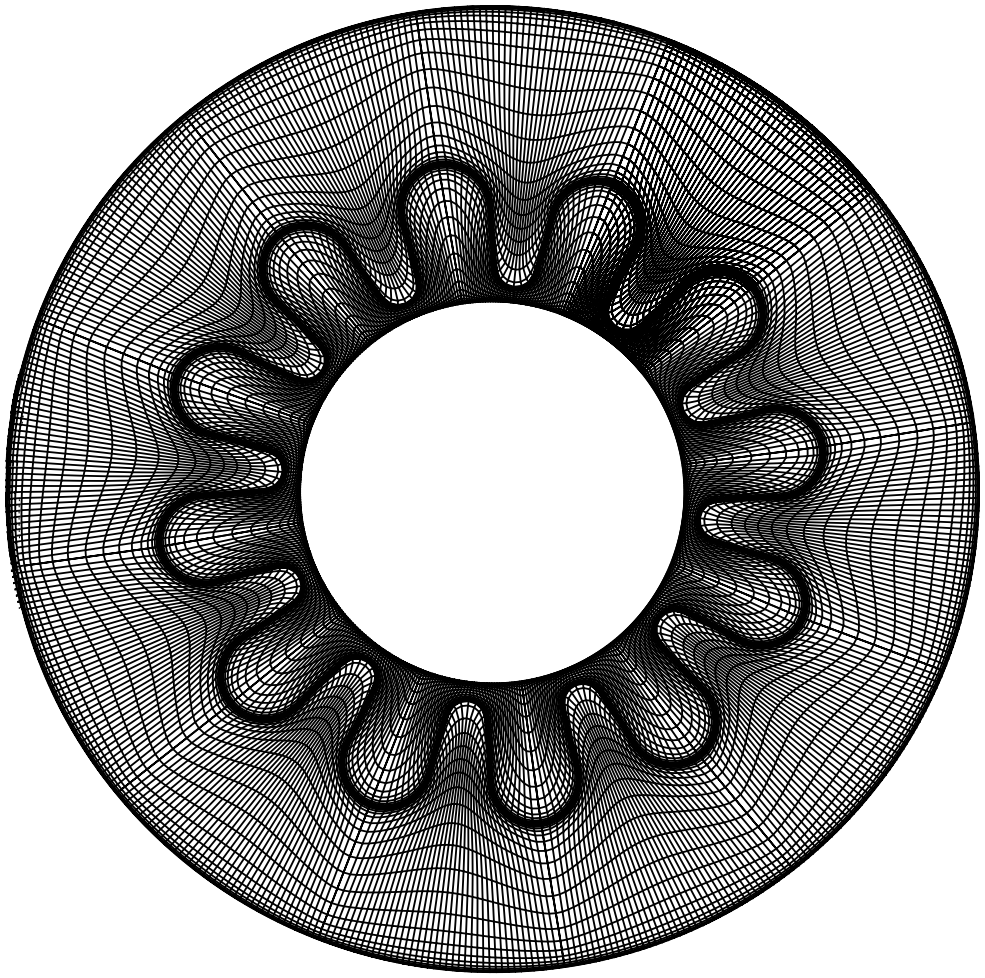

Figure 9.29: Illustration of EEE lobed exhaust mixer exit plane mesh system employed during the component validation study (analysis employs one lobe and assumes periodicity from lobe to lobe).

possible due to uncertainty between the modeled mixer and the geometries described in the rig tests.

Figure 9.30 illustrates the predicted surface static pressure contours from the design point analysis for the EEE lobed exhaust mixer. Total temperature contours on an axial plane roughly one diameter downstream of the nozzle exit plane are also illustrated on this figure. The symmetric horseshoe-shaped total temperature regions result from the secondary flow vorticies which develop as a result of the lobed mixer. Figure 9.31 illustrates a series of iso-surfaces defining boundaries of constant total temperature for temperature ratios varying from 1.8 to 1.1. The high temperature surfaces are confined within the mixer as the large temperature differences between the two streams are initially reduced rather rapidly. At lower temperature ratios, and consequently farther downstream, the lobed mixer flow patterns control the shapes of the constant temperature surfaces. The vortical nature of the flow displays a bifurcation of the iso-surface (24 segments as opposed to 12) for the iso-surface defined by a total temperature ratio of 1.3. The iso-surface returns to a 12-segment configuration for lower temperature ratios.

Spanwise total temperature profiles at the mixer/nozzle exit are illustrated in Figure 9.32. Predicted and experimental total temperature ratios are plotted against a normalized nozzle area distribution along several circumferentially spaced arrays spanning a single half-lobe of the mixer. The test data was derived from a study [36] of mixer configurations of varying penetration, area ratio, etc. To validate the mixer predictions, test data was derived from an essentially equivalent mixer (Configuration F3, 12 lobes, 39% penetration) which was tested under the referenced study. In general, the spanwise characteristics of the mixer are qualitatively captured, particularly along the lobe radial peak (Station A on Figure 9.32 survey. There is some noticable disagreement between prediction and test at survey Stations D and E. This discrepency is likely due to the fact that the numerical and test mixer geometries were not exactly similar, and also due to the generally accepted observation that the algebraic turbulence model employed in the present analyses is not well suited for temperature mixing problems of this sort. The algebraic model does not promote turbulent mixing at the shear layer between the two streams, and the general consequence is that predicted temperatures tend to display more abrupt profile changes than the test data.

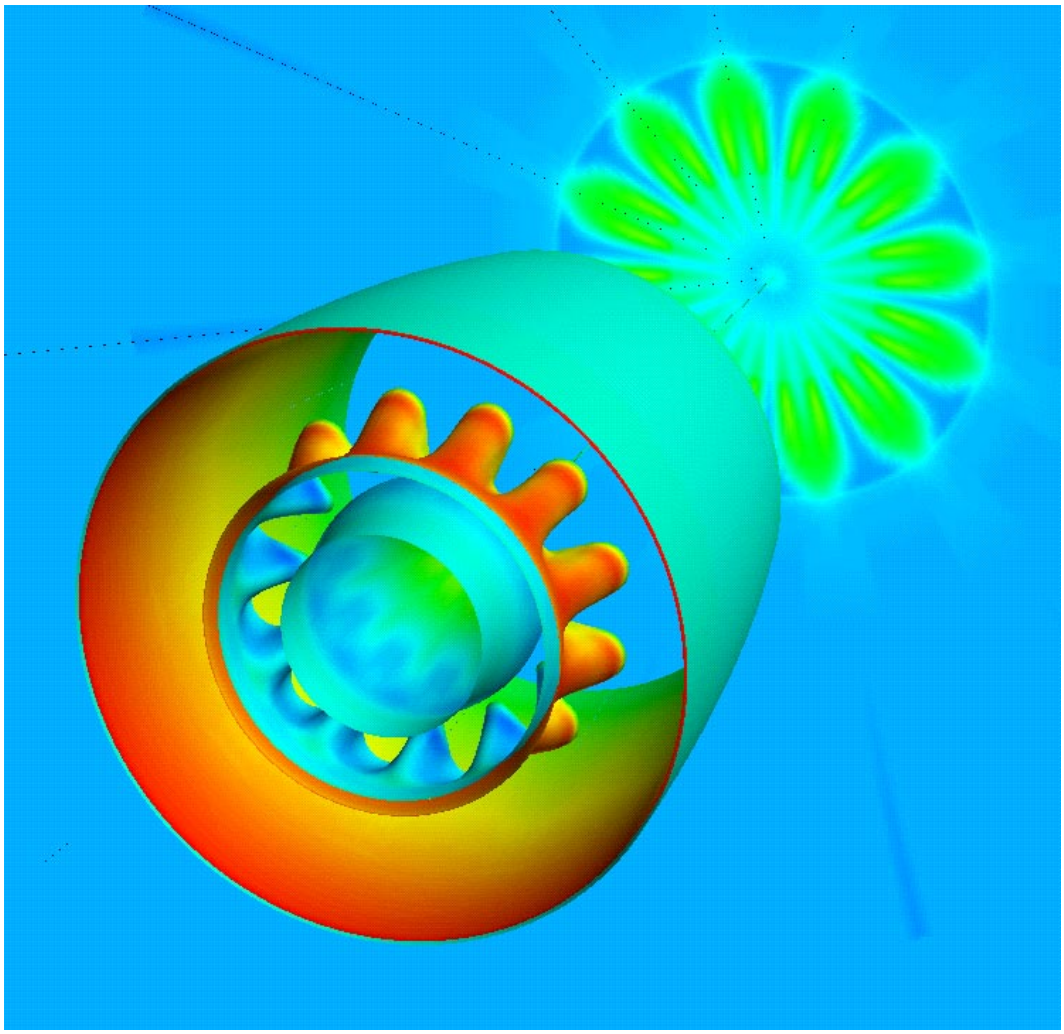

Figure 9.30: Predicted surface static pressure contours and axial plane total temperature contours (one diameter aft of nozzle exit) for the EEE lobed exhaust mixer.

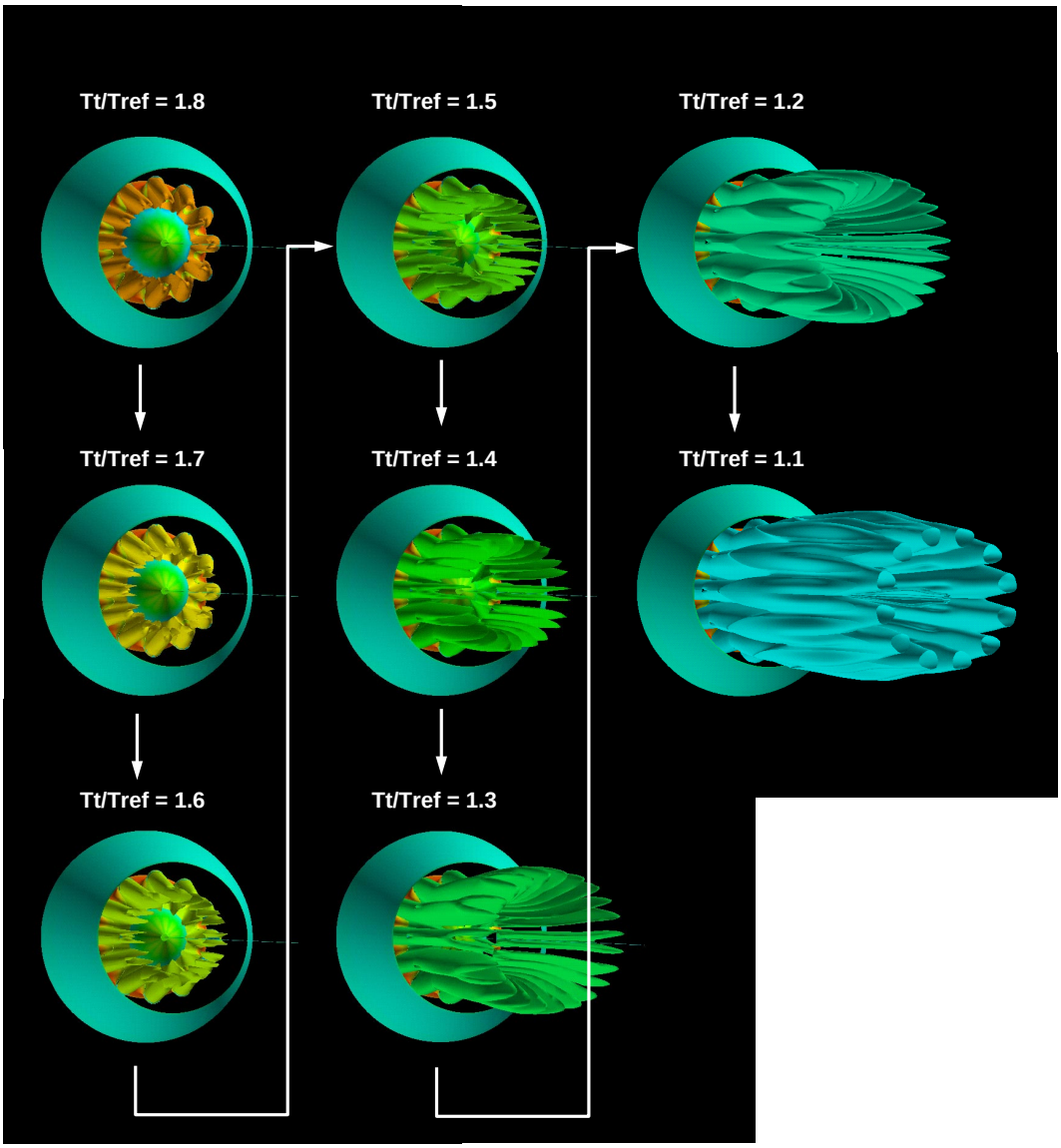

Figure 9.31: Predicted iso-temperature surfaces for EEE lobed exhaust mixer simulation illustrate temperature distribution patterns due to mixing.

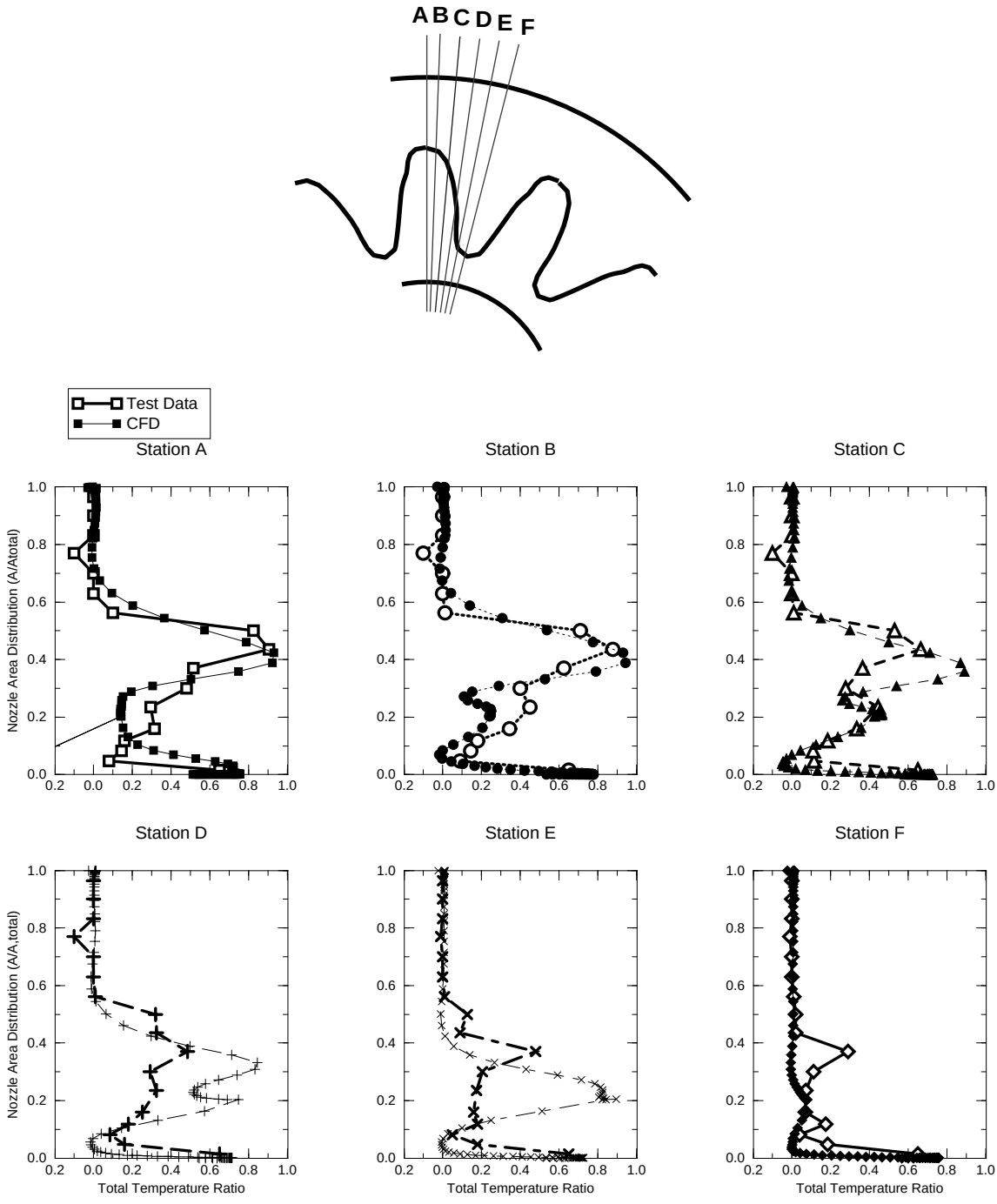

Figure 9.32: Comparison of predicted and experimental radial total temperature surveys for the EEE lobed exhaust mixer.

(This page intentionally left blank)

Chapter 10

EEE/LP Subsystem Analysis

This chapter deals with the results of numerical modeling of the Low Pressure (LP) Subsystem of the General Electric (GE) Energy Efficient Engine (EEE). The LP Subsystem model was developed following the component validation studies described in the previous chapter. The LP Subsystem analysis employed both fixed and variable core boundary specifications based on the results of an engine cycle model for the High Pressure (HP) core behavior.

10.1 LP Subsystem Mesh Construction

Grid generation for the EEE LP subsystem analysis was based essentially on collecting the individual meshes for the major subcomponents (fan, HP/LP turbines and lobed mixer) employed during the component validation study. The existing fan, quarter-height booster stage, HP turbine, LP turbine, and lobed mixer subsystem component meshes were assembled for this purpose. In addition, new meshes were generated using *GRIDGEN* to model those regions which were not discretized by any of the component validation models. These new regions included the forward-most flow in the inlet, external flow about the nacelle, and the bypass duct flow between the fan section bypass vane and the lobed exhaust mixer. For computational simplicity, these new regions were modeled in a two-dimensional fashion (the analysis is certainly not limited in this respect), and were computational coupled to the three-dimensional domains using the *ADPAC* mixing plane strategy (see e.g. Figure 10.1). It should be emphasized that all primary components (blade rows, for example) were still modeled with 3-D mesh systems. The collection and assembly of these meshes resulted in a numerical model of the entire EEE (minus the engine core compressor and combustor). It should be noted that although the high pressure compressor and combustor were not discretely modeled, the influences of these components were approximated by equivalent inflow and outflow boundary conditions. Figure 10.1 illustrates axisymmetric projections of the resulting EEE mesh/geometry model.

The resulting primary mesh for the EEE LP analysis consisted of 74 separate blocks and approximately 6.7 million grid points. The meshes and corresponding boundary data file were sequentially "coarsened" by removing every other grid point

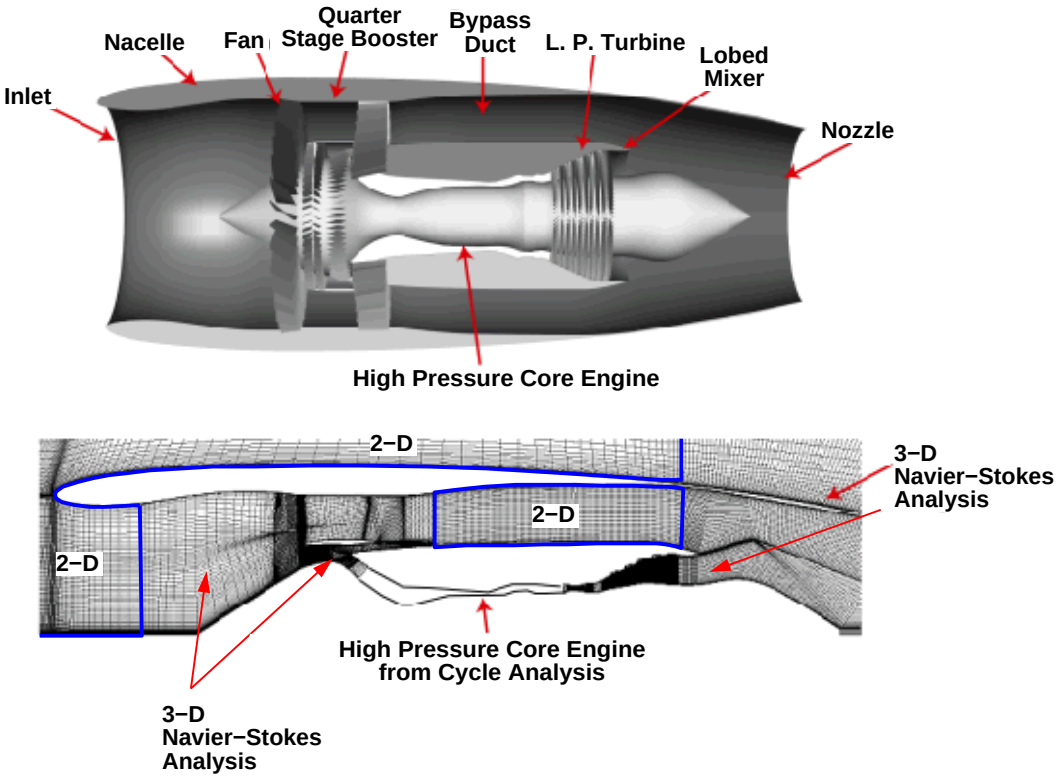

Figure 10.1: Axisymmetric projection of Energy Efficient Engine (EEE) Low Pressure (LP) Subsystem analysis component layout and mesh system.

in each computational coordinate direction to yield a mesh system of of 900,000 points. This "coarse" mesh was employed to debug the overall solution specifications, and to ease the difficulties encountered with numerical initialization of the solution caused by the high pressure ratios encountered in a complete engine solution. It was also found that the solution could be effectively initialized by employing the individual component solution data obtained from the component validation studies. This type of data would not normally be available for the analysis of a new engine design, and it was therefore deemed important to be able to demonstrate that the solution could be initialized from an arbitrary initial specification.

10.2 EEE LPS Processing Strategy

All calculations for the EEE LP Subsystem were performed on parallel computing systems. Four such systems were described in detail in Chapter 6. At the very end of this program, timing comparisons were also obtained on a 128-processor Silicon Graphics Origin 2000 computer. All parallel calculations employed the MPI [114] message passing specification, with the primary programming sublayer coded using the the APPL [112] message passing library. Conversion between the APPL specification and the MPI specification was handled by a conversion library (APPLMPI). This layered coding structure is outlined in more detail in the *ADPAC* reference manuals [107], [142]. Inter-processor communication based on the MPI programming specification was handled using two different MPI libraries. Initially, a public domain MPI library referred to as *MPICH* was employed as this package was self-contained, had an automatic configuration script, and was available for a very wide variety of computing platforms. During the latter stages of this project, Silicon Graphics Corp. developed a proprietary MPI implementation (SGI MPI 3.0) which was also employed during this study. Timing comparisons for the various computational platforms and communication libraries employed in this study for the EEE LP Subsystem analysis are provided in Table 10.1.

Several interesting conclusions can be drawn from this comparison. Solution times varied widely based on computing platform. Overall computation time (wall clock time in this instance) is governed by essentially three factors: system load, processor load, and communication load. For each of the times presented in Table 10.1, every effort was made to perform the timing study on an unloaded system. That is, the system, while not necessarily dedicated, was essentially unloaded when the timing comparison was performed. This was assumed to eliminate the system load factor as a significant contributor to the overall time. The remaining time was therefore essentially a function of CPU load and communication load. CPU load was controlled through the block/processor assignment algorithm employed by the *ADPAC* analysis. The *ADPAC* code performs parallel computations via a domain decomposition coarse grained computing strategy. The division of the computational effort is accomplished by assigning one or more blocks of the multiple block mesh to specific processors. This assignment can be directly specified by the user, or through the code predefined assignment strategy. The overall processing load for a given

Wall Clock Time Summary

(100 Iterations of EEE/LP Model)

	Coarse Mesh Number of Processors			Fine Mesh Number of Processors		
	8	**16**	**32**	**8**	**16**	**32**
LACE						
communication	**5380**	**2139**	**2707**	**N/A**	**23063**	**–**
total solver time	**7762**	**4846**	**4198**	**N/A**	**77427**	**–**
Babbage						
communication	**952**	**403**	**735**	**–**	**–**	**8763**
total solver time	**2673**	**1418**	**1089**	**–**	**–**	**17518**
Davinci						
communication	**–**	**–**	**–**	**4617**	**–**	**–**
total solver time	**–**	**–**	**–**	**18122**	**–**	**–**
Allison SGI Power Challenge						
communication	**585**	**182**	**N/A**	**N/A**	**N/A**	**N/A**
total solver time	**1278**	**673**	**N/A**	**N/A**	**N/A**	**N/A**
SGI Origin 2000						
communication	**268**	**153**	**264**	**–**	**–**	**3105**
total solver time	**781**	**403**	**327**	**–**	**–**	**5528**

N/A – not applicable (machine resources insufficient to performing the operation)

LACE: **NASA Lewis IBM RS–6000 cluster.**
Babbage: **NASA Ames IBM SP2 cluster**
Davinci: **NASA Ames SGI cluster**

Table 10.1: Tabulation of parallel computing CPU time estimates for platforms employed for the EEE LP Subsystem analysis (all times given are wall clock time on non-dedicated systems with precautions taken to eliminate outside loading factors).

processor is based on the total number of mesh cells contained within the blocks assigned to that processor. Thus, for a mesh system with widely varying mesh sizes, optimizing the block/processor assignment to balance the processor computational load can be a difficult task. This was exactly the case with the EEE LPS analysis. The smallest single mesh block in the EEE LPS mesh system contained 25 computational cells while the largest single mesh block contained 448,497 computational cells. This disparity in block size and the flexibility in the number of processors and the block/processor assignment strategy makes balancing the overall computational load in the parallel computing environment a very difficult proposition. Table 10.1 illustrates CPU time estimates based on three different numbers of processors (8, 16, 32). In each case, the block processor assignment strategy was to attempt to balance the computational load. No real bias was devoted to incorporating the communication overhead in the block/processor load balancing strategy. The block/processor assignment was not necessarily considered optimal, but should be reasonable in terms of providing a good estimate of the type of parallel computing performance which can be achieved in a production environment. The final factor controlling overall CPU time is the inter-processor communication load. The communication load, in turn, is governed by many factors including system hardware, communication library, and block/processor assignment. This area is often the limiting factor in determining the total number of processors which can be effectively applied to a large-scale CFD simulation. As more processors are added to attack a given problem, the individual CPU load goes down, while the communication requirements go up. The experience gained in this study suggests that for the current status of computer equipment (processor power, communication speed) a near optimal arrangement for multistage turbomachinery calculations was achieved when 1-2 processors was assigned for each blade row in the machine. For the complete EEE LPS simulation, this level was not acheived on every system tested as there were 15+ blade rows in every simulation, and several systems were limited to a maximum of 16 processors.

Overall, the following comments can be made concerning the parallel performance studies:

- Peak processing speed was acheived on a Silicon Graphics Origin 2000 using the SGI MPI 3.0 communication library.
- Estimated turnaround time for a single operating point was estimated to be 10 hours on the SGI Origin 2000 system using 32 processors.
- Load balance was non-optimal for the present mesh configuration. It seems entirely possible that significant improvements in parallel computing efficiency might be achieved through a more structured specification of mesh block dimensions in the overall problem.
- For the faster systems, parallel computing efficiency was still nearly linear with the addition of more processors. This implies that the problem could still be effectively acclerated if systems with larger numbers of processors (> 100) were available.

10.3 EEE LPS Design Point Simulation

Preliminary solutions for the EEE LP Subsystem model focused on demonstrating the solution convergence behavior and accuracy for engine design point analysis. For this simulation, the HP compressor and combustor were modeled through the appropriate boundary specifications for the engine HP compressor inlet and combustor exit planes. The boundary specifications were based on a design point engine cycle analysis derived from results from the NEPP computer code. Note that for this set of results, the HP turbine (normally considered a core, or HP subsystem component) was employed in the CFD model to permit a more reasonable specification of the spanwise flow profiles entering the LP turbine. Subsequent large-scale simulations of the LP Subsystem did not employ the CFD representation of the HP turbine as it was ultimately demonstrated that the LP turbine performance is relatively insensitive to inlet flow profile.

10.4 EEE LPS Shaft Power Balance

An important aspect of engine simulation, compared to component simulation, is that the mating of components often involves both aerodynamic *and* mechanical couplings. This concept is illustrated for both single-spool and twin-spool gas turbine engines in Figure 10.2. This concept is commonly employed in cycle deck analyses (e.g. *NEPP*) for components connected by a common shaft. The same concept can be applied to larger-scale simulations by providing the appropriate aerodynamic consistency between components (mass flow, etc.) as well as equating the overall power requirements for common shaft-mounted components. This balance was iteratively achieved in the present simulation through an iterative procedure which employed shaft rotational speed as the means of achieving the desired shaft power balance.

A series of solutions for the EEE/LP Subsystem was obtained for fixed shaft rotational speeds. For each shaft speed, computed power and torque for the rotating components were integrated for the rotating components of both the LP turbine and fan/booster-stage assemblies. Differences between the computed power/torque requirements for the fan and LP turbine assemblies were then employed to estimate a new shaft speed for the subsequent solution. Simple physical reasoning suggests that if there is power excess, then the shaft speed should increase, and if there is a power deficit, then the shaft speed should decrease. A simple linear interpolation was employed to estimate the updated shaft speed based on the integrated results from two previous solutions.

A portion of the iterative history of the ADPAC EEE LP shaft power balance is given in Table 10.2. As the shaft speed was reduced, the power required by the fan was reduced, while the power provided by the LP turbine increased. Eventually, these two power levels were essentially identical. The balance was deemed converged when the power balance was within 1%. Note that in spite of the changes to the LP system, the HP turbine power was relatively constant. This is essentially a result of the fact that the core performance was fixed during the shaft power balance procedure. The

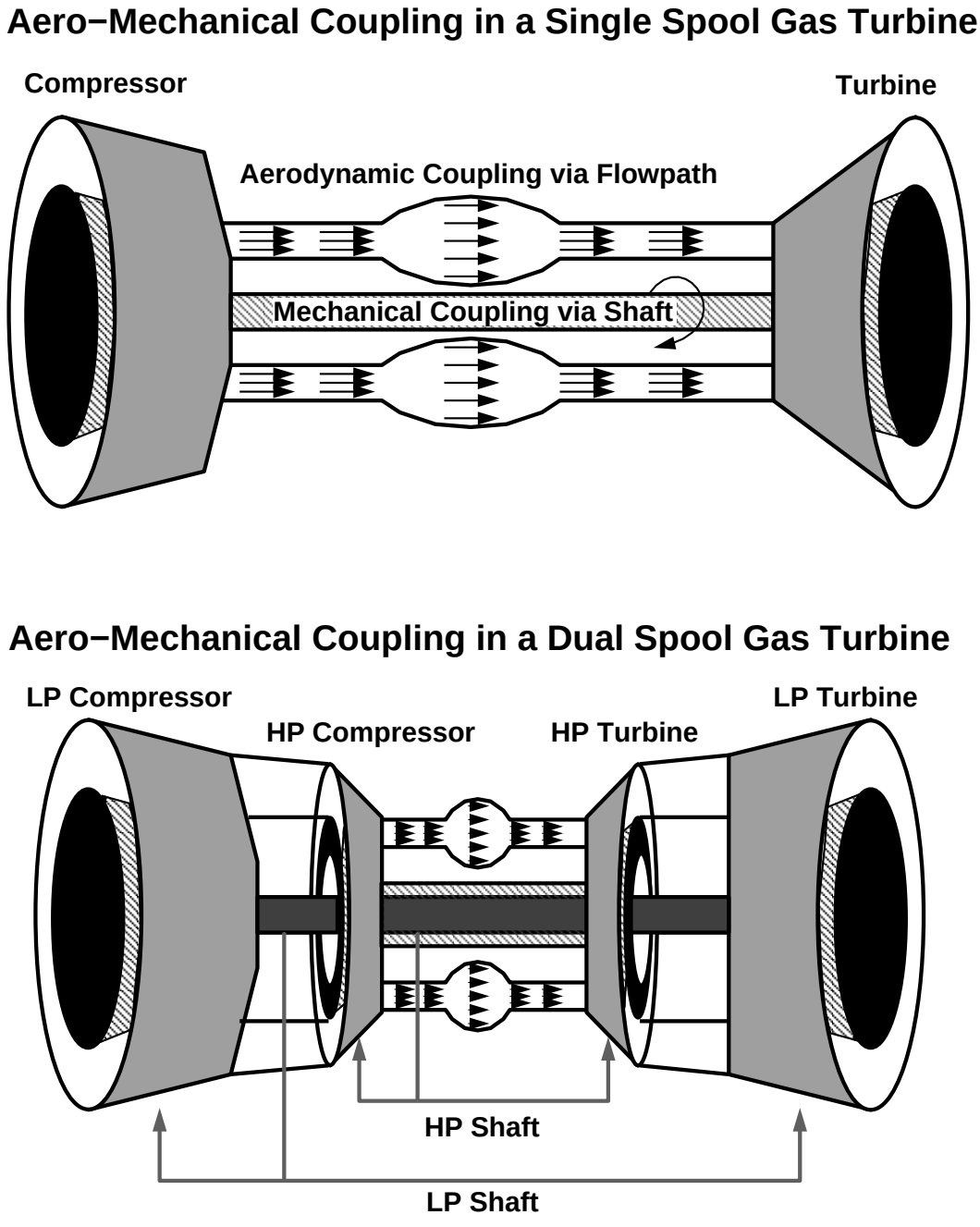

Figure 10.2: Illustration of aerodynamic/mechanical balance required for single-spool and twin-spool gas turbine engines.

ADPAC Solution (Fixed RPM/Fixed Core, ft−lbf/sec)

Shaft RPM	Fan	LP Turbine	HP Turbine
3507	8,622,000	6,947,200	12,634,000
3407	8,028,000	7,002,600	12,619,000
3250	7,522,300	7,301,400	12,557,000
3200	7,243,100	7,322,700	12,547,000

NEPP Solution (Design Point)

Shaft RPM	Fan	LP Turbine	HP Turbine
3538.5	8,182,000	8,182,000	11,625,300

Table 10.2: Tabulation of coarse mesh EEE LP Subsystem shaft power balance iterative results.

absolute power levels must be interpreted with the limitations of the CFD analysis in mind. The analysis was performed with a constant specific heat, when in fact, given the range of temperatures in the machine, the specific heat actually varies up to 5%. In addition, parasitic losses in the compressor (endwall leakages, cavity flows, etc.) have not been included in the analysis. The shaft power balance also assumes a 100% transmission efficiency (no bearing losses). These solutions were typically not run to full convergence as only an indicator of the level of power balance was required for the intermediate solutions during the balancing procedure. The primary intent at this point was to validate the convergence of the shaft power balance iterative process, and not necessarily isolate all of the individual features of the problem.

Also tabulated on Figure 10.2 are the corresponding power estimates from the NEPP cycle deck analysis for the design point. The most glaring discrepancy between the ADPAC and NEPP results is that the power generated by the HP turbine is lower and the power generated by the LP turbine is higher than the corresponding *ADPAC* predictions. It is clear that the predicted LP turbine power output is rather low compared to the NEPP cycle analysis data. This is believed to be due to the shrouded rotor cavity model applied for the LP turbine in the EEE/LP Subsystem analysis. It was demonstrated in the component validation study that the present shrouded rotor cavity model can result in a 3%-5% reduction in turbine efficiency, which would explain much of the noted discrepancy. In addition, it should be noted that the data obtained from the *NEPP* cycle model represents operation along constant *operating lines*, while the *ADPAC* simulation is obtained along fixed *speed lines*. This subtle difference is illustrated in Figure 10.3.

Other potential influences may be due to cooling flows or specific heat ratio variations.

The convergence of the shaft power balance is something of a milestone effort, representing solutions which are both aerodynamically consistent (within the limitations of the CFD model, of course), and mechanically consistent.

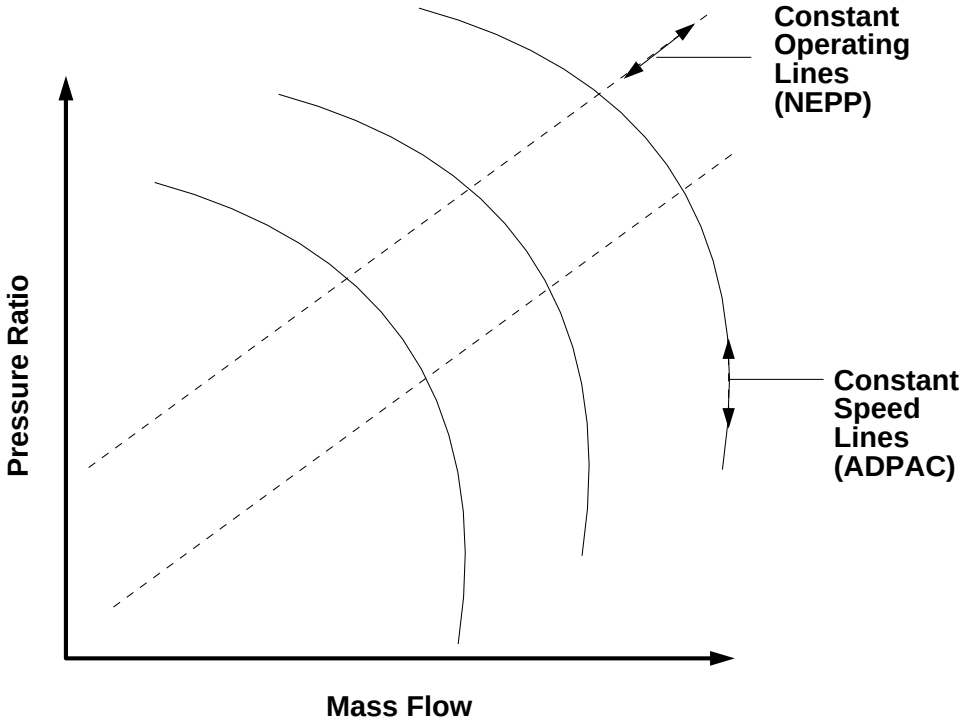

Figure 10.3: Illustration of *NEPP* solution along constant *operating lines* and *ADPAC* solution along constant *speed lines*.

(This page intentionally left blank)

Chapter 11

ADPAC/NEPP Engine Analysis

11.1 *ADPAC/NEPP* Coupling Procedure

Following the completion of the effort to develop an LP Subsystem shaft power balance computational procedure, the logical next step in the LP Subsystem analysis was to couple the 3-D ADPAC predictions with a lower order (cycle deck) analysis of the core component performance. This coupling is consistent with the "zooming" philosophy inherent in the NPSS system architecture. In the present application, the core cycle model was based on predictions from the *NEPP* code. In order to incorporate the *NEPP* results in a systematic fashion, the various interactions between the NEPP core model and the *ADPAC* LP Subsystem model must be addressed. One interpretation of these interactions is outlined schematically in Figure 11.1. The specifications required from NEPP for the ADPAC analysis are an estimate of the core compressor inlet flow (represented initially by a static pressure which is used to set the flow in the ADPAC solution), and a specification of the HP turbine inlet total pressure and total temperature profiles describing the flow out of the EEE combustor. The specifications required from the ADPAC analysis for the NEPP analysis include the core compressor inlet total pressures, temperature and velocities (which result from the CFD analysis of the fan section). Intertwined in this cross specification is the fact that the LP shaft RPM may change as the overall solution evolves, and the level and frequency by which the exchanged boundary data between the two analyses occurs may be critical. It would also be useful if the ADPAC LP Subsystem analysis solution could be initiated based on cycle predictions from the NEPP code. This would essentially eliminate the complex solution initialization process required for ADPAC analysis for this complex problem. This procedure was, unfortunately, not available for the current set of calculations.

The computational system resulting from the combined *NEPP/ADPAC* computational procedure is illustrated graphically in Figure 11.2. Since this procedure was designed for demonstration purposes, the coupling between the *ADPAC* and *NEPP* analyses was controlled by a UNIX shell script which sequentially applied the analyses in an iterative fashion. Following the application of each analyses, the appropriate flow information was extracted from output files by hardwired programs developed

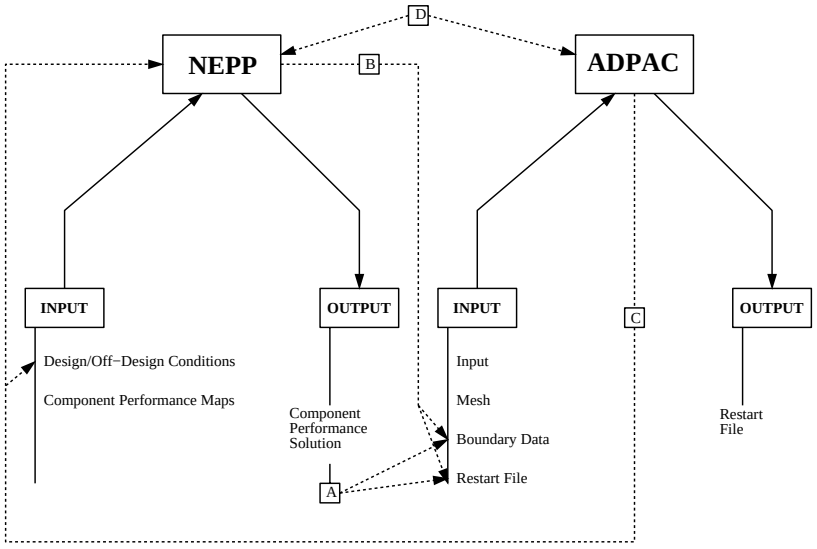

ADPAC/NEPP Interaction

A. Use NEPP output to create ADPAC Boundata and Restart files
   1. No direct link between NEPP and APAC
   2. NEPP output file updates EXIT and INLET conditions and RPM boundata file
   3. NEPP output file creates ADPAC restart file to aid in "start−up" process
B. Create coding changes in NEPP to perform A
C. Use SYSTEM call in ADPAC boundata file to run NEPP from ADPAC
D. Use front−end script to control NEPP−ADPAC interations

Figure 11.1: Coupled ADPAC/NEPP analysis schematic data flow representation.

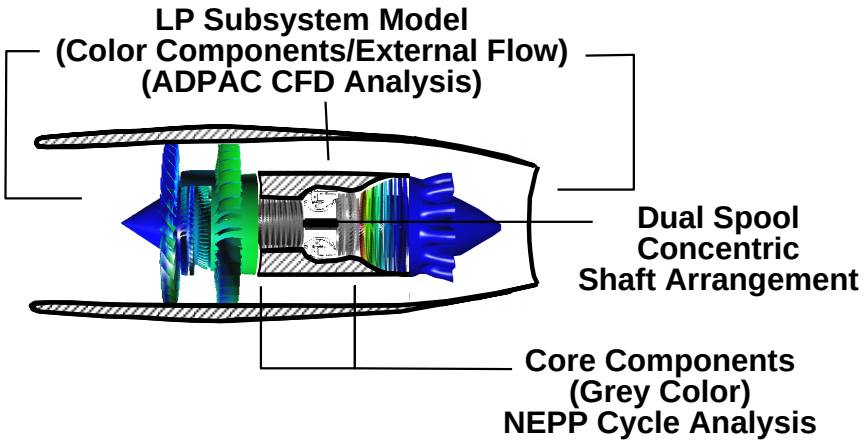

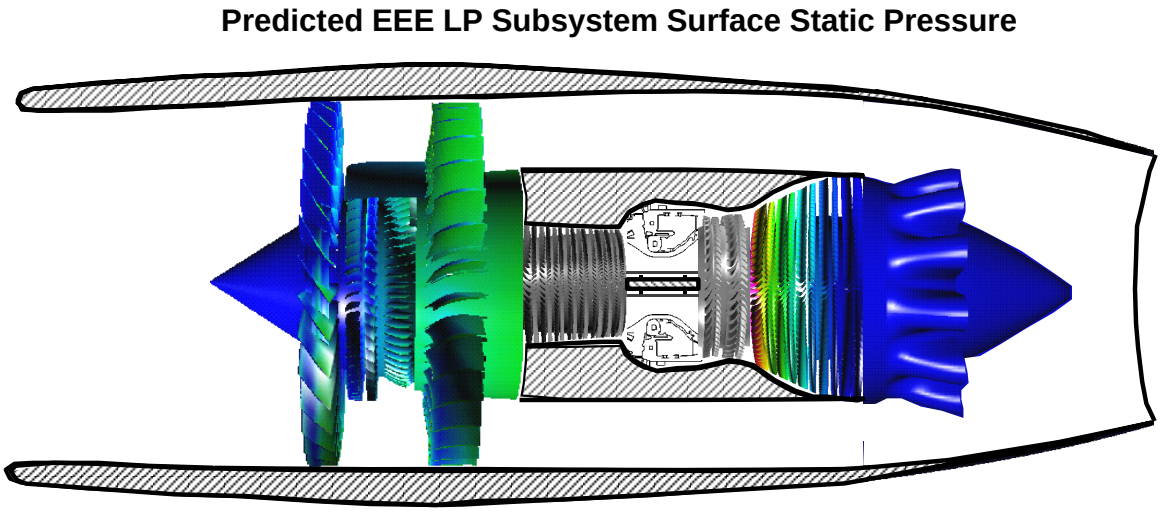

Figure 11.2: Illustration of coupled ADPAC/NEPP prediction for the EEE LP Subsystem (color contours indicate predicted static pressure ratio: red-10.0, blue-0.36, grey scale components are represented by the NEPP cycle analysis).

specifically for these two codes, and based specifically on the format of the output for each codes. This was, unfortunately an inflexible system, but did have the advantage that it could be assembled rather quickly to demonstrate the overall concept.

A solution for the EEE/LP Subsystem using the coupled *ADPAC/NEPP* solution strategy was obtained for the design operating point. Problems encountered during the initial tests of the solution procedure were traced to excessive variations in the boundary specifications during the initial phases of the calculations. These excursions were modulated using a simple under-relaxation procedure. The behavior of the overall solution procedure was then relatively stable, albeit very slow. Individual *ADPAC solutions* acquired during the iterative cycle can take up to 8 hours on a parallel system, with some 10-20 iterations required to achieve complete coupling between the ADPAC and NEPP analyses.

It should be noted that the present demonstration did not employ the LP shaft power balance procedure which would be essential to complete the coupled solution procedure. At this point, a demonstration of the concept was considered of primary importance. The capability demonstrated through this exercise validates the NPSS primary objective of "*zooming*", and can hopefully lead to further research in employing this type of analysis for future gas turbine engine studies.

Chapter 12

CONCLUSIONS

Computational Fluid Dynamics (CFD) analysis of the complete Low Pressure (LP) Subsystem of the General Electric Energy Efficient Engine (EEE) was demonstrated. This study identified several important topical areas to consider in the planning and execution of large-scale simulations of complete gas turbine engine propulsion systems. The topical areas include geometry manipulation, mesh generation, solution initialization, application of parallel computing, full-scale engine simulation, and interpretation of computational results. Each area is discussed in the sections below.

12.1 Geometry Manipulation

This study served to identify both the strengths and the weaknesses of the consistent geometry database representation strategy. The NASA EEE Master Engine Geometry Database package evaluated and updated during this study consists of a collection of IGES curve-based and surface-based entities which define the primary flowpaths and bladed elements in the EEE engine. The component validation study served to validate many of these geometry representations through both the mesh generation process and the comparison of CFD prediction with test data. The contributions to the geometry database elements derived from this study included the following:

- A one degree (open) reset was applied to the LP turbine first stage vane, based on both computational results and discussions with engineers from General Electric Corporation familiar with the design.
- The construction of an axisymmetric representation of the LP turbine shrouded rotor endwall seal cavities was also performed. These geometry elements were constructed by hand based on interpretations of published drawings of the actual test rig hardware.
- Some of the original geometry elements in the Master Engine Geometry Database package were mislabeled (rotors and stators swapped). These corrections were subsequently reported to NASA so that the database could be updated.

Shortcomings of the IGES database geometry representation identified during this study included the following:

- A lack of variable geometry capability hinders the analysis of HP compression systems. Specifically, the rotational axes of variable setting stators should be defined to permit adjustment representative of the actual compression system geometry under off-design operating conditions.

- Some identification of engine secondary flow systems such as customer bleed and cooling flow bleed from the HP compression system, coolant flow injection in the HP turbine, and drum/cavity purge flows such as found in both HP and LP turbine should be considered.

- Variations of the geometry with temperature should be identified in some fashion. At present, it is not well understood whether the geometry elements are the hot or cold (as manufactured) representations.

- The ability to model statistical variations in the geometry such as might occur due to manufacturing tolerances or erosion would also be useful.

All of these elements point to the need for a flexible geometry manipulation tool which could act in concert with the mesh generation/CFD procedures described in this report.

12.2 Mesh Generation

A relatively simple mesh generation procedure was established during this project which employed the geometry database described in Chapter 3. Based on the IGES entity blade and flowpath definitions, sheared H-type mesh systems could be rapidly generated for multistage compressor or turbine flows. It has been acknowledged that the mesh systems are non-optimal in the sense that orthogonality and mesh aspect ratio are somewhat compromised for the convenience and simplicity of this nearly automated procedure. The analyses described in this report are in no way limited to this type of mesh system. Complete automation of the mesh generation procedure for arbitrary engine configurations would be a significant accomplishment, and was beyond the scope of this study. Some estimates of the sensitivity of the solution to the mesh density was afforded through the examination of results from "coarsened" mesh systems derived by eliminating every other point from an original "fine" mesh. It is unlikely that the solutions presented for the LP Subsystem simulation were mesh independent as the number of grid points was typically minimized to reduce the overall solution computation time. A full IGES-compatible parser could also be added to the *SEARCH* program (the current version of the program is limited to specific IGES entity designations).

12.3 Solution Initialization

Some general comments regarding solution initialization seem appropriate given the magnitude of the computational effort and the numerical difficulties presented during this large-scale simulation. The ideal solution initialization procedure would be to have a collection of 3-D CFD isolated component analyses derived with appropriate boundary conditions such that an overall representation of the flow could be generated by simply assembling the individual component data. This procedure was, in effect, verified following the component validation study. Another reasonable approach would be to employ 2-D engine simulations from which an axisymmetric 3-D solution initialization field could be established. Further down the ladder defined by this type of hierarchy would be extending 1-D or cycle deck simulations to the 3-D space through some sort of interpolation system. Naturally this interplation is somewhat arbitrary as the extension of lower order data to the higher order system has many possible solutions. Finally, least desirable is initialization of the solution from an essentially meaningless initial condition (uniform flow). It was demonstrated that it is possible to generate the LP Subsystem simulations from the lowest order initialization routine, but that this process required a "stair-stepping" of the boundary pressure and temperature specifications in order to avoid overwhelming the simulation with nonrealistic pressure or temperature ratios. The development of automated couplings between the 3-D and lower order analyses of the types described above (2-D and 1-D/cycle analyses) would afford a great simplification in the solution initialization procedure, and also accelerate the generation of results when evaluating a new operating condition.

12.4 Application of Parallel Computing

Parallel computing constructs were used extensively during this project, and included architectures based on multiprocessor shared-memory computers, to distributed memory, network-connected workstation clusters. The analysis was demonstrated under four different parallel computing environments of both NASA and industry origin. Overall, the best performance was achieved by assigning approximately one blade row per processor in the parallel computing environment, as this afforded the best compromise between processor load and communication overhead. Parallel computing efficiencies on the order of 75% were achieved during this study for the large-scale simulations. Load balancing ultimately became the issue which was the greatest obstacle for improving performance. Careful planning of grid distributions would help to reduce this problem, although the large variations in length scales for the components in a complete engine simulation make grid distribution a difficult task.

12.5 Full-Scale Engine Simulation

Full-scale engine simulations of the GE EEE engine were demonstrated during this study based on the 3-D CFD LP Subsystem simulation coupled with the NEPP cycle

deck core simulation. Multidisciplinary coupling of common spool components was achieved through the application of a shaft power balance. This procedure demonstrated both aerodynamic and mechanical coupling of the LP shaft components by varying the shaft rotational speed until a mechanical power balance was achieved. This requirement is nearly always overlooked in other reported "full-scale" engine simulations. The iterative process to achieve the shaft power balance was accelerated through the use of the *ADPAC* mesh sequencing and multigrid capability, which permits early iterations of the shaft power balance on coarser meshes before proceeding with the process on the more computationally expensive finer mesh.

Direct coupled analyses of the engine operation employing both the 3-D *ADPAC* LP simulation and the *NEPP* HP/combustor simulation were also successfully developed. This procedure demonstrated a two-way coupling between the analyses to derive the engine operating condition. This type of analysis features the NPSS "zooming" concept whereby a portion of the engine is simulated on one level of fidelity, while other components are simulated at a different fidelity level.

12.6 Interpretation of Computational Results

By and large, all of the computational result developed in this study exhibited qualitative agreement with available data, and did not display any gross violations of the expected physical behavior for a given component or collection of components. Some comments on the order of accuracy of the analysis are, however, appropriate at this time. The mesh sensitivity of the results was discussed earlier, and will not be repeated here. Certain aspects of the calculations possessed known errors such as the use of non-varying specific heat ratio in the simulations. Other factors contributing to errors include omission of windage and mechanical drag in the shaft power balance, slight inconsistencies in mass flow due to the 2-D LP turbine shrouded rotor cavity model, and the application of adiabatic wall boundary conditions throughout the machine. Given these known inconsistencies, detailed evaluation of engine performance parameters (i.e., specific fuel consumption (SFC), thrust, etc.) makes little sense, and therefore no attempt was made to correlate predicted and experimental values of this nature.

12.7 Recommendations for Future Study

Given the demonstrated capability of complete engine simulation, a natural extension to this work would be to remove the inconsistencies described above, and to proceed with the effort to validate the engine operation prediction capabilities of this scheme with actual engine data. Large amounts of data exist for simpler, single-shaft engine configurations which could be used to evaluate the predicted capabilities of this scheme.

Enhancing the capabilities of the geometry database is also considered a priority. Several details related to this effort are described above under the geometry section.

Finally, additional studies directed at the evaluation of secondary flow systems effects on primary gas flowpath performance would serve to define what level of fidelity is required to incorporate the overall engine performance effect of these "real world" components. Simulations of this type have been performed for isolated compressor airfoils employing inner banded stators [143]. Similar analyses for multistage compressor and turbine systems incorporating secondary flow systems models could be performed to assess the relative impact of these gas path features.

(This page intentionally left blank)

Bibliography

[1] http://www.aero.hq.nasa.gov/hpcc/

[2] http://cas-www.arc.nasa.gov/general.html

[3] http://www.lerc.nasa.gov/WWW/CISO/projects/NPSS/

[4] Fagan, J. R., and Hall, E. J., "Mixing Mechanisms in Multistage Compressors," to appear in *Advanced Turbomachinery Design*, Mercel-Dekker, Inc., 1997.

[5] Hall, E. J., "Aerodynamic Modeling of Multistage Compressor Flowfields-Part 1: Analysis of Rotor/Stator/Rotor Aerodynamic Interaction," ASME Paper 97-GT-344, 1997.

[6] Hall, E. J., "Aerodynamic Modeling of Multistage Compressor Flowfields-Part 2: Analysis of Rotor/Stator/Rotor Aerodynamic Interaction," ASME Paper 97-GT-345, 1997.

[7] Adamczyk, J. J., Celestina, M. L., Beach, T. A., and Barnett, M., "Simulation of Three-Dimensional Viscous Flow Within a Multistage Turbine," ASME Paper 89-GT-152, 1989.

[8] Saunders, N. T., Colladay, R. S., and Macioce, L. E., "Design approaches to more energy efficient engines," AIAA and SAE 14th Joint Propulsion Conference, Las Vegas, Nevada, July 25-27, 1978.

[9] Klineberg, J. M., "The NASA Aircraft Energy Efficiency Program," *Canadian Symposium on Energy Conserving Transport Aircraft, Ottawa, Canada, October 3-4, 1977, Proceedings,* A78-31301 12-05, Ottawa, Canadian Aeronautics and Space Institute, 1978.

[10] Klineberg, J. M., "The NASA Aircraft Energy Efficiency program," *Energy and aerospace; Proceedings of the Anglo/American Conference, London, England,, December 5-7, 1978,* A79-31908 12-44, London, Royal Aeronautical Society, 1979.

[11] Chamberlin, R. and Miller, B., "Energy efficient aircraft engines," AIAA Aircraft Systems and Technology Meeting, New York, New York, 1979.

[12] Mayfield, J., "Manufacturers developing fuel-efficient engines," *Aviation Week and Space Technology,* vol. 110, May 28, 1979.

[13] Klineberg, J. M., "Technology for aircraft energy efficiency," *International Air Transportation Conference, Washington, D.C., April 4-6, 1977, Proceedings,* A79-14126 03-03, American Society of Civil Engineers, New York, 1977.

[14] Saunders, N. T., "Advanced component technologies for energy-efficient turbofan engines," AIAA, SAE, and ASME 16th Joint Propulsion Conference, Hartford, Connecticut, June 30-July 2, 1980.

[15] Kingcombe, R. C. and Dunning, S. W., "Design study for a fuel efficient turbofan engine," ASME Gas Turbine Conference and Products Show, New Orleans, Louisiana, March 10-13, 1980.

[16] Crow, D. E., Welna, H., Singer, I. D., and Vanco, M. R., "Results from tests on a high work transonic turbine for an energy efficient engine," ASME Gas Turbine Conference and Products Show, New Orleans, Louisiana, March 10-13, 1980.

[17] Kozlowski, H. and Kraft, G., "Experimental evaluation of exhaust mixers for an Energy Efficient Engine," AIAA, SAE, and ASME 16th Joint Propulsion Conference, Hartford, Connecticut, June 30-July 2, 1980.

[18] Gardner, W. B. and Gray, D. E., "The Energy Efficient Engine E^3 - Advancing the state of the art," ASME Gas Turbine Conference and Products Show, New Orleans, Louisiana, March 10-13, 1980.

[19] Kuchar, A. P. and Chamberlin, R., "Scale model performance test investigation of exhaust system mixers for an Energy Efficient Engine E^3 propulsion system," AIAA 18th Aerospace Sciences Meeting, Pasadena, California, January 14-16, 1980.

[20] Gliebe, P. R., Sandusky, G. T., and Chamberlin, R., "Mixer nozzle aeroacoustic characteristics for the energy efficient engine," AIAA 7th Aeroacoustics Conference, Palo Alto, California, October 5-7, 1981.

[21] Macioce, R, Schaefer, J. W., and Saunders, N. T., "A status report on the Energy Efficient Engine Project," SAE Aerospace Congress and Exposition, Los Angeles, California, October 13-16, 1980.

[22] Sabla, P. E., Taylor, J. R., and Gauntner, D. J., "Design and development of the combustor inlet diffuser for the NASA/GE energy efficient engine," ASME Gas Turbine Conference and Products Show, Houston, Texas, March 9-12, 1981.

[23] Sokolowski, D. E. and Rohde, J. E., "The E3 combustors - Status and challenges," AIAA, SAE, and ASME 17th Joint Propulsion Conference, Colorado Springs, Colorado, July 27-29, 1981.

[24] Gardner, W. B., Hannah, W., and Gray, D. E., "Interim review of the Energy Efficient Engine E^3 Program," ASME 27th International Gas Turbine Conference and Exhibit, London, England, April 18-22, 1982.

[25] Bucy, R. W., "Progress in the development of energy efficient engine components," ASME 27th International Gas Turbine Conference and Exhibit, London, England, April 18-22, 1982.

[26] Gardner, W. B., "Energy efficient engine E^3 technology status," AIAA, SAE, and ASME 18th Joint Propulsion Conference, Cleveland, Ohio, June 21-23, 1982.

[27] Greene, W., Tanrikut, S., and Sokolowski, D. E., "Development and operating characteristics of an advanced two-stage combustor," AIAA 20th Aerospace Sciences Meeting, Orlando, Florida, January 11-14, 1982.

[28] Sullivan, T. J. and Hager, R. D., "The aerodynamic design and performance of the General Electric/NASA EEE fan," AIAA, SAE, and ASME 19th Joint Propulsion Conference, Seattle, Washington, June 27-29, 1983.

[29] Kuchar, A. P. and Chamberlin, R., "Comparison of full-scale engine and subscale model performance of a mixed flow exhaust system for an energy efficient engine (E^3) propulsion system," AIAA 22nd Aerospace Sciences Meeting, Reno, Nevada, January 9-12, 1984.

[30] Storace, A. F. and Cline, S. J., "NASA-General Electric Energy Efficient Engine high load squeeze film damper-system analysis and test results," AIAA, SAE, and ASME 20th Joint Propulsion Conference, Cincinnati, Ohio, June 11-13, 1984.

[31] Cherry, D. G. and Dengler, R. P., "The aerodynamic design and performance of the NASA/GE E^3 low pressure turbine," AIAA, SAE, and ASME 20th Joint Propulsion Conference, Cincinnati, Ohio, June 11-13, 1984.

[32] Lavin, S. P., Ho, P. Y., and Chamberlin, R., "Measurement and prediction of Energy Efficient Engine noise," AIAA and NASA 9th Aeroacoustics Conference, Williamsburg, Virgina, October 15-17, 1984.

[33] Lavin, S. P., Ho, P. Y., and Chamberlin, R., "Comparison of scaled model data to full size energy efficient engine test results," AIAA and NASA 9th Aeroacoustics Conference, Williamsburg, Virgina, October 15-17, 1984.

[34] Ciepluch, C. C., Davis, D. Y. and Gray, D. E., "Results of NASA's Energy Efficient Engine Program," *Journal of Propulsion and Power* (ISSN 0748-4658), vol. 3, November-December 1987, p. 560-568.

[35] Hampton, T. L., "Energy efficient engine component development and integration program Semiannual Report, 1 Apr. - 30 Sep. 1980," NASA CR-175322, 1980.

[36] Rowe, R. K. and Kuchar, A. P., "Energy Efficient Engine (E^3): Scaled mixer performance report - Final Report," NASA CR-167947, November 1982.

[37] "Energy efficient engine component development and integration program: Original work plan," NASA CR-183155, May 1978.

[38] "Energy efficient engine preliminary design and integration studies - Final Report," NASA CR-183382, February 1978.

[39] "Energy efficient engine integrated core/low spool test vehicle," NASA CR-188054, 1980.

[40] Hemsworth, M. C., "Energy efficient engine flight propulsion system preliminary design review. Executive summary," NASA CR-183211, 1978.

[41] Johnston, R. P., Hemsworth, M. C., "Energy efficient engine preliminary design and integration studies," June 1978.

[42] Johnston, R. P., Hirschkron, R., Koch, C. C., Neitzel, R. E. and Vinson, P. W., "Energy efficient engine: Preliminary design and integration studies - Final Report, Jan. 1977 - Apr. 1978," NASA CR-135444, September 1978.

[43] Gray, D. E., "Energy efficient engine preliminary design and integration study," NASA CR-135396, PWA-5500-18, November 1978.

[44] Chamberlin, R. and Miller, B., "Energy efficient aircraft engines," AIAA Aircraft Systems Meeting, New York, New York, August 20-22, 1979, NASA TM-79204, 1979.

[45] Owens, R. E., "Energy efficient engine: Propulsion system-aircraft integration evaluation - Topical Report, Mar. 1978 - Sep. 1978," NASA CR-159488, PWA-5594-48, March 1979.

[46] Gardner, W. B., "Energy efficient engine flight propulsion system preliminary analysis and design report - Progress Report, Mar. 1978 - Feb. 1979," NASA CR-159487, PWA-5594-49, May 1979.

[47] Burrus, D., Sabla, P. E., and Bahr, D. W., "Energy efficient engine," NASA CR-159685, R79AEG562, June 1980.

[48] Saunders, N. T., "Advanced component technologies for energy-efficient turbofan engines," AIAA, ASME and SAE 16th Joint Propulsion Conference, Hartford, Connecticut, June 30 - July 2, 1980, NASA TM-81507, E-445, 1980.

[49] Macioce, L. E., Schaefer, J. W., and Saunders, N. T., "The energy efficient engine project - Status Report," NASA TM-81566, E-531, 1980.

[50] Clyman, M., Einhorn, S. J., and Shultz, R. S., "Compilation of energy efficient concepts in advanced aircraft design and operations. Volume 1: Technical report - Final Report, 10 Mar. - 5," AD-A094225, NADC-79239-60-VOL-1, November 1980.

[51] Patt, R. F., "Energy efficient engine flight propulsion system: Aircraft/engine integration evaluation - Status Report, Jan. 1978 - Nov. 1978," NASA CR-159584, R79AEG274, June 1980.

[52] Johnston, R. P., Beitler, R. S., Bobinger, R. O., Broman, C. L., Gravitt, R. D., Heineke, H., Holloway, P. R., Klem, J. S., Nash, D. O., and Ortiz, P., "Energy efficient engine: Flight propulsion system preliminary analysis and design - Topical Report, Jan. - Nov. 1978," NASA CR-159583, R79AEG623, June 1980.

[53] Sokolowski, D. E. and Rohde, J. E., "The E3 combustors: Status and challenges," NASA TM-82684, E-904, 1981.

[54] "A look at NASA's Aircraft Energy Efficiency program," PSAD-80-50, July 1980.

[55] Kozlowski, H., and Larkin, M., "Energy efficient engine exhaust mixer model technology," NASA CR-165459, PWA-5594-164, June 1981.

[56] Michael, C. J., "Energy efficient engine shroudless, hollow fan blade technology report," NASA CR-165586, PWA-5594-199, December 1981.

[57] Michael, C. J., and Halle, J. E., "Energy efficient engine low-pressure compressor component test hardware detailed design report," NASA CR-165354, PWA-5594-157, June 1981.

[58] Broman, C. L., "Energy efficient engine. Core engine bearings, drives and configuration: Detailed design report," NASA CR-165376, R81AEG307, June 1981.

[59] "Energy efficient engine component development and integration program - Semiannual Report, 1 Oct. 1980 - 31 Mar. 1981," NASA CR-170089, R81AEG316, SAR-6, January 1981.

[60] Dubiel, D. J., Greene, W., Sundt, C. V., Tanrikut, S., and Zeisser, M. H., "Energy efficient engine sector combustor rig test program," NASA CR-167913, PWA-5594-180, October 1981.

[61] Giamel, A. F., Salkeld, R. W., and Hayes, C. W., "Energy efficient engine high-pressure turbine single crystal vane and blade fabrication technology report," NASA CR-165400, PWA-5594-152, July 1981.

[62] Sullivan, T. J., "Energy efficient engine: Fan test hardware detailed design report," NASA CR-165148, R80AEG417, October 1980.

[63] Gardner, W. B., "Energy efficient high-pressure turbine leakage technology report," NASA CR-165202, PWA-5594-106, December 1980.

[64] Leach, K., Thulin, R. D., Howe, D. C., "Energy efficient engine: Turbine intermediate case and low-pressure turbine component test hardware detailed design report," NASA CR-167973, PWA-5594-191, January 1982.

[65] Halle, J. E. and Michael, C. J., "Energy efficient engine fan component detailed design report," NASA CR-165466, PWA-5594-165, September 1981.

[66] "Energy efficient engine component development and integration program - Semiannual Status Report, 1 Apr. - 30 Sep. 1980," NASA CR-173884, NAS 1.26:173884, SASR-5, PWA-5594-142, 1981.

[67] Batterton, P. G., "Energy efficient engine program contributions to aircraft fuel conservation," NASA TM-83741, 1981.

[68] Kopper, F. C., Milano, R., Davis, R. L., Dring, R. P., and Stoeffler, R. C., "Energy efficient engine high-pressure turbine supersonic cascade technology report," NASA CR-165567, PWA-5594-152, November 1981.

[69] Sharma, O. P., Kopper, F. C., Knudsen, L. K., and Yustinich, J. B., "Energy efficient engine: Low-pressure turbine subsonic cascade component development and integration program," NASA CR-165592, PWA-5594-167, January 1982.

[70] Stearns, E. M., "Energy efficient engine: Flight propulsion system, preliminary analysis and design update - Topical Report, Nov. 1978 - Jul. 1982," NASA CR-167980, R82AEB532, November 1982.

[71] Thulin, R. D., Howe, D. C., and Singer, I. D., "Energy efficient engine high-pressure turbine detailed design report," NASA CR-165608, PWA-5594-171, January 1982.

[72] Broman, C. L., "Energy efficient engine ICLS engine bearings, drives and configuration: Detail design report," NASA CR-167871, R81AEG821, June 1982.

[73] Nelson, W. A., and Carlson, R. G., "Energy efficient engine high pressure turbine ceramic shroud support technology report," NASA CR-168036, R82AEB399, 1982.

[74] Cline, S. J., Halter, P. H., Kutney, J. T., and Sullivan, T. J., "Energy efficient engine. Fan and quarter-stage component performance report," NASA CR-168070, R82AEB408, January 1983.

[75] Bisset, J. W., and Howe, D. C., "Energy efficient engine flight propulsion system preliminary analysis and design report - Final Update Report," NASA CR-174701, PWA-5594-248, September 1983.

[76] "Energy efficient engine component development and integration program - Semiannual Status Report, 1 Oct. 1981 - 31 Mar. 1982," NASA CR-172846, PWA-5594-202, May 1982.

[77] Leach, K. P., "Energy efficient engine high-pressure turbine component rig performance test report," NASA CR-168189, PWA-5594-243, 1983.

[78] Cherry, D., Gay, C. H., and Lenahan, D. T., "Energy efficient engine low pressure turbine test hardware detailed design report," NASA CR-167956, R81AEG597, 1982.

[79] Zeisser, M. H., Greene, W., and Dubiel, D. J., "Energy efficient engine combustor test hardware detailed design report," NASA CR-167945, PWA-5594-197, March 1982.

[80] Duderstadt, E. C. and Agarwal, P., "Energy efficient engine, high pressure turbine thermal barrier coating. Support technology report," NASA CR-168037, R82AEB293, 1983.

[81] Eskridge, R. R., Kuchar, A. P., and Stotler, C. L., "Energy efficient engine ICLS Nacelle detail design report," NASA CR-167870, R81AEG700, July 1982.

[82] "Energy efficient engine component development and integration program - Semiannual Report, 1 Apr. - 30 Sep. 1981," NASA CR-170034, R81AEG709, SAR-7, 1982.

[83] Holloway, P. R., Koch, C. C., Knight, G. L., and Shaffer, S. L., "Energy efficient engine. High pressure compressor detail design report," NASA CR-165558, R81AEG710, 1982.

[84] Halila, E. E., Lenahan, D. T., and Thomas, T. T., "Energy efficient engine high pressure turbine test hardware detailed design report," NASA CR-167955, R81AEG284, June 1982.

[85] Beitler, R. S. and Lavash, J. P., "Energy Efficient Engine (E3) controls and accessories detail design report," NASA CR-168017, R82AEB400, December 1982.

[86] Larkin, M. J., and Blatt, J. R., "Energy Efficient Engine exhaust mixer model technology report addendum; phase 3 test program," NASA CR-174799, PWA-5594-271-ADD, May 1984.

[87] Howe, D. C. and Wynosky, T. A., "Energy Efficient Engine program advanced turbofan nacelle definition study," NASA CR-174942, PWA-5394-315, May 1983.

[88] Dubiel, D. J., Lohmann, R. P., Tanrikut, S., and Morris, P. M., "Energy efficient engine pin fin and ceramic composite segmented liner combustor sector rig test report," NASA CR-179534, PWA-5594-333, September 1986.

[89] Gray, D. E., and Gardner, W. B., "Energy efficient engine program technology benefit/cost study, volume 2," NASA CR-174766-VOL-2, PWA-5594-251-VOL-2, October 1983.

[90] Burrus, D. L., Chahrour, C. A., Foltz, H. L., Sabla, P. E., Seto, S. P., and Taylor, J. R., "Energy Efficient Engine (E3) combustion system component technology performance report - Draft Report," NASA CR-168274, R82AEB401, July 1984.

[91] Davis, D. Y., and Stearns, E. M., "Energy Efficient Engine: Flight propulsion system final design and analysis - Report, Nov. 1978 - Aug. 1983," NASA CR-168219, R83AEB488, 1983.

[92] Stearns, E. M., "Energy Efficient Engine core design and performance report - Report, Jan. 1978 - Dec. 1982," NASA CR-168069, R82AEB470, 1983.

[93] Bisset, J. W. and Howe, D. C., "Energy Efficient Engine integrated core/low spool test hardware design report," NASA CR-168137, PWA-5594-231, March 1983.

[94] Lavin, S. P., and Ho, P. Y., "Energy Efficient Engine acoustic supporting technology report," NASA CR-174834, R84AEB246, June 1985.

[95] Beitler, R. S., and Bennett, G. W., "Energy Efficient Engine: Control system component performance report," NASA CR-174651, R83AEB623, October 1984.

[96] Dubiel, D. J., "Energy Efficient Engine: Combustor component performance program," NASA CR-179533, PWA-5594-329, September 1986.

[97] Gray, D. E. and Gardner, W. B., "Energy efficient engine program technology benefit/cost study. Volume 1: Executive summary," NASA CR-174766-VOL-1, PWA-5594-258-VOL-1, October 1983.

[98] Burrus, D. L., Chahrour, C. A., Foltz, H. L., Sabla, P. E., Seto, S. P., and Taylor, J. R., "Energy Efficient Engine combustor test hardware detailed design report," NASA CR-168301, R82AEB472, March 1984.

[99] Stearns, E. M., "Energy Efficient Engine integrated core/low spool design and performance report - Topical Report, Jan. 1978 - Aug. 1983," NASA CR-168211, R83AEB503, February 1985.

[100] Timko, L. P., "Energy Efficient Engine high pressure turbine component test performance report," NASA CR-168289, R82AEB406, 1984.

[101] Bridgeman, M. J., Cherry, D. G., and Pedersen, J., "NASA/GE Energy Efficient Engine low pressure turbine scaled test vehicle performance report - Topical Report, 1979-1982," NASA CR-168290, R83AEB143, July 1983.

[102] Howe, D. C., "Energy Efficient Engine: Control system preliminary definition report," NASA CR-179578, PWA-5594-331, September 1986.

[103] Howe, D. C., and Marchant, R. D., "Energy Efficient Engine: High-pressure compressor test hardware detailed design report," NASA CR-180850, PWA-5594-287, March 1988.

[104] PATRAN User's Manual, MacNeal-Schwindler Corporation Version 1.4-2.

[105] Anderson, D. A., Tannehill, J. C., and Pletcher, R. H. , "Computational Fluid Mechanics and Heat Transfer," McGraw-Hill, New York, New York, 1984.

[106] Barber, T., Choi, D., McNulty, G., Hall, E., and Delaney, R., "Preliminary Findings in Certification of ADPAC," AIAA Paper 94-2240, June 1994.

[107] Hall, E. J., and Delaney, R. A., "Investigation of Advanced Counterrotation Blade Configuration Concepts for High Speed Turboprop Systems: Task VII - ADPAC User's Manual," NASA Contract NAS3-25270, NASA CR-195472, July 1995.

[108] Jameson, A., Schmidt, W., and Turkel, E., "Numerical Solutions of the Euler Equations by Finite Volume Methods Using Runge-Kutta Time-Stepping Schemes," AIAA Paper 81-1259, 1981.

[109] Arnone, A. A., Liou, M. S., and Povinelli, L. A., "Multigrid Time-Accurate Integration of Navier-Stokes Equations," AIAA Paper 93-3361-CP, 1993.

[110] Melson, N. D., Sabetrik, M. D., and Atkins, H. L., "Time-Accurate Navier-Stokes Calculations with Multigrid Acceleration," Presented at the Sixth Copper Mountain Conference on Multigrid Methods, Copper Mountain, Colorado, April 4-9, 1993.

[111] Baldwin, B. S., and Lomax, H., "Thin Layer Approximation and Algebraic Model for Separated Turbulent Flows," AIAA Paper 78-257, 1978.

[112] Quealy, A., Cole, G. L., and Blech, R. A., "Portable Programming on Parallel/Networked Computers Using the Application Portable Parallel Library (APPL)," NASA TM-106238, 1993.

[113] Sunderam, "PVM: A Framework for Parallel Distributed Computing," Concurrency: Practice & Experience, Vol. 2, No. 4, 1990.

[114] "MPI: A Message-Passing Interface Standard, " Message Passing Interface Forum, May 5, 1994, University of Tennessee, Knoxville, Report No. CS-94-230, (see also the International Journal of Supercomputing Applications, Volume 8, Number 3/4, 1994).

[115] Saxer, A. P., "A Numerical Analysis of 3-D Inviscid Stator/Rotor Interactions Using Non-Reflecting Boundary Conditions," MIT GTL Report 209, 1992.

[116] Klann, J. L. and Snyder, C. A., "NEPP Programmers Manual (NASA Engine Performance Program) Volume 1. Technical Description," NASA TM-106575, September 1994.

[117] Klann, J. L. and Snyder, C. A., "NEPP Programmers Manual (NASA Engine Performance Program) Volume 2. Source Code Listing," NASA TM-106575, September 1994.

[118] Cours, J. T., "Design and Implementation of a Distributed Version of the NASA Engine Performance Program," NASA CR-194475, March 1994.

[119] Cours, J. T. and Curlett, B. P., "A Distributed Version of the NASA Engine Performance Program," NASA TM-106208, 1993.

[120] Berton, J. and Plencner, R. M., "An Interactive Preprocessor for the NASA Engine Performance Program," NASA TM-105786, 1992.

[121] Curlett, B. P. and Ryall, K., "A Graphical User-Interface for Propulsion System Analysis," NASA TM-105696, 1992.

[122] Gordon, S., "The NAVY/NASA Engine Program (NNEP89)–Interfacing the Program for Calculation of Complex Chemical Equilibrium Compositions (CEC)," NASA CR-187208, September 1991.

[123] Plencner, R. M. and Snyder, C. A., "The NAVY/NASA Engine Program (NNEP89)–A User's Manual," NASA TM-105186, August 1991.

[124] Berton, J., "Divergence Thrust Loss Calculations for Convergent-Divergent Nozzles: Extensions to the Classical Case," NASA TM-105176, 1991.

[125] Plencner, R. M., "Plotting Component Maps in the Navy/NASA Engine Program (NNEP)-A Method and Its Usage," NASA TM-101433, 1989.

[126] Fishbach, L. H., and Gordon, S., "NNEPEQ - Chemical Equilibrium Version of the Navy/NASA Engine Program," NASA TM-100851, 1988. (see also Journal of Engineering for Gas Turbines and Power, Vol. 111, pp. 114-116, January 1989.)

[127] Converse, G. L., "Extended Parametric Representation of Compressor, Fans and Turbines Volume III - MODFAN User's Manual (Parametric Modulating Flow Fan)," NASA CR-174647, March 1984.

[128] Converse, G. L., "Extended Parametric Representation of Compressor, Fans and Turbines Volume II - PART User's Manual (Parametric Turbine)," NASA CR-174646, March 1984.

[129] Converse, G. L. and Giffin, R. G., "Extended Parametric Representation of Compressor, Fans and Turbines Volume I - CMGEN User's Manual," NASA CR-174645, March 1984.

[130] Fishbach, L. H., "PREPWATE–An Interactive Preprocessing Computer Code to the Weight Analysis of Turbine Engines (WATE) Computer Code," NASA TM-83545, 1983.

[131] Plencner, R. M., Senty, P., and Wickenheiser, T.J., "Propeller Performance and Weight Prediction Appended to the Navy/NASA Engine Program," NASA TM-83458, 1983.

[132] Corban, R. R., "Interactive-Graphic Flowpath Plotting for Turbine Engines," NASA TM-82756, 1981.

[133] Fishbach, L. H., "KONFIG and REKONFIG–Two Interactive Preprocessing Programs to the Navy NASA Engine Program (NNEP)," NASA TM-82636, 1981.

[134] Gauntner, J. W., "Algorithm for Calculating Turbine Cooling Flow and the Resulting Decrease in Turbine Efficiency," NASA TM-81453, 1980.

[135] Fishbach, L. H., "Computer Simulation of Engine Systems.", NASA TM-79290, 1980.

[136] Kowalski, E. J. and Atkins, R. A., Jr., "Computer Code for Estimating Installed Performance of Aircraft Gas Turbine Engines, Volume II User's Manual," NASA CR-159692, December 1979.

[137] Fishbach, L. H., "Computerized System Analysis and Optimization of Aircraft Engine Performance, Weight, and Life Cycle Costs," NASA TM-79221, 1979.

[138] Onat, E. and Klees, G. W., "A Method to Estimate Weight and Dimensions of Large and Small Gas Turbine Engines," NASA CR-159481, January 1979.

[139] Gordon, S. and McBride, B. J., "Computer Program for Calculation of Complex Chemical Equilibrium Compositions, Rocket Performance, Incident and Reflected Shocks, and Chapman-Jouguet Detonations," NASA SP-273, 1976.

[140] Fishbach, L. H. and Caddy, M. J., "NNEP - The Navy NASA Engine Program," NASA TM-X-71857, 1975.

[141] Caddy, M. J. and Shapiro, S. R., "NEPCOMP - The Navy Engine

[142] Hall, E. J., Topp, D. A., Heidegger, N. J., and Delaney, R. A., "Investigation of Advanced Counterrotation Blade Configuration Concepts for High Speed Turboprop Systems: Task VII - Endwall Treatment Inlet Flow Distortion Analysis Final Report," NASA Contract NAS3-25270, NASA CR-195468, 1995.

[143] Heidegger, N. J., Hall, E. J., and Delaney, R. A., "Parameterized Study of High-Speed Compressor Seal Cavity Flow," AIAA Paper 96-2807, 1996.

(This page intentionally left blank)

Appendix A

ADPAC07 Input Files for EEE/LP Simulation

ADPAC Input File for EEE LP Analysis

```
#-------------------------------------------------
# EEE LP Analysis
#-------------------------------------------------
#VARNAME  = VARIABLE VALUE     COMMENT
#-------------------------------------------------
CASENAME    =         EEELP       Case name used for file naming
FBCWARN     =         1.0         Turn on warning for B.C. errors
RMACH       =         0.800000    Reference Mach Number
FINVVI      =         1.000000    Viscous trigger (On=1)
GAMMA       =         1.400000    Specific heat ratio
PREF        =       759.052800    Reference Total Pressure (lbf/ft^2)
TREF        =       444.319200    Reference Total Temperature (deg. R)
RGAS        =      1716.350700    Gas constant
DIAM        =         0.083333    Reference length to convert grid to feet
EPSX        =         1.000000    Residual smoothing multiplier
EPSY        =         0.500000    Residual smoothing multiplier
EPSZ        =         1.000000    Residual smoothing multiplier
VIS2        =         0.500000    2nd order dissipation coefficient
VIS4        =         0.015625    4th order dissipation coefficient
CFL         =        -5.000000    Time step multiplier (CFL number)
FNCMAX      =       300.00000     Number of iterations on fine grid
FITCHK      =         5.000000    Checkpoint restart iteration interval
FTIMEI      =         1.000000    Time step calculation interval
FTURBI      =         1.000000    Turbulence model update interval
FTURBB      =        20.000000    Turbulence model initiation iteration number
PRNO        =         0.700000    Prandtl number
PRTNO       =         0.900000    Turbulent Prandtl Number
FSOLVE      =         1.000000    Solution scheme trigger (1 = 4-stage scheme)
FRESID      =         1.000000    Residual smoothing trigger (On=1)
FREST       =         1.000000    Restart flag (=1, restart using case.restart.old)
P3DPRT      =         1.0         PLOT3D file output trigger
FUNINT      =     99999.000000    Unsteady output iteration interval
FMULTI      =         2.000000    Number of multigrid levels, =1,no multigrid
FSUBIT      =         3.000000    Number of subiterations  during multigrid
FFULMG      =         0.000000    Full multigrid trigger (start on coarser mesh=1)
FCOAG1      =         2.000000    Full multigrid starting mesh level
FCOAG2      =         2.000000    Full multigrid ending mesh level
FITFMG      =       200.000000    Full multigrid iterations (on coarse meshes)
VISCG2      =         0.125000    Coarse mesh dissipation coefficient
FGRAFIX     =         5.000000    Interactive graphics trigger (0=off)
FGRAFINT    =         1.000000    Interactive graphics update interval
FIMGSAV     =         0.000000    Interactive graphics screensave trigger
FIMGINT     =     99999.000000    Interactive graphics screesave interval
FVTSFAC     =         7.000000    Viscous time step factor
FTOTSM      =         1.000000    Multigrid smoothing trigger (on=1.0)
EPSTOT      =         0.100000    Multigrid smoothing coefficient
FWALLF      =         1.000000    Wall Function trigger (on=1)
CFMAX       =         2.200000    Ref. CFL # for implicit res. smoothing
#
#---> Set the block rotational speeds here
#
# Upstream outer nacelle
#
RPM(1)      =             0.000
RPM(2)      =             0.000

#
# Fan + Quarter stage booster
```

```
#
RPM(3)     =         3507.000
RPM(4)     =         3507.000
RPM(5)     =            0.000
RPM(6)     =         3507.000
RPM(7)     =            0.000
RPM(8)     =            0.000
RPM(9)     =            0.000
RPM(10)    =            0.000

#
# Bypass duct
#
RPM(11)    =            0.000

#
# HP turbine
#
RPM(12)    =            0.000
RPM(13)    =        12627.315
RPM(14)    =            0.000
RPM(15)    =        12627.315

#
# LP turbine
#
RPM(16)    =            0.000
RPM(17)    =         3507.000
RPM(18)    =            0.000
RPM(19)    =         3507.000
RPM(20)    =            0.000
RPM(21)    =         3507.000
RPM(22)    =            0.000
RPM(23)    =         3507.000
RPM(24)    =            0.000
RPM(25)    =         3507.000

#
# LP turbine shrouded rotor cavities
#
RPM(26)    =            0.000
RPM(27)    =            0.000
RPM(28)    =            0.000
RPM(29)    =            0.000
RPM(30)    =            0.000
RPM(31)    =            0.000
RPM(32)    =            0.000
RPM(33)    =            0.000
RPM(34)    =            0.000
RPM(35)    =            0.000
RPM(36)    =            0.000
RPM(37)    =            0.000
RPM(38)    =            0.000
RPM(39)    =            0.000
RPM(40)    =            0.000
RPM(41)    =            0.000
RPM(42)    =            0.000
RPM(43)    =            0.000
RPM(44)    =            0.000
RPM(45)    =            0.000
RPM(46)    =            0.000
RPM(47)    =            0.000
RPM(48)    =            0.000
RPM(49)    =            0.000
RPM(50)    =            0.000
RPM(51)    =            0.000
RPM(52)    =            0.000
RPM(53)    =            0.000
RPM(54)    =            0.000
RPM(55)    =            0.000
RPM(56)    =            0.000
RPM(57)    =            0.000
RPM(58)    =            0.000
RPM(59)    =            0.000
RPM(60)    =            0.000
RPM(61)    =            0.000
RPM(62)    =            0.000
RPM(63)    =            0.000
RPM(64)    =            0.000
RPM(65)    =            0.000

#
# Lobed exhaust mixer and downstream plume
#
RPM(66)    =            0.000
RPM(67)    =            0.000
RPM(68)    =            0.000
RPM(69)    =            0.000
RPM(70)    =            0.000
RPM(71)    =            0.000
RPM(72)    =            0.000
RPM(73)    =            0.000
```

```
RPM(74)    =            0.000

#
#---> Set the number of blades for each block where possible
#

#
# Upstream outer nacelle
#
NBLD(1)    =            1.000
NBLD(2)    =            1.000

#
# Fan + quarter stage booster
#
NBLD(3)    =           32.000
NBLD(4)    =           32.000
NBLD(5)    =           60.000
NBLD(6)    =           56.000
NBLD(7)    =           64.000
NBLD(8)    =           64.000
NBLD(9)    =           34.000
NBLD(10)   =           34.000

#
# Bypass duct
#
NBLD(11)   =            1.000

#
# HP turbine
#
NBLD(12)   =           46.000
NBLD(13)   =           76.000
NBLD(14)   =           48.000
NBLD(15)   =           70.000

#
# LP turbine
#
NBLD(16)   =           72.000
NBLD(17)   =          120.000
NBLD(18)   =          102.000
NBLD(19)   =          122.000
NBLD(20)   =           96.000
NBLD(21)   =          122.000
NBLD(22)   =          114.000
NBLD(23)   =          156.000
NBLD(24)   =          120.000
NBLD(25)   =          110.000

#
# LP turbine shrouded rotor cavities
#
NBLD(26)   =            1.000
NBLD(27)   =            1.000
NBLD(28)   =            1.000
NBLD(29)   =            1.000
NBLD(30)   =            1.000
NBLD(31)   =            1.000
NBLD(32)   =            1.000
NBLD(33)   =            1.000
NBLD(34)   =            1.000
NBLD(35)   =            1.000
NBLD(36)   =            1.000
NBLD(37)   =            1.000
NBLD(38)   =            1.000
NBLD(39)   =            1.000
NBLD(40)   =            1.000
NBLD(41)   =            1.000
NBLD(42)   =            1.000
NBLD(43)   =            1.000
NBLD(44)   =            1.000
NBLD(45)   =            1.000
NBLD(46)   =            1.000
NBLD(47)   =            1.000
NBLD(48)   =            1.000
NBLD(49)   =            1.000
NBLD(50)   =            1.000
NBLD(51)   =            1.000
NBLD(52)   =            1.000
NBLD(53)   =            1.000
NBLD(54)   =            1.000
NBLD(55)   =            1.000
NBLD(56)   =            1.000
NBLD(57)   =            1.000
NBLD(58)   =            1.000
NBLD(59)   =            1.000
NBLD(60)   =            1.000
NBLD(61)   =            1.000
NBLD(62)   =            1.000
NBLD(63)   =            1.000
```

```
NBLD(64)    =           1.000
NBLD(65)    =           1.000

#
# Lobed exhaust mixer and downstream
#
NBLD(66)    =          12.000
NBLD(67)    =          12.000
NBLD(68)    =          12.000
NBLD(69)    =          12.000
NBLD(70)    =          12.000
NBLD(71)    =          12.000
NBLD(72)    =          12.000
NBLD(73)    =          12.000
NBLD(74)    =          12.000
```

ADPAC Boundary Data File for EEE LP Analysis

```
#
# Block descriptions for boundary conditions
#
# BLOCK  1 - upstream and outer nacelle mesh                    (2D)
# BLOCK  2 - upstream and outer nacelle mesh                    (2D)
# BLOCK  3 - quarter stage and fan      mesh                    (3D)
#   .
#   .
#   .
# BLOCK 10 - quarter stage and fan      mesh                    (3D)
# BLOCK 11 - bypass duct                mesh                    (2D)
# BLOCK 12 - high pressure turbine      mesh                    (3D)
#   .
#   .
#   .
# BLOCK 15 - high pressure turbine      mesh                    (3D)
# BLOCK 16 - low pressure turbine       mesh                    (3D)
#   .
#   .
#   .
# BLOCK 65 - low pressure turbine       mesh                    (3D)
# BLOCK 66 - mixer and downstream       mesh                    (3D)
#   .
#   .
#   .
# BLOCK 74 - mixer and downstream       mesh                    (3D)
#



# UPSTREAM AND OUTER NACELLE GRIDDING
PATCH      1   2  J  J  P  M  I  K   1 101   1  65   1   2   1  65   1   2
PATCH      2   1  J  J  M  P  I  K 101   1   1  65   1   2   1  65   1   2

# Upper part of inlet
FREE       1   1  I  I  P  P  J  K   1   1   1  49   1   2   1  49   1   2
 PTOT     TTOT     EMINF    ALPHA
 1.0      1.0      0.8      0.0

# Nacelle top
SSVI       1   1  J  J  P  P  I  K   1   1  65 129   1   2  65 129   1   2
 RPMWALL     TWALL
       0.0         0.0

# 2D linkup w/ 3D mixer (above nacelle)
MBCAVG     1  70  I  I  M  P  J  K 129   1   1  49   1   2   1  49   1  81
NSEGS
  1
LBLOCK2B   LFACE2B  LDIR2B L2LIMB  M2LIM1B M2LIM2B  N2LIM1B N2LIM2B
   70         I       P      1        1       49       1       81

MBCAVG    70   1  I  I  P  M  J  K   1 129   1  49   1  81   1  49   1   2
NSEGS
  1
LBLOCK2B   LFACE2B  LDIR2B L2LIMB  M2LIM1B M2LIM2B  N2LIM1B N2LIM2B
   1          I        M    129       1       49       1       2

# Top nacelle farfield
FREE       1   1  J  J  M  M  I  K  49  49   1 129   1   2   1 129   1   2
 PTOT     TTOT     EMINF    ALPHA
 1.0      1.0      0.8      0.0

# Lower part of inlet
FREE       2   2  I  I  P  P  J  K   1   1   1 101   1   2   1 101   1   2
 PTOT     TTOT     EMINF    ALPHA
 1.0      1.0      0.8      0.0

# 2D linkup w/ 3D fan (inside inlet) (lower section)
MBCAVG     2   3  I  I  M  P  J  K  93   1   1  81   1   2   1  81   1  49
NSEGS
  1
LBLOCK2B   LFACE2B  LDIR2B L2LIMB  M2LIM1B M2LIM2B  N2LIM1B N2LIM2B
  3          I       P      1       1       81       1       49

MBCAVG     3   2  I  I  P  M  J  K   1  93   1  81   1  49   1  81   1   2
NSEGS
  1
LBLOCK2B   LFACE2B  LDIR2B L2LIMB  M2LIM1B M2LIM2B  N2LIM1B N2LIM2B
  2          I       M     93       1       81       1       2

# 2D linkup w/ 3D fan (inside inlet) (upper section)
MBCAVG     2   4  I  I  M  P  J  K  93   1  81 101   1   2   1  21   1  49
NSEGS
  1
LBLOCK2B   LFACE2B  LDIR2B L2LIMB  M2LIM1B M2LIM2B  N2LIM1B N2LIM2B
  4          I       P      1       1       21       1       49

MBCAVG     4   2  I  I  P  M  J  K   1  93   1  21   1  49  81  101  1   2
NSEGS
```

```
  1
LBLOCK2B   LFACE2B  LDIR2B L2LIMB  M2LIM1B M2LIM2B  N2LIM1B N2LIM2B
  2          I       M     93      81      101        1       2

# Axis of symmetry
SSIN       2   2  J  J  P  P  I  K   1   1   1  93   1   2   1  93   1   2
 RPMWALL     TWALL
      0.0         0.0

# Inside nacelle
SSVI       2   2  J  J  M  M  I  K 101 101  65  93   1   2  65  93   1   2
 RPMWALL     TWALL
      0.0         0.0



# QUARTER STAGE AND FAN
PATCH      3   4  J  J  M  P  I  K  81   1   1  57   1  49   1  57   1  49
PATCH      4   3  J  J  P  M  I  K   1  81   1  57   1  49   1  57   1  49

PATCH      3   4  J  J  M  P  I  K  81   1  81 113   1  49  81 113   1  49
PATCH      4   3  J  J  P  M  I  K   1  81  81 113   1  49  81 113   1  49

PATCH      3   3  K  K  P  M  I  J   1  49   1  33   1  81   1  33   1  81
PATCH      3   3  K  K  M  P  I  J  49   1   1  33   1  81   1  33   1  81

PATCH      3   3  K  K  P  M  I  J   1  49  97 113   1  81  97 113   1  81
PATCH      3   3  K  K  M  P  I  J  49   1  97 113   1  81  97 113   1  81

PATCH      4   4  K  K  P  M  I  J   1  49   1  33   1  21   1  33   1  21
PATCH      4   4  K  K  M  P  I  J  49   1   1  33   1  21   1  33   1  21

PATCH      4   4  K  K  P  M  I  J   1  49  97 113   1  21  97 113   1  21
PATCH      4   4  K  K  M  P  I  J  49   1  97 113   1  21  97 113   1  21

MBCAVG     3   5  I  I  M  P  J  K 113   1   1  65   1  49   1  65   1  33
NSEGS
  1
LBLOCK2B   LFACE2B  LDIR2B L2LIMB  M2LIM1B M2LIM2B  N2LIM1B N2LIM2B
  5          I       P      1       1       65        1      33

MBCAVG     5   3  I  I  P  M  J  K   1 113   1  65   1  33   1  65   1  49
NSEGS
  1
LBLOCK2B   LFACE2B  LDIR2B L2LIMB  M2LIM1B M2LIM2B  N2LIM1B N2LIM2B
  3          I       M     113      1       65        1      49

MBCAVG     3  10  I  I  M  P  J  K 113   1  65  81   1  49   1  17   1  49
NSEGS
  1
LBLOCK2B   LFACE2B  LDIR2B L2LIMB  M2LIM1B M2LIM2B  N2LIM1B N2LIM2B
 10          I       P      1       1       17        1      49

MBCAVG    10   3  I  I  P  M  J  K   1 113   1  17   1  49  65  81   1  49
NSEGS
  1
LBLOCK2B   LFACE2B  LDIR2B L2LIMB  M2LIM1B M2LIM2B  N2LIM1B N2LIM2B
  3          I       M     113      65      81        1      49

# before spinner
SSIN       3   3  J  J  P  P  I  K   1   1   1   9   1  49   1   9   1  49
 RPMWALL     TWALL
    0.0           0.0

# spinner surface
SSVI       3   3  J  J  P  P  I  K   1   1   9 113   1  49   9 113   1  49
 RPMWALL     TWALL
    3507.000        0.0

SSVI       3   3  J  J  M  M  I  K  81  81  57  81   1  49  57  81   1  49
 RPMWALL     TWALL
   3507.000         0.0

SSVI       3   3  K  K  P  P  I  J   1   1  33  97   1  81  33  97   1  81
 RPMWALL     TWALL
    3507.000        0.0

SSVI       3   3  K  K  M  M  I  J  49  49  33  97   1  81  33  97   1  81
 RPMWALL     TWALL
    3507.000        0.0

MBCAVG     4  10  I  I  M  P  J  K 113   1   1  21   1  49  17  37   1  49
NSEGS
  1
LBLOCK2B   LFACE2B  LDIR2B L2LIMB  M2LIM1B M2LIM2B  N2LIM1B N2LIM2B
 10          I       P      1       17      37        1      49

MBCAVG    10   4  I  I  P  M  J  K   1 113  17  37   1  49   1  21   1  49
NSEGS
  1
LBLOCK2B   LFACE2B  LDIR2B L2LIMB  M2LIM1B M2LIM2B  N2LIM1B N2LIM2B
```

```
  4          I      M    113      1     21       1     49

SSVI      4   4  J  J  P  P  I  K   1   1  57  81   1  49  57  81   1  49
 RPMWALL     TWALL
    3507.000         0.0

SSVI      4   4  J  J  M  M  I  K  21  21   1 113   1  49   1 113   1  49
 RPMWALL     TWALL
    0.0          0.0

SSVI      4   4  K  K  P  P  I  J   1   1  33  97   1  21  33  97   1  21
 RPMWALL     TWALL
    3507.000         0.0

SSVI      4   4  K  K  M  M  I  J  49  49  33  97   1  21  33  97   1  21
 RPMWALL     TWALL
    3507.000         0.0

PATCH     5   5  K  K  P  M  I  J   1  33   1  17   1  65   1  17   1  65
PATCH     5   5  K  K  M  P  I  J  33   1   1  17   1  65   1  17   1  65

PATCH     5   5  K  K  P  M  I  J   1  33  81  97   1  65  81  97   1  65
PATCH     5   5  K  K  M  P  I  J  33   1  81  97   1  65  81  97   1  65

MBCAVG    5   6  I  I  M  P  J  K  97   1   1  65   1  33   1  65   1  33
NSEGS
  1
LBLOCK2B   LFACE2B  LDIR2B L2LIMB  M2LIM1B M2LIM2B  N2LIM1B N2LIM2B
  6          I       P      1        1      65        1      33

MBCAVG    6   5  I  I  P  M  J  K   1  97   1  65   1  33   1  65   1  33
NSEGS
  1
LBLOCK2B   LFACE2B  LDIR2B L2LIMB  M2LIM1B M2LIM2B  N2LIM1B N2LIM2B
  5          I       M      97       1      65        1      33

SSVI      5   5  J  J  P  P  I  K   1   1   1  97   1  33   1  97   1  33
 RPMWALL     TWALL
      0.0          0.0

SSVI      5   5  J  J  M  M  I  K  65  65   1  97   1  33   1  97   1  33
 RPMWALL     TWALL
      0.0          0.0

SSVI      5   5  K  K  P  P  I  J   1   1  17  81   1  65  17  81   1  65
 RPMWALL     TWALL
      0.0          0.0

SSVI      5   5  K  K  M  M  I  J  33  33  17  81   1  65  17  81   1  65
 RPMWALL     TWALL
      0.0          0.0

PATCH     6   6  K  K  P  M  I  J   1  33   1  17   1  65   1  17   1  65
PATCH     6   6  K  K  M  P  I  J  33   1   1  17   1  65   1  17   1  65

PATCH     6   6  K  K  P  M  I  J   1  33  81  97   1  65  81  97   1  65
PATCH     6   6  K  K  M  P  I  J  33   1  81  97   1  65  81  97   1  65

MBCAVG    6   7  I  I  M  P  J  K  97   1   1  33   1  33   1  33   1  33
NSEGS
  1
LBLOCK2B   LFACE2B  LDIR2B L2LIMB  M2LIM1B M2LIM2B  N2LIM1B N2LIM2B
  7          I       P      1        1      33        1      33

MBCAVG    7   6  I  I  P  M  J  K   1  97   1  33   1  33   1  33   1  33
NSEGS
  1
LBLOCK2B   LFACE2B  LDIR2B L2LIMB  M2LIM1B M2LIM2B  N2LIM1B N2LIM2B
  6          I       M      97       1      33        1      33

MBCAVG    6   8  I  I  M  P  J  K  97   1  33  65   1  33   1  33   1  33
NSEGS
  1
LBLOCK2B   LFACE2B  LDIR2B L2LIMB  M2LIM1B M2LIM2B  N2LIM1B N2LIM2B
  8          I       P      1        1      33        1      33

MBCAVG    8   6  I  I  P  M  J  K   1  97   1  33   1  33  33  65   1  33
NSEGS
  1
LBLOCK2B   LFACE2B  LDIR2B L2LIMB  M2LIM1B M2LIM2B  N2LIM1B N2LIM2B
  6          I       M      97      33      65        1      33

SSVI      6   6  J  J  P  P  I  K   1   1   1  97   1  33   1  97   1  33
 RPMWALL     TWALL
    3507.000         0.0

SSVI      6   6  J  J  M  M  I  K  65  65   1  97   1  33   1  97   1  33
 RPMWALL     TWALL
    0.0          0.0

SSVI      6   6  K  K  P  P  I  J   1   1  17  81   1  65  17  81   1  65
 RPMWALL     TWALL
```

```
   3507.000         0.0

SSVI      6   6  K  K  M  M  I  J  33  33  17  81   1  65  17  81   1  65
 RPMWALL     TWALL
   3507.000         0.0

PATCH     7   8  J  J  M  P  I  K  33   1   1  17   1  33   1  17   1  33
PATCH     8   7  J  J  P  M  I  K   1  33   1  17   1  33   1  17   1  33

PATCH     7   7  K  K  P  M  I  J   1  33   1  25   1  33   1  25   1  33
PATCH     7   7  K  K  M  P  I  J  33   1   1  25   1  33   1  25   1  33

PATCH     7   7  K  K  P  M  I  J   1  33  89 105   1  33  89 105   1  33
PATCH     7   7  K  K  M  P  I  J  33   1  89 105   1  33  89 105   1  33

PATCH     8   8  K  K  P  M  I  J   1  33   1  29   1  33   1  29   1  33
PATCH     8   8  K  K  M  P  I  J  33   1   1  29   1  33   1  29   1  33

# Exit from bypass (inlet to compressor)
EXITG     7   7  I  I  M  M  L  L 105 105   1  33   1  33   1  33   1  33
 PEXIT
  1.5242046  1.075  0.02

SSVI      7   7  J  J  P  P  I  K   1   1   1 105   1  33   1 105   1  33
 RPMWALL     TWALL
      0.0         0.0

SSVI      7   7  J  J  M  M  I  K  33  33  17 105   1  33  17 105   1  33
 RPMWALL     TWALL
      0.0         0.0

SSVI      7   7  K  K  P  P  I  J   1   1  25  89   1  33  25  89   1  33
 RPMWALL     TWALL
      0.0         0.0

SSVI      7   7  K  K  M  M  I  J  33  33  25  89   1  33  25  89   1  33
 RPMWALL     TWALL
      0.0         0.0

MBCAVG    8   9  I  I  M  P  J  K  29   1   1  33   1  33   1  33   1  49
NSEGS
  1
LBLOCK2B   LFACE2B  LDIR2B L2LIMB  M2LIM1B M2LIM2B  N2LIM1B N2LIM2B
  9          I       P      1        1      33        1      49

MBCAVG    9   8  I  I  P  M  J  K   1  29   1  33   1  49   1  33   1  33
NSEGS
  1
LBLOCK2B   LFACE2B  LDIR2B L2LIMB  M2LIM1B M2LIM2B  N2LIM1B N2LIM2B
  8          I       M      29       1      33        1      33

SSVI      8   8  J  J  P  P  I  K   1   1  17  29   1  33  17  29   1  33
 RPMWALL     TWALL
      0.0         0.0

SSVI      8   8  J  J  M  M  I  K  33  33   1  29   1  33   1  29   1  33
 RPMWALL     TWALL
      0.0         0.0

PATCH     9  10  J  J  M  P  I  K  33   1  25  89   1  49  73 137   1  49
PATCH    10   9  J  J  P  M  I  K   1  33  73 137   1  49  25  89   1  49

PATCH     9   9  K  K  P  M  I  J   1  49   1   9   1  33   1   9   1  33
PATCH     9   9  K  K  M  P  I  J  49   1   1   9   1  33   1   9   1  33

PATCH     9   9  K  K  P  M  I  J   1  49  73  89   1  33  73  89   1  33
PATCH     9   9  K  K  M  P  I  J  49   1  73  89   1  33  73  89   1  33

PATCH    10  10  K  K  P  M  I  J   1  49   1  49   1  37   1  49   1  37
PATCH    10  10  K  K  M  P  I  J  49   1   1  49   1  37   1  49   1  37

PATCH    10  10  K  K  P  M  I  J   1  49 121 137   1  37 121 137   1  37
PATCH    10  10  K  K  M  P  I  J  49   1 121 137   1  37 121 137   1  37

SSVI      9   9  J  J  P  P  I  K   1   1   1  89   1  49   1  89   1  49
 RPMWALL     TWALL
      0.0         0.0

SSVI      9   9  J  J  M  M  I  K  33  33   1  25   1  49   1  25   1  49
 RPMWALL     TWALL
      0.0         0.0

SSVI      9   9  K  K  P  P  I  J   1   1   9  73   1  33   9  73   1  33
 RPMWALL     TWALL
      0.0         0.0

SSVI      9   9  K  K  M  M  I  J  49  49   9  73   1  33   9  73   1  33
 RPMWALL     TWALL
      0.0         0.0

SSVI     10  10  J  J  P  P  I  K   1   1   1  73   1  49   1  73   1  49
 RPMWALL     TWALL
```

```
      0.0         0.0

SSVI      10  10  J  J  M  M  I  K  37  37   1 137   1  49   1 137   1  49
 RPMWALL     TWALL
      0.0         0.0

SSVI      10  10  K  K  P  P  I  J   1   1  49 121   1  37  49 121   1  37
 RPMWALL     TWALL
      0.0         0.0

SSVI      10  10  K  K  M  M  I  J  49  49  49 121   1  37  49 121   1  37
 RPMWALL     TWALL
      0.0         0.0

# Lower section 3D qtr-stage to 2D bypass duct
MBCAVG     9  11  I  I  M  P  J  K  89   1   1  33   1  49   1  17   1   2
NSEGS
  1
LBLOCK2B   LFACE2B  LDIR2B L2LIMB  M2LIM1B M2LIM2B  N2LIM1B N2LIM2B
 11           I       P      1       1       17       1       2

MBCAVG    11   9  I  I  P  M  J  K   1  89   1  17   1   2   1  33   1  49
NSEGS
  1
LBLOCK2B   LFACE2B  LDIR2B L2LIMB  M2LIM1B M2LIM2B  N2LIM1B N2LIM2B
  9           I       M     89       1       33       1      49

# Upper section 3D qtr-stage to 2D bypass duct
MBCAVG    10  11  I  I  M  P  J  K 137   1   1  37   1  49  17  49   1   2
NSEGS
  1
LBLOCK2B   LFACE2B  LDIR2B L2LIMB  M2LIM1B M2LIM2B  N2LIM1B N2LIM2B
 11           I       P      1      17       49       1       2

MBCAVG    11  10  I  I  P  M  J  K   1 137  17  49   1   2   1  37   1  49
NSEGS
  1
LBLOCK2B   LFACE2B  LDIR2B L2LIMB  M2LIM1B M2LIM2B  N2LIM1B N2LIM2B
 10           I       M    137       1       37       1      49



# BYPASS DUCT
SSVI      11  11  J  J  P  P  I  K   1   1   1  97   1   2   1  97   1   2
 RPMWALL     TWALL
      0.0         0.0

SSVI      11  11  J  J  M  M  I  K  49  49   1  97   1   2   1  97   1   2
 RPMWALL     TWALL
      0.0         0.0

SSVI      11  11  I  I  M  M  J  K  97  97   1  49   1   2   1  49   1   2
 RPMWALL     TWALL
      0.0         0.0

# 2D bypass duct to 3D mixer linkup
MBCAVG    11  73  I  I  M  P  J  K  97   1   1  49   1   2   1  49   1  81
NSEGS
  1
LBLOCK2B   LFACE2B  LDIR2B L2LIMB  M2LIM1B M2LIM2B  N2LIM1B N2LIM2B
 73           I       P      1       1       49       1      81

MBCAVG    73  11  I  I  P  M  J  K   1  97   1  49   1  81   1  49   1   2
NSEGS
  1
LBLOCK2B   LFACE2B  LDIR2B L2LIMB  M2LIM1B M2LIM2B  N2LIM1B N2LIM2B
 11           I       M     97       1       49       1       2




# HIGH PRESSURE TURBINE (HPT)
#PATCH     12  12  K  K  P  M  I  J   1  49   1  17   1  33   1  17   1  33
#PATCH     12  12  K  K  M  P  I  J  49   1   1  17   1  33   1  17   1  33

#PATCH     12  12  K  K  P  M  I  J   1  49  81  97   1  33  81  97   1  33
#PATCH     12  12  K  K  M  P  I  J  49   1  81  97   1  33  81  97   1  33

PATCH     12  12  K  K  P  M  I  J   1  49   1  97   1  33   1  97   1  33
PATCH     12  12  K  K  M  P  I  J  49   1   1  97   1  33   1  97   1  33

#PATCH     13  13  K  K  P  M  I  J   1  49   1  17   1  33   1  17   1  33
#PATCH     13  13  K  K  M  P  I  J  49   1   1  17   1  33   1  17   1  33

#PATCH     13  13  K  K  P  M  I  J   1  49  81  97   1  33  81  97   1  33
#PATCH     13  13  K  K  M  P  I  J  49   1  81  97   1  33  81  97   1  33

PATCH     13  13  K  K  P  M  I  J   1  49   1  97   1  33   1  97   1  33
PATCH     13  13  K  K  M  P  I  J  49   1   1  97   1  33   1  97   1  33
```

```
#PATCH     14  14  K  K  P  M  I  J   1  49   1  17   1  33   1  17   1  33
#PATCH     14  14  K  K  M  P  I  J  49   1   1  17   1  33   1  17   1  33

#PATCH     14  14  K  K  P  M  I  J   1  49  81  97   1  33  81  97   1  33
#PATCH     14  14  K  K  M  P  I  J  49   1  81  97   1  33  81  97   1  33

PATCH     14  14  K  K  P  M  I  J   1  49   1  97   1  33   1  97   1  33
PATCH     14  14  K  K  M  P  I  J  49   1   1  97   1  33   1  97   1  33

#PATCH     15  15  K  K  P  M  I  J   1  49   1  17   1  33   1  17   1  33
#PATCH     15  15  K  K  M  P  I  J  49   1   1  17   1  33   1  17   1  33

#PATCH     15  15  K  K  P  M  I  J   1  49  81  97   1  33  81  97   1  33
#PATCH     15  15  K  K  M  P  I  J  49   1  81  97   1  33  81  97   1  33

PATCH     15  15  K  K  P  M  I  J   1  49   1  97   1  33   1  97   1  33
PATCH     15  15  K  K  M  P  I  J  49   1   1  97   1  33   1  97   1  33

#

## Inlet to HPT
#INLETG    12  12  I  I  P  P  J  K   1   1   1  33   1  49   1  33   1  49
# PTOT   TTOT
# 35.66   6.632

# Vane 1

#SSVI      12  12  J  J  P  P  I  K   1   1   1  97   1  49   1  97   1  49
# RPMWALL     TWALL
#       0.0         0.0

#SSVI      12  12  J  J  M  M  I  K  33  33   1  97   1  49   1  97   1  49
# RPMWALL     TWALL
##       0.0         0.0

#SSVI      12  12  K  K  P  P  I  J   1   1  17  81   1  33  17  81   1  33
# RPMWALL     TWALL
#       0.0         0.0

#SSVI      12  12  K  K  M  M  I  J  49  49  17  81   1  33  17  81   1  33
# RPMWALL     TWALL
#       0.0         0.0

MBCAVG    12  13  I  I  M  P  J  K  97   1   1  33   1  49   1  33   1  49
NSEGS
  1
LBLOCK2B   LFACE2B  LDIR2B L2LIMB  M2LIM1B M2LIM2B  N2LIM1B N2LIM2B
 13           I       P      1       1       33        1      49

MBCAVG    13  12  I  I  P  M  J  K   1  97   1  33   1  49   1  33   1  49
NSEGS
  1
LBLOCK2B   LFACE2B  LDIR2B L2LIMB  M2LIM1B M2LIM2B  N2LIM1B N2LIM2B
 12           I       M     97       1       33        1      49

# Blade 1

#SSVI      13  13  J  J  P  P  I  K   1   1   1  97   1  49   1  97   1  49
# RPMWALL     TWALL
#    12627.315         0.0

#SSVI      13  13  J  J  M  M  I  K  33  33   1  97   1  49   1  97   1  49
# RPMWALL     TWALL
#   0.0        0.0

#
#
###### HERE BE THE TEST - ADD HYPERSPACE TIP CLEARANCE
#SSVI      13  13  K  K  P  P  I  J   1   1  17  81   1  33  17  81   1  33
## RPMWALL     TWALL
##    12627.315         0.0
##
#SSVI      13  13  K  K  M  M  I  J  49  49  17  81   1  33  17  81   1  33
# RPMWALL     TWALL
#    12627.315         0.0
#
#SSVI      13  13  K  K  P  P  I  J   1   1  17  81   1  29  17  81   1  29
# RPMWALL     TWALL
#    12627.315         0.0

#SSVI      13  13  K  K  M  M  I  J  49  49  17  81   1  29  17  81   1  29
# RPMWALL     TWALL
#    12627.315         0.0
#
#PATCH     13  13  K  K  P  M  I  J   1  49  17  81  29  33  17  81  29  33
#PATCH     13  13  K  K  M  P  I  J  49   1  17  81  29  33  17  81  29  33



MBCAVG    13  14  I  I  M  P  J  K  97   1   1  33   1  49   1  33   1  49
NSEGS
  1
```

```
LBLOCK2B   LFACE2B  LDIR2B L2LIMB  M2LIM1B M2LIM2B  N2LIM1B N2LIM2B
 14          I       P      1       1       33       1      49
#
MBCAVG    14  13  I  I  P  M  J  K   1  97   1  33   1  49   1  33   1  49
NSEGS
  1
LBLOCK2B   LFACE2B  LDIR2B L2LIMB  M2LIM1B M2LIM2B  N2LIM1B N2LIM2B
 13          I       M      97      1       33       1      49
#
## Vane 2
#
##SSVI      14  14  J  J  P  P  I  K   1   1   1  97   1  49   1  97   1  49
# RPMWALL     TWALL
#       0.0         0.0
#
#SSVI      14  14  J  J  M  M  I  K  33  33   1  97   1  49   1  97   1  49
# RPMWALL     TWALL
#       0.0         0.0
#
#SSVI      14  14  K  K  P  P  I  J   1   1  17  81   1  33  17  81   1  33
# RPMWALL     TWALL
#       0.0         0.0

#SSVI      14  14  K  K  M  M  I  J  49  49  17  81   1  33  17  81   1  33
# RPMWALL     TWALL
#       0.0         0.0

MBCAVG    14  15  I  I  M  P  J  K  97   1   1  33   1  49   1  33   1  49
NSEGS
  1
LBLOCK2B   LFACE2B  LDIR2B L2LIMB  M2LIM1B M2LIM2B  N2LIM1B N2LIM2B
 15          I       P      1       1       33       1      49
#
MBCAVG    15  14  I  I  P  M  J  K   1  97   1  33   1  49   1  33   1  49
NSEGS
  1
LBLOCK2B   LFACE2B  LDIR2B L2LIMB  M2LIM1B M2LIM2B  N2LIM1B N2LIM2B
 14          I       M      97      1       33       1      49
#
## Blade 2
#
##SSVI      15  15  J  J  P  P  I  K   1   1   1  97   1  49   1  97   1  49
# RPMWALL     TWALL
#    12627.315        0.0

#SSVI      15  15  J  J  M  M  I  K  33  33   1  97   1  49   1  97   1  49
# RPMWALL     TWALL
#       0.0         0.0


##### HERE BE THE TEST - ADD HYPERSPACE TIP CLEARANCE
#SSVI      15  15  K  K  P  P  I  J   1   1  17  81   1  33  17  81   1  33
# RPMWALL     TWALL
#    12627.315        0.0
#
#SSVI      15  15  K  K  M  M  I  J  49  49  17  81   1  33  17  81   1  33
# RPMWALL     TWALL
#    12627.315        0.0


#SSVI      15  15  K  K  P  P  I  J   1   1  17  81   1  29  17  81   1  29
# RPMWALL     TWALL
#    12627.315        0.0

#SSVI      15  15  K  K  M  M  I  J  49  49  17  81   1  29  17  81   1  29
# RPMWALL     TWALL
#    12627.315        0.0

#PATCH     15  15  K  K  P  M  I  J   1  49  17  81  29  33  17  81  29  33
#PATCH     15  15  K  K  M  P  I  J  49   1  17  81  29  33  17  81  29  33



# HPT to LPT linkup
#MBCAVG    15  16  I  I  M  P  J  K  97   1   1  33   1  49   1  49   1  33
#NSEGS
#  1
#LBLOCK2B   LFACE2B  LDIR2B L2LIMB  M2LIM1B M2LIM2B  N2LIM1B N2LIM2B
# 16          I       P      1       1       49       1      33
#
#MBCAVG    16  15  I  I  P  M  J  K   1  97   1  49   1  33   1  33   1  49
#NSEGS
#  1
#LBLOCK2B   LFACE2B  LDIR2B L2LIMB  M2LIM1B M2LIM2B  N2LIM1B N2LIM2B
# 15          I       M      97      1       33       1      49
#
#---> This is the fake HPT exit
#
#EXITG     15  15  I  I  M  M  J  K  97  97   1  33   1  49   1  33  1  49
#PEXIT
#9.2424
```

```
#
#---> Shut off the HP turbine which is in the grid file
#     (Essentially remove this from the LP analysis)
#
KILL       12  12  I  I  P  P  J  K   1   1   1  33   1  49   1  33  1  49
LSTART LEND
1  97
KILL       13  13  I  I  P  P  J  K   1   1   1  33   1  49   1  33  1  49
LSTART LEND
1  97
KILL       14  14  I  I  P  P  J  K   1   1   1  33   1  49   1  33  1  49
LSTART LEND
1  97
KILL       15  15  I  I  P  P  J  K   1   1   1  33   1  49   1  33  1  49
LSTART LEND
1  97


#
#---> LPT INLET SPECIFICATION
#

INLETG 16 16  I  I  P  P  J  K   1   1   1  49   1  33   1  49   1  33
PTOT   TTOT
9.2424 5.01216
6.8    4.45




# LOW PRESSURE TURBINE (LPT)
# Blocks 16-25 are alternating stator/rotor in 3d
# Blocks 26-65 are seal cavity geometries in 2d
PATCH     16  16  K  K  P  M  I  J   1  33   1  17   1  49   1  17   1  49
PATCH     16  16  K  K  M  P  I  J  33   1   1  17   1  49   1  17   1  49

PATCH     16  16  K  K  P  M  I  J   1  33  81  97   1  49  81  97   1  49
PATCH     16  16  K  K  M  P  I  J  33   1  81  97   1  49  81  97   1  49

PATCH     17  17  K  K  P  M  I  J   1  49   1  17   1  49   1  17   1  49
PATCH     17  17  K  K  M  P  I  J  49   1   1  17   1  49   1  17   1  49

PATCH     17  17  K  K  P  M  I  J   1  49  81  97   1  49  81  97   1  49
PATCH     17  17  K  K  M  P  I  J  49   1  81  97   1  49  81  97   1  49

PATCH     18  18  K  K  P  M  I  J   1  49   1  17   1  49   1  17   1  49
PATCH     18  18  K  K  M  P  I  J  49   1   1  17   1  49   1  17   1  49

PATCH     18  18  K  K  P  M  I  J   1  49  81  97   1  49  81  97   1  49
PATCH     18  18  K  K  M  P  I  J  49   1  81  97   1  49  81  97   1  49

PATCH     19  19  K  K  P  M  I  J   1  49   1  17   1  49   1  17   1  49
PATCH     19  19  K  K  M  P  I  J  49   1   1  17   1  49   1  17   1  49

PATCH     19  19  K  K  P  M  I  J   1  49  81  97   1  49  81  97   1  49
PATCH     19  19  K  K  M  P  I  J  49   1  81  97   1  49  81  97   1  49

PATCH     20  20  K  K  P  M  I  J   1  49   1  17   1  49   1  17   1  49
PATCH     20  20  K  K  M  P  I  J  49   1   1  17   1  49   1  17   1  49

PATCH     20  20  K  K  P  M  I  J   1  49  81  97   1  49  81  97   1  49
PATCH     20  20  K  K  M  P  I  J  49   1  81  97   1  49  81  97   1  49

PATCH     21  21  K  K  P  M  I  J   1  49   1  17   1  49   1  17   1  49
PATCH     21  21  K  K  M  P  I  J  49   1   1  17   1  49   1  17   1  49

PATCH     21  21  K  K  P  M  I  J   1  49  81  97   1  49  81  97   1  49
PATCH     21  21  K  K  M  P  I  J  49   1  81  97   1  49  81  97   1  49

PATCH     22  22  K  K  P  M  I  J   1  49   1  17   1  49   1  17   1  49
PATCH     22  22  K  K  M  P  I  J  49   1   1  17   1  49   1  17   1  49

PATCH     22  22  K  K  P  M  I  J   1  49  81  97   1  49  81  97   1  49
PATCH     22  22  K  K  M  P  I  J  49   1  81  97   1  49  81  97   1  49

PATCH     23  23  K  K  P  M  I  J   1  49   1  17   1  49   1  17   1  49
PATCH     23  23  K  K  M  P  I  J  49   1   1  17   1  49   1  17   1  49

PATCH     23  23  K  K  P  M  I  J   1  49  81  97   1  49  81  97   1  49
PATCH     23  23  K  K  M  P  I  J  49   1  81  97   1  49  81  97   1  49

PATCH     24  24  K  K  P  M  I  J   1  49   1  17   1  49   1  17   1  49
PATCH     24  24  K  K  M  P  I  J  49   1   1  17   1  49   1  17   1  49

PATCH     24  24  K  K  P  M  I  J   1  49  81  97   1  49  81  97   1  49
PATCH     24  24  K  K  M  P  I  J  49   1  81  97   1  49  81  97   1  49

PATCH     25  25  K  K  P  M  I  J   1  49   1  17   1  49   1  17   1  49
```

```
PATCH     25  25  K  K  M  P  I  J  49   1   1  17   1  49   1  17   1  49

PATCH     25  25  K  K  P  M  I  J   1  49  81 129   1  49  81 129   1  49
PATCH     25  25  K  K  M  P  I  J  49   1  81 129   1  49  81 129   1  49


# Blocks 26-33 compose seal cavity for rotor 1
PATCH     26  27  I  I  M  P  J  K  17   1   9  29   1   2   1  21   1   2
PATCH     27  26  I  I  P  M  J  K   1  17   1  21   1   2   9  29   1   2

PATCH     27  28  I  I  M  P  J  K  17   1  17  21   1   2   1   5   1   2
PATCH     28  27  I  I  P  M  J  K   1  17   1   5   1   2  17  21   1   2

PATCH     28  29  I  I  M  P  J  K   5   1   1   5   1   2  13  17   1   2
PATCH     29  28  I  I  P  M  J  K   1   5  13  17   1   2   1   5   1   2

PATCH     29  30  I  I  M  P  J  K  21   1   1  17   1   2   1  17   1   2
PATCH     30  29  I  I  P  M  J  K   1  21   1  17   1   2   1  17   1   2

PATCH     30  31  I  I  M  P  J  K  21   1  29  33   1   2   1   5   1   2
PATCH     31  30  I  I  P  M  J  K   1  21   1   5   1   2  29  33   1   2

PATCH     31  32  I  I  M  P  J  K   5   1   1   5   1   2  13  17   1   2
PATCH     32  31  I  I  P  M  J  K   1   5  13  17   1   2   1   5   1   2

PATCH     32  33  I  I  M  P  J  K  17   1   1  17   1   2  13  29   1   2
PATCH     33  32  I  I  P  M  J  K   1  17  13  29   1   2   1  17   1   2

# Blocks 34-41 compose seal cavity for rotor 2
PATCH     34  35  I  I  M  P  J  K  17   1   9  29   1   2   1  21   1   2
PATCH     35  34  I  I  P  M  J  K   1  17   1  21   1   2   9  29   1   2

PATCH     35  36  I  I  M  P  J  K  17   1  17  21   1   2   1   5   1   2
PATCH     36  35  I  I  P  M  J  K   1  17   1   5   1   2  17  21   1   2

PATCH     36  37  I  I  M  P  J  K   5   1   1   5   1   2  13  17   1   2
PATCH     37  36  I  I  P  M  J  K   1   5  13  17   1   2   1   5   1   2

PATCH     37  38  I  I  M  P  J  K  21   1   1  17   1   2   1  17   1   2
PATCH     38  37  I  I  P  M  J  K   1  21   1  17   1   2   1  17   1   2

PATCH     38  39  I  I  M  P  J  K  21   1  29  33   1   2   1   5   1   2
PATCH     39  38  I  I  P  M  J  K   1  21   1   5   1   2  29  33   1   2

PATCH     39  40  I  I  M  P  J  K   5   1   1   5   1   2  13  17   1   2
PATCH     40  39  I  I  P  M  J  K   1   5  13  17   1   2   1   5   1   2

PATCH     40  41  I  I  M  P  J  K  17   1   1  17   1   2  13  29   1   2
PATCH     41  40  I  I  P  M  J  K   1  17  13  29   1   2   1  17   1   2

# Blocks 42-49 compose seal cavity for rotor 3
PATCH     42  43  I  I  M  P  J  K  17   1   9  29   1   2   1  21   1   2
PATCH     43  42  I  I  P  M  J  K   1  17   1  21   1   2   9  29   1   2

PATCH     43  44  I  I  M  P  J  K  17   1  17  21   1   2   1   5   1   2
PATCH     44  43  I  I  P  M  J  K   1  17   1   5   1   2  17  21   1   2

PATCH     44  45  I  I  M  P  J  K   5   1   1   5   1   2  13  17   1   2
PATCH     45  44  I  I  P  M  J  K   1   5  13  17   1   2   1   5   1   2

PATCH     45  46  I  I  M  P  J  K  21   1   1  17   1   2   1  17   1   2
PATCH     46  45  I  I  P  M  J  K   1  21   1  17   1   2   1  17   1   2

PATCH     46  47  I  I  M  P  J  K  21   1  29  33   1   2   1   5   1   2
PATCH     47  46  I  I  P  M  J  K   1  21   1   5   1   2  29  33   1   2

PATCH     47  48  I  I  M  P  J  K   5   1   1   5   1   2  13  17   1   2
PATCH     48  47  I  I  P  M  J  K   1   5  13  17   1   2   1   5   1   2

PATCH     48  49  I  I  M  P  J  K  17   1   1  17   1   2  13  29   1   2
PATCH     49  48  I  I  P  M  J  K   1  17  13  29   1   2   1  17   1   2

# Blocks 50-57 compose seal cavity for rotor 4
PATCH     50  51  I  I  M  P  J  K  17   1   9  29   1   2   1  21   1   2
PATCH     51  50  I  I  P  M  J  K   1  17   1  21   1   2   9  29   1   2

PATCH     51  52  I  I  M  P  J  K  17   1  17  21   1   2   1   5   1   2
PATCH     52  51  I  I  P  M  J  K   1  17   1   5   1   2  17  21   1   2

PATCH     52  53  I  I  M  P  J  K   5   1   1   5   1   2  13  17   1   2
PATCH     53  52  I  I  P  M  J  K   1   5  13  17   1   2   1   5   1   2

PATCH     53  54  I  I  M  P  J  K  21   1   1  17   1   2   1  17   1   2
PATCH     54  53  I  I  P  M  J  K   1  21   1  17   1   2   1  17   1   2

PATCH     54  55  I  I  M  P  J  K  21   1  25  29   1   2   1   5   1   2
PATCH     55  54  I  I  P  M  J  K   1  21   1   5   1   2  25  29   1   2

PATCH     55  56  I  I  M  P  J  K   5   1   1   5   1   2  17  21   1   2
PATCH     56  55  I  I  P  M  J  K   1   5  17  21   1   2   1   5   1   2

PATCH     56  57  I  I  M  P  J  K  17   1   1  21   1   2  13  33   1   2
```

```
PATCH     57  56  I  I  P  M  J  K   1  17  13  33   1   2   1  21   1   2

# Blocks 58-65 compose seal cavity for rotor 5 flow order 58-59-61-60-62...
PATCH     58  59  I  I  M  P  J  K  17   1   9  29   1   2   1  21   1   2
PATCH     59  58  I  I  P  M  J  K   1  17   1  21   1   2   9  29   1   2

PATCH     59  61  I  I  M  P  J  K  17   1  17  21   1   2   1   5   1   2
PATCH     61  59  I  I  P  M  J  K   1  17   1   5   1   2  17  21   1   2

PATCH     60  61  I  I  P  M  J  K   1   5  17  21   1   2   1   5   1   2
PATCH     61  60  I  I  M  P  J  K   5   1   1   5   1   2  17  21   1   2

PATCH     60  62  I  I  M  P  J  K  21   1   1  21   1   2   1  21   1   2
PATCH     62  60  I  I  P  M  J  K   1  21   1  21   1   2   1  21   1   2

PATCH     62  63  I  I  M  P  J  K  21   1  17  21   1   2   1   5   1   2
PATCH     63  62  I  I  P  M  J  K   1  21   1   5   1   2  17  21   1   2

PATCH     63  64  I  I  M  P  J  K   5   1   1   5   1   2  13  17   1   2
PATCH     64  63  I  I  P  M  J  K   1   5  13  17   1   2   1   5   1   2

PATCH     64  65  I  I  M  P  J  K  17   1   1  17   1   2   9  25   1   2
PATCH     65  64  I  I  P  M  J  K   1  17   9  25   1   2   1  17   1   2


# Stator 1

SSVI      16  16  J  J  P  P  I  K   1   1   1  97   1  33   1  97   1  33
 RPMWALL     TWALL
       0.0         0.0

# Old tip w/ no seals
#SSVI      16  16  J  J  M  M  I  K  49  49   1  97   1  49   1  97   1  49
# RPMWALL     TWALL
#       0.0         0.0

# Tip w/ seal
SSVI      16  16  J  J  M  M  I  K  49  49   1  81   1  33   1  81   1  33
 RPMWALL     TWALL
       0.0         0.0

SSVI      16  16  K  K  P  P  I  J   1   1  17  81   1  49  17  81   1  49
 RPMWALL     TWALL
       0.0         0.0

SSVI      16  16  K  K  M  M  I  J  33  33  17  81   1  49  17  81   1  49
 RPMWALL     TWALL
       0.0         0.0

MBCAVG    16  17  I  I  M  P  J  K  97   1   1  49   1  33   1  49   1  49
NSEGS
  1
LBLOCK2B   LFACE2B  LDIR2B L2LIMB  M2LIM1B M2LIM2B  N2LIM1B N2LIM2B
 17           I       P      1       1       49       1      49

MBCAVG    17  16  I  I  P  M  J  K   1  97   1  49   1  49   1  49   1  33
NSEGS
  1
LBLOCK2B   LFACE2B  LDIR2B L2LIMB  M2LIM1B M2LIM2B  N2LIM1B N2LIM2B
 16           I       M      97      1       49       1      33


# Rotor 1

SSVI      17  17  J  J  P  P  I  K   1   1   1  97   1  49   1  97   1  49
 RPMWALL     TWALL
    3507.000         0.0

SSVI      17  17  J  J  M  M  I  K  49  49   1  97   1  49   1  97   1  49
 RPMWALL     TWALL
    3507.000         0.0

SSVI      17  17  K  K  P  P  I  J   1   1  17  81   1  49  17  81   1  49
 RPMWALL     TWALL
    3507.000         0.0

SSVI      17  17  K  K  M  M  I  J  49  49  17  81   1  49  17  81   1  49
 RPMWALL     TWALL
    3507.000         0.0

MBCAVG    17  18  I  I  M  P  J  K  97   1   1  49   1  49   1  49   1  49
NSEGS
  1
LBLOCK2B   LFACE2B  LDIR2B L2LIMB  M2LIM1B M2LIM2B  N2LIM1B N2LIM2B
 18           I       P      1       1       49       1      49

MBCAVG    18  17  I  I  P  M  J  K   1  97   1  49   1  49   1  49   1  49
NSEGS
  1
LBLOCK2B   LFACE2B  LDIR2B L2LIMB  M2LIM1B M2LIM2B  N2LIM1B N2LIM2B
 17           I       M      97      1       49       1      49
```

```
# Stator 2

SSVI      18  18  J  J  P  P  I  K   1   1   1  97   1  49   1  97   1  49
 RPMWALL     TWALL
       0.0         0.0

# Old tip w/ no seal
#SSVI      18  18  J  J  M  M  I  K  49  49   1  97   1  49   1  97   1  49
# RPMWALL     TWALL
#       0.0         0.0

# New tip w/ seal
SSVI      18  18  J  J  M  M  I  K  49  49  17  81   1  49  17  81   1  49
 RPMWALL     TWALL
       0.0         0.0

SSVI      18  18  K  K  P  P  I  J   1   1  17  81   1  49  17  81   1  49
 RPMWALL     TWALL
       0.0         0.0

SSVI      18  18  K  K  M  M  I  J  49  49  17  81   1  49  17  81   1  49
 RPMWALL     TWALL
       0.0         0.0

MBCAVG    18  19  I  I  M  P  J  K  97   1   1  49   1  49   1  49   1  49
NSEGS
  1
LBLOCK2B   LFACE2B  LDIR2B L2LIMB  M2LIM1B M2LIM2B  N2LIM1B N2LIM2B
 19           I       P      1       1       49        1      49

MBCAVG    19  18  I  I  P  M  J  K   1  97   1  49   1  49   1  49   1  49
NSEGS
  1
LBLOCK2B   LFACE2B  LDIR2B L2LIMB  M2LIM1B M2LIM2B  N2LIM1B N2LIM2B
 18           I       M      97      1       49        1      49


# Rotor 2

SSVI      19  19  J  J  P  P  I  K   1   1   1  97   1  49   1  97   1  49
 RPMWALL     TWALL
    3507.000         0.0

SSVI      19  19  J  J  M  M  I  K  49  49   1  97   1  49   1  97   1  49
 RPMWALL     TWALL
    3507.000         0.0

SSVI      19  19  K  K  P  P  I  J   1   1  17  81   1  49  17  81   1  49
 RPMWALL     TWALL
    3507.000         0.0

SSVI      19  19  K  K  M  M  I  J  49  49  17  81   1  49  17  81   1  49
 RPMWALL     TWALL
    3507.000         0.0

MBCAVG    19  20  I  I  M  P  J  K  97   1   1  49   1  49   1  49   1  49
NSEGS
  1
LBLOCK2B   LFACE2B  LDIR2B L2LIMB  M2LIM1B M2LIM2B  N2LIM1B N2LIM2B
 20           I       P      1       1       49        1      49

MBCAVG    20  19  I  I  P  M  J  K   1  97   1  49   1  49   1  49   1  49
NSEGS
  1
LBLOCK2B   LFACE2B  LDIR2B L2LIMB  M2LIM1B M2LIM2B  N2LIM1B N2LIM2B
 19           I       M      97      1       49        1      49


# Stator 3

SSVI      20  20  J  J  P  P  I  K   1   1   1  97   1  49   1  97   1  49
 RPMWALL     TWALL
       0.0         0.0

# Old tip w/ no seal
#SSVI      20  20  J  J  M  M  I  K  49  49   1  97   1  49   1  97   1  49
# RPMWALL     TWALL
#       0.0         0.0

# New tip w/ seal
SSVI      20  20  J  J  M  M  I  K  49  49  17  81   1  49  17  81   1  49
 RPMWALL     TWALL
       0.0         0.0

SSVI      20  20  K  K  P  P  I  J   1   1  17  81   1  49  17  81   1  49
 RPMWALL     TWALL
       0.0         0.0

SSVI      20  20  K  K  M  M  I  J  49  49  17  81   1  49  17  81   1  49
 RPMWALL     TWALL
       0.0         0.0
```

```
MBCAVG    20  21  I  I  M  P  J  K  97   1   1  49   1  49   1  49   1  49
NSEGS
  1
LBLOCK2B   LFACE2B  LDIR2B L2LIMB  M2LIM1B M2LIM2B  N2LIM1B N2LIM2B
 21          I       P      1       1       49       1      49

MBCAVG    21  20  I  I  P  M  J  K   1  97   1  49   1  49   1  49   1  49
NSEGS
  1
LBLOCK2B   LFACE2B  LDIR2B L2LIMB  M2LIM1B M2LIM2B  N2LIM1B N2LIM2B
 20          I       M      97      1       49       1      49


# Rotor 3

SSVI      21  21  J  J  P  P  I  K   1   1   1  97   1  49   1  97   1  49
 RPMWALL     TWALL
    3507.000         0.0

SSVI      21  21  J  J  M  M  I  K  49  49   1  97   1  49   1  97   1  49
 RPMWALL     TWALL
    3507.000         0.0

SSVI      21  21  K  K  P  P  I  J   1   1  17  81   1  49  17  81   1  49
 RPMWALL     TWALL
    3507.000         0.0

SSVI      21  21  K  K  M  M  I  J  49  49  17  81   1  49  17  81   1  49
 RPMWALL     TWALL
    3507.000         0.0

MBCAVG    21  22  I  I  M  P  J  K  97   1   1  49   1  49   1  49   1  49
NSEGS
  1
LBLOCK2B   LFACE2B  LDIR2B L2LIMB  M2LIM1B M2LIM2B  N2LIM1B N2LIM2B
 22          I       P      1       1       49       1      49

MBCAVG    22  21  I  I  P  M  J  K   1  97   1  49   1  49   1  49   1  49
NSEGS
  1
LBLOCK2B   LFACE2B  LDIR2B L2LIMB  M2LIM1B M2LIM2B  N2LIM1B N2LIM2B
 21          I       M      97      1       49       1      49


# Stator 4

SSVI      22  22  J  J  P  P  I  K   1   1   1  97   1  49   1  97   1  49
 RPMWALL     TWALL
       0.0         0.0

# Old tip w/ no seal
#SSVI      22  22  J  J  M  M  I  K  49  49   1  97   1  49   1  97   1  49
# RPMWALL     TWALL
#       0.0         0.0

# New tip w/ seal
SSVI      22  22  J  J  M  M  I  K  49  49  17  81   1  49  17  81   1  49
 RPMWALL     TWALL
       0.0         0.0

SSVI      22  22  K  K  P  P  I  J   1   1  17  81   1  49  17  81   1  49
 RPMWALL     TWALL
       0.0         0.0

SSVI      22  22  K  K  M  M  I  J  49  49  17  81   1  49  17  81   1  49
 RPMWALL     TWALL
       0.0         0.0

MBCAVG    22  23  I  I  M  P  J  K  97   1   1  49   1  49   1  49   1  49
NSEGS
  1
LBLOCK2B   LFACE2B  LDIR2B L2LIMB  M2LIM1B M2LIM2B  N2LIM1B N2LIM2B
 23          I       P      1       1       49       1      49

MBCAVG    23  22  I  I  P  M  J  K   1  97   1  49   1  49   1  49   1  49
NSEGS
  1
LBLOCK2B   LFACE2B  LDIR2B L2LIMB  M2LIM1B M2LIM2B  N2LIM1B N2LIM2B
 22          I       M      97      1       49       1      49


# Rotor 4

SSVI      23  23  J  J  P  P  I  K   1   1   1  97   1  49   1  97   1  49
 RPMWALL     TWALL
    3507.000         0.0

SSVI      23  23  J  J  M  M  I  K  49  49   1  97   1  49   1  97   1  49
 RPMWALL     TWALL
    3507.000         0.0
```

```
SSVI      23  23  K  K  P  P  I  J   1   1  17  81   1  49  17  81   1  49
 RPMWALL     TWALL
    3507.000         0.0

SSVI      23  23  K  K  M  M  I  J  49  49  17  81   1  49  17  81   1  49
 RPMWALL     TWALL
    3507.000         0.0

MBCAVG    23  24  I  I  M  P  J  K  97   1   1  49   1  49   1  49   1  49
NSEGS
  1
LBLOCK2B   LFACE2B  LDIR2B L2LIMB  M2LIM1B M2LIM2B  N2LIM1B N2LIM2B
 24           I       P      1       1       49        1      49

MBCAVG    24  23  I  I  P  M  J  K   1  97   1  49   1  49   1  49   1  49
NSEGS
  1
LBLOCK2B   LFACE2B  LDIR2B L2LIMB  M2LIM1B M2LIM2B  N2LIM1B N2LIM2B
 23           I       M      97      1       49        1      49


# Stator 5

SSVI      24  24  J  J  P  P  I  K   1   1   1  97   1  49   1  97   1  49
 RPMWALL     TWALL
       0.0         0.0

# Old tip w/ no seal
#SSVI      24  24  J  J  M  M  I  K  49  49   1  97   1  49   1  97   1  49
# RPMWALL     TWALL
#       0.0         0.0

# New tip w/ seal
SSVI      24  24  J  J  M  M  I  K  49  49  17  81   1  49  17  81   1  49
 RPMWALL     TWALL
       0.0         0.0

SSVI      24  24  K  K  P  P  I  J   1   1  17  81   1  49  17  81   1  49
 RPMWALL     TWALL
       0.0         0.0

SSVI      24  24  K  K  M  M  I  J  49  49  17  81   1  49  17  81   1  49
 RPMWALL     TWALL
       0.0         0.0

MBCAVG    24  25  I  I  M  P  J  K  97   1   1  49   1  49   1  49   1  49
NSEGS
  1
LBLOCK2B   LFACE2B  LDIR2B L2LIMB  M2LIM1B M2LIM2B  N2LIM1B N2LIM2B
 25           I       P      1       1       49        1      49

MBCAVG    25  24  I  I  P  M  J  K   1  97   1  49   1  49   1  49   1  49
NSEGS
  1
LBLOCK2B   LFACE2B  LDIR2B L2LIMB  M2LIM1B M2LIM2B  N2LIM1B N2LIM2B
 24           I       M      97      1       49        1      49


# Rotor 5

SSVI      25  25  J  J  P  P  I  K   1   1   1 129   1  49   1 129   1  49
 RPMWALL     TWALL
    3507.000         0.0

# Split to accept tip seal
SSVI      25  25  J  J  M  M  I  K  49  49   1  97   1  49   1  97   1  49
 RPMWALL     TWALL
    3507.000         0.0

# Split to accept tip seal
SSVI      25  25  J  J  M  M  I  K  49  49 113 129   1  49 113 129   1  49
 RPMWALL     TWALL
    3507.000         0.0

SSVI      25  25  K  K  P  P  I  J   1   1  17  81   1  49  17  81   1  49
 RPMWALL     TWALL
    3507.000         0.0

SSVI      25  25  K  K  M  M  I  J  49  49  17  81   1  49  17  81   1  49
 RPMWALL     TWALL
    3507.000         0.0

# LPT to mixer linkup
MBCAVG    25  66  I  I  M  P  J  K 129   1   1  49   1  49   1  45   1  81
NSEGS
  1
LBLOCK2B   LFACE2B  LDIR2B L2LIMB  M2LIM1B M2LIM2B  N2LIM1B N2LIM2B
  66          I       P      1       1       45        1      81

MBCAVG    66  25  I  I  P  M  J  K   1 129   1  45   1  81   1  49   1  49
NSEGS
  1
```

```
LBLOCK2B   LFACE2B  LDIR2B L2LIMB  M2LIM1B M2LIM2B  N2LIM1B N2LIM2B
 25          I       M     129       1      49         1     49


# Rotor 1 seal cavity 2d/3d mixing plane linkup and outer boundaries
SSVI      26  26  I  I  P  P  J  K   1   1   1  29   1   2   1  29   1   2
 RPMWALL      TWALL
       0.0          0.0

SSVI      26  26  I  I  M  M  J  K  17  17   1   9   1   2   1   9   1   2
 RPMWALL      TWALL
    3507.000          0.0

SSVI      26  26  J  J  M  M  I  K  29  29   1  17   1   2   1  17   1   2
 RPMWALL      TWALL
       0.0          0.0

MBCAVG    16  26  J  J  M  P  I  K  49   1  81  97   1  33   1  17   1   2
NSEGS
  1
LBLOCK2B   LFACE2B  LDIR2B L2LIMB  M2LIM1B M2LIM2B  N2LIM1B N2LIM2B
  26          J       P       1       1      17         1       2

MBCAVG    26  16  J  J  P  M  I  K   1  49   1  17   1   2  81  97   1  33
NSEGS
  1
LBLOCK2B   LFACE2B  LDIR2B L2LIMB  M2LIM1B M2LIM2B  N2LIM1B N2LIM2B
 16          J       M      49      81      97         1      33

SSVI      27  27  I  I  M  M  J  K  17  17   1  17   1   2   1  17   1   2
 RPMWALL      TWALL
    3507.000          0.0

SSVI      27  27  J  J  P  P  I  K   1   1   1  17   1   2   1  17   1   2
 RPMWALL      TWALL
    3507.000          0.0

SSVI      27  27  J  J  M  M  I  K  21  21   1  17   1   2   1  17   1   2
 RPMWALL      TWALL
       0.0          0.0

SSVI      28  28  J  J  P  P  I  K   1   1   1   5   1   2   1   5   1   2
 RPMWALL      TWALL
    3507.000          0.0

SSVI      28  28  J  J  M  M  I  K   5   5   1   5   1   2   1   5   1   2
 RPMWALL      TWALL
       0.0          0.0

SSVI      29  29  I  I  P  P  J  K   1   1   1  13   1   2   1  13   1   2
 RPMWALL      TWALL
    3507.000          0.0

SSVI      29  29  J  J  P  P  I  K   1   1   1  21   1   2   1  21   1   2
 RPMWALL      TWALL
    3507.000          0.0

SSVI      29  29  J  J  M  M  I  K  17  17   1  21   1   2   1  21   1   2
 RPMWALL      TWALL
       0.0          0.0

SSVI      30  30  I  I  P  P  J  K   1   1  17  33   1   2  17  33   1   2
 RPMWALL      TWALL
       0.0          0.0

SSVI      30  30  I  I  M  M  J  K  21  21   1  29   1   2   1  29   1   2
 RPMWALL      TWALL
    3507.000          0.0

SSVI      30  30  J  J  P  P  I  K   1   1   1  21   1   2   1  21   1   2
 RPMWALL      TWALL
    3507.000          0.0

SSVI      30  30  J  J  M  M  I  K  33  33   1  21   1   2   1  21   1   2
 RPMWALL      TWALL
       0.0          0.0

SSVI      31  31  J  J  P  P  I  K   1   1   1   5   1   2   1   5   1   2
 RPMWALL      TWALL
    3507.000          0.0

SSVI      31  31  J  J  M  M  I  K   5   5   1   5   1   2   1   5   1   2
 RPMWALL      TWALL
       0.0          0.0

SSVI      32  32  I  I  P  P  J  K   1   1   1  13   1   2   1  13   1   2
 RPMWALL      TWALL
    3507.000          0.0

SSVI      32  32  J  J  P  P  I  K   1   1   1  17   1   2   1  17   1   2
 RPMWALL      TWALL
```

```
   3507.000        0.0

SSVI     32  32  J  J  M  M  I  K  17  17   1  17   1   2   1  17   1   2
 RPMWALL     TWALL
      0.0        0.0

SSVI     33  33  I  I  P  P  J  K   1   1   1  13   1   2   1  13   1   2
 RPMWALL     TWALL
   3507.000        0.0

SSVI     33  33  I  I  M  M  J  K  17  17   1  29   1   2   1  29   1   2
 RPMWALL     TWALL
      0.0        0.0

SSVI     33  33  J  J  M  M  I  K  29  29   1  17   1   2   1  17   1   2
 RPMWALL     TWALL
      0.0        0.0

MBCAVG   18  33  J  J  M  P  I  K  49   1   1  17   1  49   1  17   1   2
NSEGS
  1
LBLOCK2B   LFACE2B  LDIR2B L2LIMB  M2LIM1B M2LIM2B  N2LIM1B N2LIM2B
  33          J       P       1       1      17        1       2

MBCAVG   33  18  J  J  P  M  I  K   1  49   1  17   1   2   1  17   1  49
NSEGS
  1
LBLOCK2B   LFACE2B  LDIR2B L2LIMB  M2LIM1B M2LIM2B  N2LIM1B N2LIM2B
 18           J       M      49       1      17        1      49


# Rotor 2 seal cavity 2d/3d mixing plane linkup and outer boundaries

SSVI     34  34  I  I  P  P  J  K   1   1   1  29   1   2   1  29   1   2
 RPMWALL     TWALL
      0.0        0.0

SSVI     34  34  I  I  M  M  J  K  17  17   1   9   1   2   1   9   1   2
 RPMWALL     TWALL
   3507.000        0.0

SSVI     34  34  J  J  M  M  I  K  29  29   1  17   1   2   1  17   1   2
 RPMWALL     TWALL
      0.0        0.0

MBCAVG   18  34  J  J  M  P  I  K  49   1  81  97   1  49   1  17   1   2
NSEGS
  1
LBLOCK2B   LFACE2B  LDIR2B L2LIMB  M2LIM1B M2LIM2B  N2LIM1B N2LIM2B
  34          J       P       1       1      17        1       2

MBCAVG   34  18  J  J  P  M  I  K   1  49   1  17   1   2  81  97   1  49
NSEGS
  1
LBLOCK2B   LFACE2B  LDIR2B L2LIMB  M2LIM1B M2LIM2B  N2LIM1B N2LIM2B
 18           J       M      49      81      97        1      49

SSVI     35  35  I  I  M  M  J  K  17  17   1  17   1   2   1  17   1   2
 RPMWALL     TWALL
   3507.000        0.0

SSVI     35  35  J  J  P  P  I  K   1   1   1  17   1   2   1  17   1   2
 RPMWALL     TWALL
   3507.000        0.0

SSVI     35  35  J  J  M  M  I  K  21  21   1  17   1   2   1  17   1   2
 RPMWALL     TWALL
      0.0        0.0

SSVI     36  36  J  J  P  P  I  K   1   1   1   5   1   2   1   5   1   2
 RPMWALL     TWALL
   3507.000        0.0

SSVI     36  36  J  J  M  M  I  K   5   5   1   5   1   2   1   5   1   2
 RPMWALL     TWALL
      0.0        0.0

SSVI     37  37  I  I  P  P  J  K   1   1   1  13   1   2   1  13   1   2
 RPMWALL     TWALL
   3507.000        0.0

SSVI     37  37  J  J  P  P  I  K   1   1   1  21   1   2   1  21   1   2
 RPMWALL     TWALL
   3507.000        0.0

SSVI     37  37  J  J  M  M  I  K  17  17   1  21   1   2   1  21   1   2
 RPMWALL     TWALL
      0.0        0.0

SSVI     38  38  I  I  P  P  J  K   1   1  17  33   1   2  17  33   1   2
 RPMWALL     TWALL
```

```
      0.0         0.0

SSVI      38  38  I  I  M  M  J  K  21  21   1  29   1   2   1  29   1   2
 RPMWALL     TWALL
    3507.000         0.0

SSVI      38  38  J  J  P  P  I  K   1   1   1  21   1   2   1  21   1   2
 RPMWALL     TWALL
    3507.000         0.0

SSVI      38  38  J  J  M  M  I  K  33  33   1  21   1   2   1  21   1   2
 RPMWALL     TWALL
      0.0         0.0

SSVI      39  39  J  J  P  P  I  K   1   1   1   5   1   2   1   5   1   2
 RPMWALL     TWALL
    3507.000         0.0

SSVI      39  39  J  J  M  M  I  K   5   5   1   5   1   2   1   5   1   2
 RPMWALL     TWALL
      0.0         0.0

SSVI      40  40  I  I  P  P  J  K   1   1   1  13   1   2   1  13   1   2
 RPMWALL     TWALL
    3507.000         0.0

SSVI      40  40  J  J  P  P  I  K   1   1   1  17   1   2   1  17   1   2
 RPMWALL     TWALL
    3507.000         0.0

SSVI      40  40  J  J  M  M  I  K  17  17   1  17   1   2   1  17   1   2
 RPMWALL     TWALL
      0.0         0.0

SSVI      41  41  I  I  P  P  J  K   1   1   1  13   1   2   1  13   1   2
 RPMWALL     TWALL
    3507.000         0.0

SSVI      41  41  I  I  M  M  J  K  17  17   1  29   1   2   1  29   1   2
 RPMWALL     TWALL
      0.0         0.0

SSVI      41  41  J  J  M  M  I  K  29  29   1  17   1   2   1  17   1   2
 RPMWALL     TWALL
      0.0         0.0

MBCAVG    20  41  J  J  M  P  I  K  49   1   1  17   1  49   1  17   1   2
NSEGS
  1
LBLOCK2B   LFACE2B  LDIR2B L2LIMB  M2LIM1B M2LIM2B  N2LIM1B N2LIM2B
  41          J       P       1       1      17        1       2

MBCAVG    41  20  J  J  P  M  I  K   1  49   1  17   1   2   1  17   1  49
NSEGS
  1
LBLOCK2B   LFACE2B  LDIR2B L2LIMB  M2LIM1B M2LIM2B  N2LIM1B N2LIM2B
 20           J       M      49       1      17        1     49


# Rotor 3 seal cavity 2d/3d mixing plane linkup and outer boundaries

SSVI     42  42  I  I  P  P  J  K   1   1   1  29   1   2   1  29   1   2
 RPMWALL     TWALL
      0.0         0.0

SSVI      42  42  I  I  M  M  J  K  17  17   1   9   1   2   1   9   1   2
 RPMWALL     TWALL
    3507.000         0.0

SSVI      42  42  J  J  M  M  I  K  29  29   1  17   1   2   1  17   1   2
 RPMWALL     TWALL
      0.0         0.0

MBCAVG    20  42  J  J  M  P  I  K  49   1  81  97   1  49   1  17   1   2
NSEGS
  1
LBLOCK2B   LFACE2B  LDIR2B L2LIMB  M2LIM1B M2LIM2B  N2LIM1B N2LIM2B
  42          J       P       1       1      17        1       2

MBCAVG    42  20  J  J  P  M  I  K   1  49   1  17   1   2  81  97   1  49
NSEGS
  1
LBLOCK2B   LFACE2B  LDIR2B L2LIMB  M2LIM1B M2LIM2B  N2LIM1B N2LIM2B
 20           J       M      49      81      97        1     49

SSVI      43  43  I  I  M  M  J  K  17  17   1  17   1   2   1  17   1   2
 RPMWALL     TWALL
    3507.000         0.0

SSVI      43  43  J  J  P  P  I  K   1   1   1  17   1   2   1  17   1   2
 RPMWALL     TWALL
    3507.000         0.0
```

```
SSVI     43  43  J  J  M  M  I  K  21  21   1  17   1   2   1  17   1   2
 RPMWALL     TWALL
      0.0         0.0

SSVI     44  44  J  J  P  P  I  K   1   1   1   5   1   2   1   5   1   2
 RPMWALL     TWALL
   3507.000         0.0

SSVI     44  44  J  J  M  M  I  K   5   5   1   5   1   2   1   5   1   2
 RPMWALL     TWALL
      0.0         0.0

SSVI     45  45  I  I  P  P  J  K   1   1   1  13   1   2   1  13   1   2
 RPMWALL     TWALL
   3507.000         0.0

SSVI     45  45  J  J  P  P  I  K   1   1   1  21   1   2   1  21   1   2
 RPMWALL     TWALL
   3507.000         0.0

SSVI     45  45  J  J  M  M  I  K  17  17   1  21   1   2   1  21   1   2
 RPMWALL     TWALL
      0.0         0.0

SSVI     46  46  I  I  P  P  J  K   1   1  17  33   1   2  17  33   1   2
 RPMWALL     TWALL
      0.0         0.0

SSVI     46  46  I  I  M  M  J  K  21  21   1  29   1   2   1  29   1   2
 RPMWALL     TWALL
   3507.000         0.0

SSVI     46  46  J  J  P  P  I  K   1   1   1  21   1   2   1  21   1   2
 RPMWALL     TWALL
   3507.000         0.0

SSVI     46  46  J  J  M  M  I  K  33  33   1  21   1   2   1  21   1   2
 RPMWALL     TWALL
      0.0         0.0

SSVI     47  47  J  J  P  P  I  K   1   1   1   5   1   2   1   5   1   2
 RPMWALL     TWALL
   3507.000         0.0

SSVI     47  47  J  J  M  M  I  K   5   5   1   5   1   2   1   5   1   2
 RPMWALL     TWALL
      0.0         0.0

SSVI     48  48  I  I  P  P  J  K   1   1   1  13   1   2   1  13   1   2
 RPMWALL     TWALL
   3507.000         0.0

SSVI     48  48  J  J  P  P  I  K   1   1   1  17   1   2   1  17   1   2
 RPMWALL     TWALL
   3507.000         0.0

SSVI     48  48  J  J  M  M  I  K  17  17   1  17   1   2   1  17   1   2
 RPMWALL     TWALL
      0.0         0.0

SSVI     49  49  I  I  P  P  J  K   1   1   1  13   1   2   1  13   1   2
 RPMWALL     TWALL
   3507.000         0.0

SSVI     49  49  I  I  M  M  J  K  17  17   1  29   1   2   1  29   1   2
 RPMWALL     TWALL
      0.0         0.0

SSVI     49  49  J  J  M  M  I  K  29  29   1  17   1   2   1  17   1   2
 RPMWALL     TWALL
      0.0         0.0

MBCAVG   22  49  J  J  M  P  I  K  49   1   1  17   1  49   1  17   1   2
NSEGS
  1
LBLOCK2B   LFACE2B  LDIR2B L2LIMB  M2LIM1B M2LIM2B  N2LIM1B N2LIM2B
  49          J       P       1       1      17        1       2

MBCAVG   49  22  J  J  P  M  I  K   1  49   1  17   1   2   1  17   1  49
NSEGS
  1
LBLOCK2B   LFACE2B  LDIR2B L2LIMB  M2LIM1B M2LIM2B  N2LIM1B N2LIM2B
 22          J       M      49       1      17        1      49


# Rotor 4 seal cavity 2d/3d mixing plane linkup and outer boundaries

SSVI     50  50  I  I  P  P  J  K   1   1   1  29   1   2   1  29   1   2
 RPMWALL     TWALL
      0.0         0.0
```

```
SSVI      50  50  I  I  M  M  J  K  17  17   1   9   1   2   1   9   1   2
 RPMWALL     TWALL
    3507.000         0.0

SSVI      50  50  J  J  M  M  I  K  29  29   1  17   1   2   1  17   1   2
 RPMWALL     TWALL
       0.0         0.0

MBCAVG    22  50  J  J  M  P  I  K  49   1  81  97   1  49   1  17   1   2
NSEGS
  1
LBLOCK2B   LFACE2B  LDIR2B L2LIMB  M2LIM1B M2LIM2B  N2LIM1B N2LIM2B
  50          J       P       1       1      17        1       2

MBCAVG    50  22  J  J  P  M  I  K   1  49   1  17   1   2  81  97   1  49
NSEGS
  1
LBLOCK2B   LFACE2B  LDIR2B L2LIMB  M2LIM1B M2LIM2B  N2LIM1B N2LIM2B
 22           J       M      49      81      97        1      49

SSVI      51  51  I  I  M  M  J  K  17  17   1  17   1   2   1  17   1   2
 RPMWALL     TWALL
    3507.000         0.0

SSVI      51  51  J  J  P  P  I  K   1   1   1  17   1   2   1  17   1   2
 RPMWALL     TWALL
    3507.000         0.0

SSVI      51  51  J  J  M  M  I  K  21  21   1  17   1   2   1  17   1   2
 RPMWALL     TWALL
       0.0         0.0

SSVI      52  52  J  J  P  P  I  K   1   1   1   5   1   2   1   5   1   2
 RPMWALL     TWALL
    3507.000         0.0

SSVI      52  52  J  J  M  M  I  K   5   5   1   5   1   2   1   5   1   2
 RPMWALL     TWALL
       0.0         0.0

SSVI      53  53  I  I  P  P  J  K   1   1   1  13   1   2   1  13   1   2
 RPMWALL     TWALL
    3507.000         0.0

SSVI      53  53  J  J  P  P  I  K   1   1   1  21   1   2   1  21   1   2
 RPMWALL     TWALL
    3507.000         0.0

SSVI      53  53  J  J  M  M  I  K  17  17   1  21   1   2   1  21   1   2
 RPMWALL     TWALL
       0.0         0.0

SSVI      54  54  I  I  P  P  J  K   1   1  17  29   1   2  17  29   1   2
 RPMWALL     TWALL
       0.0         0.0

SSVI      54  54  I  I  M  M  J  K  21  21   1  25   1   2   1  25   1   2
 RPMWALL     TWALL
    3507.000         0.0

SSVI      54  54  J  J  P  P  I  K   1   1   1  21   1   2   1  21   1   2
 RPMWALL     TWALL
    3507.000         0.0

SSVI      54  54  J  J  M  M  I  K  29  29   1  21   1   2   1  21   1   2
 RPMWALL     TWALL
       0.0         0.0

SSVI      55  55  J  J  P  P  I  K   1   1   1   5   1   2   1   5   1   2
 RPMWALL     TWALL
    3507.000         0.0

SSVI      55  55  J  J  M  M  I  K   5   5   1   5   1   2   1   5   1   2
 RPMWALL     TWALL
       0.0         0.0

SSVI      56  56  I  I  P  P  J  K   1   1   1  17   1   2   1  17   1   2
 RPMWALL     TWALL
    3507.000         0.0

SSVI      56  56  J  J  P  P  I  K   1   1   1  17   1   2   1  17   1   2
 RPMWALL     TWALL
    3507.000         0.0

SSVI      56  56  J  J  M  M  I  K  21  21   1  17   1   2   1  17   1   2
 RPMWALL     TWALL
       0.0         0.0

SSVI      57  57  I  I  P  P  J  K   1   1   1  13   1   2   1  13   1   2
 RPMWALL     TWALL
    3507.000         0.0
```

```
SSVI      57  57  I  I  M  M  J  K  17  17   1  33   1   2   1  33   1   2
 RPMWALL     TWALL
       0.0         0.0

SSVI      57  57  J  J  M  M  I  K  33  33   1  17   1   2   1  17   1   2
 RPMWALL     TWALL
       0.0         0.0

MBCAVG    24  57  J  J  M  P  I  K  49   1   1  17   1  49   1  17   1   2
NSEGS
  1
LBLOCK2B   LFACE2B  LDIR2B L2LIMB  M2LIM1B M2LIM2B  N2LIM1B N2LIM2B
  57          J       P       1       1      17        1       2

MBCAVG    57  24  J  J  P  M  I  K   1  49   1  17   1   2   1  17   1  49
NSEGS
  1
LBLOCK2B   LFACE2B  LDIR2B L2LIMB  M2LIM1B M2LIM2B  N2LIM1B N2LIM2B
 24           J       M      49       1      17        1     49


# Rotor 5 seal cavity 2d/3d mixing plane linkup and outer boundaries

SSVI      58  58  I  I  P  P  J  K   1   1   1  29   1   2   1  29   1   2
 RPMWALL     TWALL
       0.0         0.0

SSVI      58  58  I  I  M  M  J  K  17  17   1   9   1   2   1   9   1   2
 RPMWALL     TWALL
    3507.000         0.0

SSVI      58  58  J  J  M  M  I  K  29  29   1  17   1   2   1  17   1   2
 RPMWALL     TWALL
       0.0         0.0

MBCAVG    24  58  J  J  M  P  I  K  49   1  81  97   1  49   1  17   1   2
NSEGS
  1
LBLOCK2B   LFACE2B  LDIR2B L2LIMB  M2LIM1B M2LIM2B  N2LIM1B N2LIM2B
  58          J       P       1       1      17        1       2

MBCAVG    58  24  J  J  P  M  I  K   1  49   1  17   1   2  81  97   1  49
NSEGS
  1
LBLOCK2B   LFACE2B  LDIR2B L2LIMB  M2LIM1B M2LIM2B  N2LIM1B N2LIM2B
 24           J       M      49      81      97        1     49

SSVI      59  59  I  I  M  M  J  K  17  17   1  17   1   2   1  17   1   2
 RPMWALL     TWALL
    3507.000         0.0

SSVI      59  59  J  J  P  P  I  K   1   1   1  17   1   2   1  17   1   2
 RPMWALL     TWALL
    3507.000         0.0

SSVI      59  59  J  J  M  M  I  K  21  21   1  17   1   2   1  17   1   2
 RPMWALL     TWALL
       0.0         0.0

# Remember blocks 45 and 46 are switched from logical sequence
SSVI      60  60  I  I  P  P  J  K   1   1   1  17   1   2   1  17   1   2
 RPMWALL     TWALL
    3507.000         0.0

SSVI      60  60  J  J  P  P  I  K   1   1   1  21   1   2   1  21   1   2
 RPMWALL     TWALL
    3507.000         0.0

SSVI      60  60  J  J  M  M  I  K  21  21   1  21   1   2   1  21   1   2
 RPMWALL     TWALL
       0.0         0.0

SSVI      61  61  J  J  P  P  I  K   1   1   1   5   1   2   1   5   1   2
 RPMWALL     TWALL
    3507.000         0.0

SSVI      61  61  J  J  M  M  I  K   5   5   1   5   1   2   1   5   1   2
 RPMWALL     TWALL
       0.0         0.0

SSVI      62  62  I  I  M  M  J  K  21  21   1  17   1   2   1  17   1   2
 RPMWALL     TWALL
    3507.000         0.0

SSVI      62  62  J  J  P  P  I  K   1   1   1  21   1   2   1  21   1   2
 RPMWALL     TWALL
    3507.000         0.0

SSVI      62  62  J  J  M  M  I  K  21  21   1  21   1   2   1  21   1   2
 RPMWALL     TWALL
       0.0         0.0
```

```
SSVI      63  63  J  J  P  P  I  K   1   1   1   5   1   2   1   5   1   2
 RPMWALL      TWALL
    3507.000         0.0

SSVI      63  63  J  J  M  M  I  K   5   5   1   5   1   2   1   5   1   2
 RPMWALL      TWALL
       0.0         0.0

SSVI      64  64  I  I  P  P  J  K   1   1   1  13   1   2   1  13   1   2
 RPMWALL      TWALL
    3507.000         0.0

SSVI      64  64  J  J  P  P  I  K   1   1   1  17   1   2   1  17   1   2
 RPMWALL      TWALL
    3507.000         0.0

SSVI      64  64  J  J  M  M  I  K  17  17   1  17   1   2   1  17   1   2
 RPMWALL      TWALL
       0.0         0.0

SSVI      65  65  I  I  P  P  J  K   1   1   1   9   1   2   1   9   1   2
 RPMWALL      TWALL
    3507.000         0.0

SSVI      65  65  I  I  M  M  J  K  17  17   1  25   1   2   1  25   1   2
 RPMWALL      TWALL
       0.0         0.0

SSVI      65  65  J  J  M  M  I  K  25  25   1  17   1   2   1  17   1   2
 RPMWALL      TWALL
       0.0         0.0

MBCAVG    25  65  J  J  M  P  I  K  49   1  97 113   1  49   1  17   1   2
NSEGS
  1
LBLOCK2B   LFACE2B  LDIR2B L2LIMB  M2LIM1B M2LIM2B  N2LIM1B N2LIM2B
  65          J       P       1       1      17        1       2

MBCAVG    65  25  J  J  P  M  I  K   1  49   1  17   1   2  97 113   1  49
NSEGS
  1
LBLOCK2B   LFACE2B  LDIR2B L2LIMB  M2LIM1B M2LIM2B  N2LIM1B N2LIM2B
  25          J       M      49      97     113        1      49
```

```
# MIXER AND EXIT GRIDDING
#
#
#
#
#
#
# B       L  L  L  L  L  L  L  L   L   L   M   M   N   N   M   M   N   N
# C       B  B  F  F  D  D  S  S   1   2   1   1   1   1   2   2   2   2
# T       L  L  A  A  I  I  P  P   L   L   L   L   L   L   L   L   L   L
# Y       O  O  C  C  R  R  E  E   I   I   I   I   I   I   I   I   I   I
# P       C  C  E  E  1  2  C  C   M   M   M   M   M   M   M   M   M   M
# E       K  K  1  2        1  2           1   2   1   2   1   2   1   2
#         1  2
# ------ -- -- -- -- -- -- -- -- --- --- --- --- --- --- --- --- --- ---
PATCH     66  72  I  I  M  P  J  K  65   1   1  45   1  81   1  45   1  81
PATCH     72  66  I  I  P  M  J  K   1  65   1  45   1  81   1  45   1  81

PATCH     66  66  K  K  M  P  I  J  81   1   1  65   1  45   1  65   1  45
PATCH     66  66  K  K  P  M  I  J   1  81   1  65   1  45   1  65   1  45

PATCH     67  68  J  J  M  P  I  K   9   1   1  81   1  81   1  81   1  81
PATCH     68  67  J  J  P  M  I  K   1   9   1  81   1  81   1  81   1  81

PATCH     67  67  K  K  M  P  I  J  81   1   1  81   1   9   1  81   1   9
PATCH     67  67  K  K  P  M  I  J   1  81   1  81   1   9   1  81   1   9

PATCH     68  72  I  I  P  M  J  K   1  49   1  49   1  81   1  49   1  81
PATCH     72  68  I  I  M  P  J  K  49   1   1  49   1  81   1  49   1  81

PATCH     68  69  J  J  M  P  I  K  49   1   1  81   1  81   1  81   1  81
PATCH     69  68  J  J  P  M  I  K   1  49   1  81   1  81   1  81   1  81

PATCH     68  68  K  K  M  P  I  J  81   1   1  81   1  49   1  81   1  49
PATCH     68  68  K  K  P  M  I  J   1  81   1  81   1  49   1  81   1  49

PATCH     69  74  I  I  P  M  J  K   1  49   1  49   1  81   1  49   1  81
PATCH     74  69  I  I  M  P  J  K  49   1   1  49   1  81   1  49   1  81
```

```
PATCH     69  70  J  J  M  P  I  K  49   1   1   9   1  81  65  73   1  81
PATCH     70  69  J  J  P  M  I  K   1  49  65  73   1  81   1   9   1  81

PATCH     69  71  J  J  M  P  I  K  49   1   9  81   1  81   1  73   1  81
PATCH     71  69  J  J  P  M  I  K   1  49   1  73   1  81   9  81   1  81

PATCH     69  69  K  K  M  P  I  J  81   1   1  81   1  49   1  81   1  49
PATCH     69  69  K  K  P  M  I  J   1  81   1  81   1  49   1  81   1  49

PATCH     70  70  K  K  M  P  I  J  81   1   1  73   1  49   1  73   1  49
PATCH     71  71  K  K  M  P  I  J  81   1   1  73   1  49   1  73   1  49

PATCH     70  70  K  K  P  M  I  J   1  81   1  73   1  49   1  73   1  49
PATCH     71  71  K  K  P  M  I  J   1  81   1  73   1  49   1  73   1  49

PATCH     72  74  J  J  M  P  I  K  49   1   1  49   1  81   1  49   1  81
PATCH     74  72  J  J  P  M  I  K   1  49   1  49   1  81   1  49   1  81

PATCH     72  72  K  K  M  P  I  J  81   1   1  49   1  49   1  49   1  49
PATCH     72  72  K  K  P  M  I  J   1  81   1  49   1  49   1  49   1  49

PATCH     73  74  I  I  M  P  J  K  65   1   1  49   1  81   1  49   1  81
PATCH     74  73  I  I  P  M  J  K   1  65   1  49   1  81   1  49   1  81

PATCH     73  73  K  K  M  P  I  J  81   1   1  65   1  49   1  65   1  49
PATCH     73  73  K  K  P  M  I  J   1  81   1  65   1  49   1  65   1  49

PATCH     74  74  K  K  M  P  I  J  81   1   1  49   1  45   1  49   1  45
PATCH     74  74  K  K  P  M  I  J   1  81   1  49   1  45   1  49   1  45

PATCH     74  74  K  K  M  P  I  J  81   1   1  33  45  49   1  33  45  49
PATCH     74  74  K  K  P  M  I  J   1  81   1  33  45  49   1  33  45  49

SSVI      66  66  J  J  P  P  I  K   1   1   1  65   1  81   1  65   1  81
 RPMWALL    TWALL
 0.000000E+00 0.000000E+00

SSVI      66  66  J  J  M  M  I  K  45  45   1  65   1  81   1  65   1  81
 RPMWALL    TWALL
 0.000000E+00 0.000000E+00

SSVI      67  67  I  I  P  P  J  K   1   1   1   9   1  81   1   9   1  81
 RPMWALL    TWALL
 0.000000E+00 0.000000E+00

SSIN      67  67  J  J  P  P  I  K   1   1   1  81   1  81   1  81   1  81
 RPMWALL    TWALL
 0.000000E+00 0.000000E+00

FREE      67  67  I  I  M  M  J  K  81  81   1   9   1  81   1   9   1  81
 PTOT    TTOT     EMINF    ALPHA
1.0      1.0      0.8      0.0

FREE      68  68  I  I  M  M  J  K  81  81   1  49   1  81   1  49   1  81
 PTOT    TTOT     EMINF    ALPHA
1.0      1.0      0.8      0.0

# This BC caused a problem in bigC.  Now using EXITG
#FREE      69  69  I  I  M  M  J  K  81  81   1  49   1  81   1  49   1  81
# PTOT    TTOT     EMINF    ALPHA
#1.0      1.0      0.8      0.0

EXITG  69 69  I  I  M  M  J  K  81  81   1  49   1  81   1  49   1   81
PTOT
  0.6560215

FREE      71  71  I  I  M  M  J  K  73  73   1  49   1  81   1  49   1  81
 PTOT    TTOT     EMINF    ALPHA
1.0      1.0      0.8      0.0

SSVI      70  70  J  J  P  P  I  K   1   1   1  65   1  81   1  65   1  81
 RPMWALL    TWALL
 0.0        0.0

FREE      70  70  J  J  M  M  I  K  49  49   1  73   1  81   1  73   1  81
 PTOT    TTOT     EMINF    ALPHA
 1.0     1.0      0.8      0.0

FREE      71  71  J  J  M  M  I  K  49  49   1  73   1  81   1  73   1  81
 PTOT    TTOT     EMINF    ALPHA
 1.0     1.0      0.8      0.0

SSVI      72  72  I  I  P  P  J  K   1   1  45  49   1  81  45  49   1  81
 RPMWALL    TWALL
 0.000000E+00 0.000000E+00

SSVI      72  72  J  J  P  P  I  K   1   1   1  49   1  81   1  49   1  81
 RPMWALL    TWALL
 0.000000E+00 0.000000E+00

SSVI      73  73  J  J  P  P  I  K   1   1   1  65   1  81   1  65   1  81
 RPMWALL    TWALL
```

```
 0.000000E+00 0.000000E+00

SSVI      73  73  J  J  M  M  I  K  49  49   1  65   1  81   1  65   1  81
 RPMWALL    TWALL
 0.000000E+00 0.000000E+00

SSVI      74  74  J  J  M  M  I  K  49  49   1  49   1  81   1  49   1  81
 RPMWALL    TWALL
 0.000000E+00 0.000000E+00

SSVI      74  74  K  K  P  P  I  J   1   1  33  49  45  49  33  49  45  49
 RPMWALL    TWALL
 0.000000E+00 0.000000E+00

SSVI      74  74  K  K  M  M  I  J  81  81  33  49  45  49  33  49  45  49
 RPMWALL    TWALL
 0.000000E+00 0.000000E+00

PATCH     70  71  I  I  M  P  J  K  73   1   1  49   1  81   1  49   1  81
PATCH     71  70  I  I  P  M  J  K   1  73   1  49   1  81   1  49   1  81
```

Appendix B

SEARCH Program Source Code

The source code for the *SEARCH* mesh generation utility program developed during this study is printd below for reference.

```
      program search

      parameter(mxdim=1100,idim=150,jdim=100,kdim=49,nblks=50)

      real t(-5:mxdim),s(-5:mxdim),w(0:mxdim,0:mxdim),
     .     x(0:mxdim,0:mxdim),y(0:mxdim,0:mxdim),
     .     z(0:mxdim,0:mxdim),u(0:1),v(0:1),
     .     sle(mxdim),ste(mxdim),tle(mxdim),tte(mxdim),
     .     xte(mxdim),yte(mxdim),zte(mxdim),rte(mxdim),
     .     xle(mxdim),yle(mxdim),zle(mxdim),rle(mxdim)

      real csle(mxdim),cste(mxdim),cxle(mxdim),cxte(mxdim),
     .     cyle(mxdim),cyte(mxdim),czle(mxdim),czte(mxdim)

      real xn(idim,jdim,kdim),
     .     yn(idim,jdim,kdim),
     .     zn(idim,jdim,kdim),
     .     x2d(idim,jdim),r2d(idim,jdim),
     .     thet(idim,jdim,kdim),rthet(kdim)
      integer il(nblks),jl(nblks),kl(nblks)

      character*80 filnm
c
      common/surfdata/ s,t,w,x,y,z
      common/paramlim/ u,v
      common/murbsize/ k1,k2
      common/aximesh/  x2d,r2d
      common/fullmesh/ xn,yn,zn
      common/meshlim/  il,jl,kl,mg
      common/xyzedges/ xle,xte,yle,yte,zle,zte,rle,rte,
     .                 cxle,cxte,cyle,cyte,czle,czte
      common/st_edges/ sle,ste,tle,tte,csle,cste
      common/xrpoint/  xx,rr
      common/ttval/    tt
      common/ssval/    ss
      common/iflags/   isearch,idebug,lin,lout,lgrid
*
*** Inititialize I/O, flags and constants ***
*
      lin = 5
      lout = 6
      lgrid = 12
      idebug = 0
      pi = 4.0*atan(1.0)

*
*** Read in IGES excerpt file ***
*
      write(lout,*) 'Enter NASA IGES filename:'
      read(lin,'(a)') filnm
      write(lout,*) 'Filename: ',filnm
      call readiges(filnm)
*
*** Find radial distributions of Xmin and Xmax ***
*
      write(lout,*) 'Enter number of spline points: (- to debug NURBS)'
      read(lin,*) nsp
      write(lout,*) 'Number of spline points:',nsp
      if (nsp.lt.0) idebug = 1
      nsp = abs(nsp)
```

```
      call letefind(nsp)

      write(lout,*) 'Meridional leading and trailing edges written.'
      write(lout,*) 'Continue? (1=y)'
      read(lin,*) ians
      if (ians.ne.1) stop

*** Calculate spline coefficients ***
      call spcoef(tle,sle,csle,nsp)
      call spcoef(tte,ste,cste,nsp)

      call spcoef(rle,xle,cxle,nsp)
      call spcoef(rte,xte,cxte,nsp)

      call spcoef(rle,yle,cyle,nsp)
      call spcoef(rte,yte,cyte,nsp)

      call spcoef(rle,zle,czle,nsp)
      call spcoef(rte,zte,czte,nsp)
*
*** Interrogate NURBS surface using search routines (idebug = 1) ***
*
      if (idebug.ne.0) then

 5      write(lout,*) 'Enter s,t value: (s = 999 to quit)'
        read(lin,*) ss,tt
        if (ss.ne.999.) then
          call getsurfxrt(ss,tt,xs,rs,ts)
          write(lout,*) 'xrt =>',xs,rs,ts*180./pi
          go to 5
        end if
 7       write(lout,*) 'Enter x,r value to match:(x=999 to quit)'
        read(lin,*) xx,rr
        if (xx.ne.999) then
          isurf = 1
          ss = u(0)+0.25*(u(1)-u(0))
          tt = v(0)+0.50*(v(1)-v(0))

          write(lout,*) 'Using alternating secant search...'
          isearch = 1
          call findst(nsp,isurf)
          call getsurfxrt(ss,tt,xs,rs,ts)
          write(lout,*) 's,t => ',ss,tt
          write(lout,*) 'xrt => ',xs,rs,ts*180./pi

          write(lout,*) 'Using under-relaxed gradient search...'
          isearch = 2
          call findst(nsp,isurf)
          call getsurfxrt(ss,tt,xs,rs,ts)
          write(lout,*) 's,t => ',ss,tt
          write(lout,*) 'xrt => ',xs,rs,ts*180./pi

          go to 7
        else
         stop
        end if
      end if
*
*** Read in 2-D PLOT3D mesh for meridional point distribution ***
*
      write(lout,*) 'Enter 2-D axisym. PLOT3D binary mesh filename:'
      read(lin,'(a80)') filnm
      write(lout,*) 'Filename: ',filnm
      call readaximesh(filnm)

      write(lout,*) 'Enter leading edge indice:'
      read(lin,*) ile
      write(lout,*) 'Leading edge: ',ile
      write(lout,*) 'Enter trailing edge indice:'
      read(lin,*) ite
      write(lout,*) 'Trailing edge: ',ite

      write(lout,*) 'Enter number of blades in wheel:'
      read(lin,*) nblades
      write(lout,*) 'Blade count: ',nblades
      pitch = 2.*pi/nblades
      write(lout,*) 'Pitch: ',pitch*180./pi

      write(lout,*) 'Enter number of points across passage:'
      read(lin,*) kl(1)
      write(lout,*) 'Kpts: ',kl(1)

      write(lout,*) 'Enter near blade spacing for first point'
      write(lout,*) 'off the blade surface:'
      read(lin,*) drth1
      write(lout,*) 'Near-wall spacing: ',drth1
      drth2=drth1
*
*** assign leading and trailing edge values from splines ***
*
      l = 1
```

```
      do  50 j=1,jl(l)
        ytemp = speval(r2d(ile,j),rle,yle,cyle,nsp)
        ztemp = speval(r2d(ile,j),rle,zle,cyle,nsp)
        thet(ile,j,1) = atan2(ztemp,ytemp)
        thet(ile,j,kl(l)) = thet(ile,j,1)

        ytemp = speval(r2d(ite,j),rte,yte,cyte,nsp)
        ztemp = speval(r2d(ite,j),rte,zte,cyte,nsp)
        thet(ite,j,1) = atan2(ztemp,ytemp)
        thet(ite,j,kl(l)) = thet(ite,j,1)
 50   continue
*
*** find theta values for interior x,r pairs ***
*
      write(lout,*) 'Enter search method:'
      write(lout,*) '  1. Alternating secant search'
      write(lout,*) '  2. Under-relaxed gradient search'
      read(lin,*) isearch
      write(lout,*) 'Search method: ',isearch
      do 100 l = 1,mg
        kl(l) = kl(1)
        do 100 isurf = 1,2
         write(lout,*) 'Surface #',isurf
         do 100 i=ile+1,ite-1
           write(lout,*) i-ile+1,' of ',ite-ile+1
           idebug = 0
           do 100 j=1,jl(l)
             xx = x2d(i,j)
             rr = r2d(i,j)
             call findst(nsp,isurf)
             call getsurfxrt(ss,tt,xs,rs,ts)
             if (isurf.eq.1) thet(i,j,1)=ts
             if (isurf.eq.2) thet(i,j,kl(l))=ts
 100  continue
*
***  Set thetas upstream and downstream of blade ***
*
      l = 1
      if (ile.ne.1) then
** upstream **
        do 200 i=1,ile-1
          do 200 j=1,jl(l)
            thet(i,j,1) = thet(ile,j,1)
            thet(i,j,kl(l)) = thet(ile,j,kl(l))
 200    continue
      end if

      if (ite.ne.il(l)) then
** downstream **
        do 210 i=ite+1,il(l)
          do 210 j=1,jl(l)
            thet(i,j,1) = thet(ite,j,1)
            thet(i,j,kl(l)) = thet(ite,j,kl(l))
 210    continue
      end if

*
*** Distribute points across passage ***
*

*** switch surfaces 1 & 2 ? ***
      im = int(0.5*(ile+ite))
      jm = int(0.5*jl(l))
      thet1 = thet(im,jm,1)
      thet2 = thet(im,jm,kl(1))+pitch
      delthet = abs(thet1 - thet2)
      write(lout,*) 'delthet = ',delthet*180./pi
      write(lout,*) 'pitch   = ',pitch*180./pi
      if (delthet.gt.pitch) then
*** swap surfaces
        write(lout,*) 'swapping theta surfaces...'
        l = 1
        do 350 i=1,il(l)
          do 350 j=1,jl(l)
            temp=thet(i,j,1)
            thet(i,j,1)=thet(i,j,kl(l))
            thet(i,j,kl(l))=temp
 350    continue
      end if

      l = 1
      do 400 i=1,il(l)
        do 400 j=1,jl(l)

*** shift surface by pitch
          thet(i,j,kl(l)) = thet(i,j,kl(l))+pitch

          kase = 0
          ierr = 0
          kpts = kl(l)
          rt1=r2d(i,j)*thet(i,j,1)
          rt2=r2d(i,j)*thet(i,j,kl(l))
```

```
          eqspc = (rt2 - rt1) / real(kpts-1)
          if (abs(eqspc).gt.drth1) then

*** use Vinokur clustered  spacing ***
            call VINOKUR(rthet,kpts,rt1,rt2,drth1,drth2,KASE,IERR)
            if (ierr.ne.0) then
              write(lout,*) 'Error in VINOKUR routine...stopping'
              stop
            end if

          else

*** use equal rthet spacing ***
            do 390 k=2,kl(l)-1
              rthet(k)=rt1+eqspc*real(k-1)
 390        continue

          end if

          do 400 k=2,kl(l)-1
            thet(i,j,k)=rthet(k)/r2d(i,j)
 400  continue
*
*** Angle upstream and downstream grid points to match blade angle ***
*
      write(lout,*) 'Enter circumferential angle for upstream: (deg)'
      read(lin,*) ucang
      write(lout,*) 'Upstream: ',ucang

      if (ucang.ne.0) then
        ucang=ucang*pi/180.
*
**** shift extension block ***
*
        l = 1
        do 800 i=ile-1,1,-1
          do 800 j=1,jl(l)
            do 800 k=1,kl(l)
* tangential location
              dx = xn(i,j,k)-xn(ile,j,k)
              dt = dx/yn(i,1,k)*atan(ucang)
              zn(i,j,k)=zn(ile,j,k)+dt
 800    continue
      end if

      write(lout,*) 'Enter circumferential angle for downstream: (deg)'
      read(lin,*) dcang
      write(lout,*) 'Downstream: ',dcang
      if (dcang.ne.0) then
        dcang=dcang*pi/180.
*
**** shift extension block ***
*
        l = 1
        do 810 i=ite+1,il(l)
          do 810 j=1,jl(l)
            do 810 k=1,kl(l)
* tangential location
              dx = xn(i,j,k)-xn(ite,j,k)
              dt = dx/yn(i,1,k)*atan(dcang)
              zn(i,j,k)=zn(ite,j,k)+dt
 810    continue
      end if

*
*** Convert back to cartesian coordinates ***
*
      write(lout,*) 'Converting to cartesian coordinates...'
      l=1
        write(lout,*) 'Block: ',l
        do 700 i=1,il(l)
          do 700 j=1,jl(l)
            do 700 k=1,kl(l)
              xn(i,j,k)=x2d(i,j)
              yn(i,j,k)=r2d(i,j)*cos(thet(i,j,k))
              zn(i,j,k)=r2d(i,j)*sin(thet(i,j,k))
  700 continue

*
*** Output PLOT3D file ***
*
      write(lout,*) '----- OUTPUT -----'
c     write(lout,*) 'Enter 3-D PLOT3D binary mesh filename:'
c     read(lin,'(a80)') filnm
      filnm = 'blade.mesh'
      write(lout,*) 'Filename: ',filnm
      call qdopen(lgrid,filnm,je)
      call qdputi(lgrid,mg,je)
      write(lout,*) 'Number of grids: ',mg
      do 899 l = 1, mg
        call qdputi(lgrid,il(l),je)
```

```
        call qdputi(lgrid,jl(l),je)
        call qdputi(lgrid,kl(l),je)
 899  continue
      l = 1
        write(lout,*) 'Block: ',l,il(l),jl(l),kl(l)
        do 911 k = 1, kl(l)
          do 911 j = 1, jl(l)
          length = il(l)
          call qdpuea(lgrid,xn(1,j,k),length,je)
 911    continue
        do 912 k = 1, kl(l)
          do 912 j = 1, jl(l)
          length = il(l)
          call qdpuea(lgrid,yn(1,j,k),length,je)
 912    continue
        do 913 k = 1, kl(l)
          do 913 j = 1, jl(l)
          length = il(l)
          call qdpuea(lgrid,zn(1,j,k),length,je)
 913    continue

      call qdclos(lgrid,je)

      stop
      end

*************************************************
****              SUBROUTINES                ****
*************************************************

      subroutine readaximesh(filmm)
      parameter(idim=150,jdim=100,nblks=50)

      real x2d(idim,jdim),r2d(idim,jdim)
      integer il(nblks),jl(nblks),kl(nblks)

      character*80 filmm

      common/aximesh/  x2d,r2d
      common/meshlim/  il,jl,kl,mg
      common/iflags/   isearch,idebug,lin,lout,lgrid

      call qdopen(lgrid,filmm,je)
      call qdgeti(lgrid,mg,je)
      write(lout,*) 'Number of grids: ',mg
      if (mg.gt.1) then
        write(lout,*) 'Warning!! Multiple grids in 2-D file...'
        write(lout,*) 'Only using grid block #1.'
      end if
      do 9 l = 1, mg
        call qdgeti(lgrid,il(l),je)
        call qdgeti(lgrid,jl(l),je)
        call qdgeti(lgrid,kl(l),je)
  9   continue

*** only single mesh now (l=1) ***
        l = 1
        mg = 1
        write(lout,*) 'Block: ',l,il(l),jl(l)
         do 111 j = 1, jl(l)
            length = il(l)
            call qdgeea(lgrid,x2d(1,j),length,je)
 111    continue
        do 112 j = 1, jl(l)
          length = il(l)
          call qdgeea(lgrid,r2d(1,j),length,je)
 112    continue

      call qdclos(lgrid,je)

      return
      end


      subroutine findst(nsp,isurf)

      parameter(mxdim=1100)
      real t(-5:mxdim),s(-5:mxdim),w(0:mxdim,0:mxdim),
     .     x(0:mxdim,0:mxdim),y(0:mxdim,0:mxdim),
     .     z(0:mxdim,0:mxdim),u(0:1),v(0:1),
     .     sle(mxdim),ste(mxdim),tle(mxdim),tte(mxdim),
     .     csle(mxdim),cste(mxdim)
      real p(2),xi(2,2)

      common/surfdata/ s,t,w,x,y,z
      common/paramlim/ u,v
      common/murbsize/ k1,k2
      common/st_edges/ sle,ste,tle,tte,csle,cste
      common/xrpoint/  xx,rr
      common/ssval/    ss
      common/ttval/    tt
      common/iflags/   isearch,idebug,lin,lout,lgrid
```

```
*
*** initial guess point and set bounds for (s,t) ***
*
      tt = v(0)+0.5*(v(1)-v(0))

      tmin = v(0)
      tmax = v(1)
      smin = speval(tt,tle,sle,csle,nsp)
      smax = speval(tt,tte,ste,cste,nsp)

      if (smin.gt.smax) then
        stemp = smin
        smin = smax
        smax = stemp
      end if

      if (isurf.eq.2) then
*** swap smin and smax ***
        stemp = smin
        smin = smax
        smax = stemp+u(1)
      end if

      ss = 0.5*(smin+smax)

      if (isearch.eq.1) then


*****************************************
*** Alternating secant search (inew = 0) ***
*****************************************

      ftol = 0.0005
      tol = 0.1
      ipass = 1

  5   if (tol.lt.0.0001) tol = 0.0001
*
*** SWEEP T at CONST S ***
*
 15   told = 0.95*tt
      if (told.lt.0.1) then
        tt = 0.1
        told = tt+0.5
      end if
      delt = tt - told
      if (idebug.ne.0) write(lout,*) 'tt,told,delt = ',tt,told,delt
      call getsurfxrt(ss,told,xs,rs,ts)
c     write(3,*) xs,rs
      frold=  rr - rs

      iter = 1

      if (idebug.ne.0) write(lout,*) 'rr,frold = ',rr,frold

 20   call getsurfxrt(ss,tt,xs,rs,ts)
c     write(3,*) xs,rs
      frnew = rr - rs
      if (idebug.ne.0) write(lout,*) 'ss,tt,rr,frnew = ',ss,tt,rr,frnew

      delt = -frnew / (frnew - frold)*delt

      ttemp = tt + delt

      if (idebug.ne.0) write(lout,*) 'ttemp,delt,tmin,tmax =',
     .      ttemp,delt,tmin,tmax

      if (ttemp.lt.tmin) then
        delt = tmin - tt
        ttemp = tmin
      end if
      if (ttemp.gt.tmax) then
        delt = tmax - tt
        ttemp = tmax
      end if

      tt = ttemp
      if (idebug.ne.0) write(lout,*) 'iter, tt, delt = ',iter,tt,delt

*** try until tolerance is met or 10 times exceeded ***
      if (abs(delt).gt.tol) then
        frold = frnew
        iter = iter + 1
        if (iter.lt.11) go to 20
      end if

*
*** SWEEP S at CONST T ***
*
 7    iter = 1
```

```
      smin = speval(tt,tle,sle,csle,nsp)
      smax = speval(tt,tte,ste,cste,nsp)

      if (idebug.ne.0) write(lout,*) 'leS, teS: ',smin,smax

      if (smin.gt.smax) then
        stemp = smin
        smin = smax
        smax = stemp
        if (idebug.ne.0) write(lout,*) 'swapped: min,max:', smin,smax
      end if

      if (isurf.eq.2) then
*** swap smin and smax ***
        stemp = smin
        smin = smax
        smax = stemp+u(1)
      end if

      sold = 0.95*ss
      if (sold.le.smin) sold = smin + 0.1
      if (ss.eq.smax) sold = smax - 0.1
      dels = ss - sold

      if (idebug.ne.0) write(lout,*) 'ss,sold,dels = ',ss,sold,dels

      call getsurfxrt(sold,tt,xs,rs,ts)
c     write(3,*) xs,rs
      fxold= xx - xs
      if (idebug.ne.0) write(lout,*) 'smin,smax = ',smin,smax

 10   call getsurfxrt(ss,tt,xs,rs,ts)
c     write(3,*) xs,rs
      fxnew = xx - xs

      dels = -fxnew / (fxnew - fxold)*dels

      stemp = ss + dels

      if (stemp.lt.smin) then
        dels = smin - ss
        stemp = smin
      end if
      if (stemp.gt.smax) then
        dels = smax - ss
        stemp = smax
      end if

      ss = stemp

*** try until tolerance is met or 10 times exceeded ***
      if (abs(dels).gt.tol) then
        fxold = fxnew
        iter = iter + 1
        if (iter.lt.11) go to 10
      end if
*
*** calculate distance ***
*
 25   call getsurfxrt(ss,tt,xs,rs,ts)
c     write(3,*) xs,rs
      dist = sqrt((xx-xs)**2 + (rr-rs)**2)

      ipass = ipass + 1

      if (idebug.ne.0) then
        write(lout,*) 'PASS #',ipass
        write(lout,*) 'DIST,s,t = ',dist,ss,tt
        write(lout,*) 'smin,smax= ',smin,smax
        write(lout,*) 'dx,dr    = ',xx-xs,rr-rs
      end if

      if (ipass.gt.7) then
        write(lout,*) 'giving up.....retry #',ipass
        write(lout,*) 'DIST,s,t = ',dist,ss,tt
        write(lout,*) 'smin,smax= ',smin,smax
        write(lout,*) 'dx,dr    = ',xx-xs,rr-rs
        return
      end if

      if (dist.lt.ftol) then
*** solution found ***
        return
      else
*** try to get closer (tighten tolerance) ***
        tol = tol/10.
        if (idebug.ne.0) write(lout,*) '---------------'
        if (idebug.ne.0) write(lout,*) 'NEW tol = ',tol
        go to 5
      end if

      else
```

```
**********************
*  simple derivative search
**********************

      iter = 1

      call getsurfxrt(ss,tt,xs,rs,ts)

 23   call derivs(ss,tt,dxds,drds,dxdt,drdt,nsp,isurf)

      dx = xx - xs
      dr = rr - rs

      if (dxds.ne.0) then
        dels1 = dx / dxds
      else
        dels1 = 0.0
      end if

      if (drds.ne.0) then
        dels2 = dr / drds
      else
        dels2 = 0.0
      end if

      ds = dels1 + dels2

      if (dxdt.ne.0) then
        delt1 = dx / dxdt
      else
        delt1 = 0.0
      end if

      if (drdt.ne.0) then
        delt2 = dr / drdt
      else
        delt2 = 0.0
      end if

      dt = delt1 + delt2

*** under-relax value ***
      omega = 0.1
      snew = ss + ds*omega
      tnew = tt + dt*omega

      if (tnew.lt.v(0)) tnew = v(0)
      if (tnew.gt.v(1)) tnew = v(1) - 0.0001

      tt = tnew

      smin = speval(tt,tle,sle,csle,nsp)
      smax = speval(tt,tte,ste,cste,nsp)

      if (smin.gt.smax) then
        stemp = smin
        smin = smax
        smax = stemp
      end if

      if (isurf.eq.2) then
*** swap smin and smax ***
        stemp = smin
        smin = smax
        smax = stemp+u(1)
      end if

      if (snew.le.smin) snew = smin + 0.01
      if (snew.ge.smax) snew = smax - 0.01
      ss = snew

      call getsurfxrt(ss,tt,xs,rs,ts)
      dist = sqrt((xx-xs)**2 + (rr-rs)**2)

      if (iter.ge.100) then
        write(lout,*) 'Deriv search FAILED!!!'
        write(lout,*) 'iter,dist =',iter,dist
        return
      end if

        if (dist.lt.ftol) then
*** solution found ***
          return
        else
         iter = iter + 1
         go to 23
        end if


      end if
```

```
      end



      subroutine derivs(ss,tt,dxds,drds,dxdt,drdt,nsp,isurf)
      parameter(mxdim=1100)
      real u(0:1),v(0:1),
     .     sle(mxdim),ste(mxdim),tle(mxdim),tte(mxdim),
     .     csle(mxdim),cste(mxdim)

      common/paramlim/ u,v
      common/st_edges/ sle,ste,tle,tte,csle,cste

c     if (isurf.eq.2) write(lout,*) '----- derivs -----'
c     if (isurf.eq.2) write(lout,*) 'ss,tt = ',ss,tt

      smin = speval(tt,tle,sle,csle,nsp)
      smax = speval(tt,tte,ste,cste,nsp)

c     if (isurf.eq.2) write(lout,*) 'u,v = ',u(0),u(1),v(0),v(1)

      if (smin.gt.smax) then
        stemp = smin
        smin = smax
        smax = stemp
      end if

      if (isurf.eq.2) then
*** swap smin and smax ***
        stemp = smin
        smin = smax
        smax = stemp+u(1)
      end if

c     if (isurf.eq.2) write(lout,*) 'smin,smax = ',smin,smax

      delsm = 0.001
      deltm = 0.001
      delsp = 0.001
      deltp = 0.001

      s1 = ss-delsm
      if (s1.le.smin) then
        s1=smin
        delsm = ss - s1
      end if

      t2 = tt+deltp
      if (t2.ge.v(1)) then
        t2 = v(1)
        deltp = t2 - tt
      end if

      s3 = ss + delsp
      if (s3.ge.smax) then
        s3=smax
        delsp = s3 - ss
      end if

      t4 = tt-deltm
      if (t4.le.v(0)) then
        t4 = v(0)
        deltp = tt - t4
      end if

      call getsurfxrt(s1,tt,x1,r1,t1)
      call getsurfxrt(ss,t2,x2,r2,t2)
      call getsurfxrt(s3,tt,x3,r3,t3)
      call getsurfxrt(ss,t4,x4,r4,t4)

      dels = delsp + delsm
c     if (isurf.eq.2) write(lout,*) 'dels =',dels,delsp,delsm

      dxds = 0.5*(x3-x1)/dels
      drds = 0.5*(r3-r1)/dels

      delt = deltp + deltm
c     if (isurf.eq.2) write(lout,*) 'delt =',delt

      dxdt = 0.5*(x2-x4)/delt
      drdt = 0.5*(r2-r4)/delt

      return
      end



      subroutine getsurfxrt(ss,tt,xs,rs,ts)

c     parameter(mxdim=1100)
c     real t(-5:mxdim),s(-5:mxdim),
c    .     w(0:mxdim,0:mxdim),
```

```
c     .     x(0:mxdim,0:mxdim),y(0:mxdim,0:mxdim),
c     .     z(0:mxdim,0:mxdim),u(0:1),v(0:1)
c     common/surfdata/ s,t,w,x,y,z
c     common/paramlim/ u,v
c     common/nurbsize/ k1,k2

      call getsurfxyz(ss,tt,xs,ys,zs)
      rs = sqrt(ys**2 + zs**2)
      ts = atan2(zs,ys)

      return
      end


      subroutine getsurfxyz(ssin,tt,xs,ys,zs)
*
*** calculate point along the NURBS curve ***
*
      parameter(mxdim=1100)
      real t(-5:mxdim),s(-5:mxdim),
     .     w(0:mxdim,0:mxdim),
     .     x(0:mxdim,0:mxdim),y(0:mxdim,0:mxdim),
     .     z(0:mxdim,0:mxdim),u(0:1),v(0:1),
     .     rN0(0:mxdim,2),rN1(0:mxdim,2),
     .     rN2(0:mxdim,2),rN3(0:mxdim,2)

      common/surfdata/ s,t,w,x,y,z
      common/paramlim/ u,v
      common/nurbsize/ k1,k2
      common/iflags/   isearch,idebug,lin,lout,lgrid

*** account for periodicity in s ***
        ss = ssin
        if (ssin.lt.0.) ss = u(1) + ssin
        if (ssin.ge.u(1)) ss = ssin - u(1)

        if (tt.lt.v(0)) tt = v(0)
        if (tt.ge.v(1)) tt = v(1)-0.0001

*** calculate basis function: bi(s) ***
         do 1810 ii=0,k1
** initialize rN3 to 0 **
           rN3(ii,1) = 0.0
           rN2(ii,1) = 0.0
           rN1(ii,1) = 0.0
           rN0(ii,1) = 0.0

           if (ss.ge.s(ii).and.ss.lt.s(ii+1)) then
             rN0(ii,1) = 1.0
             imid = ii
           end if
 1810    continue


         do 1811 ii=imid-1,imid
c        do 1811 ii=0,k1
            term1 = 0.0
            if (rN0(ii,1).ne.0.0.and.
     .          (s(ii+1)-s(ii)).ne.0.0)
     .        term1 = (ss-s(ii)) / (s(ii+1)-s(ii)) * rN0(ii,1)

            term2 = 0.0
            if (rN0(ii+1,1).ne.0.0.and.
     .          (s(ii+2)-s(ii+1)).ne.0.)
     .        term2 = (s(ii+2)-ss) / (s(ii+2)-s(ii+1)) * rN0(ii+1,1)

            rN1(ii,1) = term1 + term2
 1811    continue

         do 1812 ii=imid-2,imid
c        do 1812 ii=0,k1
            term1 = 0.0
            if (rN1(ii,1).ne.0.0.and.
     .          (s(ii+2)-s(ii)).ne.0.)
     .        term1 = (ss-s(ii)) / (s(ii+2)-s(ii)) * rN1(ii,1)

            term2 = 0.0
            if (rN1(ii+1,1).ne.0.0.and.
     .          (s(ii+3)-s(ii+1)).ne.0.)
     .        term2 = (s(ii+3)-ss) / (s(ii+3)-s(ii+1)) * rN1(ii+1,1)

            rN2(ii,1) = term1 + term2
 1812    continue

         do 1813 ii=imid-3,imid
c        do 1813 ii=0,k1
            term1 = 0.0
            if (rN2(ii,1).ne.0.0.and.
     .          (s(ii+3)-s(ii)).ne.0.)
     .        term1 = (ss-s(ii)) / (s(ii+3)-s(ii)) * rN2(ii,1)

            term2 = 0.0
```

```
            if (rN2(ii+1,1).ne.0.0.and.
     .          (s(ii+4)-s(ii+1)).ne.0.)
     .        term2 = (s(ii+4)-ss) / (s(ii+4)-s(ii+1)) * rN2(ii+1,1)

            rN3(ii,1) = term1 + term2
 1813     continue


*** calculate basis function: bj(t) ***
          do 1820 jj=0,k2
            rN3(jj,2) = 0.0
            rN2(jj,2) = 0.0
            rN1(jj,2) = 0.0
            rN0(jj,2) = 0.0
            if (tt.ge.t(jj).and.tt.lt.t(jj+1)) then
              rN0(jj,2) = 1.0
              jmid = jj
            end if
 1820     continue

c         if (jmid.lt.ijdel) jmid = ijdel
c         if (jmid.gt.(k2-ijdel)) jmid = k2-ijdel

          do 1821 jj=jmid-1,jmid
c         do 1821 jj=0,k2
            term1 = 0.0
            if (rN0(jj,2).ne.0.0.and.
     .          (t(jj+1)-t(jj)).ne.0.)
     .        term1 = (tt-t(jj)) / (t(jj+1)-t(jj)) * rN0(jj,2)

            term2 = 0.0
            if (rN0(jj+1,2).ne.0.0.and.
     .          (t(jj+2)-t(jj+1)).ne.0.)
     .        term2 = (t(jj+2)-tt) / (t(jj+2)-t(jj+1)) * rN0(jj+1,2)

            rN1(jj,2) = term1 + term2
 1821     continue

          do 1822 jj=jmid-2,jmid
c         do 1822 jj=0,k2
            term1 = 0.0
            if (rN1(jj,2).ne.0.0.and.
     .          (t(jj+2)-t(jj)).ne.0.)
     .        term1 = (tt-t(jj)) / (t(jj+2)-t(jj)) * rN1(jj,2)

            term2 = 0.0
            if (rN1(jj+1,2).ne.0.0.and.
     .          (t(jj+3)-t(jj+1)).ne.0.)
     .        term2 = (t(jj+3)-tt) / (t(jj+3)-t(jj+1)) * rN1(jj+1,2)

            rN2(jj,2) = term1 + term2
 1822     continue

          do 1823 jj=jmid-3,jmid
c         do 1823 jj=0,k2
            term1 = 0.0
            if (rN2(jj,2).ne.0.0.and.
     .          (t(jj+3)-t(jj)).ne.0.)
     .        term1 = (tt-t(jj)) / (t(jj+3)-t(jj)) * rN2(jj,2)

            term2 = 0.0
            if (rN2(jj+1,2).ne.0.0.and.
     .          (t(jj+4)-t(jj+1)).ne.0.)
     .        term2 = (t(jj+4)-tt) / (t(jj+4)-t(jj+1)) * rN2(jj+1,2)

            rN3(jj,2) = term1 + term2
 1823      continue

         sum1=0.0
         sum2=0.0
         sum3=0.0
         sum4=0.0

         do 1830 i=imid-3,imid
           do 1830 j=jmid-3,jmid

           bis = rN3(i,1)
           bjt = rN3(j,2)

           if (bis.ne.0.0.and.bjt.ne.0.0) then
             sum1 = sum1+w(i,j)*x(i,j)*bis*bjt
             sum2 = sum2+w(i,j)*y(i,j)*bis*bjt
             sum3 = sum3+w(i,j)*z(i,j)*bis*bjt
             sum4 = sum4+w(i,j)*bis*bjt
           end if
 1830    continue

         xs = sum1/sum4
         ys = sum2/sum4
         zs = sum3/sum4

        return
```

```
       end


      subroutine readiges(filnm)

      parameter(mxdata=100000,mxdim=1100)
      real data(mxdata),t(-5:mxdim),s(-5:mxdim),
     .     w(0:mxdim,0:mxdim),
     .     x(0:mxdim,0:mxdim),y(0:mxdim,0:mxdim),
     .     z(0:mxdim,0:mxdim),u(0:1),v(0:1)

      character*80 filnm
      character*70 chline, parse, chtemp, blank
      character*70 aline

      common/surfdata/ s,t,w,x,y,z
      common/paramlim/ u,v
      common/murbsize/ k1,k2

      blank(1:)  = '                                '
      blank(41:) = '                                '

      open(unit=2,file=filnm,status='unknown')

*
*** initialize data array ***
*
c     write(lout,*) 'Initializing data array...'
      do 50 n=1,mxdata
        data(n) = -9999.0
 50   continue
*
*** read IGES file into data array ***
*
      ifound = 0
  90  read(2,99,end=100) aline
  99  format(a70)
      if (aline(:4).eq.'128,'.and.ifound.eq.0) then
        print*,'IGES type 128 found...'
        ifound = 1
        itype = 128
        aline = aline(5:)
        idata = 1
      else if (ifound.eq.0) then
        go to 90
      end if
*
*** parse out data from aline ***
*
 95   chtemp  = parse(aline)
      if(chtemp.ne.blank) then
         read(chtemp,*,err=100) data(idata)
         idata = idata + 1
      else
        go to 90
      endif
      go to 95

c     read(2,*,err=100) itype,(data(i),i=1,mxdata)
 100  close(2)

      write(lout,*) 'IGES type =',itype
c     write(lout,*) '----------------'
      ndata = 0
      do 200 n=1,mxdata
        if (data(n).ne.-9999.0) ndata = n
 200  continue
      write(lout,*) 'ndata = ',ndata,data(ndata)

      if (itype.eq.128) then
****************************************
*** IGES entity 128: B-Spline Surface ***
****************************************
        write(lout,*) 'IGES entity 128: B-Spline Surface'
*
*** assign variables from data array ***
*
      iptr = 1
      k1     = int(data(iptr))
      k2     = int(data(iptr+1))
      m1     = int(data(iptr+2))
      m2     = int(data(iptr+3))
      iprop1 = int(data(iptr+4))
      iprop2 = int(data(iptr+5))
      iprop3 = int(data(iptr+6))
      iprop4 = int(data(iptr+7))
      iprop5 = int(data(iptr+8))

      n1 = k1-m1+1
      n2 = k2-m2+1
      ia = n1+2*m1
```

```
      ib = n2+2*m2
      ic = (k1+1)*(k2+1)
      write(lout,*) 'n1,n2,a,b,c = ',n1,n2,ia,ib,ic

*** knot points ***
      write(lout,*) 'knot points'
      iptr = 10
      do 1500 i=0,ia
        s(i) = data(iptr+i)
c     write(4,*) 's=',s(i)
 1500 continue
      iptr = 11+ia
      do 1502 i=0,ib
        t(i) = data(iptr+i)
c     write(4,*) 't=',t(i)
 1502 continue

*** weights ***
      write(lout,*) 'weights'
      iptr = 12+ia+ib
      do 1600 j=0,k2
        do 1600 i=0,k1
        w(i,j) = data(iptr)
c       write(4,*) 'i,j,w=',i,j,w(i,j)
        iptr = iptr + 1
 1600 continue

*** control points ***
      write(lout,*) 'control pts'
      iptr = 12+ia+ib+ic
      do 1700 j=0,k2
        do 1700 i=0,k1
          x(i,j) = data(iptr)
          y(i,j) = data(iptr+1)
          z(i,j) = data(iptr+2)
c         write(4,*) i,j,x(i,j),y(i,j),z(i,j)
          iptr = iptr + 3
 1700 continue

      iptr = 12+ia+ib+4*ic
      u(0)  = data(iptr)
      u(1)  = data(iptr+1)
      v(0)  = data(iptr+2)
      v(1)  = data(iptr+3)
      write(lout,*) 'End of data at: ',iptr+3
      write(lout,*) 'u0,u1,v0,v1 = ',u(0),u(1),v(0),v(1)

      else
        write(lout,*) 'IGES entity ',itype,' not supported.'
        write(lout,*) 'Must be surface (128)'
        write(lout,*) 'Program terminating...'
        stop
      end if

      return
      end



      function xofs(ss)
*** axial location for ss value at constant tt value ***
      common/ttval/    tt

      call getsurfxyz(ss,tt,xs,ys,zs)
      xofs = xs

      return
      end


      function xofsm(ss)
*** negative of xofs ***
      common/ttval/    tt

      xofsm = -xofs(ss)

      return
      end


      subroutine letefind(njpts)

      parameter(mxdim=1100)
      real t(-5:mxdim),s(-5:mxdim),w(0:mxdim,0:mxdim),
     .     x(0:mxdim,0:mxdim),y(0:mxdim,0:mxdim),
     .     z(0:mxdim,0:mxdim),u(0:1),v(0:1),
     .     xte(mxdim),yte(mxdim),zte(mxdim),rte(mxdim),
     .     xle(mxdim),yle(mxdim),zle(mxdim),rle(mxdim),
     .     sle(mxdim),ste(mxdim),tle(mxdim),tte(mxdim)

      real csle(mxdim),cste(mxdim),cxle(mxdim),cxte(mxdim),
     .     cyle(mxdim),cyte(mxdim),czle(mxdim),czte(mxdim)
```

```
      real st(15),xt(15)

      common/surfdata/ s,t,w,x,y,z
      common/paramlim/ u,v
      common/nurbsize/ k1,k2
      common/xyzedges/ xle,xte,yle,yte,zle,zte,rle,rte,
     .                 cxle,cxte,cyle,cyte,czle,czte
      common/st_edges/ sle,ste,tle,tte,csle,cste
      common/ttval/    tt

      external xofs,xofsm

      open(unit=13,file='le.pts',status='unknown')
      open(unit=14,file='te.pts',status='unknown')
      write(13,*) njpts
      write(14,*) njpts
*
*** Find edges
*
      tol = 0.001
      delta2 = ((v(1)-0.0001)-v(0)) / real(njpts-1)
      do 1750 nj=1,njpts

c       write(lout,*) 'Finding min/max for: ',nj,' of ',njpts
        tt = v(0) + delta2*real(nj-1)
        if (tt.eq.0.) tt = 1.e-4

*** find trailing (max X) value for tt ***

** bracket max X point **

        do 100 i=1,13
          fact = real(i-2)/10.
          st(i)=u(0)+fact*(u(1)-u(0))
          xt(i)=xofs(st(i))
 100    continue

        do 110 i=3,13
          if (xt(i-1).gt.xt(i-2).and.
     .        xt(i-1).gt.xt(i)) then
            s1 = st(i-2)
            s2 = st(i-1)
            s3 = st(i)
          end if
 110    continue

        xmax=brent(s1,s2,s3,xofsm,tol,smax)

        call getsurfxyz(smax,tt,xs,ys,zs)
        xte(nj) = xs
        yte(nj) = ys
        zte(nj) = zs
        rte(nj) = sqrt(ys**2+zs**2)
        ste(nj) = smax
        tte(nj) = tt

*** find leading (min X) value for tt ***

        do 120 i=3,13
          if (xt(i-1).lt.xt(i-2).and.
     .        xt(i-1).lt.xt(i)) then
            s1 = st(i-2)
            s2 = st(i-1)
            s3 = st(i)
          end if
 120    continue

        xmin=brent(s1,s2,s3,xofs,tol,smin)

        call getsurfxyz(smin,tt,xs,ys,zs)
        xle(nj) = xs
        yle(nj) = ys
        zle(nj) = zs
        rle(nj) = sqrt(ys**2+zs**2)
        sle(nj) = smin
        tle(nj) = tt

        write(13,997) xle(nj),rle(nj),0.0
        write(14,997) xte(nj),rte(nj),0.0
 997    format(1x,4(f12.5,1x))

*** next tt value ***
 1750 continue

      close(13)
      close(14)

      return
      end
```

```
*
*** spline routines
*
      subroutine spcoef(spt,spf,coeff,nsp)
      real coeff(*),spt(*),spf(*),
     .     b(200),h(200),uu(200),vv(200)

*  spt(200) = t
*  spf(200) = y
*  coeff(200) = z

        do i=1,nsp-1
          h(i)=spt(i+1)-spt(i)
          b(i)=6.0*(spf(i+1)-spf(i))/h(i)
        end do

        uu(1)=2.0*(h(1)+h(2))
        vv(1)=b(2)-b(1)

        do i=2,nsp-2
          uu(i)=2.0*(h(i)+h(i-1))-h(i-1)**2/uu(i-1)
          vv(i)=b(i)-b(i-1)-h(i-1)*vv(i-1)/uu(i-1)
        end do

        coeff(nsp-1)=0.0

        do i=nsp-2,2,-1
          coeff(i)=(vv(i)-h(i)*coeff(i+1))/uu(i)
        end do

        coeff(1)=0.0

      return
      end


      function speval(xx,spt,spf,coeff,nsp)

      real coeff(*),spt(*),spf(*)

*  spt(200) = t
*  spf(200) = y
*  coeff(200) = z

      if (xx.lt.spt(1)) then
c        write(lout,*) xx,spt(1),nsp
c        write(lout,*) 'Warning... outside (for) orig data -- extrapolating'
         h=spt(2)-spt(1)
         a=(coeff(2)-coeff(1))/6.0/h
         b=coeff(1)/2.0
         c=-h/6.0*coeff(2)-h/3.0*coeff(1)+
     .     (spf(2)-spf(1))/h
         dx=xx-spt(1)
         speval=spf(1)+dx*(c+dx*(b+dx*a))
         return
      end if

      do i=1,nsp-1
        if (xx.ge.spt(i).and.xx.le.spt(i+1)) then
          h=spt(i+1)-spt(i)
          a=(coeff(i+1)-coeff(i))/6.0/h
          b=coeff(i)/2.0
          c=-h/6.0*coeff(i+1)-h/3.0*coeff(i)+
     .      (spf(i+1)-spf(i))/h
          dx=xx-spt(i)
          speval=spf(i)+dx*(c+dx*(b+dx*a))
          return
        end if
      end do

      if (xx.gt.spt(nsp)) then
c        write(lout,*) xx,spt(nsp),nsp
c        write(lout,*) 'Warning... outside (aft) orig data -- extrapolating'
         h=spt(nsp)-spt(nsp-1)
         a=(coeff(nsp)-coeff(nsp-1))/6.0/h
         b=coeff(nsp-1)/2.0
         c=-h/6.0*coeff(nsp)-h/3.0*
     .     coeff(nsp-1)+(spf(nsp)-spf(nsp-1))/h
         dx=xx-spt(nsp-1)
         speval=spf(nsp-1)+dx*(c+dx*(b+dx*a))
         return
      end if

*** error trap ***
      write(lout,*) 'Error occurred in SPEVAL rotuine!'
      write(lout,*) 'Value of spline index = ',xx
      stop

      end
```

```
      FUNCTION BRENT(AX,BX,CX,F,TOL,XMIN)
      PARAMETER (ITMAX=200,CGOLD=.3819660,ZEPS=1.0E-10)
      real brent,ax,bx,cx,tol,xmin,f
      external f
      A=MIN(AX,CX)
      B=MAX(AX,CX)
      V=BX
      W=V
      X=V
      E=0.
      FX=F(X)
      FV=FX
      FW=FX
      DO 11 ITER=1,ITMAX
        XM=0.5*(A+B)
        TOL1=TOL*ABS(X)+ZEPS
        TOL2=2.*TOL1
        IF(ABS(X-XM).LE.(TOL2-.5*(B-A))) GOTO 3
        IF(ABS(E).GT.TOL1) THEN
          R=(X-W)*(FX-FV)
          Q=(X-V)*(FX-FW)
          P=(X-V)*Q-(X-W)*R
          Q=2.*(Q-R)
          IF(Q.GT.0.) P=-P
          Q=ABS(Q)
          ETEMP=E
          E=D
          IF(ABS(P).GE.ABS(.5*Q*ETEMP).OR.P.LE.Q*(A-X).OR.
     *       P.GE.Q*(B-X)) GOTO 1
          D=P/Q
          U=X+D
          IF(U-A.LT.TOL2 .OR. B-U.LT.TOL2) D=SIGN(TOL1,XM-X)
          GOTO 2
        ENDIF
1       IF(X.GE.XM) THEN
          E=A-X
        ELSE
          E=B-X
        ENDIF
        D=CGOLD*E
2       IF(ABS(D).GE.TOL1) THEN
          U=X+D
        ELSE
          U=X+SIGN(TOL1,D)
        ENDIF
        FU=F(U)
        IF(FU.LE.FX) THEN
          IF(U.GE.X) THEN
            A=X
          ELSE
            B=X
          ENDIF
          V=W
          FV=FW
          W=X
          FW=FX
          X=U
          FX=FU
        ELSE
          IF(U.LT.X) THEN
            A=U
          ELSE
            B=U
          ENDIF
          IF(FU.LE.FW .OR. W.EQ.X) THEN
            V=W
            FV=FW
            W=U
            FW=FU
          ELSE IF(FU.LE.FV .OR. V.EQ.X .OR. V.EQ.W) THEN
            V=U
            FV=FU
          ENDIF
        ENDIF
11    CONTINUE
      PAUSE 'Brent exceed maximmm iterations.'
3     XMIN=X
      BRENT=FX
      RETURN
      END



      SUBROUTINE VINOKUR(S,LMAX,SMIN,SMAX,DSAE,DSBE,KASE,IERR)
C
C VINKITER - CONTROL ROUTINE TO SATISFY STRETCHING CONSTRAINTS IN
C            VINOKUR'S FUNCTION EXACTLY
C
      REAL    S(*)
      TOLMIN  = 1.0E-6
      TOLMIN2 = 1.0E-6
      IERR    = 0
```

```
C
C  VINOKUR'S FUNCTION CREATES A DISTRIBUTION OF GRID POINTS WHICH
C  SATISFY A SPECIFIED DERIVATIVE CONDITION, BUT WE REQUIRE A DELTA-S
C  CONSTRAINT INSTEAD.  THESE TWO VALUES ARE EQUIVALENT ONLY TO FIRST
C  ORDER, AND HENCE, WE RESORT TO AN ITERATIVE PROCEDURE TO OBTAIN
C  MORE ACCURATE DELTA-S'S. UP TO TEN ITERATIVE SWEEPS ARE
C  MADE.  THE FIRST GUESS SETS DS/DXI = DELTA-S.  THE NEXT GUESS
C  RECALCULATES DS/DXI USING THE LEADING TERM IN THE TRUNCATION ERROR
C  (D2S/D(XI)**2).  THE NEXT EIGHT ITERATIONS USE A 2-D SECANT
C  ALGORITHM TO HOME IN ON THE DS/DXI'S AT BOTH ENDS WHICH WILL GIVE
C  THE CORRECT DELTA-S.
C
C  IN THE CASES WHERE A SINGLE-SIDED STRETCHING FUNCTION IS REQUIRED,
C  (KASE = 1 OR 2) A SECANT ALGORITHM IN 1-D IS APPLIED INSTEAD.
C
C.... KASE = 0
C     STRETCHING ON BOTH ENDS, SO USE A 2-D SECANT METHOD TO ARRIVE AT THE
C     VALUES OF DSA AND DSB WHICH WILL SATISFY DS1E AND DS2E WITHIN
C     ROUNDOFF.
C
      IF (KASE .EQ. 0 )THEN
C
C....... INITIAL GUESS -  AN = DSAE, BN = DSBE
         AN2 = DSAE
         BN2 = DSBE
C
         CALL VINK(S,LMAX,SMIN,SMAX,AN2,BN2,ESA,ESB,KASE )
C
         FN2 = ESA/DSAE - 1
         GN2 = ESB/DSBE - 1
C
C....... SECOND GUESS - CALCULATE DS1 AND DS2 FROM A TRUNCATED TAYLOR SERIES
         DSSA = 2.*S(   1)-5.*S(     2)+4.*S(     3)   -S(     4)
         DSSB = 2.*S(LMAX)-5.*S(LMAX-1)+4.*S(LMAX-2)   -S(LMAX-3)
         AN1 = DSAE-0.5*DSSA
         BN1 = DSBE+0.5*DSSB
C
         CALL VINK(S,LMAX,SMIN,SMAX,AN1,BN1,ESA,ESB,KASE )
C
         FN1 = ESA/DSAE - 1
         GN1 = ESB/DSBE - 1
         AN  = AN1
         BN  = BN1
C
C....... 3RD THRU 10TH GUESSES , USE 2-D SECANT METHOD
         DO N = 3,20
C
C.......... CALCULATE OFFSET DERIVATIVES
            CALL VINK(S,LMAX,SMIN,SMAX,AN2,BN1,ESA21,ESB21,KASE )
            CALL VINK(S,LMAX,SMIN,SMAX,AN1,BN2,ESA12,ESB12,KASE )
            FA = ( ESA - ESA21 )/DSAE
            FB = ( ESA - ESA12 )/DSAE
            GA = ( ESB - ESB21 )/DSBE
            GB = ( ESB - ESB12 )/DSBE
            DEN = FA*GB - FB*GA
            DELA = -(AN1 - AN2)
            DELB = -(BN1 - BN2)
C
C.......... STICK WITH LAST GUESS IF APPROACHING ROUNDOFF
            IF (ABS(DEN).LT.TOLMIN2) THEN
               CALL VINK(S,LMAX,SMIN,SMAX,AN,BN,ESA,ESB,KASE )
               RETURN
            ENDIF
C
C.......... CALCULATE NEXT DISTRIBUTION
            AN = AN1 + DELA*(  GB*FN1 - FB*GN1 )/DEN
            BN = BN1 + DELB*(- GA*FN1 + FA*GN1 )/DEN
C
            CALL VINK(S,LMAX,SMIN,SMAX,AN,BN,ESA,ESB,KASE )
C
            FN = ESA/DSAE - 1
            GN = ESB/DSBE - 1
C
C.......... UPDATE N, N-1, N-2 AND CONTINUE
            AN2 = AN1
            BN2 = BN1
            AN1 = AN
            BN1 = BN
            FN1 = FN
            GN1 = GN
C
C....... NEXT GUESS
         ENDDO
C
C.... KASE = 1
C     STRETCHING AT THE LAST ENDPOINT ONLY, SO USE A 1-D SECANT METHOD
C     TO ARRIVE AT THE VALUES OF DSB WHICH WILL SATISFY DSBE WITHIN
C     ROUNDOFF.
C
      ELSEIF (KASE.EQ.1) THEN
C
C....... INITIAL GUESS -  BN = DSBE
```

```
         BN2 = DSBE
         CALL VINK(S,LMAX,SMIN,SMAX,DSAE,BN2,ESA,ESB,KASE )
         FN2 = ESB/DSBE - 1
C
C....... SECOND GUESS - CALCULATE DS1 AND DS2 FROM A TRUNCATED TAYLOR SERIES
         DSSB = 2.*S(LMAX)-5.*S(LMAX-1)+4.*S(LMAX-2)   -S(LMAX-3)
         BN1 = DSBE-0.5*DSSB
         CALL VINK(S,LMAX,SMIN,SMAX,DSAE,BN1,ESA,ESB,KASE )
         FN1 = ESB/DSBE - 1
         BN = BN1
C
C....... 3RD THRU 10TH GUESSES , USE 1-D SECANT METHOD
         DO N = 3,20
C
C.......... STICK WITH LAST GUESS IF APPROACHING ROUNDOFF
            DEN = FN1-FN2
            IF (ABS(DEN).LT.TOLMIN2) THEN
               CALL VINK(S,LMAX,SMIN,SMAX,DSAE,BN,ESA,ESB,KASE )
               RETURN
            ENDIF
C
C.......... CALCULATE NEXT DISTRIBUTION
            BN = BN1 - FN1*(BN1-BN2)/DEN
            CALL VINK(S,LMAX,SMIN,SMAX,DSAE,BN,ESA,ESB,KASE )
            FN = ESB/DSBE - 1
C
C.......... UPDATE N, N-1, N-2 AND CONTINUE
            BN2 = BN1
            BN1 = BN
            FN2 = FN1
            FN1 = FN
C
C....... NEXT GUESS
         ENDDO
C
C.... KASE = 2
C     STRETCHING AT THE FIRST ENDPOINT ONLY, SO USE A 1-D SECANT METHOD
C     TO ARRIVE AT THE VALUES OF DSA WHICH WILL SATISFY DS1E WITHIN
C     ROUNDOFF.
C
      ELSEIF (KASE.EQ.2) THEN
C
C....... INITIAL GUESS -  AN = DSAE
         AN2 = DSAE
         CALL VINK(S,LMAX,SMIN,SMAX,AN2,DSBE,ESA,ESB,KASE )
         FN2 = ESA/DSAE - 1
C
C....... SECOND GUESS - CALCULATE DS1 AND DS2 FROM A TRUNCATED TAYLOR SERIES
         DSSA = 2.*S(   1)-5.*S(     2)+4.*S(     3)   -S(     4)
         AN1 = DSAE-0.5*DSSA
         CALL VINK(S,LMAX,SMIN,SMAX,AN1,DSBE,ESA,ESB,KASE )
         FN1 = ESA/DSAE - 1
         AN = AN1
C
C....... 3RD THRU 10TH GUESSES , USE 1-D SECANT METHOD
         DO N = 3,20
C
C.......... STICK WITH LAST GUESS IF APPROACHING ROUNDOFF
            DEN = FN1-FN2
            IF (ABS(DEN).LT.TOLMIN2) THEN
             CALL VINK(S,LMAX,SMIN,SMAX,AN,DSBE,ESA,ESB,KASE )
             RETURN
            ENDIF
C
C.......... CALCULATE NEXT DISTRIBUTION
            AN = AN1 - FN1*(AN1-AN2)/DEN
            CALL VINK(S,LMAX,SMIN,SMAX,AN,DSBE,ESA,ESB,KASE )
            FN = ESA/DSAE - 1
C
C.......... UPDATE N, N-1, N-2 AND CONTINUE
            AN2 = AN1
            AN1 = AN
            FN2 = FN1
            FN1 = FN
C
C....... NEXT GUESS
         ENDDO
C
C.... END CASE TEST
      END IF
C
C.... ERROR TEST
      IERR = 1
      WRITE(*,*) 'ERROR IN VINOKUR'
      WRITE(*,*) KASE,ABS(DEN)
C
C.... RETURN TO CALLING ROUTINE
      RETURN
      END
C
C---------------------------------------------------------------------
C
```

```
C VINK - STRETCHES POINTS ON A LINE SO THAT SPECIFIED DERIVATIVES
C     AT THE EDGES ARE SATISFIED (TAKEN FROM NASA CR 3313 BY
C     VINOKUR (1980))
C
      SUBROUTINE VINK(S,LMAX,SMIN,SMAX,DS1,DS2,ES1,ES2,KASE )
C
C   VINOKUR'S ALGORITHM IS DESIGNED TO DISTRIBUTE A SPECIFIED
C   NUMBER OF POINTS ALONG A CURVE, GIVEN THE NUMBER OF POINTS,
C   THE LENGTH OF THE CURVE, AND THE DERIVIATIVE CONDITIONS AT
C   BOTH ENDS OF THE CURVE.  IN CFD APPLICATIONS, THE USER WOULD
C   USUALLY RATHER SPECIFY THE DELTA-S'S AT THE ENDS OF THE CURVE,
C   WHICH ARE EQUIVALENT TO THE DERIVATIVES ONLY TO FIRST ORDER.
C   THEREFORE, THE USER MAY WISH TO APPLY THIS ALGORITHM ITERATIVELY
C   TO OBTAIN AN EXACT DELTA-S SPECIFICATION.  SUBROUTINE
C   VINKITER WILL ITERATE ON THIS SCHEME UNTIL THE PROPER DELTA-S
C   CONSTRAINTS ARE SATISFIED.
C
C
C  INPUT:
C     LMAX - NUMBER OF POINTS ON THE CURVE
C     SMIN, SMAX - BEGINNING AND END VALUES OF S
C     DS1,  DS2  - THE DERIVATIVE END CONDITIONS INPUT INTO
C                  VINOKUR'S FUNCTION
C     KASE = 0   - SATISFY DELTA-S ON BOTH ENDS
C          = 1   - SATISFY DELTA-S ONLY AT XI=XIMAX
C          = 2   - SATISFY DELTA-S ONLY AT XI=XIMIN
C  OUTPUT:
C     S( XI )    - RESULTING S DISTRIBUTION FROM VINOKUR'S FUNCTION
C     ES1  -       ( S(XIMIN+1)-S(XIMIN) ) <-  CALCULATED DELTA-S
C     ES2  -       ( S(XIMAX)-S(XIMAX-1) ) <-
C
C
C  ADDITIONALLY, THIS VERSION USES THE APPROXIMATE INVERSE SOLUTION
C  FOR Y=SIN(X)/X AND Y=SINH(X)/X RATHER THAN A NEWTON ITERATION.  THE
C  APPROXIMATE SOLUTION WAS ALSO TAKEN FROM NASA CR 3313.
C
      COMMON /PIVAL/ PI
      DIMENSION S(*), D1(4,2),D2(4,2)

C
C.... CALCULATE CONSTANTS
      SDEL = SMAX-SMIN
      SO=SDEL/FLOAT(LMAX-1)/DS1
      S1=SDEL/FLOAT(LMAX-1)/DS2
      B=SQRT(SO*S1)
      A=SQRT(SO/S1)
C
C.... USE VARIUOS KASE TYPE
      IF (KASE.EQ.1) THEN
        B=S1
      ELSEIF (KASE.EQ.2) THEN
        B=SO
      ENDIF
C
C.... CALCULATE X BASED ON VALUE OF B
      IF ( B.LT.1.0 ) THEN
C
C....... X IS REAL
         IF(B.LT.0.26938972)THEN
            X = PI*(1.   -B     +          B**2 - (1.+PI**2/6.)*B**3
     >        + 6.794732*B**4  -13.205501*B**5     + 11.726095*B**6)
         ELSE
            C =1.-B
            X = SQRT(6.*C)*(1.
     >        +0.15*C    + 0.057321429*C**2 +0.048774238*C**3
     >                   -0.053337753*C**4 + 0.075845134*C**5)
         ENDIF
C
C....... X IS ZERO
         ELSEIF ( B.EQ.1.0 ) THEN
         X=0.
C
C....... X IS IMAGINARY
         ELSE
            IF (B.LT.2.7829681) THEN
               C = B-1.
               X = SQRT(6.*C)*(1.
     *           -0.15*C   + 0.0573214290*C**2 - 0.0249072950*C**3
     *                     + 0.0077424461*C**4 - 0.0010794123*C**5)
            ELSE
               V = ALOG(B)
               W = 1./B - 0.028527431
               X = V + (1.+1./V)*ALOG(2.*V) -0.02041793
     *           + 0.24902722*W     +  1.9496443*W**2
     *           -  2.6294547*W**3  + 8.56795911*W**4
            ENDIF
         ENDIF
C
C....... DISTRIBUTE POINTS ALONG EDGE
         IF ( KASE.EQ.1 .OR. KASE.EQ.2 ) THEN
            S(1   ) = 0.0
            S(LMAX) = SDEL
```

```
            DO I = 2,LMAX-1
               J  = LMAX+1-I
               XI = FLOAT(I-1)/(LMAX-1)
               IF (B.GT.1.0001) THEN
                  U1 = 1. + TANH(X/2.*(XI-1.))/TANH(X/2.)
               ELSEIF (B.LT.0.9999) THEN
                  U1 = 1. + TAN (X/2.*(XI-1.))/TAN (X/2.)
               ELSE
                  U1 = XI*(1.-.5*(B-1.)*(1.-XI)*(2.-XI))
               ENDIF
               U2 = SINH(XI*X)/SINH(X)
               IF (KASE.EQ.1) THEN
                  FACT = ABS(DS1)
                  S(J) = ((1.-FACT)*(1.-U1) + FACT*(1.-U2) ) *SDEL
               ELSEIF (KASE.EQ.2) THEN
                  FACT = ABS(DS2)
                  S(I) = ((1.-FACT)*    U1  + FACT*    U2  ) *SDEL
               ENDIF
            ENDDO
C
C..... KASE = 0
         ELSE
            DO I=1,LMAX
               XI=FLOAT(I-1)/FLOAT(LMAX-1)
               CNUM=X*(XI-0.5)
               CDEN=X/2.
               IF (B.LT.0.9999) THEN
                  CC = TAN(CNUM)/TAN(CDEN)
                  U  = 0.5*(1.+CC)
               ELSEIF (B.GE.0.9999.AND.B.LE.1.0001) THEN
                  U=XI*(1.+2.*(B-1.)*(XI-0.5)*(1.-XI))
               ELSEIF (B.GT.1.0001) THEN
                  CC = TANH(CNUM)/TANH(CDEN)
                  U  = 0.5*(1.+CC)
               ENDIF
               S(I) = U*SDEL/(A+(1.-A)*U)
            ENDDO
         ENDIF
C
         DO L = 1,LMAX
            S(L) = S(L) + SMIN
         ENDDO
         ES1 = S(   2)-S(     1)
         ES2 = S(LMAX)-S(LMAX-1)
C
C.... RETURN TO CALLING ROUTINE
      RETURN
      END

      character*70 function PARSE(s)
C-----------------------------------------------------------------------
C
C  parse  parse out a substring
C
C  901017 cjm
C
C-----------------------------------------------------------------------
        character s*70, stmp*70, c*1
integer   slen, i, j, sl
        logical   delim
c
c---> Strip leading whitespace and delimiters
c
  100   if ( (.not.delim(s(1:1))) .or. (slen(s).eq.0) ) goto 101
          stmp = s(2:slen(s))
  s = stmp
          goto 100
  101   continue
c
c---> Search for the next delimiter
c
sl = slen(s)
i  = sl +1
do 110 j = sl,2,-1
          c = s(j:j)
  if (delim(c)) i = j -1
  110 continue
c
c---> Return the substring and reduce s
c
        if (i.gt.0) then
          parse = s(1:i)
          stmp  = s(i+1:len(s))
  s = stmp
        else
          parse = ' '
          s(1:1) = ' '
        endif
        return
      end
```

```
      logical function DELIM(c)
C-----------------------------------------------------------------------
C
C  Return true if the variable c is a delimiter
C
C  cjm 901214
C
C-----------------------------------------------------------------------
        character c*1
integer   tstc(6), i
data      tstc/32, 9, 44, 47, 58, 59/
c
delim = .false.
do 100 i = 1,6
  if ( ichar(c) .eq. tstc(i) ) delim = .true.
  100   continue
return
      end
      integer function SLEN(s)
C-----------------------------------------------------------------------
C
C  return the actual string length (i.e., strip trailing spaces)
C
C  jch 901017
C
C-----------------------------------------------------------------------
        character s*70
        integer   i, iara(70)
        logical   delim
C
C strip trailing white space and delimiters to find actual length
        i = len(s) +1
  100   continue
          i = i-1
        if ( (i.gt.0) .and. delim(s(i:i)) ) goto 100
        slen = i
        return
      end
```

REPORT DOCUMENTATION PAGE

Form Approved
OMB No. 0704-0188

1. AGENCY USE ONLY (*Leave blank*)	2. REPORT DATE	3. REPORT TYPE AND DATES COVERED
	April 1998	Final Contractor Report

4. TITLE AND SUBTITLE

Energy Efficient Engine Low Pressure Subsystem Flow Analysis

5. FUNDING NUMBERS

WU–509–10–11–00
NAS3–27394

6. AUTHOR(S)

Edward J. Hall, Sean R. Lynn, Nathan J. Heidegger, and Robert A. Delaney

7. PERFORMING ORGANIZATION NAME(S) AND ADDRESS(ES)

Allison Engine Company
P.O. Box 420 T-14A
Indianapolis, Indiana 46206–0420

8. PERFORMING ORGANIZATION REPORT NUMBER

E–11067

9. SPONSORING/MONITORING AGENCY NAME(S) AND ADDRESS(ES)

National Aeronautics and Space Administration
Lewis Research Center
Cleveland, Ohio 44135–3191

10. SPONSORING/MONITORING AGENCY REPORT NUMBER

NASA CR—1998-206597

11. SUPPLEMENTARY NOTES

Responsible person, Joseph P. Veres, organization code 2900, (216) 433–2436.

12a. DISTRIBUTION/AVAILABILITY STATEMENT

Unclassified - Unlimited
Subject Categories: 07 and 64 Distribution: Nonstandard

This publication is available from the NASA Center for AeroSpace Information, (301) 621–0390.

12b. DISTRIBUTION CODE

13. ABSTRACT ***(Maximum 200 words)***

The objective of this project is to provide the capability to analyze the aerodynamic performance of the complete low pressure subsystem (LPS) of the Energy Efficient Engine (EEE). The analyses were performed using three-dimensional Navier-Stokes numerical models employing advanced clustered processor computing platforms. The analysis evaluates the impact of steady aerodynamic interaction effects between the components of the LPS at design and off-design operating conditions. Mechanical coupling is provided by adjusting the rotational speed of common shaft-mounted components until a power balance is achieved. The Navier-Stokes modeling of the complete low pressure subsystem provides critical knowledge of component aero/mechanical interactions that previously were unknown to the designer until after hardware testing.

14. SUBJECT TERMS

Gas turbine; Turbofan; Engine simulation; Modeling, System; Computational; Numerical; Flow, CFD

15. NUMBER OF PAGES

176

16. PRICE CODE

A08

17. SECURITY CLASSIFICATION OF REPORT	18. SECURITY CLASSIFICATION OF THIS PAGE	19. SECURITY CLASSIFICATION OF ABSTRACT	20. LIMITATION OF ABSTRACT
Unclassified	Unclassified	Unclassified	